UPoN 2008

Unsolved Problems on Noise

5th International Conference on

Unsolved Problems on Noise and Fluctuations
in Physics, Biology & High Technology

École Normale Supérieure de Lyon (France)
June 2–6, 2008

Organizers: S. Ciliberto, L. Bellon, E. Bertin, T. Dauxois, S. Deschanel, S. Roux and L. Vanel

CENTRE NATIONAL DE LA RECHERCHE SCIENTIFIQUE

DGA

ECOLE NORMALE SUPERIEURE DE LYON

Région RhôneAlpes

Institut des Systèmes Complexes Complex Systems Institute Rhône-Alpes IXXI

Foreword

The aim of the conferences "Unsolved Problems on Noise", which are organized every three years, is to provide a forum for researchers working on noise and fluctuations, where they can present and discuss their scientific problems which do resist solutions. The first edition held in 1996 in Szeged (Hungary) was mostly devoted to devices. The second edition held in Adelaide (Australia) in 1999 focused on the mathematical aspects of noise and fluctuation research. In the third one, organized in the National Institutes of Health in Bethesda (USA), the main topics were centered around the problems of noise in biology and biomedical engineering. The fourth conference, which took place in Gallipoli (Italy), focused mainly on noise and fluctuations at the nanometric scale-length in electronic devices, bio-materials and mesoscopic systems. The conference organized in Lyon wants to keep a strong interdisciplinary aspect and we hope that we will succeed in reaching this goal. The Scientific Committee selected seven main topics that will be introduced by several invited speakers who will point out which, in their opinion, are the open problems in their specific field of interest. The selected topics are:

1. Applications of noise in measurements, technologies and informatics
2. Biological noise
3. Crackling noise
4. Noise in complex and non-linear systems
5. Noise in materials and devices
6. Quantum noise and coherence
7. Theoretical trends in fluctuations

Several subjects in this list are within the framework of the Gallipoli conference and previous ones. The real novelty of the Lyon edition is the section on "Crackling Noise", which has been introduced because such a kind of noise appears in many physical, biological, geological and technological problems. It presents many open aspects which merit to be discussed in details.

Focusing on unsolved problems requires a more thorough, more open-minded, and less biased refereeing process than the presentation of solved problems typical in the publications of the standard literature. The conference tradition dictates that to be accepted each proposal (contributed oral and poster papers) has to be reviewed using double-blind refereeing process by appropriate members of the Scientific Committee. For this edition we received about 130 contributions. Using the above mentioned procedure the committee selected 50 talks and 70 posters. The proceedings of the conference will be published in a special issue "Unsolved problems of noise in physics, biology and technology" of the "Journal of Statistical Mechanics: Theory and Experiment". The deadline for submitting your contributions has been postponed to June 15^{th}.

We hope that you will enjoy your stay in Lyon and profit from the workshop.

The organizers

S. Ciliberto, L. Bellon, E. Bertin, T. Dauxois, S. Deschanel, S. Roux and L. Vanel

Acknowledgements

The financial support which helped the conference organization came from several Institutions that we warmly acknowledge: l'École Normale Supérieure de Lyon (ENSL), le Centre National de la Recherche Scientifique (CNRS), la Direction Générale de l'Armement (DGA), la Fédération de Physique André Marie Ampère, l'Institut des Systèmes Complexes (IXXI), la Région Rhône-Alpes, le GDR-CNRS Phénix.

The organization of the Lyon edition of UPON has been made possible by the work of the local organizers that I thank for their essential contribution: L. Bellon, E. Bertin, T. Dauxois, S. Deschanel, S. Roux and L. Vanel. A specially warm acknowledge is addressed to Dr. L. Bellon, who edited and managed in a very efficient way the web page of the conference.

I also thank for their useful help the two secretaries of the Laboratoire de Physique de l'ENSL, N. Clervaux and L. Mauduit.

I finally acknowledge all the members of the Scientific Committee who helped in the double blind referee process of the abstract selection.

The Conference Chairman

Sergio Ciliberto

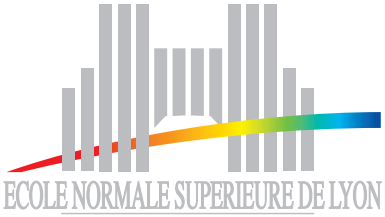

Contents

Foreword **1**

Table of contents **3**

Schedule **5**

Talks **9**
Applications of noise in measurements, technologies and informatics . . . 9
Biological noise . . . 13
Crackling noise . . . 26
Noise in complex and non-linear systems . . . 35
Noise in materials and devices . . . 45
Quantum noise and coherence . . . 59
Theoretical trends in fluctuations . . . 63

Posters **69**
Applications of noise in measurements, technologies and informatics . . . 69
Biological noise . . . 76
Crackling noise . . . 88
Noise in complex and non-linear systems . . . 92
Noise in materials and devices . . . 101
Quantum noise and coherence . . . 113
Theoretical trends in fluctuations . . . 117

Scientific Committee **119**

List of participants **121**

Index of Authors **133**

Schedule

Monday June 2nd

8h00 Registration Opening

8h45-9h10 Welcome Introduction

Session: Noise in complex and non-linear systems

9h10-9h40 Laszlo B. Kish
Negative weight transients of information storage media after recording

9h40-10h00 Debjani Bagchi
Fluctuations and slow dynamics in an ageing polymer glass

10h00-10h30 Ho Bun Chan
Activation barrier scaling and switching path distribution in micromechanical parametric oscillators

10h30 Coffee Break

11h00-11h30 Francisco J. Cao
Open problems on information and feedback control of stochastic systems

11h30-11h50 Andrea Duggento
An inferential framework for nonstationary dynamics: Theory, applications, and open questions

11h50-12h10 Lukasz Machura
Order and Disorder in Coupled Mesoscopic Rings

12h10-12h30 Alexander Alexandrovich Dubkov
The problem of constructing phenomenological equations for subsystem interacting with non-Gaussian thermal bath

12h30-14h30 Lunch

14h30-15h10 Bernard Castaing – **Keynote Lecture**
Noise statistics and physical mechanisms

15h10-15h30 Freddy Bouchet
Out of equilibrium phase transitions in the two dimensional Navier Stokes equation with stochastic forces

Session: Quantum noise and coherence

15h30-16h00 Julien Gabelli
Dynamics of Quantum Noise in a Tunnel Junction under ac Excitation

16h00 Coffee Break

16h40-17h10 Tomas Novotný
Josephson junctions as detectors of the Full Counting Statistics: Theoretical issues and analysis of experiments

17h10-17h30 Xavier Oriols
High frequency noise in mesoscopic conductors: A novel algorithm for the self-consistent computations of particle and displacement currents with quantum trajectories

17h30-17h40 Human Rights Session.

18h00 Welcome drink

Tuesday, June 3rd

Session: Crackling noise

9h00-9h40 Karin DAHMEN – **Keynote Lecture**
Crackling Noise, Glassiness, and Disorder Induced Critical Scaling In and Out of Equilibrium: are they the same ?

9h40-10h00 Lasse LAURSON
Temporal avalanche correlations in crackling noise

10h00-10h30 Stéphanie DESCHANEL
Experimental study of crackling noise: conditions on power-law scaling correlated to fracture precursors

10h30-11h00 Coffee Break

11h00-11H30 Ferenc KUN
Crackling noise in fatigue fracture of heterogeneous materials

11h30-11h50 Alvaro CORRAL
Self-similar dynamical structure in catastrophic events and in written texts

11h50-12h10 Gianni NICCOLINI
Crackling noise and universality in fracture systems

Session: Biological noise

12h10-12h30 Daniele ANDREUCCI
Variability and suppression of variability in the photoresponse in the mouse rod

12h30-12h50 Igor A. KHOVANOV
Intrinsic dynamics of heart regulatory systems: from experiment to modelling

12h50-14h30 Lunch

14h30-16h00 Poster Session

16h00-16h30 Coffee Break

Session: Applications of noise in measurements, technologies and informatics

16h30-17h10 Holger KANTZ – **Keynote Lecture**
Noise in measurements and data analysis

17h10-17h30 Francois CHAPEAU-BLONDEAU
Raising the noise to improve the performance of optimal processing

17h30-18h00 Bernard ORSAL
Optical noise of a 1550 nm fiber laser as an underwater acoustic sensor

Wednesday, June 4th

Session: Theoretical trends in fluctuations

9h00-9h40 Roberto BENZI – **Keynote Lecture**
Stochastic Resonance in complex systems

9h40-10h00 Peter M. KOTELENEZ
Brownian noise and the depletion phenomenon

10h00-10h30 Giuseppe GONNELLA
Heat fluctuations in systems in contact with heat baths at different temperatures

10h30-11h00 Coffee Break

11h00-11h30 Eli BARKAI
Weakly Non-ergodic Noise: From Blinking Qunatum Dots to mRNA diffusing in a cell

11h30-11h50 Paolo PARADISI
Perturbation-induced transition from Non-Poisson to Poisson statistics

Session: Noise in materials and devices

11h50-12h10 Yossi PALTIEL
Non Gaussian Noise in Quantum Wells

12h10-12h30 Iouri GALPERINE
Many electron theory of 1/f-noise in hopping conductance

12h30-12h50 Jean-Marc ROUTOURE
Possible effect of epitaxial quality and of strain on the low frequency noise in LSMO thin films

12h50-14h30 Lunch

14h30-15h45 Poster Session / Visit of the Physics Laboratory

15h45-16h15 Coffee Break

16h15-19h00 Guided tour of the old city of Lyon

Meeting Points: 16h15 from ENS Lyon or 17h from Basilique Fourvière.

Thursday, June 5th

Session: Noise in materials and devices

9h00-9h40 Hélène BOUCHIAT – **Keynote Lecture**
Thermal and out of equilibrium noise in electronic devices: from the classical to the quantum regime

9h40-10h00 Francesco CICCARELLO
Noise of hot electrons in anisotropic semiconductors in the presence of a magnetic field

10h00-10h30 Guillem ALBAREDA
Can analog and digital applications tolerate the intrinsic noise of aggressively-scaled field-effect transistors?

10h30 Coffee Break

11h00-11h30 Luca VARANI
Problems of noise modeling in the presence of total current branching in HEMTs and FETs channels

11h30-11h50 Eugene SUKHORUKOV
Stochastic dynamics of a Josephson junction threshold detector

11h50-12h10 Jesús Enrique VELÁZQUEZ-PÉREZ
Noise in strained-Si MOSFET for low-power applications

12h10-12h30 Jean-Francois MILLITHALER
A Monte Carlo investigation of plasmonic noise in nanometric n-$In_{0.53}Ga_{0.47}As$ channels

12h30-14h30 Lunch

14h30-16h00 Poster Session

16h00-16h30 Coffee Break

16h30-16h50 Kamal Kumar BARDHAN
1/f Noise in systems with multiple transport mechanisms

16h50-17h10 Shih CHUN-HSING
Latent Noise in Schottky Barrier MOSFETs

Session: Theoretical trends in fluctuations

17h10-17h50 Eric VANDEN-EIJNDEN – **Keynote Lecture**
Pathway of maximum likelihood of rare noise-induced events

20h00 Banquet: Restaurant *Le Caro de Lyon* 25, rue Bât d'Argent 69001 Lyon

Friday, June 6th

Session: Biological noise

9h00-9h40 Benjamin LINDNER – **Keynote Lecture**
Biological noise - from neural shot noise to diffusive transport

9h40-10h00 Kai DIERKES
Enhancement of sensitivity gain and frequency tuning by coupling of active noisy hair bundles

10h00-10h30 Francesca DI PATTI
Can a microscopic stochastic model explain the emergence of pain cycles in patients?

10h30 Coffee Break

11h00-11h30 Zbigniew R. STRUZIK
Is Complexity of Heart Rate Decreased or Increased in Congestive Heart Failure

11h30-11h50 Noboru TANIZUKA
Predictability of Consciousness States Studied with Human Brain Magnetism

11h50-12h10 Mark Damian MCDONNELL
On the Interaction Between Lossy Compression, Randomness and Redundancy in Biological Neurons

12h10-12h30 Steeve ZOZOR
Does the eye tremor provide the hyperacuity phenomenon?

12h30-14h30 Lunch

14h30-14h50 Ekkehard ULLNER
Noise-induced rhythmicity in an ensemble of circadian oscillators

14h50-15h10 Josep Maria HUGUET
Towards DNA sequencing by force

Session: Crackling Noise

15h10-15h30 Fergal DALTON
Stick-slip of a sheared granular medium

15h30-15h50 Ferenc F. CSIKOR
Dislocation avalanches and the intermittency of crystal plasticity

15h50-16h10 Edvige CELASCO
Correlated avalanches in TES noise power spectra

16h10-17h00 Coffee Break

Talks

Applications of noise in measurements, technologies and informatics

Holger Kantz – **Keynote Lecture**
Noise in measurements and data analysis *10*

Bernard Orsal
Optical noise of a 1550 nm fiber laser as an underwater acoustic sensor *11*

Francois Chapeau-Blondeau
Raising the noise to improve the performance of optimal processing *12*

Noise in measurements and data analysis

Holger Kantz
Max-Planck-Institute for the Physics of Complex Systems
Nöthnitzer Str. 38, 01187 Dresden, Germany

Open problems in the way how noisy measurements can be used in signal processing and data analysis will be discussed. Noise on data obscures our knowledge about the true state of the observed system. We raise issues in noise reduction, statistical inference, and modeling based on noisy time series data or images, but also the difficulty of assessing uncertainties of measurements of time dependent quantities.

Optical noise of a 1550 nm fiber laser as an underwater acoustic sensor

B. Orsal, R. Vacher**, D. Dureisseix****

*** Research team "Bruit Optoélectronique", Institut d'Electronique du Sud (IES), CNRS UMR 5214 / University Montpellier 2, CC 084, Place Eugène Bataillon, F-34095 Montpellier Cedex 05, France**

**** Société d'études, de recherche et de développement industriel et commercial (Serdic), 348 avenue du Vert-Bois, F-34090 Montpellier, France**

**** Research team "Systèmes Multi-contacts", Laboratoire de Mécanique et de Génie Civil (LMGC), CNRS UMR 5508 / University Montpellier 2, CC 048, Place Eugène Bataillon, F-34095 Montpellier Cedex 05, France**

The goal of this presentation is to provide the first results we get concerning the optical noise of a fiber laser used as an underwater acoustic sensor. The main sensor characteristics are:
- a sensitivity allowing detection of all noise levels over background sea noise (the so-called *deep-sea state 0*). Among other applications, one may mention: seismic risk prevention, oil prospection, ship detection, etc.
- an optical noise reduced at its minimal value: it is the lower bound below which no acoustic pressure variation is detectable.

The studied sensor we are concerned with is a fiber-laser based deep-sea hydrophone. Its basic principle lies in the measurement of a laser emission frequency from an erbium-doped optic fiber, with two imprinted mirrors acting as an optical cavity. The length variations of the fiber, proportional to the acoustic pressure levels, induce a change in frequency of the emitted light. To allow for an accurate detection of these length variations, the fiber laser is embedded into an acoustic/mechanical device whose aim is to amplify strains arising from acoustic waves. The device principles and designs, architectures of the detection channel and performances are well described in the literature.

Excitation power is produced by a pump laser located on an emission/reception station on shore. A transmission fiber, whose length may be up to several dozens of kilometers, guides the pump power (with a 1480 nm wavelength) up to the fiber lasers acting as sensors. These fiber lasers emit a backtracking beam with a different wavelength. Several sensors may be located on the same line, provided that they all respond with different wavelengths, close to 1550 nm, in order to increase detection area radius. Once they reach the reception station, the different signals are first separated with a wavelength demultiplexer, and second, driven to a Mach-Zehnder interferometer shifted by using 300m optical fiber that detects both the acoustic signal frequency and the optical noise generated by the fiber laser. To improve the detection phase, the two separated beams in the interferometer are modulated with different frequencies, to get the heterodyne detection, using a FFT analyzer for low frequency analysis of main signal and optical noise.
We therefore present herein the first results on the expected sensitivity of the acoustic/optic device, on the frequency and amplitude optical noises induced by the fiber laser and all the devices on the optical line, on the interactions between optical channels when close laser wavelengths are used. These results exemplify the possible detection of signal levels as low as the *deep-sea state 0*, especially for low frequency bandwidths, from several Hertz up to several kiloHertz.

Raising the noise to improve the performance of optimal processing

François Chapeau-Blondeau, David Rousseau,
Laboratoire d'Ingénierie des Systèmes Automatisés (LISA),
Université d'Angers, 62 avenue Notre Dame du Lac, 49000 Angers, France.

Abstract

We formulate, in general terms, the classic theory of optimal detection and optimal estimation of signal in noise. In this framework, we exhibit specific examples of optimal detectors and estimators endowed with a performance which can be improved by injecting more noise. From this proof of feasibility by examples, we suggest a general mechanism by which noise improvement of optimal processing, although seemingly paradoxical, may indeed occur. Beyond specific examples, this leads us to the formulation of open problems concerning the general characterization, including the conditions of feasibility, of such situations of optimal processing improved by noise.

(1) A general optimal processing problem: An input signal $s(t)$ is coupled to a native random noise $\xi(t)$ by some physical process, so as to produce an observable signal $x(t)$. At N distinct times t_j which are given, N observations are collected $x(t_j) = x_j$, for $j = 1$ to N. From the N observations $(x_1, \dots x_N) = \boldsymbol{x}$, one wants to perform, about the input signal $s(t)$, some inference that would be optimal in the sense of a meaningful criterion of performance that is denoted Q.

(2) A detection problem: An embodiment of the situation of (1) is a standard two-hypothesis detection problem, where the input signal $s(t)$ can be any one of two known signals, i.e. $s(t) \equiv s_0(t)$ with prior probability P_0 or $s(t) \equiv s_1(t)$ with prior probability $P_1 = 1 - P_0$. Input signal $s(t)$ is mixed in some way to the "corrupting" noise $\xi(t)$ to yield the observable signal $x(t)$. From the observations $\boldsymbol{x} = (x_1, \dots x_N)$ one has then to detect whether $s(t) \equiv s_0(t)$ or $s(t) \equiv s_1(t)$ hold. In this context, a meaningful criterion of performance Q is (other criteria of Neynman-Pearson or minimax types are also possible) the probability of detection error $Q = \Pr\{s_1 \text{ decided } | s_0 \text{ true }\}P_0 + \Pr\{s_0 \text{ decided } | s_1 \text{ true }\}P_1$, the two conditional probabilities in Q being dependent upon the probabilization established by the noise $\xi(t)$. Classic detection theory [1] tells us that the optimal detector to minimize this Q is to compare the likelihood ratio $\Pr\{\boldsymbol{x}|s_1\}/\Pr\{\boldsymbol{x}|s_0\}$ to the decision threshold P_0/P_1.

(3) An estimation problem: Another embodiment of the general situation (1) is a standard parameter estimation problem, where the input signal $s(t)$ is dependent upon an unknown parameter a, i.e. $s(t) \equiv s_a(t)$. Input signal $s_a(t)$ is mixed to the noise $\xi(t)$ to yield the observable signal $x(t)$. From the observations $\boldsymbol{x} = (x_1, \dots x_N)$ one has then to estimate a value $\widehat{a}(\boldsymbol{x})$ for the unknown parameter. In this context, a meaningful criterion of performance Q can be the rms estimation error $Q = \mathrm{E}^{1/2}\{[\widehat{a}(\boldsymbol{x}) - a]^2\}$. In this Q, the expectation $\mathrm{E}(\cdot)$ can be according to the probabilization established by the noise $\xi(t)$ alone, in the case of a deterministic unknown parameter a; or it can be according to the probabilization established in conjunction by the noise $\xi(t)$ and the prior probability on a, in the (Bayesian) case of a stochastic unknown parameter a. Classic estimation theory [1] tells us that the optimal estimator is the maximum likelihood estimator $\widehat{a} = \arg\max_a \Pr\{\boldsymbol{x}|a\}$ in the asymptotic regime $N \to \infty$ for the deterministic parameter case, and the a posteriori mean for the Bayesian stochastic parameter case.

(4) Noise-improved optimal processing: The amount of noise is quantified by a standard measure such as the noise variance $\mathrm{var}[\xi(t)] = \sigma^2$. At a given noise level $\sigma^2 = \sigma_1^2$, the optimal processor for the problem at hand achieves the optimal performance $Q = Q_1$. At a strictly superior noise level $\sigma^2 = \sigma_2^2 > \sigma_1^2$, the optimal processor for the problem achieves the optimal performance $Q = Q_2$. The outcome is that situations are possible where Q_2 can be strictly better than Q_1, i.e. when the optimal processor operates at a higher noise level, its optimal performance is improved.

Another related situation, is the case where in the original setup of (1), a supplementary noise $\eta(t)$ is purposely injected into the process in some way to influence the production of the observable signal $x(t)$, with $\eta(t)$ independent of both the native noise $\xi(t)$ and the input signal $s(t)$. The amount of the injected noise is quantified, for instance, by its variance $\mathrm{var}[\xi(t)] = \sigma_\eta^2$. With no injected noise, i.e. at $\sigma_\eta^2 \equiv 0$, the optimal processor for the problem at hand achieves the optimal performance $Q = Q_1$. With a nonzero amount of injected noise, i.e. at $\sigma_\eta^2 > 0$, the optimal processor for the problem achieves the optimal performance $Q = Q_2$. The outcome is that situations are possible where Q_2 can be strictly better than Q_1, i.e. when some nonzero extra noise is injected into the process, the optimal processor achieves a better performance.

In the line of the studies on stochastic resonance and useful-noise effects [2], specific examples establishing the feasibility of such improvement by noise have been reported for optimal detection in [3, 4], and for optimal estimation in [5]. New examples will be proposed in the full presentation.

(5) The basic mechanism: It may at first sight seem paradoxical that optimal processors in the sense of (1), which include the classic optimal detectors of (2) and optimal estimators of (3), can be improved by raising the noise. The point is that these processors are optimal in the sense that they represent the best possible *deterministic* processing that can be done on the data $\boldsymbol{x}$ to optimize the performance Q. In the classic theory of these optimal processors, the performance Q is a functional of the probabilization established by the native noise $\xi(t)$, and this probabilization is kept fixed. The classic optimal theory then derives the best *deterministic* processing of the data $\boldsymbol{x}$ to optimize the performance Q at a level Q_1. This level Q_1 is therefore the best value of the performance that can be achieved by *deterministic* processing of the data $\boldsymbol{x}$ in the presence of a *fixed* probabilization of the problem and of the functional Q. What is realized by injection of more noise, is a change of this probabilization of the problem. If the probabilization in the functional Q is changed, then the optimal processor, which is now optimal in the presence of the new probabilization of the functional Q, may achieve an improved performance $Q_2 > Q_1$. It is even possible that a suboptimal processor in the sense of Q based on the new probabilization, achieve a performance strictly better than the performance Q_1 optimal in the sense of the initial probabilization.

(6) Open problems of noise: In this perspective, several open problems will be discussed:
• To obtain a general characterization of the optimal processing problems according to (1) that can benefit from an improved performance through a change of their probabilization.

The change of probabilization, to be interpretable as a noise-improved performance, should be what can be called an "overprobabilization", i.e. a change of probabilization that goes in the direction of raising the noise. A formal change of probabilization that would only amount to reduce the level of the native noise $\xi(t)$ would in general trivially lead to an improved performance of the optimal processor; but the direction which is interesting to explore is the opposite: an improved performance by raising the noise.
• To characterize the beneficial overprobabilizations that are compatible with the underlying physics of the problem. No all formally conceivable changes of probabilization are physically realizable in a given process.
• Finally, for a given optimal-processing problem, one would like to be able to characterize, when it exists and among those physically realizable, the optimal overprobabilization, i.e. that yielding the best improvement by raising the noise.

References

[1] H. L. Van Trees, *Detection, Estimation, and Modulation Theory, Part 1.* New York: Wiley, 2001.

[2] L. Gammaitoni, P. Hänggi, P. Jung, and F. Marchesoni, "Stochastic resonance," *Reviews of Modern Physics*, vol. 70, pp. 223–287, 1998.

[3] F. Chapeau-Blondeau, "Stochastic resonance for an optimal detector with phase noise," *Signal Processing*, vol. 83, pp. 665–670, 2003.

[4] F. Chapeau-Blondeau and D. Rousseau, "Constructive action of additive noise in optimal detection," *International Journal of Bifurcation and Chaos*, vol. 15, pp. 2985–2994, 2005.

[5] F. Chapeau-Blondeau and D. Rousseau, "Noise-enhanced performance for an optimal Bayesian estimator," *IEEE Transactions on Signal Processing*, vol. 52, pp. 1327–1334, 2004.

Biological noise

Benjamin Lindner – **Keynote Lecture**
Biological noise - from neural shot noise to diffusive transport 14

Kai Dierkes
Enhancement of sensitivity gain and frequency tuning by coupling of active noisy hair bundles 15

Francesca Di Patti
Can a microscopic stochastic model explain the emergence of pain cycles in patients? 16

Zbigniew R. Struzik
Is Complexity of Heart Rate Decreased or Increased in Congestive Heart Failure 17

Igor A. Khovanov
Intrinsic dynamics of heart regulatory systems: from experiment to modelling 18

Mark Damian McDonnell
On the Interaction Between Lossy Compression, Randomness and Redundancy in Biological Neurons 19

Steeve Zozor
Does the eye tremor provide the hyperacuity phenomenon? 20

Paolo Paradisi
Perturbation-induced transition from Non-Poisson to Poisson statistics 21

Ekkehard Ullner
Noise-induced rhythmicity in an ensemble of circadian oscillators 22

Josep Maria Huguet
Towards DNA sequencing by force 23

Noboru Tanizuka
Predictability of Consciousness States Studied with Human Brain Magnetism 24

Daniele Andreucci
Variability and suppression of variability in the photoresponse in the mouse rod 25

Biological noise - from neural shot noise to diffusive transport

Benjamin Lindner
Max-Planck-Institute for the Physics of Complex Systems
Nöthnitzer Str. 38, 01187 Dresden, Germany

Solved and open problems in two general biophysical problems involving noise are reviewed: transfer of information through stochastic neurons and directed intracellular transport by molecular motors.

1 Noise in neural systems

All our sensations are mediated by small electric discharges across the cell membrane of nerve cells (neurons) [1]. These discharges are called action potentials or spikes; their occurrence in time is thought to encode information solely by means of the instances in time (not by the shape of the stereotypic action potential).

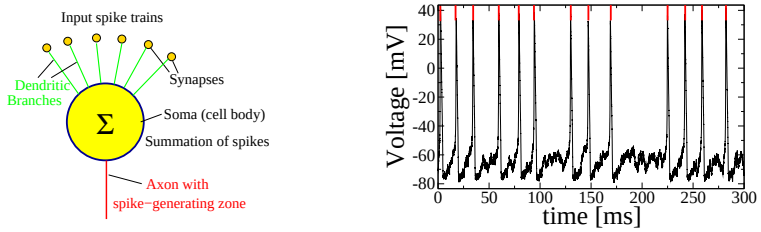

Figure 1: Left: Scheme of a neuron that receives many $(10^2 - 10^4)$ spike train inputs from other neurons via synapses on the dendritic branches. If the input is sufficiently strong, an action potential or spike is generated in the axon. Right: Voltage trace of a stochastic model neuron (Hodgkin-Huxley model) showing randomly occurring action potentials due to the noisy synaptic input. Information is entirely encoded in the spike train (red bars).

There are several internal and external sources of fluctuations that require a statistical description of neural activity [2]. The generation and statistics of *spike trains* and their relation to sensory stimuli has long been studied within the framework of stochastic dynamical systems and stochastic point processes. The last decade has seen considerable progress in the analytical approaches to these models. I will review some of them and discuss their limitations. Problems will include correlations in the sequence of interspike intervals [3, 4, 5], spike train correlations induced by common noise [6], multiplicative shot noise (conductance noise) in single neurons [7], and the role of synaptic plasticity in shaping neural signal transfer [8].

2 Noise in intracellular transport

Self-propelled motion is a fascinating aspect of living systems. This motion can be observed on various levels ranging from motion within single cells [12, 13] to swarming of flocks of animals. Simple phenomenological models help to understand the dynamics of self-propelled entities, their statistics and, possibly, how their dynamics and statistics is related to their biological task (for instance, a reliable transport of cargo for molecular motors or an optimized food search for the motion of animals). One class of models successfully studied during the last 15 years are active Brownian particles [14, 15, 16]. I review analytical results on the mean velocity and the diffusion coefficient of such models [17, 10, 11], present open problems regarding the diffusion of active particles in nonlinear spatial potentials, and try to illustrate how these coarse grained models are related to more realistic microscopic models of self-propelled motion.

References

[1] F. Rieke, D. Warland, R. de Ruyter van Steveninck, and W. Bialek. *Spikes: Exploring the neural code*. MIT Press, Cambridge, Massachusetts, 1996.

[2] H. C. Tuckwell. *Stochastic Processes in the Neuroscience*. Society for industrial and applied mathematics, Philadelphia, Pennsylvania, 1989.

[3] B. Lindner. Interspike interval statistics of neurons driven by colored noise. *Phys. Rev. E*, 69:022901, 2004.

[4] M. J. Chacron, B. Lindner, and A. Longtin. Noise shaping by interval correlations increases neuronal information transfer. *Phys. Rev. Lett.*, 92:080601, 2004.

[5] B. Lindner, M. J. Chacron, and A. Longtin. Integrate-and-fire neurons with threshold noise - a tractable model of how interspike interval correlations affect neuronal signal transmission. *Phys. Rev. E*, 72:021911, 2005.

[6] B. Lindner, B. Doiron, and A. Longtin. Theory of oscillatory firing induced by spatially correlated noise and delayed inhibitory feedback. *Phys. Rev. E*, 72:061919, 2005.

[7] L. Wolff and B. Lindner. A method to calculate the moments of the membrane voltage in a model neuron driven by multiplicative filtered shot noise. *submitted*, 2008.

[8] B. Lindner, J. E. Lewis, and A. Longtin. Broadband coding with dynamic synapses. *submitted*, 2008.

[9] B. Lindner. The diffusion coefficient of nonlinear Brownian motion. *New J. Phys.*, 9:136, 2007.

[10] B. Lindner. The diffusion coefficient of a Brownian particle with friction function according to a power law. *J. Stat. Phys.*, 130:523, 2007.

[11] B. Lindner and E. M. Nicola. Diffusion in different models of active Brownian motion. *submitted*, 2008.

[12] J. Howard. *Mechanics of motor proteins and the cytoskeleton*. Sinauer Associates, Sunderland, Mass., 2001.

[13] F. Jülicher, A. Ajdari, and J. Prost. Modeling molecular motors. *Rev. Mod. Phys.*, 69:1269, 1997.

[14] F. Schweitzer, W. Ebeling, and B. Tilch. Complex motion of Brownian particles with energy depots. *Phys. Rev. Lett.*, 80:5044, 1998.

[15] U. Erdmann, W. Ebeling, L. Schimansky-Geier, and F. Schweitzer. Brownian particles far from equilibrium. *Eur. Phys. J. B*, 15:105, 2000.

[16] L. Schimansky-Geier, U. Erdmann, and N. Komin. Advantages of hopping on a zig-zag course. *Physica A*, 351:51, 2005.

[17] B. Lindner. The diffusion coefficient of nonlinear Brownian motion. *New J. Phys.*, 9:136, 2007.

Enhancement of sensitivity gain and frequency tuning by coupling of active noisy hair bundles

Kai Dierkes, Benjamin Lindner, and Frank Jülicher
Max Planck Institute for the Physics of Complex Systems
Nöthnitzer Str. 38, 01187 Dresden, Germany

Numerical results performed on the basis of an existing model for noisy hair bundle dynamics suggest that collective effects within arrays of coupled hair bundles could play a beneficial role in signal detection by inner ear organs.

Hair bundles and signal tranduction

In all vertebrates the hair bundle constitutes the universal mechano-electrical transducer in both the auditory and the vestibular system. In contrast to purely passive resonators hair bundles from the sacculus of the bullfrog have been shown to possess the ability to amplify weak periodic stimuli by means of an active process [1]. Spontaneous and evoked oscillations of single hair bundles in lower vertebrates have been studied in order to probe the underlying mechanism. Recently, Nadrowski at al. [2] have proposed a stochastic model for active hair bundle motility that very well captures the experimental findings. They have shown that in order to faithfully describe the observed response characteristics of hair bundles it is crucial to take into account the influence of noise stemming from various sources within the system.

In vivo hair bundles in the sacculus of the bullfrog are attached to an overlying viscoelastic structure that effectively mediates a coupling between them: the otolithic membrane. The same holds true for the hair bundles of outer hair cells in the mammalian cochlea whose tips are connected to the overlying tectorial membrane. We report on numerical results that suggest that collective effects in arrays of coupled hair bundles could indeed lead to an increase in the quality of spontaneous oscillations, as well as the enhancement of sensitivity gain and frequency tuning as compared to the performance of a single hair bundle.

We are dealing with a set of strongly coupled noisy oscillators. A deeper theoretical insight into the effects observed in our stochastic simulations could lead to a better understanding of the mechanisms involved in signal detection by inner ear organs. However, the analytical treatment of our results is still wanting.

References

[1] P. Martin and A.J. Hudspeth. 1999. Active hair-bundle movements can amplify a hair cell's response to oscillatory mechanical stimuli. *PNAS* 96:14306-14311

[2] B. Nadrowkski, P. Martin, and F. Jülicher. 2004. Active hair-bundle motility harnesses noise to operate near an optimum of mechanosensitivity. *PNAS* 101:12195-12200

Can a microscopic stochastic model explain the emergence of pain cycles in patients?

Francesca Di Patti[1,2] and Duccio Fanelli[1,2,3]

1. CSDC Centro Interdipartimentale per lo Studio delle Dinamiche Complesse, via di Santa Marta 3, 50139 Firenze, Italy.
2. INFN, sez. Firenze, via G. Sansone 1, 50019 Sesto Fiorentino, Italy.
3. Dip. Energetica, Florence University, via di Santa Marta 3, 50139 Firenze, Italy.

Pain in animals, including humans, is triggered by the so-called nociceptors, sensory neurons that react to potentially damaging stimulus. Analgesic drugs relieve the pain by acting on the peripheral and central nervous system. Drug molecules binds in fact their target receptors and consequently induce a cascade of reactions which eventually inhibits the pain perception. To elucidate the chemical and molecular pathways that drive the aforementioned process would represent a crucial leap forward for both applied and fundamental biomedical research.

Current mathematical models approach the problem via deterministic paradigms, thus neglecting the crucial role which is certainly played by the noise, intrinsic to the phenomenon under scrutiny. These aspects become particularly important when accounting for the presence of diverse chemical species, which populate the stream flow in a spatially diffusive environment. Different chemical entities may compete with the drug molecules and occupy the sites located in close vicinity of the receptors, thus effectively hindering the binding event. Under specific conditions, such competition sustained by the stochastic component of the dynamics result in large temporal oscillations for the amount of bound receptors, a mechanism which could explain the emergence of macroscopic cycles for the sensation of pain in response to medicament.

In this paper, we shall speculate on the above scenario by putting forward a network of chemical reactions and performing a system-size expansion through the celebrated van Kampen theory [1]. This enables us to derive a set of linear equations for the fluctuations, with coefficients related to the steady-state concentrations predicted from the first-order theory (i.e. the deterministic rate equations). Solutions are identified for which the deterministic steady-state occurs via damped oscillations: the inclusion of second-order fluctuations leads then to the amplification of sustained oscillations. These conclusions are discussed with reference to the existing medical literature.

References

[1] See e.g. N. G. van Kampen, *Stochastic Processes in Physics and Chemistry* (North Holland, Amsterdam, 1992).

Is Complexity of Heart Rate Decreased or Increased in Congestive Heart Failure

Ken Kiyono[1], Zbigniew R. Struzik[2], and Yoshiharu Yamamoto[2]
1 College of Engineering, Nihon University, 1 Naka-gawara,
Tokusada, Tamura-machi, Koriyama City, Fukushima, 963-8642, Japan
2 Educational Physiology Laboratory, Graduate School of Education,
The University of Tokyo, 7–3–1 Hongo, Bunkyo-ku, Tokyo 113–0033, Japan

Over the past decade, human heart rate research has attracted considerable interest in the physical and biomedical science communities. Especially since the discovery of 1/f noise in human heart rate more than two decades ago, it has become one of the 'benchmarks' for studies of biological complexity. Specifically, reduced variability and complexity of human heart rate in severe heart disease, including congestive heart failure (CHF), has become one of the key yardsticks by which new complexity measures are validated [1, 2, 3, 4, 5, 6, 7, 8, 9]. Consideration of reduced variability in severe heart disease has become one of the recommendations for the interpretation of HRV by the influential standardising work [10], now registering 1,500 citations. Indeed, there is an emergent belief that the lower variability and lower complexity of heart rate observed in CHF are associated with a higher risk of mortality, yet the focus of attention of the past research on HRV complexity in CHF has been limited to CHF diagnosis from HRV.

In our recent work, we counter this belief, showing on carefully prepared, high-quality data that not a decrease but an increase in complex fluctuations of heart rate predicts mortality of patients suffering from CHF. The increased variability and complexity of heart rate is reflected in the intermittent large deviations, forming non-Gaussian 'fat' tails in the probability density function of heart rate increments and breaking the critical scale invariance observed in healthy heart rate [11, 12, 13]. We characterise this intermittency using our novel methodology [11, 12, 13], stemming from the previous work on fully developed turbulence [14, 15], of multiscale PDF evaluation, and multiscale evaluation of magnitude correlations.

By examining a multiscale description of probability density function (PDF) of beat-to-beat fluctuations of heart rate, or heart rate variability (HRV), we have found that congestive heart failure (CHF) patients with intermittent and non-Gaussian HRV have higher mortality compared with patients with reduced and less complex variability [16]. Such an increase in intermittent and non-Gaussian HRV is also in stark contrast with the robust scale-invariance, i.e. scale-independence, of the multiscale PDF of heart rate fluctuations observed in healthy individuals [12, 13]. Compared with healthy human HRV, heart rate fluctuations in CHF patients, especially those in non-survivors during about four years of the follow-up period, are characterised by a scale specific increase in non-Gaussianity in the short scale (< 40 beats) [16]. Such non-Gaussianity is numerically captured using the λ_s index, where s denotes scale, e.g. λ_{40} probes non-Gaussianity at 40 beats. This λ_s describes a tail of PDF for sums of s successive interbeat intervals after detrending – filtering away a smooth, polynomial trend. A random or simply periodic sequence within this scale would result in the successive sums having a Gaussian distribution, due to a well-known statistics law called the central limit theorem. The existence of fatter tails of PDF in non-survivors than in survivors thus suggests that the non-survivors have a larger number of episodes with correlated tachycardia or bradycardia within this (time)scale.

This likely implies that the patients, particularly non-survivors, have a selective breakdown in the short-term neural regulation of heart rate (e.g. baroreflexes). Indeed, insufficiency or instability in the negative feedback control results in HRV dynamics with unresponsive quiescent phases characteristic of cardiac congestion, interwoven with intermittent compensatory bursts. This view is further supported by the fact that CHF is characterised by impaired or down-regulated baroreflex systems [17]. The short-term non-Gaussianity index proposed (Kiyono et al [16]), possibly probing the existence of such controller instability in intermittent, episodically large increments/decrements of heart rate, has become a significant and independent risk stratifier for CHF mortality.

The concept of heteroscedasticity and intermittent dynamics and its implications for the complexity of the systems under study has previously been addressed in such classical examples of complex dynamics as turbulence, financial markets, solar activity or other physical, natural or man-made complex systems displaying intermittent behaviour in time series from such phenomena. Our notion of complexity and intermittency/heteroscedasticity stems from studies of (the physics of) such phenomena. In particular, heteroscedasticity, i.e., temporal non-homogeneity of variance, observed in CHF patients at high risk of mortality as a result of increased correlations in the system, is characterised by the breaking of the functional PDF scalewise invariance which is observed in healthy subjects [1] and as such, implies breaking the invariance - or symmetry - of the system under renormalization.

Such intermittent behaviour therefore suggests a more complex dynamics of the system under study in terms of a generally recognised concept of complexity in statistical physics, referring to the compactness of the description of the system. An example of a formal treatment is given in, e.g., Ref [18]. The intuitive basis of 'complexity' in such a description reflects 'the average amount of mathematical work required to produce a fluctuation'. Stationary fluctuations require less mathematical work than intermittent, heteroscedastic fluctuations, therefore a system producing such is a more complex one in our interpretation.

Therefore, we expect that our findings will have consequences for the interpretability of the results from the analysis of benchmark data such as the Physionet CHF database `http://www.physionet.org`. They also shed light on stability properties of complex systems, as captured in the evaluation of intermittency and clustering of non-Gaussian fluctuations through magnitude correlations. Finally, our findings are also a demonstration that heart rate control remains a benchmark of biocomplexity. Indeed, future research is required to provide insight into the intermittency and complexity increase/decrease controversy, and further understanding of the neuro-physiological origins of heart rate intermittency.

References

[1] Peng C.-K., et al., *Phys. Rev. Lett.*, **70**, p. 1343, (1993)

[2] Poon C.-S., et al., *Nature* **389**, p. 492, (1997)

[3] [Thurner S., et al., *Phys. Rev. Lett.*, **80**, p. 1544, (1998)

[4] [Amaral L.A.N., et al., *Phys. Rev. Lett.*, **81**, p. 2388, (1998)

[5] Ivanov PC, et al., *Nature* **399** pp. 461–465, (1999)

[6] Chialvo D.R., et al., *Nature* **419**, p. 263, (2002)

[7] [Ashkenazy Y. et al., 2001] *Phys. Rev. Lett.*, **86**, p. 1900, (2001)

[8] Costa M. et al., *Phys. Rev. Lett.*, **89**, p. 068102, (2002)

[9] Yang A.C.-C., et al., *Phys. Rev. Lett.*, **90**, p. 108103, (2003)

[10] Task Force ..., *Circulation* **93** pp. 1043–1065, (1996)

[11] Kiyono K, et al., *IEEE Trans. Biomed. Eng.* **53** pp. 95–102, (2006)

[12] Kiyono K, et al., *Phys. Rev. Lett.* **93** pp. 178103–1–4, (2004)

[13] Kiyono K, et al., *Phys. Rev. Lett.* **95** pp. 058101–1–4, (2005)

[14] Castaing B, et al., *Physica D* **46** pp. 177–200, (1990)

[15] A. Arneodo A., et al. *Phys. Rev. Lett.*, **80**, p. 708, (1998)

[16] Kiyono K, et al., *Heart Rhythm* **5** pp. 261–268, (2008)

[17] Packer M. *Circulation* **77** pp. 721–730, (1988)

[18] Crutchfield J. P. et al., *Phys. Rev. Lett.* **63**, p.105 (1989)

Intrinsic dynamics of heart regulatory systems: from experiment to modelling

I. A. Khovanov
Physics Department,
Lancaster University,
Lancaster LA14YB, United Kingdom

The complexity of heart rate variability (HRV) presents a major challenge to the physics of living systems. Heart rate represents the output of an integrative control system [1] that reacts to external and internal perturbations and to regulatory antagonistic reflexes to produce the observed HRV. The control system consists of a set of complex signaling networks distributed within the body and includes a rhythm center in the brain [1]. Currently the complete structure of the control system is unknown and we can characterize the system via HRV mainly, i.e. by solving the inverse problem: what kind of systems can produce observed HRV?

Recently [2] we experimentally study the intrinsic dynamics of the heart regulatory system, i.e. dynamics in the absence of explicit perturbations by temporarily removing the continuing perturbations caused by respiration. The experimental study leads to a number of new conclusions which are based on analysis of RR-intervals within the framework of a random walk approach. It was shown that nonstationarity of HRV is observed on timescales of less than a minute, taking the form of free diffusion close to classical Brownian motion, but with weak correlation, intermittent periodic oscillations and small deviations from Gaussianity of an increments (of RR-intervals) distribution in the form of the stable distribution.

Recalling that RR-intervals corresponds to time intervals between two activation events of neuron cluster, i.e. passage times, and that without signals from the heart regulatory system, the cluster has shown periodic self-oscillations, we are able to tackle the inverse problem: what are properties of the control system to produce the described above statistics of RR-intervals and increments of RR-intervals. This inverse problem is open now. Evidently non-Gaussianity of increments is most interesting property that requests exploring even on level of phenomenological models of statistical physics.

In this contribution I am going to present experimental results, outline state-of-art understanding of the heart regulatory system and sources of stochasticity in the system, and finally, formulate the inverse problem mentioned above.

References

[1] J. A. Armour, *Am. J. Physiol. Regulatory Integrative Comp. Physiol.* **287** pp. R262-R271 (2004).

[2] I. A. Khovanov, N. A. Khovanova, P. V. E. McClintock, and A. Stefanovska, *New J Physics* (submitted).

On the Interaction Between Lossy Compression, Randomness and Redundancy in Biological Neurons

Mark D. McDonnell*, Pierre-Olivier Amblard† and Nigel G. Stocks‡

Overview: Stochastic Pooling Networks

Two challenges are ubiquitous for many forms of signal and information processing tasks, whether in biology, or artificial technology. These are (i) robustness to the effects of random noise, and (ii) extraction of only the 'information' which is relevant for the task. The latter challenge can require the use of *lossy compression*, where 'information' is intentionally discarded because the lost information is either redundant or irrelevant.

Robustness to random noise is often achieved using a network or array of sensors. It is less obvious that a network approach could lead to lossy compression. We are investigating a generic biologically inspired information processing model in which noise reduction and lossy compression can be simultaneously achieved. This model is called a *stochastic pooling network* (SPN) [1], and in this abstract we outline some of the interesting unsolved questions about this model.

This work is motivated by two fundamental unsolved research questions we are addressing as part of this research:

1. *What mechanisms do biological neural systems use to compress information about external stimuli at the sensory periphery?*
2. *Do unpredictable fluctuations in neural activity in sensory transduction processes contribute to coding/compression effectiveness? If so, is this achieved in conjunction with redundancy?*

A special case of an SPN is the model first discussed in [2] that was designed to encapsulate the most important properties of a population of parallel sensory neurons. When this model was first considered in [2], the context was that of Stochastic Resonance (SR) [3, 4]. The model of [2] exhibits SR in a much more pronounced way than usual, in that 'noise benefits' occur for suprathreshold signals and very large input SNRs. Due to this, the effect was labeled Suprathreshold Stochastic Resonance (SSR).

However, the general SPN defined here goes well beyond that original model, and has far broader applications and interesting features beyond SSR. Our definition of an SPN requires the following three features (which are certainly **not** restricted to neuron or simple comparator models):

- **Non-identical random noise corrupts each node**: each node in the network operates on noisy versions of the *same* signal where no two noise sources can be perfectly correlated;
- **Lossy compression in each node**: each node in the network performs a *lossy* operation on its inputs, so that each output has less possible states than its input;
- **Node outputs are pooled; nodes are unlabeled**: the outputs of each node in the network are 'pooled' to form an overall network output, meaning that no labeling of the output of any individual network node is allowed. The consequence of this is that the 'pooling function' cannot assign weights to the responses from individual nodes, based on the characteristics of that node.

We emphasize the following in the above features: *multiple noise sources, redundancy, lossy compression* and *pooling of unlabeled measurements*. The remainder of this abstract outlines some of the unsolved problems about SPNs that we have encountered.

*Mark D. McDonnell is with the Institute for Telecommunications Research, University of South Australia, Mawson Lakes, SA 5095, Australia (email: mark.mcdonnell@unisa.edu.au).

†Pierre-Olivier Amblard is with GIPSA-lab, Dept. Images & Signals (UMR CNRS 5216) BP 46, 38 402 Saint Martin d'Hères cedex, France (email: bidou.amblard@gipsa-lab.inpg.fr)

‡N. G. Stocks is with the School of Engineering, The University of Warwick, Coventry, CV4 7AL, UK (email: ngs@eng.warwick.ac.uk)

Unsolved Questions on the Optimality of SPNs

The simple case of an SPN first discussed in [2] consists of identical binary nodes. If the restriction that each node is identical is relaxed, then a natural question that arises is how to optimize the nodes at a network level. Since the nodes are binary, this means optimizing N 'threshold levels' for an N-node network. This problem has been solved numerically in [5]. However, the solution is far from intuitive. A series of bifurcations occurs in the optimal levels as the noise intensity in the system decreases. The end result is that the optimal levels cluster to fewer values when fluctuations are larger. In the absence of fluctuations, the optimal levels are unique. This structure has not been explained, and yet we have found similar structures occur in optimization of far more complex topologies, such as when each node is a Poisson neuron. Further complicating the picture is that in some cases our optimality results indicate removal of certain elements from the network completely is the best solution. There are also synergies with problems of recent interest to the information theory community, where it has been proven that information capacity can be achieved by signals which are discrete in nature, rather than continuous [6]. We are currently investigating the optimization of populations of sensory neurons in the SPN context, and anticipate similar bifurcation structures in the solution.

Is the SPN framework applicable to more complex topologies?

A recent neuroscience study has suggested that populations of neurons need to be able to encode probability distributions [8]. Furthermore, in this paper the authors argue that the summation of the output of two populations of neurons encoding information about one stimulus is Bayes optimal for the estimation of the stimulus if the likelihood of the population is 'Poisson-like'. 'Poisson-like' means that the likelihood is an exponential family with linear sufficient statistics. SPNs with identical nodes that are all stochastic neurons, such as Poisson neurons are in the class discussed in [8]. However, the situation is not clear if the individual nodes are different. This raises the question of what changes when the geometry of the network is changed: is the optimal 'pooling function' different when the nature of the nodes is changed?

Are SPNs Relevant to Modern Communications Technology?

Biology significantly outperform even state-of-the-art engineered systems at many tasks. There are many success stories of bio-mimetic and bio-inspired technology and the potential for future innovations based on improved understanding of biological mechanisms is vast. In particular, biological processes have evolved over millions of years, and it is highly feasible that they are optimized for considerations such as energy efficiency, simplicity, adaptability and robustness [7]. One obvious advantage that biology – at least in the brain and nervous system – has over standard silicon based computation, is that of massive parallelism. One way this might be utilized is through noise reduction via averaging effects obtained from redundancy. While highly sophisticated forms of redundancy are used to achieve error correction and communication at rates close to channel capacity, is it possible that biology can achieve fast rates of communication through noisy channels, via *parallel* redundancy, such as is inherent to SPNs?

References

[1] S. Zozor, P. Amblard, and C. Duchêne. *Fluct. Noise Lett.*, 7:L39–L60, 2007.

[2] N. G. Stocks. *Phys. Rev. Lett.*, 84:2310–2313, 2000.

[3] K. Wiesenfeld and F. Moss. *Nature*, 373:33–36, 1995.

[4] L. Gammaitoni, P. Hänggi, P. Jung, and F. Marchesoni. *Rev. Mod. Phys.*, 70:223–287, 1998.

[5] M. D. McDonnell, N. G. Stocks, C. E. M. Pearce, and D. Abbott. *Phys. Lett. A*, 352:183–189, 2006.

[6] T. H. Chan, S. Hranilovic, and F. R. Kschischang. *IEEE Trans. Info. Theory*, 51:2073–2088, 2005.

[7] S. B. Laughlin. *Current Optinion in Neurobiology*, 11:475–480, 2001.

[8] W. J. Ma, J. M. Beck, P. E. Latham, and A. Pouget. *Nature Neuroscience*, 9:1432–1438, 2006.

Does the eye tremor provide the hyperacuity phenomenon?

S. Zozor[1], P.-O. Amblard[1] and C. Duchêne[2]

[1] GIPSA-Lab, 961 rue de la Houille Blanche, 38402 Saint Martin d'Hères Cedex, France

[2] Institut de Traitement du Signal, EPFL, 1015 Lausanne, Switzerland

steeve.zozor@gipsa-lab.inpg.fr, bidou.amblard@gipsa-lab.inpg.fr, cedric.duchene@epfl.ch

Our aim is to understand if the intrinsic biological noise in the visual process provides noise-enhanced processing. Indeed, many fluctuations affect the human visual process. In addition to the well known neural variability, fluctuations affect the retina itself: (i) retina randomly sampled by the photoreceptors; (ii) rods and cones, sensitive to different spectral band of the light, are randomly distributed [1]; (iii) the eyes are subjected to perpetual random oscillations called tremor [2, 3]. The precise role of these fluctuations and especially the saccades is still debated and investigated [4]. However, these random sources seem to be fundamental in the visual process [2, 3, 4] since, for example, suppressing the eye tremor can lead to a fading of vision [4]. Moreover, the tremor is often evoked in the hyperacuity of a sensor, *i.e.* its capability to perform discrimination finer than its resolution [5]. Effects of noise-enhanced resolution of sensors raised up to several engineering application such as contour detection tasks in image processing [6] or improvement of the resolution of sensors [7].

In a previous work [8], we tried to answer the question using an elementary model of retina. Roughly speaking, we showed that a given photoreceptor, at a given time, is able to acquire "information" that is not on its visual field. However, both the model of retina and the measure of similarity considered are elementary. Moreover the study did not precisely show if, as time goes on, the tremor allows the whole ensemble of sensors to improve the information acquisition and if such an improvement is fundamental and is at the origin of the hyperacuity phenomenon.

1 Previous works

In [8], we consider d-dimensional regular samplers, where the noise-free positions of the sensors x_n are affected to spatial noise $\gamma\boldsymbol{\epsilon}_n$ of amplitude γ. In addition, vibrations $\sigma\boldsymbol{\xi}_t$ of amplitude σ shake the ensemble of sensors. Finally we assumed the sensor to perform a linear spatial filtering of impulse response $\alpha^{-d}a_0(\alpha\boldsymbol{f})$ where α tunes the resolution of the sensor. The d-dimensional scene S_r acquired by the n-th sensor from the scrutinized scene S is then modeled as

$$S_r(n,t) = \int_{\mathbb{R}^d} S(\boldsymbol{x}_n + \gamma\boldsymbol{\epsilon}_n + \sigma\boldsymbol{\xi}_t + \boldsymbol{u})\,\alpha^{-d}a_0(\boldsymbol{u}/\alpha)\,d\boldsymbol{u}$$

Our investigation aimed at quantifying the information contained in the *discrete-space* acquisition S_r about the observed *continuous-space* scene S. Due to the different nature of S and S_r and technical difficulties, we restricted our measure of information to a local one: common information between the acquisition of sensor n (noise-free position $\boldsymbol{x}_n$) on point $\boldsymbol{x}_n+\boldsymbol{y}$ of scene S (point at a distance $\boldsymbol{y}$ from $\boldsymbol{x}_n$), at a fixed time t. Even with these restrictions, to be able to quantify of possible noise-enhanced information acquisition, we simplify further the study the a second order measure, namely a correlation coefficient C between the acquisition of a sensor and a given point of the image. Assuming the problem completely isotropic (statistics of the scene, fluctuations and filter), we were able to express this correlation coefficient under a simple integral form. Using specific model of scene, noise statistics, and spatial filter, we then showed the existence of an *optimal stochastic control*: correlation coefficient C is maximized for a non-zero noise amplitude (see fig. 1).

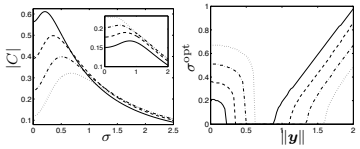

Figure 1: Typical shapes of $|C|$ versus σ for a model of natural scene, a realistic model of a_0 (with excitatory and inhibitory parts) and a bounded tremor noise (Pearson type II), for several resolutions α (different lines) and two different distances between the noise free position $\boldsymbol{x}_n$ of the sensor and point $\boldsymbol{x}_n+\boldsymbol{y}$ of the scene acquired by the sensor (principal panel and inset). Right: typical shape of the optimal noise magnitude versus $\|\boldsymbol{y}\|$.

2 Open questions

Our previous work provided preliminary interpretations about the beneficial role fluctuations may have in the visual process. Before any further neural processing, the first layer of the retina may use the fluctuations to acquire information on a whole scene and not only on a set of discrete points of the scene. However it does not really answer the question whether the noise play a role in the hyperacuity phenomenon, and it did not show that the noise is more than helpful but fundamental in the visual process. To show that tremor compensate a fading effect, time must be taken into account in the study. Furthermore, since the roles of spatial noise and temporal noise are symmetric in our model, the same noise-enhanced behavior occurs when considered versus the spatial noise amplitude. Random sampling is known since many years for its property of alias free sampling [9]: under specific spatial noise, in (ensemble) average random sampling allows to reduce the aliasing effect compared to regular sampling. With this point of view, the tremor can also be viewed as a way to perform an ensemble average (or mathematical expectation) via a time-average. This interpretation may link the statistics of the random sampling and that of the tremor, as tentatively done in [2]. But to validate this claim, again, time-processing must be taken into account in our previous study (*e.g.* via the spatiotemporal filtering made by the photoreceptors, more likely than only a spatial filtering).

Furthermore, we concentrate here on a second order measure to quantify the information acquired by the sensors. A mutual information rate (both in time and space) in the sense of Shannon or Rényi [10] should be preferred, to take into account in some sense the whole statistics of the scene and of the fluctuations. Indeed, two variables can be uncorrelated while sharing information But using such a measure is not an easy task. As an example, let us write the Shannon mutual information between $S_r(n,t)$ and $S(\boldsymbol{x}_n+\boldsymbol{y})$, *i.e.* $I(S(\boldsymbol{x}_n+\boldsymbol{y});S_r(n,t)) = H(S(\boldsymbol{x}_n+\boldsymbol{y})) + H(S_r(n,t)) - H(S(\boldsymbol{x}_n+\boldsymbol{y}),S_r(n,t))$ and assume that S is a Gaussian process of variance σ_S^2. The Shannon entropy $H(S(\boldsymbol{x}_n+\boldsymbol{y}))$ has the explicit form $H(S(\boldsymbol{x}_n+\boldsymbol{y})) = \frac{1}{2}\log(2\pi e\sigma_S^2)$ [10]. $S_r(\boldsymbol{x}_n,t)$ has a Gaussian distribution since, conditionally to the fluctuations, it is Gaussian. Its variance, and hence its entropy, can easily be evaluated; The difficulty lies in the joint entropy. Indeed, the probability density function of couple $(S(\boldsymbol{x}_n+\boldsymbol{y})\,,\ S_r(n,t))$ is no longer Gaussian. This probability density function is a mixture of Gaussian: when conditioned to the fluctuations, the probability density function is Gaussian but of covariance matrix depending on the fluctuations, *e.g.*

$$E\left[S(\boldsymbol{x}_n+\boldsymbol{y})S_r(n,t)|_{\epsilon_n,\xi_t}\right] = \int R_S(\boldsymbol{y}-\gamma\boldsymbol{\epsilon}_n-\sigma\boldsymbol{\xi}_t-\boldsymbol{u})a(\boldsymbol{u})d\boldsymbol{u}$$

Hence, the joint entropy cannot be explicitly evaluated. Even numerically the problem remains difficult. The technical difficulties raise up when, in addition, we would like to take into account a whole scene and all the photoreceptors. The entropy of the continuous-space Gaussian process S can be evaluated [10], but that of S_r is not calculable since the whole vector S_r is no longer Gaussian but is a mixture of Gaussian. Taking into account the whole map of sensors is crucial since, for a fixed magnitude of the eye tremor, a given photoreceptor can gain information on certain areas of the image, while it can lose information on other parts. But in parallel, other photoreceptors can capture information the first one is not able to. Moreover, in the brain the information acquired by a layer of neurons is merged and treated to be sent to the the next layer of neurons (*e.g.* from the photoreceptors up to the optical nerve). Such a posterior processing has to be taken into account.

These steps may help us to quantify how beneficial can by the noise in term of information acquisition and processing. But this model must be used, as an example, in a discrimination task, to clearly show whether the noise provide hyperacuity phenomenon or not.

References

[1] H. Hofer, J. Carroll, J. Neitz, and D. R. Williams. Organization of the human trichromatic cone mosaic. *The Journal of Neurosciences*, 25(42):9669–9679, 2005.

[2] A. Lewis, R. Garcia, and L. Zhaoping. Understanding cone distribution from saccadis dynamics. is information rate maximised? *Neurocomputing*, 58-60:807–813, 2004.

[3] M. H. Hennig, N. J. Kerscher, K. Funke, and F. Wörgötter. Stochastic resonance in visual cortical neurons: Does the eye-tremor actually improve visual acuity? *Neurocomputing*, 44-46:115–121, 2002.

[4] S. Martinez-Conde, S. L. Macknik, and D. H. Hubel. The role of fixational eye movements in visual perception. *Nature Reviews. Neurosciences*, 5(3):229–240, 2004.

[5] W. S. Geisler. Physical limits of acuity and hyperacuity. *J. of Optical Soc. of America A*, 1(7):775–782, 1984.

[6] M.-O. Hongler, Y. Lopez de Meneses, A. Beyeler, and J. Jacot. The resonant retina: Exploiting vibration noise to optimally detect edges in an image. *IEEE Trans. on Pattern Analysis and Machine Intelligence*, 25(9):1051–1062, 2003.

[7] O. Landolt and A. Mitros. Visual sensor with resolution enhancement by mechanical vibrations. *Autonomous Robots*, 11(3):233–239, 2001.

[8] S. Zozor, P.-O. Amblard, and C. Duchêne. Fluctuation in the retina: noise-enhanced processing via random sampling and microsaccads? In *SPIE Int. Symposium on Fluctuations and Noise*, Florence, Italy, May 2007.

[9] F. J. Beutler. Alias-free randomly timed sampling of stochastic processes. *IEEE Trans. on Information Theory*, 16(2):147–152, 1970.

[10] T. M. Cover and J. A. Thomas. *Elements of Information Theory*. John Wiley & Sons, New-York, 1991.

Perturbation-induced transition from Non-Poisson to Poisson statistics

Paolo Paradisi[1], Osman C. Akin[2], Paolo Grigolini[2,3,4]

[1]Istituto di Scienze dell'Atmosfera e del Clima (ISAC-CNR), Lecce Unit, Strada Provinciale Lecce-Monteroni, km 1.2, 73100 Lecce, Italy.
[2]Center for Nonlinear Science, University of North Texas, P.O. Box 311427, Denton, Texas,USA 76203-1427
[3]Dipartimento di Fisica "E. Fermi"- University of Pisa, Largo Pontecorvo 3, 56127 Pisa,Italy.
[4]Istituto dei Processi Chimico Fisici (IPCF-CNR), Area della Ricerca di Pisa, Via G. Moruzzi 1, 56124 Pisa, Italy

Introduction

The response of a statistical system of neuro-physiological interest to an external perturbation is a problem of fundamental importance in physics, insofar as the perturbation is a probe, the response to which brings information on the physical nature of the system under study. The remarkable work done by Moss and coworkers [1, 2] in the understanding of the neuron dynamics is a seminal work that triggered much interest. These authors investigated the effect of an external harmonic perturbation on the dynamics of a neuron firing process. The main effect found by these authors was a reordering of the time distances, or Waiting Times (WT), between two successive firing events. This is found by evaluating the hystogram of perturbed WTs, resulting in a sequel of equally spaced peaks, whose intensity decays with an exponential envelope. The time interval between two consecutive peaks is equal to the perturbation period.

As a general result, the exponential envelope is a typical structure arising in the WT hystogram as the response, to a harmonic signal, of a dynamical system with Poisson statistics of the unperturbed firing events, associated with a pure exponential decay in the unperturbed WT hystogram [3]. In fact, the authors of Refs. [1, 2] found this result using a model describing the motion of a particle in a double-well potential, in presence of a white noise and a harmonic signal. This model, which is also a basic model in the research field of *stochastic resonance*, is in agreement with Poisson statistics of the firing events, here identified as the jumps between the potential wells.

A crucial point is that the exponential envelope is displayed also by several (perturbed) neural models, such as the Hodgkin-Huxley model [4, 5], but the unperturbed firing events in some of these models do not follow a Poisson statistics. As an example, the authors of Ref. [6] reveal the emergence of an anomalous scaling in the Hodgkin-Huxley model, which is a condition incompatible with Poisson statistics, typically associated with ordinary scaling (i.e., ordinary Brownian motion). This result confirms that Non-Poisson systems (i.e., systems with Non-Poisson statistics of the unperturbed firing events) can display the Poisson-like structure identified by the exponential envelope of Refs. [1, 2, 3]. Further, according to some neuro-physiologists, neurons are renewal [7] and Non-Poisson processes [8], *i.e.*, the WTs are mutually independent random variables with non-exponential decay of the hystogram [9].

Aims and results

From the above discussions, it is clear that the transition to a Poisson-like behaviour must be related to the way the unperturbed Non-Poisson system interacts with the external perturbation. However, a general explanation and a quantitative description of this transition is still lacking.

The main aim of this work is to shed light into this issue. To this goal, we make the assumption, supported by the results of Refs. [7, 8], that the WT sequence, generated by the neuron firing process, is described by a renewal Non-Poisson process. In particular, the unperturbed WT hystogram is given by the following class of Pareto-Nutting power-law densities:

$$\psi(\tau) = (\mu_0 - 1)\frac{T_0^{\mu_0 - 1}}{(\tau + T_0)^{\mu_0}}, \qquad (1)$$

with $\mu_0 > 1$. The time scale T_0 defines the transition to the long-time limit, where the inverse power-law $1/\tau^{\mu_0}$ appears. The power index μ_0 signals the specificity of the cooperative properties that establish the complex nature of the neuron firing process. The parameters μ_0 and T_0 afford complete information about the unperturbed system dynamics. Other parameters, characterizing the external perturbing signal, are the time period T_ω and the intensity ϵ of the perturbation itself. The ratio between the time period T_ω and the internal time T_0 is a crucial quantity allowing to establish if the perturbation is slow or fast with respect to the system. Depending on the particular kind of external signal, the perturbation can affect T_0, μ_0 or both of them, and turning them into time dependent parameters $T(t)$ and $\mu(t)$. We use different models generating WT sequences distributed according to Eq. (1) and satisfying the renewal condition and we investigate the effect of an external harmonic signal, affecting T_0 or μ_0.

We will show some results on the different qualitative behaviours of the perturbed system in the different regions of the parameter space, finding under which conditions the system displays the emergence of a Poisson-like behaviour. To this goal, we evaluate the WT hystogram and we perform the Diffusion Entropy (DE) analysis [10] to reveal the diffusion scaling. We recall that an anomalous scaling is a signature of the Non-Poisson nature of the system under study, whereas normal scaling signals a Poisson behaviour. As an example, in Fig. 1 it is reported the WT hystogram of a renewal Non-Poisson model, affected by a strong and fast harmonic perturbation, displaying the typical Poisson-like structure given by the exponential envelope of the maxima.

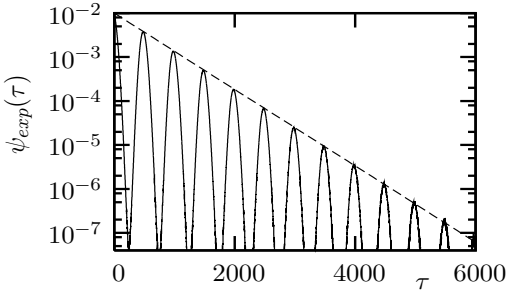

Figure 1: Histogram of perturbed Waiting Times. The dashed line is the exponential envelope of the maxima.

References

[1] A. Longtin, A. Bulsara, F. Moss, *Phys. Rev. Lett.* **67**, 656 (1991).

[2] T. Zhou, F. Moss, P. Jung, *Phys. Rev. A* **42**, 3161 (1990).

[3] O. C. Akin, P. Paradisi, P. Grigolini, *Physica A* **371** (2), 157-170 (2006).

[4] A.L. Hodgkin and A.F. Huxley, *J. Physiol. (London)* **117**, 500 (1952).

[5] F. Liu, Y. Yu and W. Wang, *Phys. Rev. E* **63**, 051912 (2001).

[6] H. Yang, F. Zhao, W. Zhang, Z. Li, *Physica A* **347**, 704 (2005).

[7] C. van Vreeswijk, *Neurocomputing* **38-40**, 417 (2001).

[8] R. Baddeley, L.F. Abbott, M. C.A. Booth, F. Sengpiel, T. Freeman, E.A. Wakeman, E.T. Rolls, *Proc. R. Soc. Lond B* **264**, 1775 (1997).

[9] D. R. Cox, *Renewal Theory* Chapman and Hall, New York (1967).

[10] P. Grigolini, L. Palatella, G. Raffaelli, *Fractals* **9**, 439 (2001).

Noise-induced rhythmicity in an ensemble of circadian oscillators

Ekkehard Ullner, Jordi García-Ojalvo
Departament de Física i Enginyeria Nuclear, Universitat Politècnica de Catalunya,
Colom 11, E–08222 Terrassa, Spain

Trinitat Cambras Riu, Antoni Díez Noguera
Department of Physiology, Faculty of Pharmacy, University of Barcelona,
Av. Joan XXIII s/n, E-08028 Barcelona ,Spain

Javier Buceta Fernández
Computer Simulation and Modeling (Co.S.Mo.) Lab & IQTC-UB
Parc Cientific de Barcelona, C. Josep Samitier 1-5, E-08028 Barcelona, Spain

The circadian rhythm is one of the most dominant and precise rhythm in living organisms, and pervades the whole organism from the level of the proteins to the activity of the whole body and its interaction with the environment. Normally, the circadian clock is controlled by a periodic and very reliable external light-dark cycle to which it is phase-locked. In mammals the circadian pacemaker is located in the suprachiasmatic nucleus of the hypothalamus and consists of two paired nuclei, each containing $\sim$ 10,000 neurons, each of which is controlled by a genetic clock circuit. The circadian genetic clock is not a passive element driven by the external day-light cycle, but rather an autonomous oscillator, which produces precise self-sustained oscillations even in constant darkness. The circadian clock undergoes a transition from the rhythmic regime to an arrhythmic behaviour without any clear rhythm in the global activity at high and constant light.

We model the circadian pacemaker on the genetic level. The genetic dynamics in each neuron were described by non-identical Goodwin oscillators and we assume a cell-to-cell communication by neurotransmitters [1]. The Goodwin oscillator describes the interplay amongst the clock mRNA, the clock protein, and the transcriptional inhibitor. All the genetic oscillators contribute to the so called overt rhythm that can be e.g. the motor activity or the body temperature. The genetic oscillators are not affected by the light directly and remain in the self-oscillatory regime in the arrhythmic state where there is no overt rhythm [2]. The dynamics of a single cell is influenced by intercellular coupling. According to ref. [3] we assume an effect of the light intensity on the coupling strength in such a way that increasing light reduces the coupling. The different eigen-frequencies of the non-identical Goodwin oscillators cause a de-synchronisation in the uncoupled or weakly case. The overt-rhythm undergoes a transition from self-oscillations to a steady state for increasing light whereas the individual non-identical genetic oscillators preserve their self-oscillations for all light conditions. The de-synchronisation amongst them for large light levels leads to reduced or vanishing self-oscillations of the overt rhythm.

We are interested in constructive effects of noise in the environmental light on the circadian overt rhythm. We found a noise induced overt rhythm generation for constant light intensities, which normally evoke an arrhythmic response in the noise-free case. The noise has a resonance-like influence on the overt rhythm, with a clear maximum at an optimal noise intensity. Due to the absence of any external pacemaker or periodic signal, because we are working under constant light conditions, the resonance found in the overt rhythm versus the noise intensity is a kind of Coherence Resonance (CR) [4]. The resonance can be observed only in the overt rhythm and not at the level of the individual oscillators, hence we found a joint effect of noise, coupling and the synchronisation amongst the oscillators. Noteworthy, the noise-induced rhythm generation only needs a very small synchronisation level.

Recent experiments gave the hint, that the overt rhythm not only shows a simple transition between rhythmicity and arrhythmicity, but behaves like a bistable system with a hysteresis in the transition zone. It is an open question whether the model of coupled Goodwin oscillators can be improved to include these additional dynamics. Maybe genetic noise or a certain distribution of the eigen-frequencies of the coupled oscillators can render the bistability in the phase distribution.

References

[1] D. Gonze, S. Bernard, C. Waltermann, A. Kramer and H. Herzel, "Spontaneous Synchronization of Coupled Circadian Oscillators", *Biophysical Journal* **89**, pp. 120-129 (2005).

[2] Hidenobu Ohta, Shin Yamazaki and Douglas G. McMahon, "Constant light desynchronizes mammalian clock neurons ", *Nature Neuroscience* **8**, pp. 267-269 (2005).

[3] A. Díez-Noguera, " A functional model of the circadian system based on the degree of intercommunication in a complex system", *Am J Physiol.* **267**, R1118 (1994).

[4] A. Pikovsky, J. Kurths, "Coherence Resonance in a Noise-Driven Excitable System", *Phys. Rev. Lett.* **78**, 775 (1997).

Towards DNA sequencing by force

J.M. Huguet*, N. Forns*†, S.B. Smith†, C. Bustamante†‡, F. Ritort*§

*Departament de Física Fonamental, Facultat de Física, Universitat de Barcelona, Diagonal 647, 08028 Barcelona, Spain; §CIBER-BBN deBioingeniería, Biomateriales y Nanomedicina, Instituto de Sanidad Carlos III, Madrid, Spain; †Department of Physics, ‡Department of Molecular and Cell Biology and Howard Hughes Medical Institute, University of California, Berkeley, California.

We present experimental measurements of the mechanical unzipping of double-stranded DNA using dual counter-propagating optical tweezers. A fragment of 2252 base pairs of λ-DNA ending in a loop is unzipped by pulling apart the handles attached to each strand of the DNA [1]. These two handles are short dsDNA oligos (27 bps) labeled at one end so that they can be attached to coated beads. One bead is fixed at the tip of a micropipette and the other one is held in an optical trap so that forces can be applied to the molecule (see figure 1a). The instrument measures forces in the range of piconewtons (0.01-80 pN) and extensions in the range of nanometers to microns with a resolution of 3 Å. Figure 1b shows a typical force vs. extension curve (FEC) obtained from one DNA pulling experiment. As the two strands of DNA are pulled apart, the reading of the force shows a pattern that looks like a sawtooth. The slopes of the sawtooth show the elastic response of the ssDNA released by unzipping (rezipping) and the steps of the sawtooth correspond to the opening (closing) of groups of base pairs. At low pulling rates (25 nm/s), the process of unzipping is nearly quasistatic and the curves of unzipping and rezipping almost overlap. We perform all the experiments at this pulling regime so that we can use thermodynamical models of DNA duplex formation.

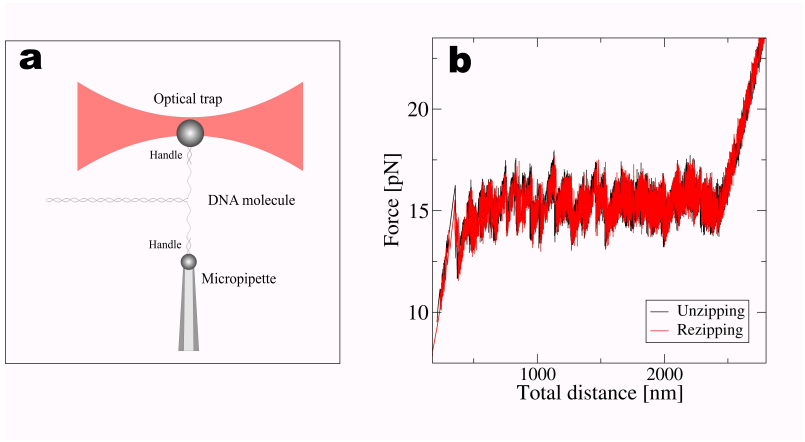

Figure 1: **a.** Experimental setup (not to scale). **b.** Force vs. extension curves. At low pulling rates (25 nm/s), unzipping and rezipping curves almost overlap due to the quasistatic pulling process.

Raw data obtained from the experiment is quite noisy due to thermal fluctuations of the bead in the trap, the dsDNA handles and the breathing of base pairs. Despite the noise, some thermodynamical properties of DNA can be inferred using polymer theory and statistical techniques. The mechanism of opening of base pairs can also be characterized by treating correctly the raw data. We have observed that the separation of the double helix is composed of a series of avalanches (see figure 2) that sequentially open different number of base pairs along the molecule. We are capable of identifying avalanches of size greater than 10 base pairs. We test the nearest-neighbor (NN) model of nucleic acids [1] and provide accurate values for the stacking energies of the bases that have been previously estimated by calorimetric techniques [2]. Two other sequences that have been analyzed confirm our results.

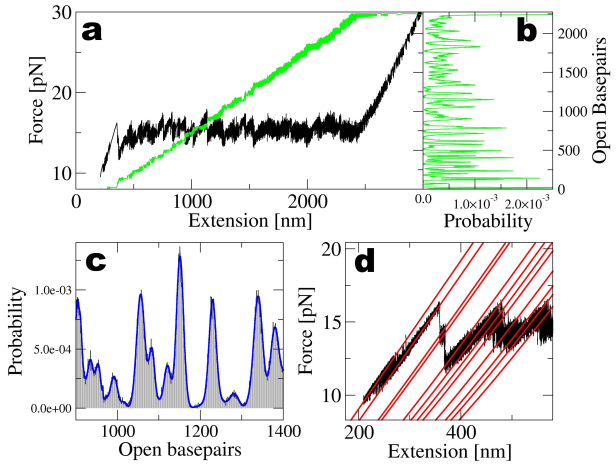

Figure 2: Avalanche analysis. **a.** From the experimental data we determine the most probable number of open base pairs of the molecule along the sequence. **b.** Histogram of open basepairs. **c.** Each peak of the histogram can be fit to a Gaussian profile. The distance between two peaks represents an opening avalanche. **d.** This method detects intermediate states with a different number of open base pairs

Because the pattern of the FEC is entirely characteristic of the DNA sequence that is pulled, unzipping by force provides a way to infer the sequence of the molecule from the force-extension data. Statistical inference of DNA sequences from unzipping data poses formidable and exciting experimental and theoretical challenges where information about the primary nucleotide sequence has to be extracted from highly noisy data due to thermal fluctuations. Experiments and the corresponding data analysis currently allow us to detect avalanche sizes down to 10 base pairs.

The improvement in both experiment and theory might help us to infer the DNA sequence from unzipping data.

References

[1] U. Bockelmann, *et. al.*, *Biophys. J.* **82** pp. 1537-1553 (2002)

[2] J. Santalucia Jr., *PNAS* **95** pp. 1460-1465 (1998)

[3] M. Manosas, F. Ritort. *Biophys. J* **88** pp. 3224-3242 (2005)

Predictability of Consciousness States Studied with Human Brain Magnetism

Noboru Tanizuka, Mostafizur R. Khan*
Graduate School of Science, Osaka Prefecture University,
1-1 Gakuen-cho, Naka-ku, Sakai, Osaka, 599-8531 Japan
Teruhisa Hochin
Graduate School of Science and Technology, Kyoto Institute of Technology
1 Hashigami-cho, Matsugazaki, Sakyou-ku, Kyoto, 606-8585 Japan

The predictability of the brain magnetism is discussed based on the analysis of the data at different consciousness states with nonlinear methods. External reading of the mental activity is concerned.

1 Measurement of brain magnetism

The brain magnetism for some human consciousness states was measured with a magnetoencephalogram (MEG, Neuromag-122TM 4-D Neuroimaging Ltd, Finland) at Kansai Center, Institute for Human Science and Biomedical Engineering, National Institute of Advanced Industrial Science and Technology (AIST), Ikeda, Osaka. The system covers 61 locations of the measurement over full human scalp, each location with 2 channels (planer-differential coils) for measureing the orthogonal magnetic fields which is caused by the synaptic electric currents in the cerebral cortex. The system detects a few femtotesla (10^{-15}T) of the magnetism as small as 10^{-10} times of the geomagnetism. The noise level of the system was 2 femtotesla. The measurements were done for some subjects in the magnetic shield room by the different consciousness states of eyes closed at rest, eyes opened at mental count and eyes opened at rest, every time for more than three minutes at the sampling rate of 2.5 milliseconds.

2 Analysis methods and results

There are frequency bands of rhythms, defined as $\delta\,(0.5 \sim 4\,\mathrm{Hz})$, $\theta\,(4 \sim 8\,\mathrm{Hz})$, $\alpha\,(8 \sim 13\,\mathrm{Hz})$, $\beta\,(13 \sim 35\,\mathrm{Hz})$ and $\gamma\,(35 \sim 100\,\mathrm{Hz})$, associated with each role activities in the brain global and local circuits. The frequency bands change according to the state, degree and kind of the consciousness. The alpha rhythm, though not fully understood even up to now[1], is the activity usually appears on the occipital lobe in the resting state with eyes closed for most of the subjects. It seems to be caused by a stochastic resonance of dynamical random oscillations in a group of the circuits. The other bands might act in a manner similar to the alpha rhythm in the different scales and roles of related circuits. In the first place, we analysed the alpha rhythm in the following methods. Take a time series data of an occipital channel: $y(1), y(2), y(3), \ldots, y(n)$. The nature of the system in which the series data is generated is analysed by reconstructing the time series in the form of vector $\boldsymbol{v}(t) = (y(t), y(t+\tau), \ldots, y(t+(m-1)\tau))$ in the $m-$th embedding dimension, with t the discrete time and τ the properly chosen time lag,[2] by computing the correlation probability $C_m(r)$, with $I(\cdot)$ the Heaviside's function, and by estimating the Kolmogorov-Sinai entropy K_2 in the following formula, with D_2 the correlation dimension; [2, 3, 4]

$$\ln C_m(r) = \ln\left\{\frac{1}{N(N-1)}\sum_{i,j;i\neq j}^{N} I\left(r - |\boldsymbol{v}(i) - \boldsymbol{v}(j)|\right)\right\} \approx D_2 \ln r - mK_2.$$

In Fig.1 is given a result of the correlation dimension analysis of the alpha rhythm for a young male in normal health, in which the result of Judd method assures justification of the result of the dimension where the small number of data (about 10^3) was used[2]. From Fig.1 the correlation dimension D_2 was estimated to be $3 < D_2 < 4$ for the clipped alpha rhythm of 2.5 sec [5]. In Fig.2 are given some results

*at present, Summit System Servece, Inc., Osaka

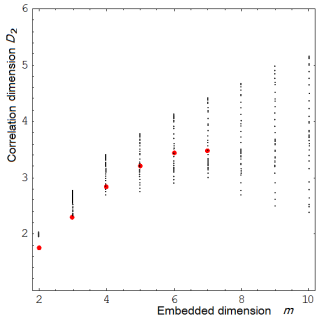

Figure 1: Correlation dimension calculated by G-P method (·) and by Judd method (|) for the alpha rhythm, 2.5sec.

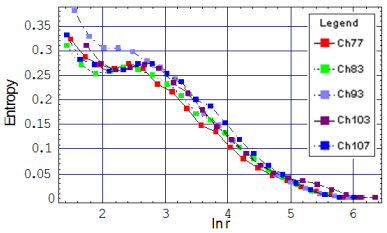

Figure 2: K-S entropy changing with $\ln r$ for the clipped alpha rhythms of 2.5 seconds measured simultaneously at several channels on the occipital lobe. sampling rate: 2.5ms. $\tau = 6$ (15ms), subject: y.i. 23 y.o. normal health male. Calculated by the recurrent plots method[4].

of the K-S entropy for the alpha rhythm. As the amplitude scale decreases from $\ln r = 3$ ($r \approx 20$fT) the entropy begins to increase at $\ln r = 2$ ($r \approx 7$fT) after passing the narrow plateau region of $\ln r$; the 7 fT should be the noise level for the system of alpha rhythm, while the 20 fT may be related to the system's dynamics if a bit problem in the calculation process is permitted. To have an image of the dynamics, the map function $f_s : \boldsymbol{x}(t) \to x_{t+1}$ where $\boldsymbol{x}(t) = \boldsymbol{v}(t) \in R^m$ and $x_{t+1} = y\,(t + (m-1)\tau + 1) \in R$ with $m = 4$, the optimum embedding dimension, was solved from the data by using the radial basis function network (RBF-net). A sample of the solved map is shown in Fig.3 [6]. A result was that the alpha rhythm of 2.5 sec was unpredictable, while the alpha rhysm of 250 ms was made sure predictable on an optimum RBF condition by more than the probability 0.8 at 100 ms in the inexperienced range. That the behavior is chaotic or not is yet uncertain because the map for 2.5 sec fluctuates. The magnetic vectors at 61 locations, each composed of the outputs of 2 channels, made patterns different according to the consciousness state by successive instants. The global behaviour of the vectors will be also discussed.
This work is partially supported by MEXT Grant-in-Aid for Scientific Research (C), 18500163.

References

[1] J. C. Shaw, *The Brain's Alpha Rhythms and the Mind* (Elsevier, Amsterdam, 2003)

[2] K. Aihara, *Fundamentals and Applications for Chaos Timeseries Analysis* (Sangyotosho, Tokyo, 2000)

[3] R.C. Hilborn, *Chaos and Nonlinear Dynamics* (Oxford Univ. Press, Oxford, 2000)

[4] Faure, P., Korn, H.,*Physica D*,**122** pp. 265-279 (1998)

[5] Nakaoka, T., Khan, M. R., Tanizuka, N., *IEICE Trans. Fundamentals* No.4,**J86-A** pp. 507-512 (2003)

[6] Fukushima, T., Tanizuka, N., *IEICE Trans. Fundamentals* No.5, **J88-A** pp. 682-686 (2005)

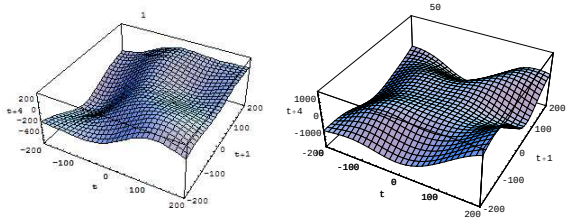

Figure 3: Map function $x_{t+1} = f_s\,(\boldsymbol{x}(t))$ solved from the clipped alpha rhythm of 2.5 sec: sampl. rate: 25ms, $\tau = 1$ (25ms), subject: y.i., two elements fixed at proper values, 2.5 sec lag between the maps. The map fluctuates as the time proceeds.

Variability and Suppression of Variability in the Photoresponse in the Mouse Rod

Daniele Andreucci
Dipartimento Modelli e Metodi Matematici
Via A.Scarpa 16
00161 Roma, Italy

In the retina of vertebrates, the rod outer segment (ROS) is an elongated cylinder containing a stack of membraneous flat cilinders, called discs. The discs host, among other chemical species, the photopigment Rhodopsin. The spaces between the discs, and between the stack and the lateral boundary of the cylinder, are occupied by cytosol, and available for diffusion of Calcium ions Ca^{2+} and cyclic guanosine monophosphate cGMP.

In the phototransduction cascade, a photon activates a molecule of Rhodopsin, denoted by R^*, initiating a process which eventually leads to the transmission of an electrical signal to the optical nerve. As long as R^* stays active, it maintains a mechanism of depletion of the concentration of cGMP in the cytosol, causing the closure of cGMP-gated ionic channels permeable to Ca^{2+} on the outer cell membrane. This causes a drop in the electrical transmembrane potential, and the signal to the nerve (see e.g., [3]).

It is remarkable that one photon can elicit an appretiable electric response from the ROS (known as Single Photon Response, or SPR). While the activation mechanism is highly random the final photocurrent is reproduced with high fidelity, as required by the visual system. The fact that the SPR is less random than one could expect is a major problem in understanding phototransduction.

In this presentation we address the problem of estimating quantitatively the relative significance of the different sources of variability, and, on the other hand, of the different processes which enhance reproducibility of the SPR.

We have identified some key components of variability, and some key mechanisms of variability suppression. We investigate their relevance and mutual influence numerically and analytically, by making use of several variations of the matematical model [1, 2], where we take into account one (or more) of the different mechanisms sketched below.

Sources of variability

- The main source of variability is the random lifetime of the activated molecule of rhodopsin (see [3]): a longer lifetime, in principle, draws a stronger response. In fact, the activated R^* is shut off by binding to a molecule of Arrestin, that is by an inherently stochastic process.
- Other possible sources are: the random position of the activated pigment molecule; the random motion of this molecule on the disc. These turn out to be in practice negligible in the case of the Mouse rod, owing to its geometry (the ROS is very thin).

Suppression of variability

However, the coefficient of variation (CV) of the SPR is considerably lower than the CV in an exponentially distributed random process (i.e., CV = 1). Depending on the way it is measured, the experimentally determined values are reported in the range 0.2–0.4.

- The activated photopigment molecule in fact undergoes a somewhat more complex process than a one-step abrupt shut off: it is progressively deactivated by repeated bindings with rhodopsin kinase, and finally quenched by Arrestin. Clearly, this multistep mechanism allows for a reduction of variability, as proposed in [5].
- A phenomenon of saturation taking place on the disc itself has also been proposed as the cause of reduced variability, see [4].

We examine also other factors of suppression of variability, taking place in the cytosol compartment of the cascade:

- The fact that Ca^{2+} and cGMP diffuse in the cytosol with finite diffusivity may cause a saturation effect preventing exceptionally long living R^* from depleting a too large amount of cGMP.
- The decrease in Ca^{2+} causes by a feedback effect an increase in cGMP. This translates into a typically second-order damping phenomenon, which also reduces variability.
- Finally, the nonlinearity of the phenomenon also influences variability. Nonlinear constitutive functions appear in the model in the standard form of Michaelis-Menten and Hill kinetics.

References

[1] Andreucci D., P. Bisegna, G. Caruso, H. Hamm and E. DiBenedetto, *Mathematical Model of The Spatio-Temporal Dynamics of Second Messengers in Visual Transduction*, Biophys. J., volume 85, pages 1358–1376, 2003.

[2] Bisegna P., G. Caruso, D. Andreucci, L. Shen, V.V. Gurevich, H. Hamm, E. DiBenedetto, *Diffusion of Second Messengers in the Cytoplasm Acts As a Variability Suppressor of the Single Photon Response in Vertebrate Phototransduction*, Biophys. J., in press.

[3] Pugh E. N. Jr., and T. D. Lamb, *Phototransduction in Vertebrate Rods and Cones: Molecular Mechanisms of Amplification, Recovery and Light Adaptation*, volume 3 of Handbook of Biological Physics, chapter 5, pages 183–255. Elsevier Science, St. Louis, U.S.A., 2000.

[4] Ramanathan S., P. B. Detwiler, A. M. Sengupta and B. I. Shraiman, *G-protein-coupled Enzyme Cascades Have Intrinsic Properties That Improve Signal Localization and Fidelity*, Biophys. J., volume 88, pages 3063–3071, 2005.

[5] Rieke, F. and D. A. Baylor, *Origin of Reproducibility in the Responses of Retinal Rods to Single Photons*, Biophys. J., volume 75, pages 1836–1857, 1998.

Crackling noise

Karin Dahmen – **Keynote Lecture**
Crackling Noise, Glassiness, and Disorder Induced Critical Scaling In and Out of Equilibrium: are they the same ? 27

Lasse Laurson
Temporal avalanche correlations in crackling noise 28

Stéphanie Deschanel
Experimental study of crackling noise: conditions on power-law scaling correlated to fracture precursors 29

Ferenc Kun
Crackling noise in fatigue fracture of heterogeneous materials 30

Alvaro Corral
Self-similar dynamical structure in catastrophic events and in written texts 31

Ferenc F. Csikor
Dislocation avalanches and the intermittency of crystal plasticity 32

Gianni Niccolini
Crackling noise and universality in fracture systems 33

Fergal Dalton
Stick-slip of a sheared granular medium 34

Crackling Noise, Glassiness, and Disorder Induced Critical Scaling In and Out of Equilibrium: are they the same ?

Karin Dahmen and Yang Liu
Department of Physics
1110 West Green St.
Urbana, IL 61801-3080
U.S.A.

We plan to discuss open questions on the relation between crackling noise and glassiness. Glasses are stuck in metastable states; crackling noise results from transitions between metastable states triggered by a slowly changing driving force. Are the metastable states in both cases the same, or are the typical thermal metastable states different from those sampled by transitions in a slowly forced system ? We show that for the random-field Ising model, the two types of states are governed by the same universal fixed point – at least near the transition where the correlation lengths diverge. Open questions motivated by these results and implications for a number of different physical systems are discussed.

Temporal avalanche correlations in crackling noise

Lasse Laurson and Mikko J. Alava
Laboratory of Physics, Helsinki University of Technology ,
FIN-02015 HUT, Finland

In systems exhibiting an intermittent, avalanche-like "crackling noise" response to slow external driving, a typical feature is the presence of complex temporal correlations in the bursty activity time series. These can be classified into two categories according to the time scales involved: Short time (or high frequency) correlations arising from the dynamics within individual avalanches, and correlations between different avalanches, visible in longer time (and lower frequency) scales. Thanks to recent advances [1], the former can now be understood by a relation between avalanche statistics and the scaling of the high frequency part of the power spectrum. In addition to the case of Barkhausen noise as originally proposed in Ref. [1], this relation appears to be valid in a number of slowly driven non-equilibrium systems ranging from sandpile models of self-organized criticality [2] to avalanches of plastic activity in a simple dislocation dynamics model [3] to fluctuations in fluid invasion into disordered media [4].

The latter case, correlations between different avalanches, is a less well understood phenomenon. In experiments, one typically observes that apparently distinct avalanches are correlated in time, as evidenced e.g. by correlation integral analysis of the avalanche initiation times, or by studies of the waiting times between consecutive avalanches. The origin of these correlations is usually not clear. We discuss some of the possible mechnanisms leading to such correlations.

References

[1] M. C. Kuntz and J. P. Sethna, Noise in disordered systems: The power spectrum and dynamic exponents in avalanche models, *Phys. Rev. B* **62**, 11699 (2000).

[2] L. Laurson, M. J. Alava and S. Zapperi, Power spectra of self-organized critical sandpiles, *J. Stat. Mech.: Theory Exp.* (2005) L11001.

[3] L. Laurson and M. J. Alava, $1/f$ noise and avalanche scaling in plastic deformation, *Phys. Rev. E* **74**, 066106 (2006).

[4] M. Rost, L. Laurson, M. Dube, and M. Alava, Fluctuations in Fluid Invasion into Disordered Media, *Phys. Rev. Lett.* **98**, 054502 (2007).

Experimental study of crackling noise: conditions on power-law scaling correlated to fracture precursors

S.Deschanel, N.Godin, G.Vigier
Laboratory MATEIS, CNRS UMR 5510, INSA de Lyon
Bâtiment Blaise Pascal, 20 Av Albert Einstein, 69621 Villeurbanne Cedex
stephanie.deschanel@insa-lyon.fr,

L.Vanel, S.Ciliberto
Physics Laboratory, CNRS UMR 672, Ecole Normale Supérieure de Lyon,
46 Allée d'Italie, 69364 Lyon cedex 07

Crackling noise has been defined as a series of discrete events that are widely distributed in size as a consequence of the material disorder. Common examples are earthquakes, Barkhausen noise, vortex motion in superconductors, sounds emitted during martensitic transformation or during paper crumpling. The rupture dynamics of heterogeneous materials usually involves many rupture events at a microscale that are precursors of the macroscopic failure. These precursors generate ultrasonic elastic wave trains called acoustic emissions (A.E) that are characterized by power law distributions and thus presents the general features of crackling noise. The scaling laws' exponents associated to fracture precursors are material-dependent, although the range of values is somewhat restricted, typically between 1.3 and 2 [1-5].

In order to shed some light on the parameters influencing the value of the power law exponent, we have probed in Polyurethane (PU) foams (simple vitreous polymer foams composed of a single constituent), the influence of test conditions, mechanical properties and morphology on the probability distributions of the released A.E energy and of the elapsed time between two acoustic events. Two loading modes, tensile and creep tests, were compared. The mechanical properties were altered from ductile to brittle behaviour by changing temperature over a wide range (from -65° C to 50°C). The morphology was changed through the elaboration of the materials by tuning the amount of voids in the foam, thus changing the material density and degree of heterogeneity.

We have found that the probability distributions of energy are power-law distributed with a stable exponent value, independently of the material density, the loading mode or the mechanical behaviour. Therefore, we ascertained experimental evidences that scale invariance in energy is a robust property of microfracturing processes. Nevertheless, the existence of a power-law for time intervals between events seems to require a quasi constant stress during damaging. Indeed, such a power-law was observed when A.E occurred either during the plastic stress plateau for tensile tests at a temperature greater than -10°C or for creep tests at any temperatures. Moreover, we highlighted that the time evolution of the normalized cumulative number of events and cumulative energy of the localized events varies with temperature in the case of tensile tests, but not in the case of creep tests.

The fact that the A.E energy released has an invariant power-law distribution is an important property that is still in need of a full theoretical explanation. Alternatively, our experiments give some indications that could help to understand the time evolution of the rupture precursors. In the case of creep tests where an imposed constant force is applied, the material can deform freely. In the case of tensile tests however, there is a competition between the relaxation times spectrum of the polymer and the characteristic time imposed by the applied constant strain rate. Since the relaxation times of the polymer become very large at temperatures well below the glass transition, such a competition might be at the origin of the difference in behaviour at low temperature between creep and tensile tests.

The most remarkable result of our study is that in creep tests, the distribution of time intervals between acoustic events and the time evolution of the rate at which events occur have universal features when properly rescaled by taking into account the time until macroscopic rupture, or lifetime, of the sample. This means that it is possible to relate the lifetime with the dynamical properties of the rupture precursors. However, it remains unclear if such a connection can be extended or not to the case of more complex loading conditions, as usually obtained in practical situations.

References

[1] A. Guarino, et al., *European Phys J B* **6**, pp. 13-24 (1998).

[2] D. Lockner, *Int J Rock Mech Min Sci Geomech Abstr* **30**, pp. 883-899 (1993).

[3] C. Maes, et al., *Phys Rev B* **57**, pp. 4987-4990 (1998).

[4] P. Diodati, et al., *Phys Rev Lett* **67**, pp. 2239-2243 (1991).

[5] S. Deschanel, et al., *International Journal of Fracture* **140**, pp. 87–98 (2006).

Crackling noise in fatigue fracture of heterogeneous materials

F. Kun[1], Z. Halász[1], J. S. Andrade Jr.[2,3], and H. J. Herrmann[2]
[1]Department of Theoretical Physics, University of Debrecen
P. O. Box:5, H-4010 Debrecen, Hungary,
[2]Computational Physics, IfB, HIF, E12, ETH
Hönggerberg, 8093 Zürich, Switzerland
[3]Departamento de Física, Universidade Federal do Ceará
60451-970 Fortaleza, Ceará, Brazil

1 Motivations

It has long been recognized by industry that structural components exposed to periodic loading can fail after a certain number of cycles even if the load amplitude is much below the safety limit. In the everyday life the mysterious sudden breakdown of car or kitchen equipment is a similar experience. The material seems to get tired due to the long time usage and therefore the phenomenon is called "fatigue". This sub-critical failure typically occurs unexpectedly and has been responsible for a large number of airplane and railway crashes with considerable human loss. The most striking quantitative feature of fatigue fracture is expressed by the classical empirical Basquin law, which states that the lifetime decreases as a power law of the load amplitude. On the microlevel, the fatigue fracture of heterogeneous materials is accompanied by crackling noise due to the nucleating and growing cracks, which can be monitored experimentally by the acoustic emission technique and by direct optical observations.

2 Results

In order to understand the origin of Basquin's law and its relation to the underlying jerky fracture process, we worked out a theoretical approach for the fatigue fracture of disordered materials which provides a direct connection between the microscopic fracture mechanisms and the macroscopic time evolution of fatigue. Our approach is based on the classical fiber bundle model which is extended to capture the relevant mechanisms of fatigue [1, 2]. In the model, material elements fail either due to immediate breaking or undergo a damage accumulating ageing process. The accumulated damage $c(t)$ up to time t is obtained by integrating over the entire loading history of the specimen $c(t) = a\int_0^t e^{-\frac{(t-t')}{\tau}} p(t')^\gamma dt'$, where $a > 0$ is a scale parameter, while the exponent $\gamma > 0$ controls the rate of damage accumulation. Since load redistribution and immediate breaking occur on a much shorter time scale than damage accumulation, the entire fatigue process can be viewed on the microlevel as a jerky sequence of bursts of immediate breakings triggered by a series of damage events happening during waiting times T, *i.e.*, the time intervals between the bursts. The microscopic failure process is characterized by the size distribution of bursts $P(\Delta)$, damage sequences $P(\Delta_d)$, and by the distribution of waiting times $P(T)$.

We show by analytic calculations and computer simulations that the size distribution of damage sequences $P(\Delta_d)$ and of the waiting times $P(T)$ have a universal power law behavior

$$P(\Delta_d) \sim \Delta_d^{-1} \exp\left(-\Delta_d / \langle \Delta_d \rangle\right), \qquad P(T) \sim T^{-1} \exp\left(-T / \langle T \rangle\right), \tag{1}$$

where dependence on the external load amplitude σ_0 only occurs in the average values $\langle \Delta_d \rangle \sim \sigma_0^{-1}$, and $\langle T \rangle \sim \sigma_0^{-(1+\gamma)}$. The size distribution of bursts $P(\Delta)$ have a similar behavior to the one observed in quasi-static fracture, *i.e.* a power law distribution of burst sizes emerges whose exponent shows a crossover to a lower value when the external load approaches the fracture strength of the material [2].

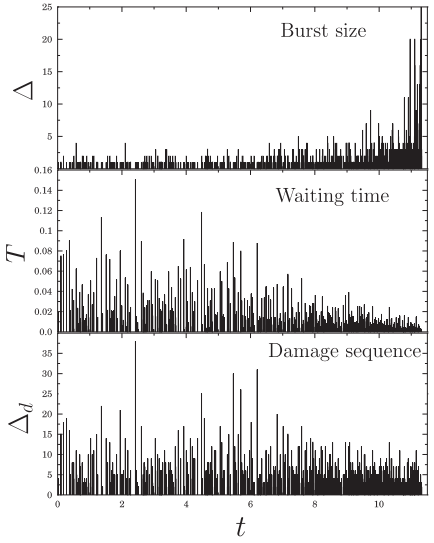

Figure 1: On the micro-scale, fatigue fracture of disordered materials proceeds in bursts triggered by damage sequences. Due to the quenched disorder, the size of bursts Δ and of damage sequences Δ_d, furthermore, the waiting times T between bursts have strong fluctuations. The figure shows the jerky breaking sequence of a specimen at the load amplitude $\sigma_0/\sigma_c = 0.5$, where σ_c denotes the fracture strength.

Astonishingly, the macroscopic Basquin law appears to be the fingerprint of this scale-free microscopic bursting activity, where material dependence enters only through the specific damage accumulation mechanism. When micro-cracks can heal leading to damage recovery, we found that a threshold load (fatigue limit) emerges below which only partial failure occurs and the material has an infinite lifetime [2]. Based on the model calculations, we propose a generic scaling form for the macroscopic deformation obtained at different load amplitudes, and show that at the fatigue limit the system undergoes a continuous phase transition when changing the external load. Our work opens up new experimental challenges [2].

References

[1] F. Kun, M. H. Costa, R. N. Costa Filho, J. S. Andrade Jr, J. B. Soares, S. Zapperi, and H. J. Herrmann, *J. Stat. Mech.* P02003 (2007).

[2] F. Kun, H. A. Carmona, J. S. Andrade Jr, H. J. Herrmann, arXiv:0801.3664, appearing in Phys. Rev. Lett.

Self-similar dynamical structure in catastrophic events and written texts

Alvaro Corral
Centre de Recerca Matemàtica, Edifici Cc, Campus UAB Bellaterra,
E-08193 Cerdanyola (Barcelona), Spain

Crackling noise is usually defined through the statistics of the size of the response events that a nonlinear system develops when it is slowly driven – the so famous power-law distribution of avalanche sizes [1, 2]. Less attention has been paid to the dynamical structure that all these events define in time; however, recent research has unveiled a complex, self-similar hierarchy of waiting times, far from the trivial Poisson behavior expected previously for some of these systems. The distributions of waiting times between these events verify a scaling law for different event sizes, which can be viewed as equivalent to the invariance of the system under a renormalization-group transformation, analogous to the Ising model in its critical point [3]. Further, this is linked in a fundamental way with the existence of correlations in the process, probably long-range correlations.

We briefly review results obtained from observational or experimental data on diverse systems, including earthquakes [4], fractures [5, 6], extreme-climatic-event records [7], solar flares [8], forest fires [9], and financial indices [10]. In the case of the fracture-earthquake system the same scaling law is surprisingly valid from nanofractures to very large earthquakes, covering more than 30 orders of magnitude in the range of energies (sizes) for its validity. Further, the dynamics of this system is strikingly similar to the spatial structure of written texts, which has been tested in English, French, Spanish, and Finnish.

References

[1] P. Bak. *How Nature Works: The Science of Self-Organized Criticality.* Copernicus, New York, 1996.

[2] J. P. Sethna, K. A. Dahmen, and C. R. Myers. Crackling noise. *Nature*, 418:242–250, 2001.

[3] A. Corral. Renormalization-Group Transformations and Correlations of Seismicity. *Phys. Rev. Lett.*, 95:028501, 2005.

[4] A. Corral. Long-term clustering, scaling, and universality in the temporal occurrence of earthquakes. *Phys. Rev. Lett.*, 92:108501, 2004.

[5] J. Davidsen, S. Stanchits, and G. Dresen. Scaling and universality in rock fracture. *Phys. Rev. Lett.*, 98:125502, 2007.

[6] J. Åström, P. C. F. Di Stefano, F. Pröbst, L. Stodolsky, J. Timonen, C. Bucci, S. Cooper, C. Cozzini, F.v. Feilitzsch, H. Kraus, J. Marchese, O. Meier, U. Nagel, Y. Ramachers, W. Seidel, M. Sisti, S. Uchaikin, and L. Zerle. Fracture processes observed with a cryogenic detector. *Phys. Lett. A*, 356:262–266, 2006.

[7] A. Bunde, J. F. Eichner, J. W. Kantelhardt, and S. Havlin. Long-term memory: a natural mechanism for the clustering of extreme events and anomalous residual times in climate records. *Phys. Rev. Lett.*, 94:048701, 2005.

[8] M. Baiesi, M. Paczuski, and A. L. Stella. Intensity thresholds and the statistics of the temporal occurrence of solar flares. *Phys. Rev. Lett.*, 96:051103, 2006.

[9] A. Corral, L. Telesca, and R. Lasaponara. Scaling and correlations in the dynamics of forest-fire occurrence. *Phys. Rev. E*, 77:016101, 2008.

[10] K. Yamasaki, L. Muchnik, S. Havlin, A. Bunde, and H. E. Stanley. Scaling and memory in volatility return intervals in financial markets. *Proc. Natl. Acad. Sci. USA*, 102:9424–9428, 2005.

Dislocation avalanches and the intermittency of crystal plasticity

Ferenc F. Csikor*, Christian Motz†, Daniel Weygand‡, Michael Zaiser§, Stefano Zapperi¶
*Department of Materials Physics, Eötvös University Budapest
Pázmány Péter sétány 1/a, H-1117 Budapest, Hungary
†Erich Schmid Institute of Materials Science, Austrian Academy of Sciences
A-8700 Leoben, Austria
‡Institut für die Zuverlässigkeit von Bauteilen und Systemen,
Universität Karlsruhe (TH), Kaiserstrasse 12, 76131 Karlsruhe, Germany
§Centre for Materials Science and Engineering, The University of Edinburgh
The King's Buildings, Sanderson Building, Edinburgh EH8 3JL, UK
¶CNR-INFM, S3, Dipartimento di Fisica, Università di Modena e Reggio Emilia
via Campi 213/A, I-41100, Modena, Italy

While plastic deformation of crystalline solids is traditionally viewed as a smooth and homogeneous process, recent experimental and theoretical studies have demonstrated the presence of large intrinsic spatio-temporal fluctuations with scale invariant characteristics. In time, plastic deformation proceeds through intermittent bursts, associated with collective dislocation avalanches, with power law size distributions. In space, deformation patterns and deformation induced surface morphology are characterized by long range correlations and self similarity. This scale invariant behavior is usually discussed in terms of a robust scaling associated with a non-equilibrium critical point, the *yielding transition* [1].

In the presentation the authors will briefly review the existing experimental and theoretical knowledge on scale free strain burst statistics and self similar surface patterns. Special focus will be given to recent three-dimensional simulations [2] and experiments [3, 4] on the quasi-static deformation of single crystals which helped to i) clarify the nontrivial dependence of strain burst size distributions on crystal size due to the lamellar character of dislocation avalanches and ii) provided strong evidence about the universal intermittency of plastic deformation and the universality of strain burst size statistics.

Despite the above great leaps forward, several fundamental questions on intermittent crystal plasticity are still unsolved. For instance, the relation between the strain bursts in microcrystal deformation [3] and the crackling noise in acoustic emission experiments [4] still needs clarification. The relations between strain bursts and the size effects in the yield strength of metallic microcrystals [5] is also still unclear, just like the complex interactions between dislocation avalanches and other crystal defects, most notably grain boundaries [6].

References

[1] M. Zaiser, *Adv. Phys.* **55** pp. 185-245 (2006)

[2] F. F. Csikor, C. Motz, D. Weygand, M. Zaiser, S. Zapperi, *Science* **318** pp. 251–254 (2007)

[3] D. M. Dimiduk, C. Woodward, R. LeSar, M. D. Uchic, *Science* **312** pp. 1188–1190 (2006)

[4] J. Weiss, T. Richeton, F. Louchet, F. Chmelik, P. Dobron, D. Entemeyer, M. Lebyodkin, T. Lebedkina, C. Fressengeas, R. J. McDonald, *Phys. Rev. B* **76** 224110 (2007)

[5] M. D. Uchic, D. M. Dimiduk, J. N. Florando, W. D. Nix, *Science* **305** pp. 986-989 (2004)

[6] T. Richeton, J. Weiss, F. Louchet, *Nature Materials* **4** pp. 465-469 (2005)

Crackling noise and universality in fracture systems

G. Niccolini, G. Durin
Istituto Nazionale di Ricerca Metrologica,
Strada delle Cacce 91, 10135 Torino, Italy

ABSTRACT

Crackling noise arises when a system responds to changing external conditions through discrete, impulsive events whose sizes are distribute according to a power law. Besides phenomena in condensed-matter physics (as the motion of domain walls in soft magnetic materials), also fracture phenomena exhibit crackling noise: let us think of the well-known Gutenberg-Richter (GR) relation, which is a power law formed by plotting the number of rupture events as of a function of their size, spanning from the microscale (acoustic emissions) [1] to the geological scale (earthquakes) [2, 3]. The fact that fracture systems can share the same behaviour over many decades of size is called universality [4, 5].

Along the lines of recent works of Bak et al. [6] and Corral [7], we focus on the scale invariance in the timing of earthquakes, examining the statistical distribution of the interoccurrence times τ between the earthquakes occurred in Italy during the period 1984-2002, which obeys a scaling law:

$$D(\tau; M) = R(M) f(R(M)\tau) \qquad (1)$$

where D is the probability density of τ, M is the minimum magnitude considered, $R(M) \propto 10^{-bM}$ given by the GR relation is the mean seismic rate, and f is a scaling function.

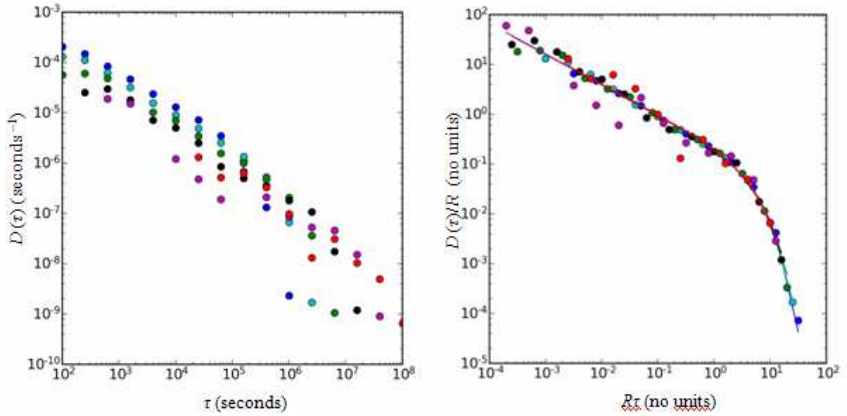

Fig. 1. Left: Probability densities of recurrence times of Italian earthquakes with magnitude $\geq M$ during the period 1984-2002, for M ranging from 2.5 to 5. Right: The same distributions rescaled by its mean seismic rate. The data collapse is the signature of the scaling law. The fitting function is the scaling function f in Eq. (1). $D(\tau)$ is $D(\tau; M)$ and R is $R(M)$.

As shown in Fig. 1, we obtain a good data collapse and the scaling function turns out to be a decreasing power law over four decades of times in agreement with the results obtained by Corral. However, the exponents describing the power-law decay in the two studies are different. In fact, the scaling function derived from our analysis:

$$f(R\tau) \propto (R\tau)^{-0.6} e^{-(R\tau)/5}, \qquad (2)$$

gives –0.6 for the exponent, while Corral obtains –0.3. This is a surprising result, since the scaling function proposed by Corral is valid for different regions and at different scales.

Therefore, we follow the same rescaling procedure for the probability densities of the time intervals between the acoustic emissions emerging from specimens of different materials experiencing damage in laboratory loading tests. We try to explore if and under which conditions earthquakes and acoustic emissions belong to the same universality class.

References

[1] Carpinteri, A., Lacidogna, G. and Niccolini, G., *Key Engineering Materials* **312** pp. 305-310 (2006).

[2] Gregori, G.P., Paparo, G., Poscolieri, M. and Zanini, A., *Natural Hazards and Earth System Sciences* **5** pp. 777-782 (2005).

[3] Turcotte, D.L., Newman, W.I. and Shcherbakov, R., *Geophys. J. Int.* **152** pp. 718-728 (2003).

[4] Sethna, J.P., Dahmen, K. and Myers, C.R., *Nature* **410** pp. 242-250 (2001).

[5] Stanley, H.E., *Reviews of Modern Physics* **71** S358-S366 (1999).

[6] Corral, A., *Proceedings of FraMCoS-6 Post-Conference Workshop Acoustic Emission and Critical Phenomena: from Structural Mechanics to Geophysics* (Catania, Italy, 2007).

[7] Bak, P., Christensen, K., Danon, L. and Scanlon, T., *Phys. Rev. Lett.* **88** 178501 (2002).

Stick-slip of a sheared granular medium

Alberto Petri[(1)], Adrea Baldassarri[(2)], Fergal Dalton[(1)]
Giorgio Pontuale[(1)], Stefano Zapperi[(3)]
(1) Istituto dei Sistemi Complessi, Consiglio Nazionale delle Ricerche,
Via del Fosso del Cavaliere 100, 00133 Roma, Italy

(2) Dipartimento di Fisica, Universita ''La Sapienza'',
Piazzale le Aldo Moro 2, 00185 Roma, Italy
(3)
(3)CNR-INFM, S3, Dipartimento di Fisica,
Universita' di Modena e Reggio Emilia,
via Campi 213/A, I-41100, Modena, Italy

The flow of one material over another can exhibit intermittent *stick-slip* motion, with examples that range from jumps of atomic sized dislocations to planet sized tectonic plate movement. Though the motion can often be periodic and thus predictable, there exist many cases in which the motion becomes irregular. Phenomenological models have been proposed that can mimic it to a greater or smaller extent. However the microscopic mechanisms determining the motion are far from understood, as in other related phenomena, e.g. friction.

In order to study this chaotic-type dynamic, we have designed and realised an apparatus in which an overhead disc is forced to shear across the surface of a granular material; the elastic nature of the forcing, together with friction between the plate and the GM, guarantees stick-slip motion, which is higly non-periodic in the investigated parameter region.

Attempts to describe this regime of motion are usually made by means of deterministic models in which a large number of degrees of freedom with non-linear interactions give rise to chaotic motion. These models are successful in reproducing some statistical features of the stick-slip motion at a qualitative level (e.g. power laws of the Gutemberg-Richter type). However, to obtain quantitative information from them is generally diffult, because a direct correspondence of their parameters with experimental situations is lacking.

In order to overcome such difficulties we have tried an alternative way, i.e. to describe the chaotic motion of the system by means of a single degree of freedom, the position of the disc, θ, in the presence of two forces: a viscous force fv (depending only on the disk velocity) and a a stochastic force fs (depending only on the position):

$$I\ \ddot{\theta} = -k\theta + f_v(\dot{\theta}) + f_s(\theta) \qquad (1)$$

where I is the disk inertia.
It turns out from the experimental measurements that fs can be well approximated by a bounded Brownian motion:

$$df_s/dt = D\eta - a f_s, \qquad (2)$$

where η is white noise and the parameters D and a (representing the noise variance and inverse correlation length) are measured directly in the experiment. The viscous force has a concave shape, which is well described by a function such as

$$f_v(\dot{\theta}) = \theta_0 + \gamma(\dot{\theta} - 2\omega_0 \ln(1 + \dot{\theta}/\omega_0)) \qquad (3)$$

Also for this equation parameters $\theta_0, \gamma, \omega_0$ are derived from the experimental measures.

The model has been shown to reproduce the experiment in a quantitative manner, and suggests that other stick-slip phenomena, unrelated to the present one apart from having a "crackling noise" signature, could be similarly modelled. In fact, a similar model is known to accurately reproduce Barkhausen noise in ferromagnets, despite the very different physical origins.

The Brownian nature of the positional force can be understood in terms of the force chains acting against the motion of the disc (during the motion, force chains are continuously disrupted and formed, and of course their configuration at a given stage of the motion must depend in some way by the configuration at the previous position). However a first principle derivation (starting from the properties of the granular medium) of the stochastic force and of its parameter is far from being obtained. In addition, the total force resulting from the combination of the three forces a acting on the disk (elastic, viscous and stochastic) presents an asymmetric distribution whose origins are not yet clear. Similar distributions have been observed in different fields where correlated events are involved, to such andextent that some authors claim it to have some universal properties [3].

References

[1] F. Dalton, F. Farrelly, A. Petri, L. Pietronero, L. Pitolli and G. Pontuale,
Phys. Rev. Lett. **95**, 138001 (2005);

[2] A. Baldassarri, F. Dalton, A. Petri, S. Zapperi, G.Pontuale and L. Pietronero,
Phys. Rev. Lett. **96**, 118002 (2006);

[3] S. T. Bramwell, T. Fennell, P. C. W. Holdsworth and B. Portelli,
Europhys. Lett. **57** 310 (2002).

Noise in complex and non-linear systems

Bernard Castaing – **Keynote Lecture**
Noise statistics and physical mechanisms 36

Debjani Bagchi
Fluctuations and slow dynamics in an ageing polymer glass 37

Ho Bun Chan
Activation barrier scaling and switching path distribution in micromechanical parametric oscillators 38

Francisco J. Cao
Open problems on information and feedback control of stochastic systems 39

Lukasz Machura
Order and Disorder in Coupled Mesoscopic Rings 40

Andrea Duggento
An inferential framework for nonstationary dynamics: Theory, applications, and open questions 41

Alexander Alexandrovich Dubkov
The problem of constructing phenomenological equations for subsystem interacting with non-Gaussian thermal bath 42

Freddy Bouchet
Out of equilibrium phase transitions in the two dimensional Navier Stokes equation with stochastic forces 43

Laszlo B. Kish
Negative weight transients of information storage media after recording 44

Noise statistics and physical mechanisms

Bernard Castaing
Ecole Normale Supérieure de Lyon, Laboratoire de Physique,
C.N.R.S. UMR5672,
46, Allée d'Italie, 69364 Lyon Cedex 07, France

When the main information about a system appears as a noise, the goal of the physicist is to go further than the simple description of this noise. He wants to relate its various characteristcs between them and each of them to the physical mechanisms driving the system. In this talk, I will show that, even when the underlying dynamics is well known, as for velocity signals in turbulence, some caution is necessary. The matter becomes rather tricky when the physical mechanisms themselves are unknown.

Fluctuations and slow dynamics in an ageing polymer glass

D. Bagchi, S. Ciliberto, A. Naert, L. Bellon
Ecole Normale Supérieure de Lyon, Laboratoire de Physique,
C.N.R.S. UMR5672,
46, Allée d'Italie, 69364 Lyon Cedex 07, France.

April 3, 2008

We present experimental explorations of the fluctuations and slow dynamics in an out of equilibrium polymer glass. The electrical impedance and the voltage fluctuations in a complex impedance consisting of a parallel-plate capacitor, with the polymer as the dielectric, are measured precisely as a function of the frequency, the waiting time after a quench below the glass transition temperature T_g of the polymer, and the speed and depth of the quench. Some aspects of the ageing dynamics are discussed. The experimental data is interpreted with respect to the fluctuation dissipation theorem (FDT). In order to extend the concepts of thermodynamics to such non-equilibrium systems, the description of a time-scale dependent 'effective temperature' for this system using the fluctuation-dissipation ratio (FDR) is analysed [1, 2]. By tuning the quench rate, we examine the range of validity of the FDT and estimate the regime in which linear response theory is valid. When the system is driven out of equilibrium, the probability distribution function (PDF) of the fluctuations is found to be non-Gaussian. A statistical analysis of the PDFs as a function of the waiting time is used to study the relaxation dynamics of fluctuations immediately following a quench.

References

[1] Buisson, L., Bellon, L., Ciliberto, S., *J. Phys. Condens. Matter* **15** pp. S1163-S1179 (2003)

[2] Cugliandolo, L. F., Kurchan, J., Peliti, L., *Phys. Rev. E* **55** pp. 3898-3914 (1997)

Activation barrier scaling and switching path distribution in micromechanical parametric oscillators

Ho Bun Chan, Corey Stambaugh, Konstantinos Ninios
Department of Physics, University of Florida,
Gainesville, FL 32611 USA

One of the unsolved questions of modern physics is whether fluctuations far from thermal equilibrium display generic features, and if so what these features are. In contrast to equilibrium systems where fluctuation probabilities can be calculated from their free energy, no general principles have been established for nonequilibrium systems. It is therefore especially important to find system-independent properties of fluctuation phenomena far from equilibrium. Recently, there has been much interest for nonlinear systems that develop multistability under sufficiently strong periodic driving, including electrons in Penning traps, Josephson junctions, micro and nanomechanical oscillators and atoms in magneto-optical traps. The presence of fluctuations enables the systems to occasionally overcome the activation barrier and switch between the coexisting states [1, 2]. Such nonequilibrium systems generally lack detailed balance, and the switching rates may not be found by a simple extension of the Kramers approach. It remains a challenge to identify generic properties of driven, nonequilibrium systems, particularly for behaviors that have no analog in their equilibrium counterparts.

Here we address some of these unsolved questions in systems far from equilibrium by investigating fluctuation induced switching in an underdamped micromechanical torsional oscillator [3] driven into parametric resonance [4]. We measure the activation barrier for switching out of an attractor as a function of frequency detuning. Near both bifurcation points, the activation barriers are found to depend on frequency detuning with critical exponents [4] that are consistent with the predicted universal scaling in parametrically driven systems [5]. We also introduce a formulation that allows us to directly measure the distribution of trajectories followed in switching. Our first results [6] indicate that even though the motion of the system in switching is random, the trajectories form narrow tubes in phase space centered at the most probable switching path (MPSP). The uphill section of this path is found to be distinct from its time-reversed downhill section, an important property for systems far from thermal equilibrium.

In our experiment, the micromechanical oscillator consists of a movable silicon plate supported by two torsional springs (Fig. 1c). Two electrodes are located underneath the top plate. In addition to the restoring torque of the torsional springs, the top plate is also subjected to an electrostatic torque when a voltage is applied to one of the underlying electrodes (Fig. 1d). The voltage is modulated at a frequency $\omega/2\pi$ close to twice the natural oscillation frequency of the plate. Torsional oscillations are detected capacitively through the other electrode. When the modulation is sufficiently strong, the plate oscillates at half the modulation frequency as a result of parametric resonance. Since the modulation is invariant upon a shift in time by its period, there exist two stable oscillation states that have the same amplitude but differ in phase by π. The dynamics is well described by the rotating wave approximation [5]. It is characterized by two dynamical variables, the quadratures X and Y of oscillations at $\omega/2$, at $\pi/2$ phase difference with each other. A lockin amplifier is used to record X and Y at regular intervals much shorter than the relaxation time. In Fig. 1a, we show the two stable oscillation states, A_1 and A_2, that are located symmetrically about the origin in the (X,Y)-plane .

When white noise is added to the excitation voltage, the system can occasionally overcome the activation barrier and switch from one stable state to the other. Transitions are identified when the oscillator begins in the vicinity of A_1 (within the left green circle in Fig. 1a) and subsequently arrives at state A_2 (within the right green circle). Figure 1a shows the switching probability distribution derived from more than 6500 transitions. While in each transition the system follows a different trajectory, the trajectories clearly lie within a narrow tube. In Fig. 1b, the location of the peak of the distribution is plotted on top of the MPSP obtained from theory. The MPSP emerges clockwise from A_1 and spirals toward the saddle point at the origin. Upon exit from the saddle point, it makes an angle and continues to spiral clockwise

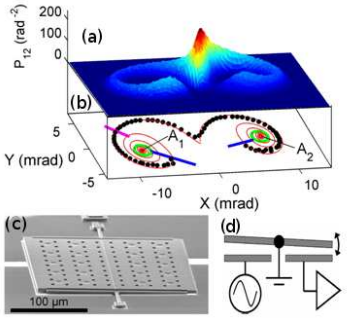

Figure 1: (left). (a) Switching probability distribution for switching out of state A_1 into state A_2 in a parametrically driven microelectromechanical oscillator. (b) The peak locations of the distribution are plotted as black circles and the theoretical MPSP is indicated by the red line. The portion of the distribution outside the blue lines is omitted. (c) Scanning electron micrograph of the micromechanical torsional oscillator. (d) Cross-sectional schematic.

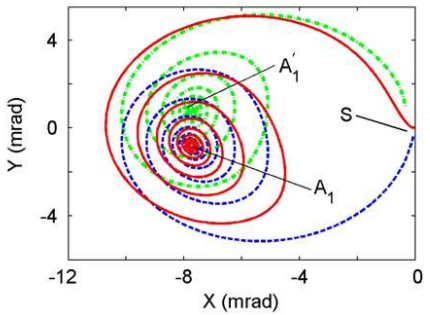

Figure 2: (right). Comparison of the MPSP (thick solid, red), the time-reversed path (dash-dotted, green) and the deterministic downhill path (dashed, blue).

toward A_2. There is excellent agreement between the measured peak in the probability distribution and the MPSP obtained from theory, with no adjustable parameters.

One important feature of the observed distribution is characteristic of systems far from thermal equilibrium [7]. For equilibrium systems, the most probable "uphill" path from an attractor to the saddle point, which results from a fluctuation, is the time reversal of the fluctuation-free "downhill" path from the saddle point back to the attractor. If the system is overdamped, these two paths coincide in space (but are opposite in direction). However, our parametric oscillator lacks detailed balance. Upon reversal of time, even the attractors are shifted away from the original locations. Our experiment provides the first demonstration of the lack of time reversal symmetry in switching of systems far from thermal equilibrium.

Apart from demonstrating the switching path distribution and the scaling of activation barriers, periodically driven micromechanical oscillators provide a well-controlled platform for future investigation on unsolved problems in systems that lack detailed balance, such as the applicability of fluctuation theorems [8] and the existence of a threshold for the onset of singularities in the optimal paths from the attractor to another state in the same attraction basin.

References

[1] Dykman, M. I. and Krivoglaz, M. A., *Sov. Phys. JETP* **50** pp. 30-37 (1979).

[2] Lehmann, J., Reimann, P. and P. Hanggi, P., *Phys. Rev. Lett.* **84** pp. 1639-1642 (2000).

[3] Stambaugh, C. and Chan, H. B., *Phys. Rev. Lett.* **97** 110602 (2006).

[4] Chan, H. B. and Stambaugh, C., *Phys. Rev. Lett.* **99** 060601 (2007).

[5] Dykman, M. I., Maloney, C. M, Smelyanskiy, V. N. and Silverstein, M., *Phys. Rev.* **E 57** pp. 5202-5232 (1998).

[6] Chan, H. B., Dykman, M. I. and Stambaugh, C., arXiv:0802.3533v1, accepted to *Phys. Rev. Lett.*

[7] Luchinsky, D. G. and McClintock, P. V. E., *Nature* **389** pp. 463-466 (1997).

[8] Douarche, F., Joubaud, S., Garnier, N. B., Petrosyan, A. and Ciliberto, S., *Phys. Rev. Lett.* **97** 140603 (2006).

Open problems on information and feedback control of stochastic systems

F. J. Cao and M. Feito
Departamento de Física Atómica, Molecular y Nuclear,
Universidad Complutense de Madrid,
Avenida Complutense s/n, 28040 Madrid, Spain.

Feedback or closed-loop control is present when there is a controller or external agent that gathers information on the state of the system and uses this information to decide the action it will perform on the system. Feedback control allows to increase the performance, and it is present in many systems with interest for physicists, engineers and biologists [1].

It is intuitively clear that the use of more information by the controller can be potentially useful to increase the performance of the system (e.g. the power output or the efficiency). However, a general formal development that justifies this statement using information theory [2] is still lacking. The development of the links between information theory and feedback control will allow to make quantitative the relation between information and performance, and to establish constraints in the increase of performance that can be reached with a given amount of information.

There have been studies of the connections between information and feedback controlled systems in the context of the study of the Maxwell's demon [3]. Recently it has been derived a relation between the decrease of entropy achievable and the information about the system that the controller has [4, 5]; also relations between the information gathered by the controller and the flux or the power output in a particular stochastic system has been recently derived [6, 7]. We will review these new results and present other recent new developments in order to introduce open questions in the connection between information theory and feedback control in the context of stochastic systems.

References

[1] J. Bechhoefer, *Rev. Mod. Phys.* **77**, 783 (2005).

[2] T. M. Cover and J. A. Thomas, *Elements of Information Theory* (John Wiley, New York, 1991).

[3] H. S. Leff and A. F. Rex, *Maxwell's Demon: Entropy, Classical and Quantum Information, Computing* (Institute of Physics, Bristol, 2003).

[4] H. Touchette and S. Lloyd, *Phys. Rev. Lett.* **84**, 1156 (2000).

[5] H. Touchette and S. Lloyd, *Physica A* **331**, 140 (2004).

[6] M. Feito and F. J. Cao, *Eur. Phys. J. B* **59**, 63 (2007).

[7] F. J. Cao, M. Feito, and H. Touchette, *arXiv:cond-mat/0703492* (2007).

Order and Disorder in Coupled Mesoscopic Rings

Lukasz Machura
Institute of Physics,
University of Silesia,
Uniwersytecka 4,
40-007 Katowice, Poland

Nowadays progress in nanotechnology lets the scientists build extremely small structures, that can exhibit new and extraordinary features. Real challenge today is to construct and controll such a small hybrid structures and bring them into play in electronic devices and maybe in future architecture of quantum computers. This systems are natural candidates for qubits and multibits in general. In mesoscopic and nanoscopic systems the geometry plays very important role, as it decides of their properties. As an example let us recall persistent currents flowing in mesoscopic devices of the cylindrical geometry, theoretically predicted by Hund in 1938 and experimentally confirmed in the early 90's. Nanotechnologists are able to produce nano- and meso- rings, tori, stripes etc., that can be treated effectively as bistable systems and, in turn, as very good candidates for qubits and qutrits for quantum computer technology.

Interaction among the nods of the network of Josephson junctions leads to fascinating phenomena like coherence, synchronisation, fluxon motion and propagation or quantum phase transitions. We aim to explore similar nets of different symmetries consisting of bistable interacting mesoscopic rings [1, 2]. From the theoretical point of view these are triangular, quadratic, hexagonal 2D networks, which can be manufactured in labs nowadays. The theory of Josephson junctions is established and well known. Yet, there is almost no analysis done on the system of interacting mesorigs providing some important and unsolved aspects:

- construction of the evolution equation,
- analysis of steady states,
- existence or nonexistence of phase transitions.

We expect that by changing one of the parameters, e.g. inductance, order state (currents will have the same sign in all rings) or some regular spatial structure can be induced. Another interesting question is the role and influence of spatial symmetry on the given properties of the system.

References

[1] J. Dajka, J. Łuczka, M. Mierzejewski, and P. Hänggi *J. Phys. - Conf. Series* **30**, pp. 321–324 (2006).

[2] J. Łuczka, J. Dajka, M. Mierzejewski, and P. Hänggi *AIP Conf. Proc.* **800**, pp. 197–202 (2005).

An inferential framework for nonstationary dynamics: Theory, applications, and open questions

Andrea Duggento[2], Dmitri G. Luchinsky[1,2],
Vadim N. Smelyanskiy[1], Peter V. E. McClintock[2]
[1]NASA Ames Research Center, Mail Stop 269-2, Moffett Field, CA 94035, USA
[2]Department of Physics, Lancaster University, Lancaster LA1 4YB, UK

April 3, 2008

Problem to be addressed. The question we address is the extent to which a Bayesian inference framework may be able to facilitate parameter evaluation in non-stationary, nonlinear, stochastic dynamical systems. The technique has many potential advantages. It does not require heavy numerical computation, it allows multiple parameter estimation, and it provides optimal compensation for dynamical noise. Moreover, it is able to reconstruct "hidden" variables which are not directly accessible to measurement. We demonstrate that the approach is also highly promising in practice by presenting preliminary results, and we discuss the problems still remaining to be solved.

Theoretical Framework. Developing our Bayesian framework from an earlier work [1], we consider the following problem: an M-dimensional time-series data $\mathcal{Y} = \{\mathbf{y}_n \equiv \mathbf{y}(t_n)\}$ $(t_n = nh)$ is given, being the observations of the following system:

$$\begin{aligned} \dot{\mathbf{x}}(t) &= \mathbf{f}(\mathbf{x}|\mathbf{c}) + \sqrt{\mathbf{D}}\,\boldsymbol{\xi}(t), \\ \mathbf{y}(t) &= \mathbf{g}(\mathbf{x}|\mathbf{b}) + \sqrt{\mathbf{M}}\,\boldsymbol{\eta}(t). \end{aligned} \tag{1}$$

The first line of (1) defines the L-dimensional underlying stochastic dynamics (with a white uncorrelated noise source) and the second defines the observed variable $\mathcal{Y}$ (with an extra observational noise source). The task is to infer the unknown model parameters and their time variations, along with the noise intensities and $\mathcal{X}$-trajectory:

$$\mathcal{M} = \{\mathbf{c}(t), \mathbf{b}(t), \mathbf{D}, \mathbf{M}, \{\mathbf{x}_n\}\} \quad .$$

Assuming $\mathbf{f}$ and $\mathbf{g}$ linear in terms of parameters, and by use of a path-integral approach, we demonstrate that the posterior distribution for parameters is a multivariate normal distribution and we present an algorithm to find it: i.e. for the $\mathbf{c}$ parameters of the driving dynamic it will be

$$\mathcal{P}_{\rm post}(\mathbf{c}) \propto \exp\left[-\frac{1}{2}(\mathbf{c}-\bar{\mathbf{c}})^{\rm T}\boldsymbol{\Xi}(\mathbf{c}-\bar{\mathbf{c}})\right]. \tag{2}$$

The explicit expressions for $\bar{\mathbf{c}}$ and $\boldsymbol{\Xi}$, along with all the other algebraical results can be found in [2]. The Covariance matrix $\boldsymbol{\Xi}$ plays a special role in our discussion. It quantifies the information content available after data elaboration and it explicitly governs the convergence process of the inferred variables towards the real ones; its behaviour is crucial in the detection of nonstationary dynamics. For this reason, special emphasis will be placed on the details, limitations and possible improvements of this aspect of the technique.

Physiological application: two coupled FHN systems. With biological applications in mind (see e.g. [3]), the technique is used to decode the parameters of a system of neurons modelled by an L-dimensional system of FitzHugh-Nagumo (FHN) oscillators (see [4]):

$$\begin{aligned} \dot{v}_j &= -v_j\,(v_j-\alpha_j)\,(v_j-1) - q_j + \eta_j + \sqrt{D_{ij}}\,\xi_j, \\ \dot{q}_j &= -\beta\,q_j + \gamma_j\,v_j\,; \qquad \langle \xi_j(t)\,\xi_i(t')\rangle = \delta_{i\,j}\delta(t-t'), \quad j = 1:L. \end{aligned} \tag{3}$$

here, v_j simulate the membrane potentials, while q_j are slow recovery variables. We assume that neither v_j nor q_j are directly read (i.e they are "hidden" variables), but the measurements are taken through an (*unknown*) measurement matrix X:

$$y_i \;=\; X_{ij}\,v_j\,. \tag{4}$$

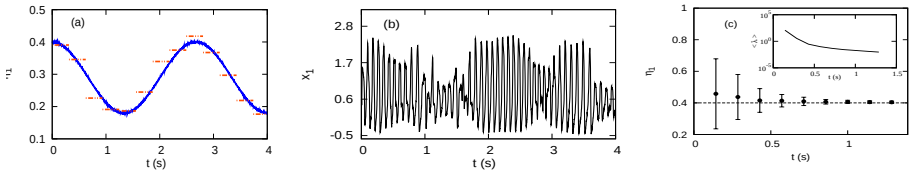

Figure 1: Inference of η_1 and η_2, while smoothly varying in the presence of noise. No prior knowledge of the model parameters is assumed. (a) The inferred values of η_1 (dashed red lines) are compared with their true values (full blue lines). (b) The measured time-trace of the mixed coordinate $x_1(t)$. (c) Typical convergence of the control parameters η_j as functions of the measurement time t; qualitative behaviour of the biggest eigenvalues of $\boldsymbol{\Xi}^{-1}$ is given in the box.

Our tasks are: (i) to reconstruct the coefficients which appears in (3); (ii) to reconstruct the mixing matrix X; (iii) to reconstruct hidden the variables q_j; (iv) to perform all three tasks taking into account that some of the parameters might have an explicit time dependence.

We find that we can detect stepwise changes of the control parameters for each oscillator, and follow continuous evolution of the control parameters in the adiabatic limit. Fig.1 shows some of our results: in this example we infer the key parameters η_j which are explicitly time-dependent. We also illustrate the parameter convergence as a function of data length together with that of the (eigenvalues of the) matrix $\boldsymbol{\Xi}$, giving practical support to the theory. A full discussion is presented in [5].

Open problems. In conclusion, we comment that, although our Bayesian framework clearly allows for inference of non-stationary stochastic dynamics, the technique is stillin its infancy. some aspects are still in the need of being brought up to discussion; especially considering that the basic algorithm might need modifications when it is applied in different disciplines and adjustments should be taken on a case-by-case basis. We therefore mention just some of the open problems to be addressed in the near future:

- The way the noise appears in the dynamics will need to be generalised to encompass multiplicative noise (leading to a non-trivial form of the parameter's likelihood);
- The form of the noise itself (at present white and uncorrelated) must be extended to the more general case of a coloured noise, and possibly to take into account the presence of correlation;
- Convergence of the algorithm might be critical in certain problems, especially in presence of many dimension and/or many coefficients, or where speed is an important.
- Extension to the more general case of nonlinear coefficients is another important problem, although ways of getting round the problem can sometimes be found [5].

The technique can readily be implemented to assist a diversity of information gaining tasks. Once answers have been found to the above problems above, we expect it to become useful across many disciplines.

References

[1] V. N. Smelyanskiy, D. G. Luchinsky, D. A. Timucin, and A. Bandrivsky, Phys. Rev. E **72**, 026202 (2005).

[2] D. G. Luchinsky, V. N. Smelyanskiy, A. Duggento, and P. V. E. McClintock, "Inferential framework for nonstationary dynamics. Part I. Theory", Submitted to Phys. Rev. E **00**, 00 (2008).

[3] V. N. Smelyanskiy, D. G. Luchinsky, A. Stefanovska, and P. V. E. McClintock, Phys. Rev. Lett. **94**, 098101 (2005).

[4] E. Izhikevich, *Dynamical Systems in Neuroscience: The Geometry of Excitability and Bursting.* (MIT Press, Cambridge, MA, 2006).

[5] A. Duggento, D. G. Luchinsky, V. N. Smelyanskiy,I. Khovanov, P. V. E. McClintock, "Inferential framework for nonstationary dynamics. Part II. Application to a model of physiological signaling", Submitted to Phys. Rev. E **00**, 00 (2008).

The problem of constructing phenomenological equations for subsystem interacting with non-Gaussian thermal bath

Alexander Dubkov
Radiophysics Faculty, Nizhniy Novgorod State University,
23 Gagarin Ave., 603950 Nizhniy Novgorod, Russia

Peter Hänggi and Igor Goychuk
Institut für Physik, Universität Augsburg,
Universitätsstr. 1, D-86135 Augsburg, Germany

A constructing the correct from thermodynamical point of view stochastic Langevin equations for macroscopic variables of subsystem interacting with thermal bath is the main problem of phenomenological theory. In most cases the influence of thermal bath can be described by introducing the additive Gaussian white noise in the equations for subsystem's phase variables. According to the basic principles of thermodynamics and statistical mechanics the intensity of such noise source should be strongly connected with the linear damping coefficient. This well-known Einstein's relation is some form of the linear fluctuation-dissipation theorem [1] reflecting indissoluble relationship between equilibrium fluctuations and irreversibility.

If we have to take into account the non-Gaussianity of thermal bath, the situation becomes more complex. All the high-order spectra of non-Gaussian white noise are nonzero, and, according to the quadratic fluctuation-dissipation theorem [2, 3], we should insert the nonlinear dissipation in the equations of motion. The open problem is how to find this nonlinear dissipation term in phenomenological equations.

A possible solution of this unsolved problem, namely, the procedure to constract the correct Langevin equation for a particle moving in some potential and interacting with the non-Gaussian thermal bath is proposed.

We start from the following Langevin equation for a particle of mass m moving in the potential $U(x)$ and interacting with the thermal bath of temperature T

$$m\dot{v} = -F(v) - \frac{dU(x)}{dx} + \xi(t), \tag{1}$$

where $x(t)$ and $v(t)$ are respectively the displacement and the velocity of a particle, $F(v)$ is unknown dissipation function, and $\xi(t)$ is the random force from the non-Gaussian thermal bath which can be represented by non-Gaussian white noise. Using the results, recently obtained in Ref. [4], we derive the closed equation for the joint probability density function $P(x, v, t)$ and taking into account the well-known Maxwell-Boltzmann form of equilibrium distribution

$$P_{st}(x, v) = c_0 \exp\left\{-\frac{1}{k_B T}\left(\frac{mv^2}{2} + U(x)\right)\right\}, \tag{2}$$

where c_0 is the normalization constant and k_B is the Boltzmann constant, we find the following expression for the nonlinear friction

$$F(v) = m \exp\left\{-\frac{mv^2}{2k_B T}\right\} \int_0^v dq \int_{-\infty}^{+\infty} \frac{\rho(z)}{z^2}\left[\exp\left\{-\frac{mq^2}{2k_B T}\right\} - \exp\left\{-\frac{(q - z/m)^2}{2k_B T}\right\}\right] dz. \tag{3}$$

Here the non-negative kernel function $\rho(z)$ defines the statistics of non-Gaussian noise source $\xi(t)$.

For Gaussian thermal bath: $\rho(z) = 2D\delta(z)$, where D is the intensity of white Gaussian noise $\xi(t)$. According to Eq. (3), the friction $F(v)$ becomes linear

$$F(v) = \gamma v \tag{4}$$

with the damping constant γ satisfying the Einstein's relation

$$\gamma = \frac{D}{k_B T}. \tag{5}$$

In the case of white shot noise

$$\xi(t) = \sum_i a_i \delta(t - t_i) \tag{6}$$

with Gaussian distribution of amplitudes a_i ($\langle a_i \rangle = 0$) from Eq. (3) we find

$$F(v) = \frac{\lambda m}{2}\sqrt{\frac{\pi}{\kappa}}\, e^{\kappa v^2}\left[\mathrm{erf}\left(\sqrt{\kappa}\,\mathrm{v}\right) - \mathrm{erf}\left(\sqrt{\frac{\kappa}{1+\varepsilon}}\,\mathrm{v}\right)\right], \tag{7}$$

where: $\langle a_i^2 \rangle = \sigma^2$, $\kappa = m/(2k_B T)$, $\varepsilon = \sigma^2/(k_B T m)$, λ is the mean rate of pulses generation, and erf (z) is the error function. The nonlinear friction (7) versus the particle velocity v is plotted in Fig. 1 for different values of dimensionless parameter ε. The first terms of nonlinear friction expansion in power series in

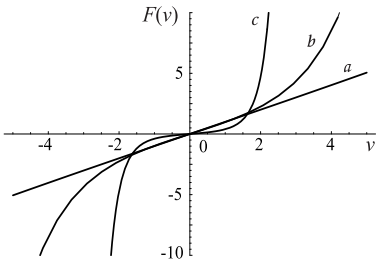

Figure 1: The dependence of nonlinear friction from the particle velocity v for different values of the dimensionless parameter ε: $a - \varepsilon = 0.001$, $b - \varepsilon = 0.1$, $c - \varepsilon = 5$. The other parameters are $\gamma = \lambda\sigma^2/(2k_B T) = 1$, $\kappa = 1$.

the velocity v read

$$F(v) = \lambda m\left\{\left(1 - \frac{1}{\sqrt{1+\varepsilon}}\right)v + \left[2 - \frac{2+3\varepsilon}{(1+\varepsilon)^{3/2}}\right]\frac{\kappa v^3}{3} + \left[8 - \frac{8+20\varepsilon+15\varepsilon^2}{(1+\varepsilon)^{5/2}}\right]\frac{\kappa^2 v^5}{30} + \ldots\right\}. \tag{8}$$

Although Eq. (3) allows to find the nonlinear friction for different non-Gaussian thermal baths, it is not evident the correctness of Eq. (2). Thus, the main hypothesis of the approach developed consists in validity of Maxwell-Boltzmann distribution for equilibrium state.

This work has been supported by Russian Foundation for Basic Research (project 08-02-01259).

References

[1] Callen, H. B. and Welton, T.A., *Phys. Rev.* **83** 34–40 (1951).

[2] Efremov, G. F., *Sov. Phys. JETP* **28** 1232–1239 (1969).

[3] Gupta, M. S., *Phys. Rev. A* **18** 2725–2731 (1978).

[4] Dubkov, A. and Spagnolo, B., *Fluct. Noise Lett.* **5** L267–L274 (2005).

Out of equilibrium phase transitions in the self organization of two dimensional turbulent flows

Freddy Bouchet, Hidetoshi Morita and Eric Simonnet
Institut Non Linéaire de Nice (INLN), CNRS UMR6618, UNSA
1361, route des lucioles, 06 560 Valbonne-Sophia Antipolis, France

April 3, 2008

One of the most important problem in turbulence is the prediction of large-scale structures of very high Reynolds' flows. We consider here the class of two dimensionnal and geostrophic flows relevant for geophysical applications (ocean and atmosphere). The main physical phenomenon is the self organization of the large scales into jets and vortices. We study the simplest academic problem including this type of phenomena : ***the two-dimensional Navier-Stokes equation with weak stochastic forces and dissipation.***

Two beautiful classical theories deal with two dimensional turbulence. The first one, the cascade theory is aimed at describing the velocity field statistics for self similar inverse energy cascade or direct enstrophy cascade. For this first approach, the main hypothesis is self similarity, which is unfortunately broken as soon as large scale structures (vortices and jets) appear. The second theory is the equilibrium statistical theory that describes the organization of inertial flows [1]. However this last approach does not take into account the effect of forces and dissipation.

Most of natural or experimental flows, as far as large scales are concerned, thus do not fall in the realm of classical theories. This is the motivation to study the two-dimensional Navier-Stokes equation with weak stochastic forcing and dissipation. *This is an example of dynamical system forced by noise, where an out of equilibrium stationary state is reached, without detailed balance.* The existence of an invariant measure has been mathematically proved recently, together with mixing and ergodic properties [2]. This problem has however never been considered from a physical point of view. We thus address the following issues: when is the measure concentrated on an inertial equilibrium, how are the large scales selected by the forcing, what is the level of the fluctuations ?

Two dimensional turbulence is an example of physical phenomena where order arises from randomness and where fluctuations play a crucial role in selecting the main structures.

1 Out of equilibrium phase transitions and stochastic Landau damping

1.1 Random switch between large scale flows with different topologies

We study the two dimensional Navier Stokes equation with stochastic forces. The most striking physical result is the existence of out of equilibrium phase transitions : one observes random bifurcations from one topology of large scale flow (dipoles) to another (unidirectional flows). The flow behaves similarly to a bistable system that switches at random times from one state to the other.

After the theoretical study of a bifurcation diagram for the stationary states of the 2D Euler equation, we have conjectured the existence of these out of equilibrium phase transitions [3]. We have verified their existence using numerical simulations and made a detailed empirical study [3]. Similar considerations leads to the predictions of out of equilibrium phase transitions in a large class of other geometries, and also for geostrophic, large rotation or 2D magnetic flows.

The system roughly behaves as a bistable one. However this analogy is extremely limited. Indeed, in our case no potential landscape exists, that would explain the phenomena. Moreover the turbulent nature of the flow (infinite number of degrees of freedom) renders the phenomena much richer than in the classical two well problem. Analogies with the Earth magnetic field reversal, and with similar phenomena in experiment of two dimensionnal and geophysical flows will be discussed.

This leads to open issues, as discussed in section 2. The major one is : in this class of phenomena where the description by a small number of modes is not valid, can we propose a theory predicting the selection of large scales flows by the balance between stochastic forces and dissipation ?

2 Stochastic Landau damping

We will present theoretical results for the prediction of the velocity and of the vorticity fluctuations, in the context of the Navier Stokes stochastic (NSS) equation, with weak stochastic forcing and dissipation [4]. Theoretical arguments and numerical evidences show that flows are then close to equilibria of the Euler equation. At leading order, fluctuations around such equilibria are then described by the linearized NSS equation.

We thus study theoretically the linearized NS equation with random forces. In the limit of zero dissipation, as expected no stationary distribution exist for the Gaussian vorticity field. By contrast, the Gaussian stream function or velocity fields strikingly converge toward a stationary Gaussian process. The velocity field thus acts similarly to a dissipative system, when dissipation is no more present. An explanation of this seemingly anomalous behavior and its relation to the deterministic Landau damping of plasma physics and Orr mechanism for 2D vortices will be given.

This suggests a class of open problems related to the effect of noise on physical systems described by partial differential equation, that are not reducible to a description by a small number of degrees of freedom.

3 Open issues

Beside the obtained theoretical results, and observed phenomena, the two dimensional Navier Stokes equation with stochastic forces open a number of issues. Many of these are common to other classes of turbulent problems, where a large number of degrees of freedom are involved. We may cite few of them :

1. In a complex system with noise where a potential landscape do not exist, how does turbulence select states that dominate the dynamics ?
2. What does select the largest scales of turbulent flows ? Why low dimensional approaches, treating unresolved scales as noise, have failed up to now ?
3. Is an adiabatic reduction possible, in the limit of weak stochastic forces and dissipation, for the two dimensional Navier Stokes equation or related models ?

References

[1] BOUCHET F. and SOMMERIA J., 2002, Emergence of intense jets and Jupiter's Great Red Spot as maximum entropy structures J. Fluid Mech.464, 165-207.

[2] KUKSIN S. B., 2004, The Eulerian limit for 2D statistical hydrodynamics, J. Stat. Physics 115:1/2, 469–492.

[3] BOUCHET F. and SIMONNET E., 2008, Out of equilibrium phase transitions in the 2D Navier Stokes stochastic equation, preprint

[4] BOUCHET F., 2008, The Stochastic Landau damping and Orr mechanism. In preparation

Negative weight transients of information storage media after recording

Laszlo B. Kish
Department of Electrical and Computer Engineering, Texas A&M University
College Station, TX77843-3128, USA

Due to the unsuccessful explanation of gravitation constant anomalies, such as the fifth force explanation, we stated a new unsolved problem: is there any attractive or repulsive interaction between similar information patterns/structures? A possible phenomenological theory is outlined. Similarity can for example measured by mutual information. At test experiments, we found that, at 1 centimeter distance, there is no observable force interaction at 100 microNewton (10 microgram) accuracy between two 4 GB Flash drives filled with the same white noise. Thus, if the effect exists it is weaker than that.

However, during these investigations, we discovered a new challenging unsolved problem of noise. The weights of information storage media, namely Flash drives, DVD and CD disks were monitored by 100 microNewton (10 microgram) accuracy after recording various types of data on them, including zeros, white noise and 1/f noise. All these media execute a negative weight transient, in the order corresponding to a milligram change, with slow relaxation back toward to the previous weight that takes about one hour. It is like a "smoking gun" after firing. The previous weight is usually not reached.

Obvious explanations are temporary water loss from some hygroscopic parts and warm air convection above the device with the corresponding updraft due to its elevated temperature. However, though the above effects certainly playing some role in the phenomena, the explanation seems to be not satisfactory. Thus a new unsolved problem is: is there any *transient* interaction between similar information patterns/structures?

Data and considerations will be presented. Some examples are shown in the two figures below.

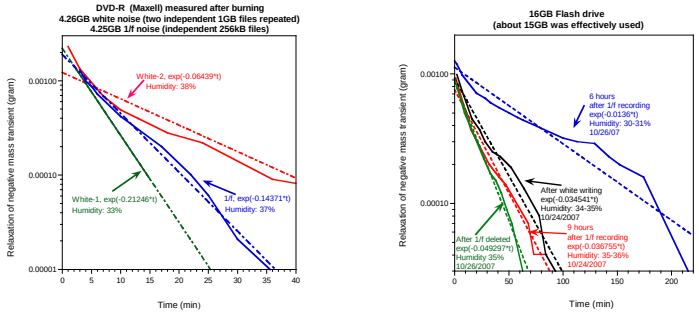

Reference

L.B. Kish, *Fluctuation and Noise Letters* **7** pp. C51-C68 (2007).

Noise in materials and devices

Hélène Bouchiat – **Keynote Lecture**
Thermal and out of equilibrium noise in electronic devices: from the classical to the quantum regime 46

Yossi Paltiel
Non Gaussian Noise in Quantum Wells 47

Iouri Galperine
Many electron theory of 1/f-noise in hopping conductance 48

Jean-Marc Routoure
Possible effect of epitaxial quality and of strain on the low frequency noise in LSMO thin films 49

Guillem Albareda
Can analog and digital applications tolerate the intrinsic noise of aggressively-scaled field-effect transistors? 50

Luca Varani
Problems of noise modeling in the presence of total current branching in HEMTs and FETs channels 51

Eugene Sukhorukov
Stochastic dynamics of a Josephson junction threshold detector 52

Jesús Enrique Velázquez-Pérez
Noise in strained-Si MOSFET for low-power applications 53

Jean-Francois Millithaler
A Monte Carlo investigation of plasmonic noise in nanometric n-$In_{0.53}Ga_{0.47}As$ channels 54

Francesco Ciccarello
Noise of hot electrons in anisotropic semiconductors in the presence of a magnetic field 55

Shih Chun-Hsing
Latent Noise in Schottky Barrier MOSFETs 57

Kamal Kumar Bardhan
1/f Noise in systems with multiple transport mechanisms 56

Edvige Celasco
Correlated avalanches in TES noise power spectra 58

Thermal and out of equilibrium noise in electronic devices: from the classical to the quantum regime

Pierre Billangeon, Richard Deblock and Hélène Bouchiat
Univ. Paris-Sud, CNRS, UMR 8502, F-91405 Orsay Cedex, France

Noise in electronic devices has been investigated for many years in various types of materials ranging from semiconductors, metals and superconductors. This noise has been classified into three main categories which are:

- Thermal equilibrium noise, measured without any current through the device.
- Shot noise, proportional to the current through the device which reveals the elementary charge of the carriers through the device as well as the nature of their statistics (bosonic, fermionic or fractional)
- 1/f or telegraphic noise proportional to the square of the current through the device. This noise is related to the internal thermal fluctuations of the defects in the device causing resistance noise revealed by the current.

After a brief review of the different characteristics of these noise sources in the low frequency limit, we would like to emphasize some of their particular aspects in the high frequency regime when $\hbar\omega$ is larger than the thermal energy k_BT. We will discuss the various possible experimental setups which enable the investigation of the noise in this regime ranging from classical to quantum detectors. We will then focus on the frequency dependence of the equilibrium and shot noise in this limit which exhibits signatures of the relevant energy scales k_BT and eV where V is the voltage bias on the device . We will present several examples such as a quantum point contact, a metallic diffusive wire and a Josephson junction.

We will then rise the important question of the asymmetry of the noise specific to the quantum regime where emission noise (corresponding to negative frequencies) is expected to be different from absorption noise (corresponding to positive frequencies). These fundamental differences between emission and absorbtion processes are very well known in the field of quantum optics. We will present some recent experiments which could also show evidence of this fundamental aspect of quantum noise in an electronic device consisting in a superconducting tunnel junction polarised with a voltage of the order of the superconducting gap. The equivalent experiment in a system at thermal equilibrium does not exist yet.

Finally we will address the quantum limit of telegraphic noise which is produced by two level systems fluctuators . This noise has been shown in certain cases to limit the performances of condensed matter Q-bits but is far from being understood.

Non-Gaussian Noise in Quantum Wells

Y. Paltiel[1], A. Ben Simon[1,2], G. Jung[2], V. Berger[3], and H. Schneider[4]
1) Solid State Physics Group, Electro-Optics Division,
Soreq NRC, Yavne 81800, Israel
2) Department of Physics, Ben Gurion University of the Negev,
Beer Sheva 84105, Israel
3) Matriaux et Phnomnes Quantiques, Universit Paris 7, 75251 Paris, France
4) Institute of Ion-Beam Physics and Materials Research,
Forschungszentrum Dresden Rossendorf, D-01314 Dresden, Germany

April 3, 2008

Generation-recombination noise is accepted to be a dominant mechanism of current noise source in quantum well systems biased by electric field normal to the layers. The central limit theorem implies that such noise has to be gaussian. In recent experiments we have found pronouncedly non-Gaussian, bias depnendent current noise in n-type and p-type multiple quantum wells. The non-Gaussianity of the noise is more pronounced in p-type wells where the time traces of current fluctuations resemble closely two-level random telegraph signal which has not been straightforwardly observed in time domain records. The non-Gaussian character of the noise in n-type wells has been revealed by measurements of nonzero skewness of the noise amplitude distributions. The origin of the nonGaussian noise and marked differences between noise properties of n- and p-type quantum wells are the UPON questions that we bring to discussion.

The nonGaussianity of the noise appears at certain bias range and is directly related to the non-linear behavior of the gain in the corresponding bias range. In p-type wells the non-linearity can be attributed to difference in tunneling rates of light and heavy holes. For n-type wells the intervalley scattering seems to be the dominant reason for the appearance of the nonlinear gain. In both cases additional non Gaussian noise can as well originate from impact ionization. The appearance of non-Gaussian noise is therefore attributed to two solutions of the continuity equation in the nonlinear differential conductivity regime. Multiple solutions of the continuity equation allow for existence of multiple metastable spatial voltage distributions. Two distinct spatial voltage distributions under a constant external bias voltage correspond to two possible states of the system: a high resistivity state with low current and a low resistivity state with high current. Each state is characterized by its specific bias dependent average lifetime. The finite time of transition between the metastable states, which is not negligible with respect to the average lifetimes, is determined by the charging time constant by the capacitance and resistance of the quantum well system.

We have tentatively attributed non-Gaussian character of the noise to the metestability of spatial configuration of electric field in the quantum well system. Quantum well system biased with a constant dc voltage may randomly switch, in a telegraphic-like way between high resistance state characterized by low current flow and low resistance state with high current flow leading to nongaussian character of current noise.

The difference between noise properties of n- and p-type systems may be attributed to small capture probability of electrons in n-type wells, as opposed to very high capture probability of holes in p-type wells. As a consequence the noise of any p-type multi-well system will be dominated by fluctuations of a single well, while in the n-type the noise appears as a superposition of many fluctuators associated with all wells constituting the system.

Many electron theory of 1/f-noise in hopping conductance

Yuri Galperin
Department of Physics, University of Oslo,
PO Box 1048 Blindern, 0316 Oslo, Norway

February 16, 2008

The talk is based on the set of papers [1, 2, 3] written in collaboration with V. I. Kozub (A. F. Ioffe Physico-Technical Institute, St. Petersburg, Russia), A. L. Burin (University of Tulane, New Orleans, USA), B. I. Shklovskii (University of Minnesota, Minneapolis, USA), A. Glatz and V. Vinokur (Argonne National Laboratory, Argonne, USA). We address long-standing problem of $1/f$ noise in hopping insulators in the regime of variable range hopping (VPH).

At low temperatures the variable-range hopping conductivity of doped semiconductors with strongly localized electrons obeys the Efros-Shklovskii (ES) law

$$\sigma_{\rm ES} = \sigma_0 e^{-(T_{\rm ES}/T)^{1/2}}, \tag{1}$$

where the temperature $T_{\rm ES}$ is defined by the electron-electron interaction at the localization radius a of electronic states. The conductivity behavior represented by Eq. (1) is observed for example in ion-implanted silicon (Si:P:B) bolometers working as detectors for high resolution astronomical X-ray spectroscopy [4].

The performance of the bolometers is limited by a $1/f$-noise, which obeys the Hooge's law [5]

$$\delta\sigma_\omega^2/\sigma^2 = \alpha_H(\omega,T)/\omega N_D\,, \tag{2}$$

where N_D is the total number of donors, $\delta\sigma_\omega^2 \equiv \int dt\, e^{i\omega t}\langle\delta\sigma(t)\delta\sigma(0)\rangle$, $\delta\sigma(t) \equiv \sigma(t) - \langle\sigma(t)\rangle$, and $\langle\cdots\rangle$ denotes ensemble average. The dimensionless Hooge factor $\alpha_H(\omega,T)$ measured for different doping levels grows by six orders of magnitude with the decreasing temperature following approximate power law [4, 6]

$$\alpha_H \propto T^{-6}\,. \tag{3}$$

This behavior strongly differs form the that observed in conductors with metallic conductance where the Hooge parameter monotonously *increases* with temperature. Ref. [6] gives a strong evidence that the noise is caused by the electron localization. This work investigates the bulk Si:P:B semiconductor in the range of dopant concentrations on both sides of the metal-insulator transition. The increase of the noise strength by several orders of magnitude, when crossing the metal-insulator transition from metal-like samples to insulating samples was observed. The noise intensity continues to increase with decreasing electron localization radius a, what proves the primal significance of the electron localization in the noise formation. A similar behavior of the normalized $1/f$-noise power has been recently reported in the low density hole system of a GaAs quantum well. These and other experiments show that $1/f$-noise is one of the manifestations of the complex correlated electronic state (Coulomb glass) formed by localized electrons coupled by the long-range Coulomb interaction.

In this work we suggest the model of many-electron fluctuators, which possess small relaxation rates ν with much larger probability then single-electron traps. A new fluctuator is made of N occupied (neutral) and N empty (positively charged) donor sites quasi-ordered into the quasi-cubic lattice with the period R. They include only donors with energies within a band with the width $U_R \equiv e^2/\kappa R$, which are required to have somewhat diminished disorder energies.

We show that $1/f$-noise of conductance in the variable range hopping regime is related to transitions of many-electrons clusters (fluctuators) between two almost degenerate states. Giant fluctuation times necessary for 1/f-noise are provided by slow rate of simultaneous tunneling of many localized electrons and by large activation barriers for their consecutive rearrangements. These fluctuations in the many-electron clusters are "read out" by the hopping cluster responsible for the conductance. We analyze statistics of the many-electron clusters responsible for noise at very low frequencies and calculate noise spectrum and intensity.

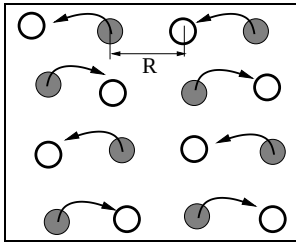

A "chess-board" cluster of donors, responsible for a $1/f-$ noise. The dark circles indicate occupied (neutral) donors, while the open circles indicate empty donors. All donors are in the energy band of the width $2e^2/\kappa R$ around the chemical potential ($E = 0$). Arrows shows the direction of the electron transition between two energy minima corresponding to two possible ways to occupy cluster sublattices. The length R stands for the size of the cluster cell.

Optimizing the "lattice constant" R and the number of electrons N we have shown that a $1/f$-noise associated with such clusters behaves as

$$-\ln\alpha_H(\omega,T) \sim \left(\frac{T}{T_{\rm ES}}\right)^{3/5} \ln^{6/5}\frac{\nu_0}{\nu} = \left[\frac{\ln(\nu_0/\omega)}{\ln(\nu_0/\nu_{\rm ES})}\right]^{6/5}. \tag{4}$$

This behavior agrees with the low temperature observations of 1/f-noise in p-type silicon and GaAs.

We also discuss relation of the 1/f noise and memory effects in hopping conductance observed in numerous experiments, as well as general aspects of dynamics in Coulomb glasses concentrating on several unsolved problems. Among them is the long-standing problem of slow relaxation and memory in conductance hopping insulators, which can be induced by slow rearrangement of electronic clusters or structural defects.

References

[1] A. L. Burin, B. I. Shklovskii, V. I. Kozub, Y. M. Galperin, and V. Vinokur, *Phys. Rev. B* 74, 075205 (2006).

[2] A. Glatz, V. M. Vinokur, and Y. M. Galperin, *Phys. Rev. Lett.* 98, 196401 (2007).

[3] A. L. Burin, V. I. Kozub, Y. M. Galperin, V. Vinokur, *Preprint: arXiv:0705.2565.*

[4] S-I. Han, R. Almy, E. Apodaca, W. Bergmann, S. Deiker, A. Lesser, D. McCammon, K. Rawlins, R. L. Kelley, S.H. Moseley, F. S. Porter, C. K. Stahle, and A. E. Szymkowiak, in *EUV, X-ray, and Gamma-Ray Instrumentation for Astronomy IX*, O. H. Seigmund and M. A. Gummin, Editors, Proceedings of SPIE **3445**, 660 (1998); D. McCammon, preprint, physics/0503086.

[5] F. N. Hooge, Physica **60**, 130 (1972).

[6] S. Kar, A. K. Raychaudhuri, A. Ghosh, H. v. Löhneysen, G.Weiss, Phys. Rev. Lett. **91**, 216603 (2003).

Possible effect of epitaxial quality and of strain on the low frequency noise in $La_{0.7}Sr_{0.3}MnO_3$ thin films

J.-M. Routoure *1, D. Fadil[1], C. Barone[1,2], P. Perna[1,3], S. Flament[1] and L. Mechin
[1] GREYC (UMR 6072) - ENSICAEN & Univ. Caen, 6 Bd Mar. Juin, 14050 Caen Cedex
[2] University of Salerno, Dipartimento di Fisica " E.R. Caianiello", 84081 Baronissi(SA)
[3] CNR-INFM Coherentia, Complesso Monte S. Angelo, via Cinthia, 80126 Napoli, It
* routoure@greyc.ensicaen.fr (+33)231452722

Introduction

The remarkable electronic and magnetic properties of manganites have raised lot of interests for applications : colossal magnetoresistance (CMR), large resistance change at the metal-to-insulator (M-I) transition temperature and high spin polarization. They are promising candidates for a new generation of electronic devices including magnetoresistive sensors, bolometers and spin-valve systems [1, 2]. Measuring the low frequency noise in these devices is necessary in order to define optimal preparation conditions and adequate geometries [3, 4]. Understanding the origin of noise in this kind of strongly correlated electron devices could also give some indications on charge transport mechanisms.

Devices and results

We report low frequency noise measurements performed in patterned $La_{0.7}Sr_{0.3}MnO_3$ ($LSMO$) thin films of various thicknesses (20 nm up to 200 nm) deposited onto different substrates : (001), (110) or vicinal $SrTi0_3$(STO) and buffered silicon. A photography of the devices is shown in figure (1). 2 current probes and several voltage probes allow to use the four-probe configuration and to select the length of the tested device.

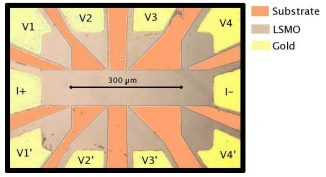

Figure 1: Photography of the devices showing the device with the current (I+ and I-) and the voltage (V1, V1'...V4, V4') contacts realized using gold.

The measurements were performed using a four-probe configuration with a high output impedance DC current source. It ensures that only the film noise is measured. As reported in [6, 7], a high contact resistance noise level can be found. Several bias points and temperatures were investigated. From noise measurements at different bias voltages V across the film, one can deduce a figure of merit called α/n using a Hooge-like empirical relation $e^2_{nRM}/V^2 = (\alpha/n) \cdot (1/(\Omega \cdot f))$ where f is the frequency, α the Hooge parameter, n the charge carrier concentration and $Omega$ the volume. Results of α/n versus Ω are plotted in figure (2).

The noise level can vary over 3 orders of magnitude depending on the type of substrates and on the layer thickness. The structural quality of the film was checked by X-ray diffraction. It showed the lower quality of the thin film deposited onto the buffered silicon substrate and as a consequence that the high value of the noise for buffered silicon substrate could have a structural origin. In the case of the STO substrates, X-ray analysis indicates a good structural quality of the film. In that case, strain in the films is strongly affected by the different substrate orientation or by the use of vicinal substrate. Consequently,

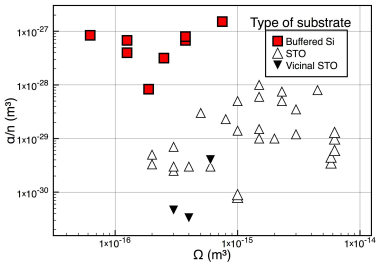

Figure 2: Evolution of α/n versus Ω for 3 different films deposited onto STO (up and down triangle symbols) and onto buffered Silicon(square symbols) . The noise level for the LSMO/buffered silicon films is three orders of magnitude higher than the noise level for LSMO/STO films.

the variations of the noise level for the different films could be correlated with the film strain : the lowest value of α/n is reported for the vicinal substrate (among the lowest value reported in the literature) which corresponds to the lowest strained films.

Conclusion

Low frequency noise have been measured in LSMO thin films deposited onto different substrates. We have shown that in the case of buffered silicon substrate, the high level for the low frequency noise could be attributed to a lower structural quality. For STO substrates of various orientation, the effect of the film strain induced by the substrate is proposed to explain the different noise levels observed. Work is in progress to find, from X ray diffraction measurements, a quantitative estimation of the strain in the film and thus demonstrate the possible correlation between the low frequency noise level and the strain.

References

[1] T. Venkatesan, M. Rajaswari, Z. Dong, S.B.Ogale and R. Ramesh, Phil. Trans. R. Soc. Lond. A 356 1661 (1998)

[2] A.-M. Haghiri-Gosnet, J.-P. Renard, J. Phys. D: Appl. Phys. 36 R127-R150 (2003)

[3] F. Yang et al., J. Appl. Phys. 99(10) (2006);

[4] L. Méchin et al.,ICNF 2005 Proceedings, pp 143-146.

[5] L. Méchin et al., Appl.Phys.Lett. 85(15) pp 3154-3156(2004).

[6] J.M. Routoure et al. : ICNF2007 Proceedings, pp 229-232

[7] C. Barone et al. Review of Scientic Instrument, 78 pp 093905 (2007)

Can analog and digital applications tolerate the intrinsic noise of aggressively-scaled field-effect transistors?

G.Albareda, D.Jiménez and X.Oriols
Departament d'Enginyeria Electrònica, ETSE
Universitat Autònoma de Barcelona,
08192, Bellaterra, Barcelona, SPAIN

For nanoscale field-effect transistors (FET) with channel lengths below 20 nm, novel structures with two, three or even four gates are developed to improve the gate control over the source-drain conductance. The advantages of these novel structures, to overcome the physical limits of traditional FETs, are clearly established in terms of size, speed or power consumption. However, few works are devoted to study the intrinsic noise performance of these novel structures. In this conference, we study the role of scaling in the intrinsic (thermal and shot) noise performance of analog and digital applications with such FET structures. We simulate a 3D (Bulk-), 2D (quantum well-) and 1D (quantum wire-) double gate FETs with a Monte Carlo (MC) simulator coupled to a full 3D Poisson solver [1] and with a novel injection model suitable for electron devices with or without electron confinement under degenerate or non-degenerate conditions [2].

1 Signal-to-noise ratio in analog amplifiers

The noise performance of an analog amplifier is quantified in terms of the signal-to-noise (S/N) ratio. One consequence of the FET dimension reduction is the presence of electron confinement (in one or two lateral directions) that reduces the number of available states at low energy. At room temperature, the states with low energy supply a large current, but low noise. In fig. 1a, we plot the current and the Fano factors for three different FET as a function of the gate voltage computed with the MC simulator. We show that the electron confinement causes a decrease of the current and an increase of the Fano Factor. As a consequence, in fig. 1b we see that the output (S/N) ratio of a simple analog amplifier is clearly degraded for 1D transistor.

2 Bit-error-ratio in digital inverters

The noise performance of a CMOS inverter (fig 2a) is quantified with the bit error ratio (BER). For any input logic level, one of the transistors is on opened-channel conditions with zero averaged current but with thermal noise. The current fluctuations of the opened-channel transistor are converted into voltage fluctuations via the gate capacitance, C, of the output transistor (i.e. $\Delta V = \Delta Q/C$) as schematically drawn in fig 2b. The reduction of FET dimensions provides a reduction of the C. In fig. 2, the probability of a drain voltage different from zero in the configuration of fig 2a is plotted for the 3D, 2D and 1D FETs. The results are in qualitative agreement with previous works [3]. A compact model [4] is used to estimate the eror probability (solid lines in fig. 2) within the assumption that the system behaves linearly (see fig 3c). Full MC simulations reveal that the estimation of errors is even worst for 1D transistors when the voltage fluctuations surpass the drain saturation voltage (~ 0.2 V) where the channel resistance is very large (see fig 3d).

Our preliminary MC numerical results suggest a negative answer to the question of the title for aggressively-scaled 1D-FETs that might imply an unexpected breakdown of Moore's law.

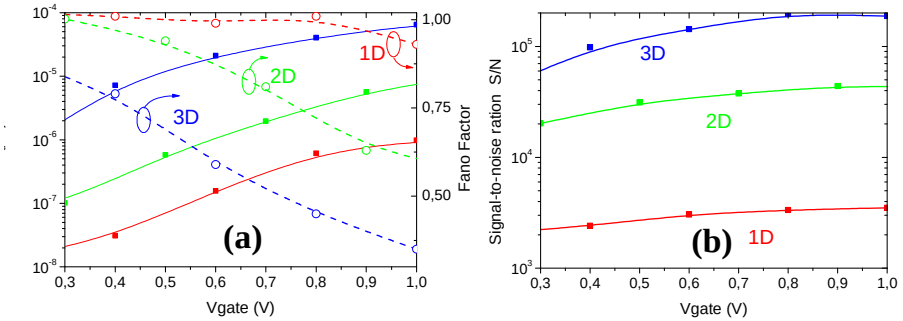

Figure 1: Monte Carlo results for average current, Fano Factor (a) and Signal-to-noise ratio (b) for a 3D (Lx=40, Ly=10, Lz=10 nm), 2D (Lx=15, Ly=10, Lz=2 nm) and 1D (Lx=15, Ly=5, Lz=2 nm) N-FET in an amplifier configuration.

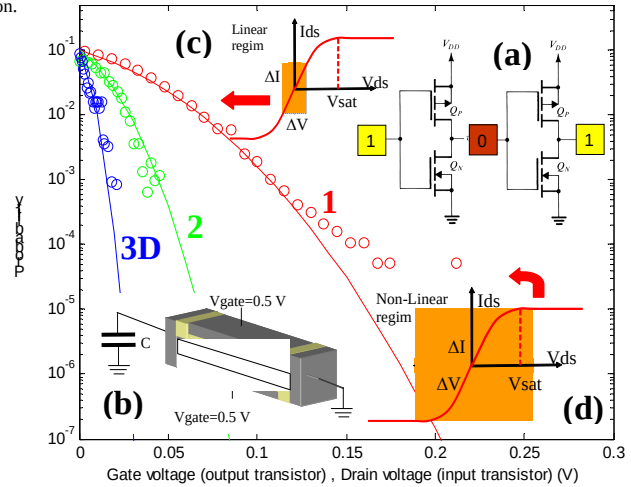

Figure 2: Probability of voltage different from zero in the CMOS inverter (a) at equilibrium computed from a time-dependent Monte Carlo simulation of a N-FET during 1e-8 seconds. The drain contact (b) is coupled to the gate capacitor of the next transistor with C_{3D}=4e-18 F, C_{2D}=1e-18 F and C_{1D}=8e-19 F. For small errors the system behaves linearly (c), but it becomes non-linearly (d) for large errors.

References

[1] G. Albareda et al, Journal of Computational Electronics, DOI 10.1007/s10825-008-0185-7 (2008).

[2] X.Oriols et al, Solid State Electronics, 51, 306 (2007).

[3] L.B.Kish, Physics Letters A. 305, 144 (2002).

[4] D. Jiménez et al., J. Appl. Phys. 94, 1061 (2003).

Problems of noise modeling in the presence of total current branching in HEMTs and FETs channels

P. Shiktorov[a], E. Starikov[a], V. Gružinskis[a],
L. Varani[b], G. Sabatini[b], H. Marinchio[b] and L. Reggiani[c]
[a]Semiconductor Physics Institute
Goštauto 11, 01108 Vilnius, Lithuania
[b]Institut d'Électronique du Sud (CNRS UMR 5214)
Université Montpellier 2, Place Eugène Bataillon, 34095 Montpellier Cedex 5, France
[c]Dipartimento di Ingegneria dell'Innovazione, Università del Salento and CNISM
Via Arnesano s/n, I-73100 Lecce, Italy

Electron transport and noise modeling in discrete-element circuits is based on Kirchhoff's law which is a direct consequence of the conservation law of the total current $\mathbf{J}_{tot}$. In its integral form, it is usually written as:

$$\int_S \mathbf{J}_{tot} d\mathbf{S} = 0 \tag{1}$$

where

$$\mathbf{J}_{tot} = \varepsilon\varepsilon_0 \frac{\partial \mathbf{E}}{\partial t} + \mathbf{j}_d \tag{2}$$

is the local total current-density consisting of the displacement and conduction components (first and second terms in the r.h.s. of Eq. (2), respectively), and $\mathbf{S}$ is a surface surrounding some volume of interest. Under the usual assumption that the directions of the electric field and conduction current density locally coincide (that is $\mathbf{j}_d || \mathbf{E}$), one can introduce current tubes along which the conservation law given by Eq. (1) reduces to a simple scalar relation:

$$\frac{\partial J_{tot}(x,t)}{\partial x} = 0 \tag{3}$$

where the x-direction is chosen along the tube. In other words, Eq. (3) implies that the total current-density is conserved in the *closed* circuit formed by such a tube which includes the conducting channel, contacts, and other external elements needed to close the circuit. It is just the case of two-terminal devices (resistors, diodes, etc.). Direct consequences of such a formulation of the total current-density conservation law are: (i) the well-known techniques based on the Ramo-Shockley theorem for the current and current-noise calculations in two-terminal devices, (ii) the duality (equivalence) of intrinsic electronic noise representation in terms of Norton and Thenevin noise generators, etc. In going from two- to three-terminal devices (shortly called as diodes and transistors, respectively) the local parallelism of $\mathbf{j}_d$ and $\mathbf{E}$ inside the device is in general violated. This can lead to the branching of the total-current tubes, so that the Eq. (3) becomes invalid at the branching points where in accordance with Eq. (1) the total current conservation is formulated as zero-sum rule for incoming/outcoming currents. Such a situation is typical in FET and HEMT structures. Here, the conduction current flows along a conducting channel while the governing local electric field direction does not coincide with the carrier flow due to presense of a gate. *In essence, it means, that under the gate action the whole channel region is practically the continuous region of the total-current branching between the source-drain and channel-gate directions.*

As a result, simplified attempts (based usually on the gradual-channel approximation and similar to it) to interpret the gated channel as a two-terminal device with the total current conservation low described by Eq. (3) fails. For example, for the total-current noise induced by an intrinsic local fluctuations of the conduction current in HEMT channels both analytical considerations and numerical simulations evidence a violation of the temporal coherence (sinhronization) of the total-current fluctuations at the source- and drain-contacts, in contrast with similar diode-like structures. As a consequence, the total-current noise spectrum at the source-terminal differs from that at the drain-terminal, what evidently contradicts our expectations for the *closed*-circuit behavior. It should be emphazised, that such a branching and related phenomena in FET and HEMT channels are mainly organized by the displacement component of the total curent-density. Therefore, the effects related with these phenomenona should be most pronounced at sufficiently high frequencies typical for expected terahertz-frequency applications of FETs and HEMTs. The aim of this communication is to discuss the problems related with intrinsic noise in FETs and HEMTs channels induced by the continuous branching of the total current between *three* terminals.

Stochastic dynamics of a Josephson junction threshold detector

Eugene V. Sukhorukov
Département de Physique Théorique, Université de Genève, CH-1211 Genève 4, Switzerla

Detecting electron counting statistics has become a major experimental challenge in mesoscopic physics. First attempts to measure non-Gaussian effects in current noise have revealed that the detection problem is quite subtle. In particular, the experiment [1] found that the third current cumulant was not described by the simple theoretical prediction [2], but was masked by the influence of the measurement circuit causing an additional "cascade" correction [3, 4]. Recent experiments demonstrated a measurement of the third current cumulant without cascade corrections [5], and the detection of individual electron counting statistics [6]. Stringent bandwidth requirements in measuring the third cumulant suggested that further experimental advances would require a new approach.

A conceptually different way to measure rare current fluctuations is with a threshold detector [7, 8], the basic idea of which is analogous to a pole vault: A detection event occurs when the measured system variable exceeds a given value. A natural candidate for such a detector is a metastable system operating on an activation principle [9]. By measuring the rate of switching out of the metastable state, information about the statistical properties of the noise driving the system may be extracted. A threshold detector using an on-chip conductor which contains a region of negative differential resistance [10, 8] was proposed by the authors and shown to be capable of measuring large deviations of current. Tobiska and Nazarov proposed a Josephson junction (JJ) threshold detector [7], the simplest variant of which operates essentially in a Gaussian regime [11]. The third cumulant contribution is small [12] and may be experimentally extracted using the asymmetry of the switching rate with respect to bias current [13].

Here we solve Kramers' problem [9] of noise-activated escape from a metastable state beyond the Gaussian noise approximation and investigate how the measurement circuit affects threshold detection. Starting with general Hamiltonian-Langevin equations which includes deterministic dynamics, dissipation, and fluctuations, we represent the solution as a stochastic path integral of Hamiltonian form [14, 15] by doubling the number of degrees of freedom. In the weak damping case, the dynamics is dominated by energy diffusion, which we account for by a change of variables, enabling an effectively two-dimensional representation. We calculate the escape rate via an instanton calculation, and obtain a formal solution of Kramers' problem [9]. Applying these general results to a JJ threshold detector, we account for the influence of the measurement circuit and find that the cascade corrections are a consequence of the non-equilibrium character of the noise.

References

[1] B. Reulet, J. Senzier, and D.E. Prober, Phys. Rev. Lett. **91**, 196601 (2003).

[2] L.S. Levitov, and M. Reznikov, Phys. Rev. B **70**, 115305 (2004).

[3] K.E. Nagaev, Phys. Rev. B **66**, 075334 (2002).

[4] C. W. J. Beenakker et al., Phys. Rev. Lett. 90, 176802 (2003).

[5] Yu. Bomze *et al.*, Phys. Rev. Lett. **95**, 176601 (2005).

[6] S. Gustavsson *et al.*, Phys. Rev. Lett. **96**, 076605 (2006).

[7] J. Tobiska and Yu.V. Nazarov, Phys. Rev. Lett. **93**, 106801 (2004).

[8] A.N. Jordan and E.V. Sukhorukov, Phys. Rev. B **72**, 035335 (2005).

[9] H.A. Kramers, Physica (Utrecht) **7**, 284 (1940).

[10] A.N. Jordan and E.V. Sukhorukov, Phys. Rev. Lett. **93**, 260604 (2004).

[11] J.P. Pekola *et al.*, Phys. Rev. Lett. 95, 197004 (2005).

[12] J. Ankerhold, cond-mat/0607020.

[13] H. Pothier, B. Huard, N. Birge, D. Esteve, unpublished.

[14] S. Pilgram et al., Phys. Rev. Lett. **90**, 206801 (2003).

[15] A.N. Jordan, E.V. Sukhorukov, and S. Pilgram, J. Math. Phys. **45**, 4386 (2004).

Noise in strained-Si MOSFET for low-power applications

K.Fobelets*, J.E. Velázquez†,
*Department of Electrical and Electronic Engineering, Imperial College, Exhibition Road, SW7 2BT London, UK
†Departamento de Física Aplicada, Pza de la Merced s/n, Universidad de Salamanca, E-37008 Salamanca, Spain

This is an example of the format of the abstract for UPoN 2008, which will be held in Lyon from to the 2 to the 6 June 2008. The abstracts have a length of 2 pages maximum, including figures, equations and bibliography.

1 Introduction

MOSFET production reached sub-100 nm dimensions in 2001 by shipping 60-nm transistors in the 130-nm bulk CMOS technology node. Recently, the semiconductor industry leaders have shifted the production to the 45-nm node involving even shorter gate lengths. It was shown that conventional CMOS was impractical for nodes under 130-nm due to heating originated from leakage currents, needs for high-doping in the channel to prevent the threshold voltage roll-off that deteriorate the channel mobility and eventually the overall device performance at high-frequency. The introduction of new alternative technologies to bulk CMOS is a pressing issue. A considerable number of research papers have been published on the possible improvements of n-channel FETs with strained Si channels, both using a buried channel [1] (s-Si MODFET) and a surface channel configuration [2] (s-Si MOSFET). Those technologies have a huge potential for analog and low-power applications. So far minimum noise figures as low as 0.4dB at 2.5GHz and cut-off frequencies (f_T) in excess of 70GHz at 300K have been reported in s-Si MODFET [3]. Encouraging results on the performance of Si/SiGe devices operating in low-power regime when compared with state of the art bulk CMOS [4].

2 Model and Simulated Devices

In this contribution we will report on the calculated noise properties of sub-100nm s-Si MOSFET operating in ultra low-power conditions at room temperature. To this aim we kept the drain to source bias at V_{DS}=50mV and the gate to source bias (V_{GS}) was varied in a voltage range around the threshold voltage (V_{th}). The vertical lay-out of the simulated devices from top to down is: a degenerately doped polysilicon gate, a SiO2 oxide layer, a quantum well (QW), a $Si_{1-x}Ge_x$ set back layer grown on top of the graded virtual substrate and a conventional high-resistivity p-Si wafer. Several gate lengths (L_g) from 100nm to 20 nm and different gating topologies have been considered. Two-dimensional (2D) simulations have been performed using an energy balance transport model incorporating impurity de-ionization, Fermi-Dirac statistics and mobility degradation due to both longitudinal and transverse electric field. For the simulation of the noise in the MOSFETs we adopted the Impedance Field Method with Langevin stochastics noise sources. We assumed that only thermal (diffusive) noise exists and other noise sources originating from processes such as recombination were not considered in this study. The Monte Carlo (MC) method is currently considered the most accurate one to simulate the transport in semiconductor devices at the microscopic level [5]. It can directly provide with the current fluctuations at the device terminals without having recourse to intermediate models like the Impedance Field Method. Nevertheless, the MC method needs long CPU times and it is not well adapted to deal with noise calculation in devices operating in the subthreshold region, like the ones considered in this paper. The model used in the calculations was previously benchmarked to a 2D MC code that has been used to calculate noise in nanometre Double Gate SOI transistors [6].

3 Main Results and Discussion

Fig 1 shows the total gate capacitance and f_T versus V_{GS} for three values of the gate length (the lateral scaling kept constant the thickness of the gate's oxide). This scaling only allows for a modest increase of the transconductance (g_m) when reducing L_g. Nevertheless, maintaining the oxide thickness pays back in terms of the cut-off frequency: as Lg is reduced from 100nm to 20nm the maximum of f_T is doubled (Fig. 1). This enhancement, not found in g_m, is essentially supported by the gate capacitance reduction.

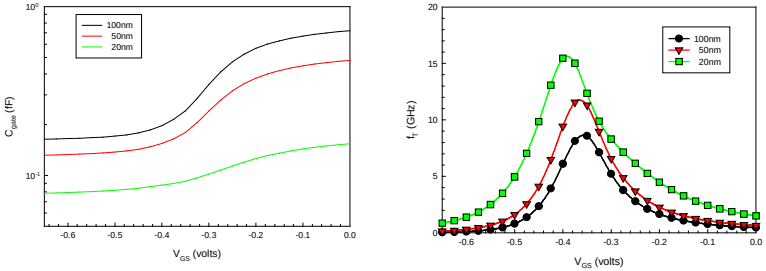

Figure 1. Total gate capacitance (left) and cut-off frequency (right) of the simulated transistors.

In this abstract we will only present some noise results (namely the noise figure, *NF*) that are useful to quick evaluate the analog noise performance of devices. In Fig. 2 we present the *NF* for the devices under study at a frequency of 1GHz. V_{GS} was swept for a few hundreds mV around V_{th} in order to maintain the drain current at values sufficiently low to allow for low-power operation. The minimum of the NF shifts towards lower values of V_{GS} as *Lg* decreases (Fig. 2, left) at a slower pace than the V_{th} roll-off. As a direct consequence of this the *NF* steadily grows when the gate length shrinks for all drain current levels under 1μA (Fig. 2, right). This is a consequence of the combination of the significant resistances across both the intrinsic device and the implanted source and drain regions. Bearing that in mind, we calculated the minimum noise figure (NF_{min}) at the same frequency. Again the shortest transistor (L_g=20nm) exhibited the largest noise value at very low drain currents, in fact, only for drain current values in excess of 0.8μA does the L_g=20nm transistor exhibit the best performance in terms of NF_{min}. This is one of the main result of this paper: there is a trade-off between increasing f_T and obtaining an optimum value of *NF* in the scaling.

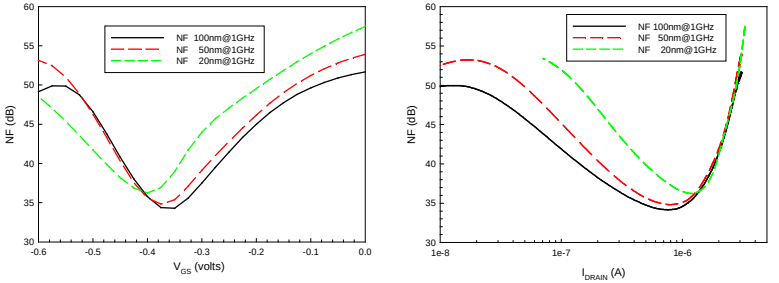

Figure 2. NF plotted against the V_{GS} (left) and the drain current (right) at 1GHz.

References

[1] M. Zeuner, *et al.*, *Jap. J. Appl. Phys.* **42**, pp. 2363-2366 (2003).
[2] S.H. Olsen, *et al.*, *IEEE Trans. Electron Dev.* **50**, pp. 1961-1969 (2003).
[3] F. Aniel, *et al.*, *Solid-State Electronics* **47**, pp. 283-289 (2003).
[4] K. Fobelets, *et al.*, *Solid-State Electronics* **48**, pp. 1401-1406 (2004).
[5] M.J. Martin, D. Pardo, J.E. Velázquez, *J. Appl. Phys* **88**, pp. 1511-1514 (2000).
[6] P. Dollfus, A. Bournel, J.E. Velázquez-Pérez, J. Comp. Electron., **5**, pp. 479-482 (2006).

A Monte Carlo investigation of plasmonic noise in nanometric n-$In_{0.53}Ga_{0.47}As$ channels

J.-F. Millithaler, L. Reggiani
Dipartimento di Ingegneria dell'Innovazione and CNISM,
Università del Salento, Lecce, Italy
J. Pousset, L. Varani, C. Palermo
Institut d'Electronique du Sud, UMR CNRS 5214, Université Montpellier II,
place Bataillon, 34095 Montpellier Cedex 5, France
W. Knap
Groupe d'Etude des Semiconducteurs, UMR CNRS 5650, Université Montpellier II,
place Bataillon, 34095 Montpellier Cedex 5, France
J. Mateos, T. González, S. Perez, D. Pardo
Departamento de Fisicà Aplicada, Universidad de Salamanca,
Pza. Merced s/n, 37008 Salamanca, Spain

Abstract

By numerical simulations we investigate the plasma frequency associated with voltage fluctuations in an n-type $In_{0.53}Ga_{0.47}As$ layer of thickness W and submicron length L embedded in a dielectric medium at T = 300 K. For W = 100 nm and carrier concentrations of $10^{16} - 10^{18}cm^{-3}$ the results are in good agreement with the standard three-dimensional (3D) expression of the plasma frequency. For $W \leq 10$ nm the results exhibit a plasma frequency that depends on L, thus implying that the oscillation mode is dispersive. The corresponding frequency values are in good agreement with the two-dimensionql (2D) expression of the plasma frequency obtained for a collisionless regime within the in-plane approximation for the self-consistent electric field. A region of cross-over between the 2D and 3D behaviors of the plasma frequency, which we address as an open problem, is evidenced for $W > 10$ nm. Problems associated with channel lengths shorter than the electron mean free path and the effects of an applied bias will be discussed.

1 Introduction and conclusions

The spectral density of voltage fluctuations of a homogeneous macroscopic resistor at thermal equilibrium evidences a peak at the classical plasma frequency ω_p when the dielectric relaxation time is shorter than the plasma time

$$\omega_p = \sqrt{\frac{e^2 n_0^{3D}}{m_0 m \varepsilon_0 \varepsilon_{mat}}} \tag{1}$$

with e the electron charge, n_0^{3D} the three-dimensional (3D) average carrier concentration and ε_{mat} the relative dielectric constant of the bulk material, ε_0 the vacuum permittivity, m_0 and m the free and effective electron masses, respectively. For a semiconductor material the plasma frequency can be controlled by an appropriate doping level in such a way to be in the TeraHertz (THz) frequency range. Recently, one of the most promising strategies to obtain THz radiation generation and detection by using electronic systems has been envisaged in exploiting the plasmonic approach. To this purpose, the scaling down of the dimensions to the nanometric length offers more possibility of modulating the value of the plasma frequency and of making use of nano-devices. In this framework, through an analytical approach, it has been considered the case of a two-dimensional electron layer as that constituted by the ungated channel of a nanometric transistor [1]. The electron gas was assumed as highly concentrated but non degenerate, and supposed to undergo only long-range electron-electron interaction. By making a small signal analysis of the self-consistent set of drift and Poisson equations within the in-plane field approximation, and adopting appropriate boundary conditions at the contacts, the electron gas is found to behave as the support of two-dimensional (2D) plasma waves with frequency

$$\omega_p^{2D} = \sqrt{\frac{e^2 n_0^{2D} k}{2 m_0 m \varepsilon_0 \varepsilon_{diel}}} \tag{2}$$

where $k = 2\pi/L$ is the wavevector, n_0^{2D} the average 2D carrier concentration and ε_{diel} the relative dielectric constant of the embedding medium. We notice that the 2D plasma frequency depends on the relative dielectric constant of the external dielectric, thus coupling the source of the fluctuations, due to the free charge, with the external medium. Through the oscillations of the plasma, nanometric High Electron Mobility Transistors (HEMT) have been suggested as possible emitters and detectors of electromagnetic radiation in the THz range [2].

The aim of this work is to investigate the same system from a microscopic point of view thus testing the limits of applicability of the analytical approach and improving the physical insight of the problem. To this purpose, we consider an n-type $In_{0.53}Ga_{0.47}As$ layer embedded in a symmetric dielectric and investigate the plasma frequency characteristics by analyzing the frequency spectrum of voltage fluctuations obtained from a Monte Carlo simulator coupled with a 2D Poissson solver. The microscopic investigation of plasmonic voltage fluctuations in nano channels evidences a complicate scenario Ref. [3], only partly in agreement with the 2D analytical approach of Ref. [1], and with several open problems. Among them, we address the following two: (i) A region of cross-over between the 2D and 3D behaviors of the plasma frequency, which is evidenced for channel width $W > 10$ nm. (ii) The role played by channel lengths shorter than the electron mean free path where transport takes a balistic regime.

References

[1] M. Dyakonov and M. S. Shur, *Appl. Phys. Lett.* **87** 111501 (2005).

[2] J. Lusakowski, W. Knap, N. Dyakonova, L. Varani, J. Mateos, T. González, Y. Roelens, S. Bollaert, A. Cappy, and K. Karpierz,*J. Appl. Phys.* **97** 064307 (2005).

[3] J.-F. Millithaler, L. Reggiani, J. Pousset, L. Varani, C. Palermo, W. Knap, J. Mateos, T. Gonzlez, S. Perez, and D. Pardo *Appl. Phys. Lett.* **92** 042113 (2008).

Noise of hot electrons in anisotropic semiconductors in the presence of a magnetic field

Francesco Ciccarello, Salvatore Zammito, and Michelangelo Zarcone
CNISM and Dipartimento di Fisica e Tecnologie Relative
Università degli Studi di Palermo, Viale delle Scienze, Edificio 18, I-90128 Palermo, Italy

Investigation of hot-electron noise in semiconductor compounds provides a well-known example of a problem which has toughly resisted analytic solutions. This is due to the formidable mathematical difficulties that arise when one attempts to solve the Boltzmann equation in the regime of high electron energies, when the system behaviour is markedly nonlinear. From the technologic perspective, the matter is of obvious interest due to the progressive miniaturization of semiconductor devices. In addition, the simultaneous interplay between different scattering mechanisms and the external applied fields, together with the peculiar structure of the conduction band at high energies, can give rise to non-trivial and very intriguing physics. The last years have witnessed a wide success of the Monte Carlo (MC) method as a powerful tool to approach such problem. A direct MC simulation of electron motion indeed represents an effective numerical solution of the Boltzmann equation. Despite the large amount of work carried out in order to characterize electron noise in the presence of applied electric fields, the case when a magnetic field is simultaneously present has been seldom addressed [1]. This is probably due to the fact that at the time when most of the MC studies on noise in semiconductor compounds were performed (see [2] and references therein) only relatively weak magnetic fields were experimentally available. Indeed, in order to observe effects competing with those induced by electric fields of the order of several kV/cm, rather intense magnetic field strengths of the order of some T are needed [3]. This is especially true for compounds such as Si having relatively high effective electron masses and thus requiring rather strong magnetic fields in order to exhibit significant cyclotron frequencies. However, present-day superconductor magnetic-field generators allow to produce fields of the order of many T. With these motivations in mind, two of us have recently investigated hot-electron noise in n-GaAs in crossed electric and magnetic fields [3]. Velocity noise spectra and correlation functions were shown to be affected in a nontrivial way in the regime when the electric and magnetic fields are competing. Among the most relevant effects are signatures of nonparabolicity, magnetic-induced cooling of electron fluctuations and, in particular, a peculiar change in the noise spectrum in the passage through the Gunn threshold[3].

Here, our aim is to perform the above analysis in n-Si. Such a task is far from being a mere academic extension of our previous studies. Indeed, apart from being the most common semiconductor, Si, unlike GaAs, offers a valid test-bed for investigating how effective-mass anisotropy affects noise under such conditions. This provides the intriguing opportunity of investigating how *both* electric *and* magnetic-field directionality affects fluctuations. The effective-mass anisotropy clearly gives rise to anisotropy in the cyclotron motion. Two cyclotron frequencies, explainable as due to the longitudinal and transverse masses, indeed appear as peaks in the noise spectrum in the case when the electric and magnetic fields are directed along the [100] and [001] directions, respectively. Interestingly, for moderate and very intense electric field strengths both frequencies are present and absent, respectively. However, as the electric field grows up, in passing from the former to the latter regime the frequencies disappear in turn. First the lowest, then the highest. The most interesting, and problematic, case takes place however when the electric is directed along the [111] direction. Here, our analysis indicates that the simultaneous presence of the magnetic field appears to enhance the intrinsic anisotropy of the material with non-trivial consequences on the features of electron noise. We aim at putting such effects to the attention of the community in order to come to a full clarification as well as to assess whether they can be exhibited by systems of a different nature.

References

[1] A. D. Boardman, W. Fawcett, and J. G. Ruch, Phys. Stat. Sol. (a), **4**, 133 (1971); R.S. Brazis, E.V. Starikov, and P.N. Shiktorov, Sov. Phys. Semicond. , **16**, 1002 (1982); R. S. Brazis, E. V. Starikov, and P. N. Shiktorov, Sov. Phys. Semicond., **17**, 8 (1983); P. Warmenbol, F. M. Peeters, J. T. Devreese, G. E. Alberga, and R. G. van Welzenis, Phys. Rev. B, **31**, 5285 (1985); P. Warmenbol, F. M. Peeters, and J. T. Devreese, Phys. Rev. B, **33**, 1213 (1986); A. D. Djikstra, Appl. Phys. Lett., **4**, 133 (1998); J. D. Albrecht, P. P. Ruden, E. Bellotti, and K. F. Brennan, MRS Internet J. Nitride Semicond. Res. 4S1, G6.6 (1999).

[2] C. Jacoboni and L. Reggiani, Rev. Mod. Phys. **55**, 645 (1983); C. Jacoboni and P. Lugli, *The Monte Carlo Method for Semiconductor Device Simulation* (Springer-Verlag, Berlin, 1989).

[3] F. Ciccarello and M. Zarcone, J. Appl. Phys. **99**, 113702 (2006); *Unsolved Problems of Noise and Fluctuations*, ed. by L. Reggiani *et al.*, AIP Conf. Proc. **800**, 492 (2005); *Noise and Fluctuations*, ed. by T. Gonzalez *et al.*, AIP Conf. Proc. **780**, 159 (2005).

1/f Noise in systems with multiple transport mechanisms

C. D. Mukherjee and K. K. Bardhan
Saha Institute of Nuclear Physics
1/AF Bidhannagar, Kolkata 700 064, INDIA

In recent years with advent of several complex systems such as mangenites, conducting polymers etc., the use of noise as a tool to gain further understanding of transport mechanisms has increased manifold. The new systems often have phases with varying degree of disorder and exhibiting more than one type of conduction mechanism. It will be then desirable to have a *systematic* study of how properties of noise may vary in course of transition from one phase to another.

For this purpose we chose two composite systems, carbon-wax (C-W) and carbon-high density polyethlyne (C- HDPE) for measurements. These systems have been recently shown to have several phases in the field-composition (F-p) plane (Fig 1)[1]. The phases are somewhat simple, induced by geometry rather than brought about by any competitive energy scales. The phases are characterized by the response to an applied electric field: dR/dF<0 in tunneling phase; dR/dF=0 in linear phase and dR/dF>0 in Joule phase. Here R is resistance and F is the field. Moreover, a composite system is a prototype of percolating system[2] which has been invoked in a great variety of physical systems. Thus knowledge of a pure percolating system will be useful to analyse data in a more complex environment.

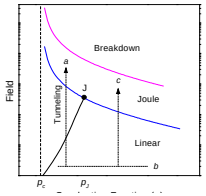

Fig. 1

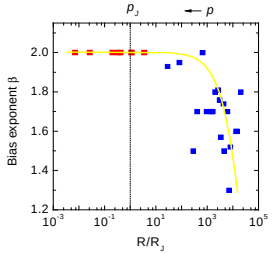

Fig. 2

Fig. 1: A schematic conduction phase diagram in the field-fraction (F-p) plane of a composite showing four regions as labeled. p_c is the percolation threshold. The three dotted lines represent measurement paths.

Fig. 2: The bias exponent as a function of sample resistance related to the fraction as $R\sim(p-p_c)^{-t}$, t being the conductivity exponent.

Noise is conveniently discussed by using an extended form of Hooge relation for the spectral power density S_V [3]:

$$S_V = aV^{\beta} \; R(\mathrm{R})/f^{\alpha} \qquad (1)$$

where a is the Hooge constant and R is a function of resistance in case of non-Ohmic conduction. In case of paths a or b we find that the frequency exponent α as a function of field / resistance suffers an abrupt change in value from about 1.17 to 1.45 signifying the change of tunneling regime to joule regime. Another interesting systematic variation takes place in the bias exponent β shown in Fig. 2 as the conducting fraction is decreased to the threshold or conversely, sample resistance increases. The value starting from the usual value of 2 progressively decreases as the system moves deeper and deeper into the tunneling regime. This is UPoN ! There are similar variation in the functional form of noise power – from power-law to polynomial – as the system moves from tunneling to joule regime. The issue of dissipation-less conduction will be examined while comparing with other systems such as variable range hopping systems.

References

[1] C D Mukherjee, K K Bardhan, M B Heaney, *Phys. Rev. Lett.* **83,** 1215 (1999).

[2] D Stauffer and A Aharony, *Introduction to percolation theory*, Taylor and Francis, London, 2nd Ed., 1992.

[3] K K Bardhan, C D Mukherjee and U N Nandi, AIP Conf. Proc. **800**, 109 (2005).

Latent Noise in Schottky Barrier MOSFETs

Sheng-Pin Yeh, Chun-Hsing Shih*, Jeng Gong, and Chenhsin Lien

Institute of Electronics Engineering, National Tsing Hua University, Hsinchu 300, Taiwan

*Department of Electrical Engineering, Yuan Ze University, Taoyuan 320, Taiwan, Email: chshih@saturn.yzu.edu.tw

By eliminating the constraints on the implanted ultra-shallow source/drain junctions, the metallic Schottky barrier source/drain MOSFETs (Fig. 1) become one of the most promising candidates for next generations CMOS devices [1, 2]. Several literatures using silicidation with (or without) Dopant Segregation (DS) had demonstrated their superior performance to the conventional MOSFETs [3-5], and their serving as high speed RF devices [5, 6]. However, since the Schottky barrier MOSFETs exhibit the unique conductions against the traditional MOSFETs, the sound examinations of noise in Schottky barrier MOSFETs become relatively troublesome and require further intense studies.

Fig. 2 illustrates the typical current-voltage (I-V) curves and the energy band diagrams of the Schottky barrier NMOSFETs. Different from the traditional MOSFETs, the moblie carriers can thermonicly emit over or laterally tunnel through the Schottky barrier with twofold subthreshold slopes of drain current. The effective Schottky barrier heights are varied as the applied gate voltage. The heavily doped layer segregated during silicidation can be adopted to modify the Schottky tunneling behavior [5, 7]. Note that the Schottky barrier MOSFETs present the ambipolar conduction as function of gate voltage [5, 7]. For positive (negative) bias, electrons (holes) are inverted (accumulated) to conduct the Schottky barrier channel. Formation of the metallic source/drain using silicidation process brings about the interface defects and the surface states generations [8] (Fig. 3). The distinguishing noise is observed for Schottky barrier MOSFETs either in inversion or accumulation [9, 10] (Fig. 4). The use of the interfacial layers [5, 11] to enhance the drain current, such as dopant segregation, is expected to aggravate further concerns on the noise.

Due to the complicate parasitic components and conduction mechanisms during device operations, the noise problems in Schottky barrier MOSFETs are really unsolved and require thorough investigations. Most concerns and possible mechanisms of noise are summarized below, and shown in Fig. 5.

1. Excepting the number fluctuation noise (due to the traps in the gate oxide) and the channel mobility fluctuations dominated the 1/f noise in traditional MOSFETs, the trap states at silicides/Si substrate interfaces should play the more important roles on the noise in Schottky barrier MOSFETs.
2. Since the hot carriers and the impact ionizations occurred near source in Schottky barrier MOSFETs [12], the number fluctuation noise is different to that of traditional MOSFETs. It will be deteriorated without the screening of the drain field.
3. Consider the ambipolar conduction in Schottky barrier MOSFETs, the trap levels in full bandgap will exacerbate a more noisy devices. Importantly, the Fermi level pinning in Schottky source/drain barriers are dependent upon the varied gate voltage during device switching.
4. Excluing surface channel, Schottky barrier diodes or nonrectifying contacts are also vertically formed at the metallic source/drain region. The presences of the trap states in the depletion region of the reversely biased junctions will lead to G-R noise, which might be minimized using SOI or double gate structures.
5. Furthermore, noise behaviors are affected by the process variations in a variety of metal silicides and dopant impurities during silicidation and segregation. However, the generation mechanisms of the interface traps incorporated with dopant segregation are not well examined previously.

References

[1] ITRS, International Technology Roadmap for Semiconductors (2003).
[2] K. Saraswat, lecture notes in IEDM Short Course (2007).
[3] J. M. Larson and J. P. Snyder, IEEE Trans. Electron Devices, vol. 53, p.1048 (2006).
[4] M. Zhang et al., IEEE Electron Device Lett., vol. 28, p.223 (2007).
[5] G. Larrieu et al., IEDM, p.147 (2007)
[6] M. Fritze et al., IEEE Electron Device Lett., vol. 25, p.220 (2004).
[7] J. Knoch et al., Appl. Phys. Lett., vol. 87, p. 263505 (2005).
[8] G. Larrieu et al., IEEE Trans. Electron Devices, vol. 52, p.2720 (2005).
[9] T. Asano et al., Jpn. J. Appl. Phys., vol. 41, p.2306 (2002).
[10] M. V. Harrtman et al., ICNF, p.307 (2005).
[11] D. Connelly et al., Appl. Phys. Lett., vol. 88, p.0121051 (2006).
[12] K. Uchida et al., Appl. Phys. Lett., vol. 76, p. 3992 (2000).

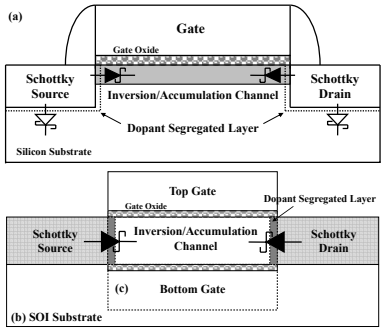

Fig. 1: Schematic view of (dopant segregated) Schottky barrier MOSFETs (a) Bulk MOSFET, (b) SOI MOSFET, and (c) Double Gate MOSFET.

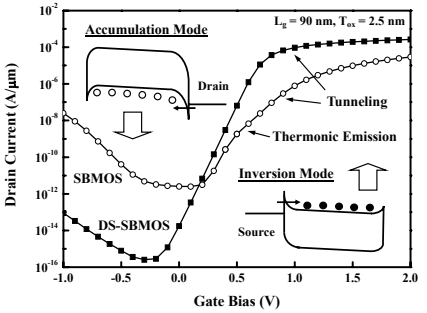

Fig. 2: Numerical illustrations of thermonic emission, barrier tunneling and ambipolar conduction for Schottky barrier NMOSFETs.

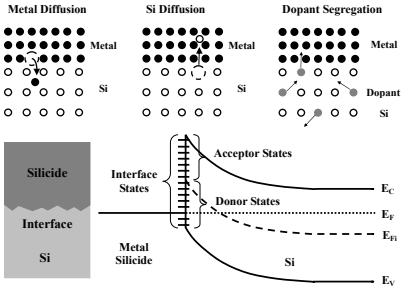

Fig. 3: Defects and interface states generated during metal silicidation and dopant segregation [8].

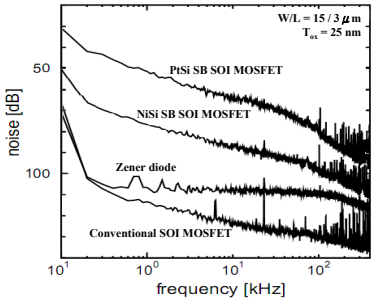

Fig. 4: Noise spectra in conventional SOI MOSFET, and NiSi, PtSi Schottky barrier SOI MOSFETs [9].

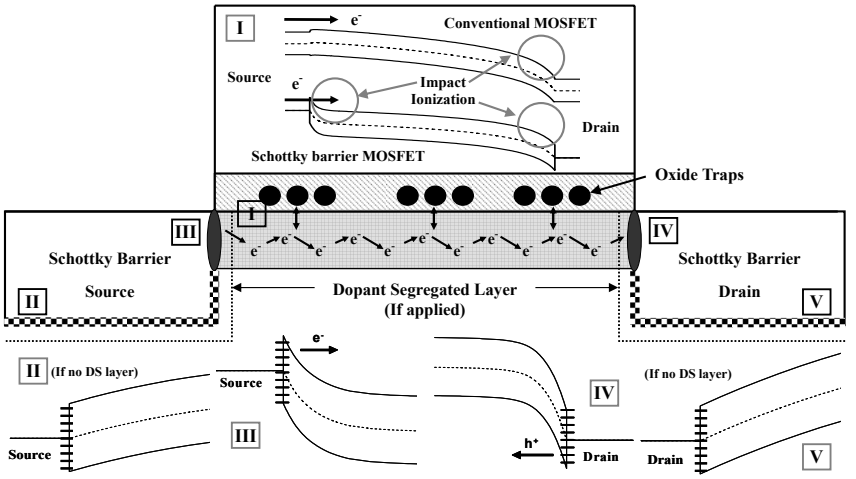

Fig. 5: Possible mechanisms of the noise in Schottky barrier MOSFET (NMOSFET as an example).

Correlated avalanches in TES noise power spectra

E.Celasco[c], D.Bagliani[a,b], M.Celasco[a], R.Eggenhöffner[a], F.Gatti[a,b], L.Ferrari[a,b], R.Valle[a,b]

[a]Dipartimento di Fisica, via Dodecaneso 33, 16146 Genova, Italy
[b]INFN of Genoa, via Dodecaneso 33, 16146 Genova, Italy
[c]Dipartimento di Fisica, Laboratorio Materiali e Microsistemi (χlab) – Unità LATEMAR, Politecnico di Torino, corso Duca degli Abruzzi 24, 10129 Torino, Italy

Superconducting transition edge sensors (TES) at temperatures below 100 mK are involved as fast and sensitive cryogenic microcalorimeters or bolometers for high resolution X-ray and single photon spectroscopy and for the detection of submillimiter and IR radiation [1]. Their detection limit is influenced by the thermal fluctuation noise beyond the Johnson and SQUID amplifier contributions to global noise power. Voltage fluctuations in superconductors were attributed temptatively to the thermal link with the radiation absorber thin film [2].

Occurrences of weak thermal links with substrates were observed in superconducting thin films. Excess noise was detected in MgB_2 thin films well below the transition temperature T_c, due to correlated fluxon avalanches, originated by thermomagnetic instabilities [3]. At temperatures $T<<T_c$, avalanches propagate through the thin film geometry with the typical features of dendritic structures. In the frequency behaviour of the noise power spectrum, a wide peak superimposed to the 1/f and other noise sources was attributed to avalanche correlation [4].

In the present work we investigate the excess noise observed in TES devices as reported by many Authors [5-6]. This noise has been characterized in detail and it has been observed by numerous groups using TES made in very different ways, but the origin of this unexplained noise is still unsolved [7,8]. The main features to be explained are twofold and concern:

a) the wide peaks in the power spectrum in the range 1-10 kHz as reported in Fig.1
b) a peak in the behaviour of noise vs the normalized electrical resistance R/R_n as reported in Fig.2.

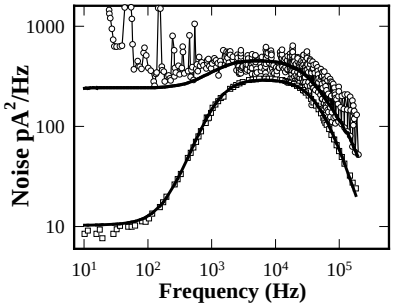

Fig. 1 Current noise power spectrum vs frequency in a Ti/Au TES device. The best fit solid curves account for quantitatively the experimental excess noise (squares) and the global noise (circles and thin line) from ref.5 and 8. The best fit curves (thick lines) are obtained with the model parameters s=1.25, $\rho\tau_0$ = 20 μs and ν_g=1200 Hz.

We explain the experimental wide peaks concerning a) in terms of our statistical model in which noise is given by sequences of generalized elementary events, by elementary events clustered in avalanches and by correlation among avalanches. In Fig.1 we report the excellent fitting of the excess and of the global noise frequency behaviour in a Ti/Au thin film. We estimate from model parameters that small mean avalanches of 20 fluxons (elementary events) and shorter elapsing timings between subsequent avalanches than in other superconductors are involved in wide peak noise processes. Since TES are operated far from equilibrium among the superconducting film, the substrate and the radiation detector, it turned out difficult to apply microscopic theories to explain noise from TES [5]. Further, the complex interactions between magnetic fields, bias current flow and the superconducting phase make it difficult to understand the internal state within the TES. In our previous investigations on superconducting thin films, the wide peaks in the power spectra vs frequency were obtained in the dendritic regime, i.e. at temperatures close to $T_c/3$, approximately.

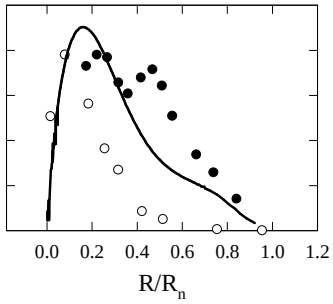

Fig. 2 Experimental excess noise (in a.u.) of a TES device (black circles) vs the normalized resistance in comparison to the behaviours from simulations from ref.7 and 9 (open circles and full line, respectively).

In operative conditions, the internal state of the superconducting portion of the device switches between the normal and the superconducting state, suggesting a percolation model as an alternative phenomenological representation of the complex thermal and electrical dynamics.

The experimental results, obtained from a series of TES impedance and noise measurements concerning b) are reported in Fig.2 (full circles). In the same figure we have reported results from simulations of the TES as a 2D network of resistive elements [7, open circles] and from a 3D network [9, full line] of resistors some of which are randomly shorted (random resistor network RRN). With respect to usual percolative approaches, we introduced in our dynamical percolative model [9], a correlation between two subsequent network configurations and we considered the entire sequence of networks as representative of the time evolution of the system.

The relationship between correlated avalanches of fluxons and correlated networks of weak-links is still an intriguing topic to be answered to pull down the excess noise in TES devices.

References

[1] H.F.C.Hoevers, A.C.Bento, M.P.Bruijn, L.Gottardi, M.A.N.Korevaar, W.A.Mels and P.A.J. de Korte, Appl. Phys. Lett. 77, 4422 (2000)
[2] A.Luukanen, K.M.Kinnunen, A.K.Nuottajärvi, H.F.Hoevers, W.M.Bergmann Tiest, and J.P.Pekola, Phys. Rev. Lett. 90, 238306 (2003)
[3] R.Eggenhöffner, E.Celasco, V.Ferrando, M.Celasco, Appl. Phys. Lett. 86, 022504 (2005)
[4] R.Eggenhöffner, E.Celasco, M.Celasco, Fluctuation and Noise Letters 7, L351 (2007)
[5] H.F.C.Hoevers, M.P.Bruijn, B.P.F.Dirks, L.Gottardi, P.A.J. de Korte, J.van der Kuur, A.M.Popescu, M.L.Ridder, Y.Takei, D.H.J.Takken, J.Low Temp.Phys. (2008) DOI- 10.1007/s10909-007-9633-1
[6] K.D.Irwin and G.C.Hilton, *Cryogenic Particle Detection*, C. Enss (Ed.), Topics Appl. Phys. 99, 63-149 (2005), Springer-Verlag Berlin Heidelberg 2005
[7] M.A.Lindeman et al., Nucl. Instrum. Methods. A559, 715 (2006)
[8] J.N.Ullom, W.B.Doriese, G.C.Hilton, J.A.Beall, S.Deiker, W.D.Duncan, L.Ferreira, K.D.Irwin, C.D.Reintsema, and L.R.Vale, Appl. Phys. Lett. **84**, 4206 (2004)
[9] M.Celasco, R.Eggenhöffner, E.Gnecco and A.Masoero, Phys. Rev. B58, 6633 (1998)

Quantum noise and coherence

Xavier Oriols
High frequency noise in mesoscopic conductors:
A novel algorithm for the self-consistent computations of particle and displacement currents with quantum trajectories 60

Julien Gabelli
Dynamics of Quantum Noise in a Tunnel Junction under ac Excitation 61

Tomas Novotný
Josephson junctions as detectors of the Full Counting Statistics: Theoretical issues and analysis of experiments 62

High frequency noise in mesoscopic conductors: A novel algorithm for the self-consistent computations of particle and displacement currents with quantum trajectories

X.Oriols and A.Alarcón
Departament d'Enginyeria Electrònica, ETSE
Universitat Autònoma de Barcelona,
08192, Bellaterra, Barcelona, SPAIN

In the DC (or zero frequency) regime of mesoscopic conductors the noise can be computed from the fluctuations of the rate at which electrons cross a given plane. However, in the high-frequency regime, one must go deeper into the meaning of current measurement. The experimental current density is not only the particle current density, $\vec{J}_p(\vec{r},t)$, but also the displacement current density, $\vec{J}_d(\vec{r},t)$, proportional to the time-dependent variations of the electric field. The total current density, $\vec{J}(\vec{r},t)=\vec{J}_p(\vec{r},t)+\vec{J}_d(\vec{r},t)$, is what is measured in the amperimeter located far from the active region of the conductor because it fulfills a conservation law, $\vec{\nabla}\cdot\vec{J}(\vec{r},t)=0$. As a consequence, the total current evaluated on a given plane inside the conductor are equal to that in the amperimeter (this is not true for the time-dependent particle current alone)

In general, most noise quantum theories for mesoscopic conductors use non-interacting electron models. These theories are incompetent to deal with high-frequency regimes of mesoscopic systems because they fail to achieve the total current conservation [1,2]. In order to ensure the conservation of the total current, one has to deal with the self-consistent solution of the Poisson equation (representing electron-electron interactions) together with a many-particle Schrodinger equation. In fact, due to the computational difficulty in directly following this path, the development of a general framework for modeling high frequency noise on mesoscopic conductors still remains an **unsolved problem**. In this conference, we propose a general and versatile solution to this problem.

2 Quantum dynamics of many-particle systems

The time-dependent evolution of a system of *N* (coulomb- and exchange-) interacting electrons is described by the following many-particle Schrödinger equation:

$$i\mathrm{h}\frac{\partial\Phi(\vec{r}_1,...,\vec{r}_N,t)}{\partial t}=\left\{\sum_{a=1}^{N}-\frac{\mathrm{h}^2}{2\cdot m}\nabla_a^2+U(\vec{r}_1,...,\vec{r}_N,t)\right\}\Phi(\vec{r}_1,...,\vec{r}_N,t) \quad (1)$$

where $\vec{r}_1,...,\vec{r}_N$ are positions of the *N* electrons. The potential energy $U(\vec{r}_1,...,\vec{r}_N,t)$ takes into account the Coulomb interaction among all electrons and the role of an external battery. However, from a computational point of view, the direct solution of equation (1) is inaccessible because (for a real space with N_L points) it implies manipulating matrixes of N_L^{3N} elements.

Alternatively, it is well-known that an "infinite" set of Bohm trajectories extracted from equation (1) do exactly reproduce the mean results obtained from $\Phi(\vec{r}_1,...,\vec{r}_N,t)$ and its fluctuations (through the uncertainty on the initial conditions of each many-particle Bohm trajectory). In principle, the computation of such quantum trajectories does also deal with the same size of matrixes. However, we have recently shown [3] that many-particle Bohm trajectories associated to (1) can be computed from a (coupled) system of single-particle time-dependent Schrödinger equations whose numerical complexity is just $N\cdot N_L^3$:

$$i\mathrm{h}\frac{\partial\Psi_a(\vec{r}_a,t)}{\partial t}=\left\{-\frac{\mathrm{h}^2}{2\cdot m}\nabla_a^2+U(\vec{r}_1[t],..,\vec{r}_a,..,\vec{r}_N[t],t)+G_a(\vec{r}_a,t)+i\cdot J_a(\vec{r}_a,t)\right\}\Psi_a(\vec{r}_a,t) \quad (2)$$

where $\{\vec{r}_1[t],...,\vec{r}_N[t]\}$ are the set of *N* Bohm trajectories. The terms $G_a(\vec{r}_a,t)$ and $J_a(\vec{r}_a,t)$ are additional potential energies whose exact value is unknown, but that can be estimated through educated guesses [3].

3 Self-consistent computations of particle and displacement currents

In this conference, we extend the work presented in [3] to high frequency regime. The relevant point of our proposal is that the evaluation of $U(\vec{r}_1[t],..,\vec{r}_a,..,\vec{r}_N[t],t)$ in (2) at each time step involves only N_L^3 variables, since all positions are fixed except $\vec{r}_a$. Therefore, this term can be related to a 3D Poisson equation where the charge density for each $\vec{r}_a$-electron is related to all Bohm trajectories except $\vec{r}_a[t]$. Then, $\vec{J}_d(\vec{r},t)$ is related (self-consistently) to the temporal variations of $U(\vec{r}_1[t],..,\vec{r}_a,..,\vec{r}_N[t],t)$ and $\vec{J}_p(\vec{r},t)$ to the velocity of these Bohm trajectories. From a numerical point of view, rather than directly computing the total current *I(t)* at one plane, it is more appropriate to use a quantum version of Ramo-Shockley theorem [4] through a volume Ω limited by a surface *S* :

$$I(t)=-\int_{\Omega}\vec{F}(\vec{r})\cdot\vec{J}_p(\vec{r},t)\cdot d^3\vec{r}+\int_{S}\vec{F}(\vec{r})\cdot\varepsilon(\vec{r})\cdot\frac{\partial}{\partial t}A_o(\vec{r},t)\cdot d\vec{s} \quad (3)$$

where $\vec{F}(\vec{r})$ is a particular solution of Laplace equation [4], $\varepsilon(\vec{r})$ is the electric permittivity and $A_o(\vec{r},t)$ is related to all the terms $U(\vec{r}_1[t],..,\vec{r}_a,..,\vec{r}_N[t],t)$ in the coupled system of equations (2).

The high-frequency power density of the current fluctuations (or higher order cumulants) are numerically obtained directly from the total current *I(t)*, computed in (3), after using autocorrelation and Fourier transform tools. The algorithm is useful for 3D systems with *N* around 100 electrons. As a relevant example, in the conference we will show numerical data testing the importance of the self-consistent simulation of $\vec{J}_d(\vec{r},t)$ and $\vec{J}_p(\vec{r},t)$ for the high-frequency noise of a double/triple barrier structure that is driven by a gate voltage working at hundreds of GHz.

4 Conclusions

Due to its computational difficulty, the development of a general framework for modeling high frequency noise on mesoscopic conductors still remains an **unsolved problem**. In this conference we present a new and versatile approach for the self-consistent simulation of particle plus displacement currents. The self-consistent coupling between the electron dynamics obtained from equation (2) and the electrostatic potential (obtained from the 3D Poisson equation) is achieved by using quantum (Bohm) trajectories [3] . Our approach allows accurate simulations of quantum THz nanoelectronics proposals and reveals information about internal time (energy) scale of mesoscopic systems, not available from previous DC (non-interacting) transport models.

References

[1] Ya. M. Blanter and M. Büttiker, Phys. Rep. 336, 1 (2000).

[2] Paraphrassing Rolf Landauer : «There are too many offenders to list, and it seems unfair to list out a few ». R.Landauer Physica Scripta T 42, 110 (1992).

[3] X.Oriols, Physical Review Letters, 98, 066803 (2007).

[4] X.Oriols A. Alarcón and E. Fernandez-Díaz, Physical Review B, 71, 245322 (2005).

Dynamics and Third Cumulant of Quantum Noise

J. Gabelli and B. Reulet
Laboratoire de Physique des Solides,
UMR8502 bâtiment 510, Université Paris-Sud 91405 ORSAY Cedex, France

The existence of the third cumulant S_3 of voltage fluctuations has demonstrated the non-Gaussian aspect of shot noise in electronic transport. Until now, measurements have been performed at low frequency, *i.e.* in the classical regime $\hbar\omega < eV, k_BT$ where voltage fluctuations arise from charge transfer process [1, 2]. We report here the first measurement of S_3 at high frequency, in the quantum regime $\hbar\omega > eV, k_BT$. In this regime, experiment cannot be seen as a charge counting statistics problem anymore. It raises central questions of the statistics of quantum noise, in particular:

1. The electromagnetic environment of the sample has been proven to strongly influence the measurement, through the possible modulation of the noise of the sample [1]. What happens to this mechanism in the quantum regime?

2. For $eV < \hbar\omega$, the noise is due to zero point fluctuations and keeps its equilibrium value: $S_2 = G\hbar\omega$ with G the conductance of the sample. Therefore, S_2 is independent of the bias voltage and no photon is emitted by the conductor. It is possible, as suggested by some theories [5, 6], that $S_3 \neq 0$ in this regime?

With regard to these questions, we give theoretical and experimental answers to the environmental effects showing they involve dynamics of the quantum noise. Using these results, we investigate the question of the third cumulant of quantum noise in the a tunnel junction.

1 Dynamics of Quantum Noise in a Tunnel Junction under ac Excitation

In the same way as the complex ac conductance $G(\omega_0)$ of a system measures the dynamical response of the *average* current to a small voltage excitation at frequency ω_0, we investigate the dynamical response of current fluctuations $\chi_{\omega_0}(\omega)$, that we name *noise susceptibility*. It measures the in-phase and out-of-phase oscillations at frequency ω_0 of the current noise spectral density $S_2(\omega)$ measured at frequency ω.
We present the first measurement of the noise susceptibility, in a tunnel junction in the quantum regime $\hbar\omega \sim \hbar\omega_0 \gg k_BT$ ($\omega/2\pi \sim 6\,\mathrm{GHz}$ and $T \sim 35\,\mathrm{mK}$) [3]. We observe that the noise responds in phase with the excitation, but not adiabatically. The results are in very good, quantitative agreement with our prediction based on a new current-current correlator that we calculate for a coherent conductor at arbitrary frequencies in the scattering matrix formalism [4]:

$$\chi_{\omega_0}(\omega) \propto \langle i(\omega) i(\omega_0 - \omega)\rangle \tag{1}$$

We show that the noise susceptibility is a central concept in the understanding of environmental effects on quantum transport. In particular, we reformulate the Dynamical Coulomb Blockade in terms of the noise susceptibility at $\omega_0 = \omega$ providing a natural extension to existing results.

2 Quantum Noise Fluctuations

The current fluctuations are usually characterized by their spectral density $S_2(\omega) = \langle i(\omega) i(-\omega)\rangle$ measured at frequency ω but are fully described by the whole of cumulants $S_n(\omega_1, ..., \omega_{n-1})$, $n \geq 2$ related to high order correlations. Whereas book knowledge is that the measurable spectral density of a current operator $\hat{i}$ is the symmetrized noise correlator, i.e. $S_2^{(meas.)}(\omega) = 1/2\,\langle \hat{i}(\omega)\hat{i}(-\omega) + \hat{i}(-\omega)\hat{i}(\omega)\rangle$, measurements of higher order cumulants are pointing out the problem of appropriate symmetrization.
We have investigated the third cumulant $S_3(\omega, 0)$ of the voltage fluctuations of a tunnel junction in the quantum regime. The experimental setup is based on "classical" detection scheme using linear amplifiers (see Fig. 1a)) and the results are in qualitative agreement with theoretical results: $S_3(\omega, 0)$ remains proportional to the average current and is frequency independent [5, 6].
Nonetheless, this result asks the intriguing question of the possibility to measure a non-zero third cumulant in the quantum regime $\hbar\omega > eV$, whereas the noise $S_2(\omega)$ is the same that at equilibrium and given by the zero-point fluctuations. It is pointing out the consequences of the detection scheme on the outcome of the measurement. Indeed, contrary to the "classical" detection scheme (see Fig. 1a)), it is clear that a detection involving a photodetector (see Fig. 1b)) would give $S_3 = 0$ for $eV < \hbar\omega$ owing to the lack of photon emission.

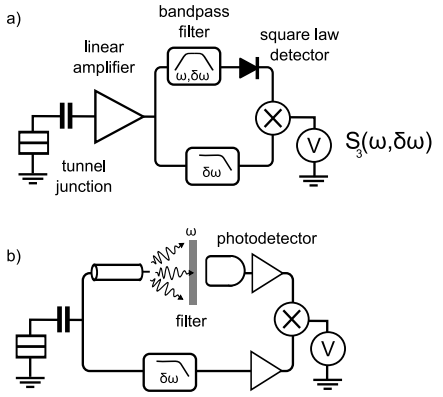

Figure 1: (a) Experimental detection scheme. The symbol $\otimes$ represents a multiplier, which output is the product of its two inputs. The diode symbol represents a square law detector, which output is proportional to the low frequency part of the square of its input. $S_3(\omega, \delta\omega \to 0)$ is given by the product of the square of high frequency fluctuations with low frequency fluctuations. (b) Equivalent detection scheme using a photodetector to measure square of high frequency fluctuations.

References

[1] B. Reulet, J. Senzier and D. E. Prober, Environmental Effects in the Third Moment of Voltage Fluctuations in a Tunnel Junction, *Phys. Rev. Lett.* **91** pp. 196601 (2003)

[2] Yu. Bomze, G. Gershon, D. Shovkun, L. S. Levitov and M. Reznikov, Measurement of Counting Statistics of Electron Transport in a Tunnel Junction, *Phys. Rev. Lett.* **95** pp. 176601 (2005)

[3] J. Gabelli and B. Reulet, Dynamics of Quantum Noise in a Tunnel Junction under ac Excitation, *Phys. Rev. Lett.* **100** pp. 026601 (2008)

[4] J. Gabelli and B. Reulet, The Noise Susceptibility of a Photo-excited Coherent Conductor, *arXiv* 0801.1432 (2008)

[5] A. Galaktionov, D. Golubev, and A. Zaikin, Statistics of current fluctuations in mesoscopic coherent conductors at nonzero frequencies, *Phys. Rev. B* **68** pp. 235333 (2003)

[6] J. Salo, F. W. J. Hekking, and J. P. Pekola , Frequency-dependent current correlation functions from scattering theory, *Phys. Rev. B* **74** pp. 125427 (2006)

Josephson Junctions as Threshold Detectors of the Full Counting Statistics

Tomáš Novotný

Department of Condensed Matter Physics, Faculty of Mathematics and Physics, Charles University, Prague, Czech Republic

Josephson junctions were theoretically proposed as threshold detectors of the Full Counting Statistics (FCS) several years ago [1, 2]. Since then there have been increasing efforts to implement the concept [3, 4] as well as to refine and extend the original theory to experimentally more relevant cases [5, 6]. Despite this intensive effort, the initial promises associated with the method haven't been realized yet.

I will review the present experimental and theoretical status of the field and afterwards I will mainly focus on the critical evaluation of the existent theories with respect to their apparent failure to give quantitative account of the experimental findings. I will argue that the persistent discrepancy is most likely due to insufficient precision of the evaluation of the escape rates under the influence of the non-Gaussian noise. Evaluation of the exponential prefactor of the escape rates seems to be the next goal which should be addressed by the theorists in order to achieve quantitative comparison with the experimental results.

Despite the fact that conceptually the problem of escape rates due to non-Gaussian noise was addressed decades ago (see Ref. [7] and references therein) the present problems stem from the necessity to perform calculations in experimentally relevant regime with stringent accuracy which pushes us beyond the achieved results and calls for the development of new insights and efficient methods. In view of these difficulties the suitability of the threshold detection of FCS, especially with Josephson junctions, may need to be reevaluated.

References

[1] J. Tobiska and Yu.V. Nazarov, *Phys. Rev. Lett.* **93**, 106801 (2004)
[2] J. Pekola, *Phys. Rev. Lett.* **93**, 206601 (2004)
[3] A. V. Timofeev *et al.*, *Phys. Rev. Lett.* **98,** 207001 (2007)
[4] B. Huard *et al.*, arXiv:0711.0646v1, to appear in *Annalen der Physik*
[5] J. Ankerhold, *Phys. Rev. Lett.* **98**, 036601 (2007)
[6] E.V. Sukhorukov and A. N. Jordan, *Phys. Rev. Lett.* **98**, 136803 (2007)
[7] P. Hänggi, P. Talkner, and M. Borkovec, *Rev. Mod. Phys.* **62**, 251 (1990)

Theoretical trends in fluctuations

Roberto Benzi – **Keynote Lecture**
Stochastic Resonance in complex systems *64*

Eric Vanden-Eijnden – **Keynote Lecture**
Pathway of maximum likelihood of rare noise-induced events *65*

Peter M. Kotelenez
Brownian noise and the depletion phenomenon *66*

Eli Barkai
Weakly Non-ergodic Noise: From Blinking Qunatum Dots to mRNA diffusing in a cell *67*

Giuseppe Gonnella
Heat fluctuations in systems in contact with heat baths at different temperatures *68*

Stochastic Resonance in complex systems

Roberto Benzi
Dip. of Physics, Univ. Roma "Tor Vergata"
Via della Ricerca Scientifica 1
00133, Roma
Italia

In this talk, I review some questions concerning the behavior of stochastic resonance in complex systems. In particular, I will discuss the case of a "random" and "regular" network whose connectivity matrix (links among the nodes) is fixed. Each node has a simple dynamical behavior with multiple equilibria. This system is the prototype of many interesting questions which are still to be analyzed in details. I will try to underline questions which might be investigated theoretically and/or experimentally.

Pathway of maximum likelihood of rare noise-induced events

Eric Vanden-Eijnden
Courant Institute, NYU
251, Mercer street
New York, NY, 10012
U.S.A.

The description of rare reactive events in nonequilibrium systems which lack detailed balance represents difcult theoretical and computational challenges. Examples of such events include phase transitions, chemical reactions, bio-chemical switches, or regime changes in climate. Brute force simulation of these events by Monte-Carlo or direct simulation of Langevin equations is difcult because of the huge disparity between the time step which must be used to perform the simulations and the time scale on which the rare events occur. Familiar concepts such as the minimum energy path which are often used to explain rare events are inappropriate because there is no energy landscape over which the system navigates.

In this talk, I will discuss techniques to describe and simulate rare events which build upon one property of these events, namely that their pathway is often predictable, even in nonequilibrium systems. The reason is that when an improbable event occurs, the probability that it does so in any other way than the most likely one is very small because all these other ways are even much less probable. This statement can be quantified within the framework of large deviation theory and it can be used to design efficient algorithms to compute the pathways of the rare events and estimate their rate of occurrence.

Browian noise and the Depletion Phenomenon

Peter M. Kotelenez*, Marshall J. Leitmanz†
Department of Mathematics
Case Western Reserve University
10900 Euclid Avenue
Cleveland, OH 44106

Summary. Kotelenez (1995a,b) introduced a model of correlated Brownian motions as a perturbation of as system of coupled stochastic ordinary differential equations (SODEs). The associated measure process is a solution of a stochastic partial differential equation (SPDE), similar to the transition from the description of N point vortices by a system of coupled ordinary differential equations (ODEs) to a first order partial differential equation (PDE - the Euler equation) for the vorticity in 2D fluid mechanics (cf. Chorin (1973) and Marchioro and Pulvirenti (1982)). In 2005 Kotelenez derived a system of N correlated Brownian motions as a kinematic mesoscopic limit from a system of nonlinear deterministic oscillators consisting of N large (solute) particles and infinitely many small (solvent) particles. The oscillators were coupled by a mean field force between the large and the small particles. The correlated Brownian motions are represented as the convolution of a $d-$dimensional kernel G_ε with standard Gaussian space-time white noise $w(dr, dt)$. The kernel G_ε is a properly rescaled version of the mean field force from the system of oscillators where ε is the correlation length. Kotelenez, Leitman and Mann (2007) carried out a careful analysis of these correlated Brownian motions in the context of modeling the depletion effect in colloids (cf. also Kotelenez, Leitman and Mann (2005)). For space dimension $d \geq 2$ they showed that two correlated Brownian particles when close have an initial tendency to attract each other further. For large times they behave like independent Brownian motions. The key to their short time result is a generalization of the one-dimensional probability flux, as defined by van Kampen (1983) to $d \geq 2$ dimensions. Refer also to Kotelenez (2008) for more details on all of the results mentioned above.

At least two **unresolved problems** arise in the work of Kotelenez, Leitman and Mann.

(1) *For $d \geq 2$ and a Maxwellian kernel G_ε (as well as similar unimodal kernels) there is an attractive zone for very short distances between the Brownian (solute) particles and a repulsive zone at moderate distances. At large distances there are no visible correlations. The presence of the repulsive zone is a mathematical fact. The problem is whether the physics requires such a zone and, if not, whether it is possible to define correlated Brownian motions without such a repulsive zone.*

(2) *Can one define correlated Brownian motions in space dimension $d \geq 2$ for which two Brownian particles are trapped for all time at a sufficiently short distance?*

References

[1] Chorin, A. J. (1973), *Numerical study of a slightly viscous flow.* J. Fluid Mech. 57, 785-796.

[2] Kampen, N.G.van (1983), *Stochastic Processes in Physics and Chemistry.* North Holland Publ. Co., Amsterdam, New York.

[3] Kotelenez, P. (1995a), *A Stochastic Navier Stokes Equation for the Vorticity of a Two-dimensional Fluid.* Ann. Applied Probab. Vol. 5, No. 4. 1126-1160.

[4] Kotelenez, P. (1995b), *A Class of Quasilinear Stochastic Partial Differential Equations of McKean-Vlasov Type with Mass conservation.* Probab. Theory Relat. Fields. 102, 159-188.

[5] Kotelenez, P. (2005a), *From Discrete Deterministic Dynamics to Stochastic Kinematics - A Derivation of Brownian Motions.* Stochastics and Dynamics, Vol 5, Number 3, 343-384.

[6] Kotelenez, P., (2008), *Stochastic Ordinary and Stochastic Partial Differential Equations: Transition from Microscopic to Macroscopic Equations*, Springer-Verlag.

*email: pxk4@cwru.edu
†email: mxl5@cwru.edu

[7] Kotelenez, P., Leitman, M. and Mann, J. Adin Jr. (2005), *Mesoscopic Modeling of Depletion Forces.* AIP Conference Proceedings, Vol. 800, Fourth International Conference on Unsolved Problems of Noise and Fluctuations in Physics, Biology and High Technology 2005, Melville, New York, 455-459.

[8] Kotelenez, P., Leitman M. and Mann, J. Adin Jr. (2007), *On the Depletion Effect in Colloids.* Preprint.

[9] Marchioro, C. and Pulvirenti M. (1982), *Hydrodynamics and Vortex Theory.* Comm. Math. Phys. 84, 483-503.

Weakly Non-ergodic Noise: From Blinking Quantum Dots to mRNA sub-diffusing in the cell

Eli Barkai
Physics Department Bar-Ilan University
Ramat Gan 52900
Israel

Time averages of intensity correlation functions of blinking quantum dots (QDs) exhibit ergodicity breaking. QDs when interacting with a continuous wave laser field turn at random times from state on in which many photons are emitted to a dark off state. The PDF of on and off times follows power law statistics $\psi(t) \sim t^{-(1+\alpha)}$ with $0 < \alpha < 1$. Hence the average on and off time diverges. In such scale free dynamics the time averages remain random even in the long time limit, since no matter how long we perform a measurement, the measurment time is shorter than the characteristic time scales of the dynamics. The time average of the intensity or intensity correlation function, measured in experiment, are irreproducible random variables as shown by the group of Maxime Dahan. We find the distribution of these Physical observables and explain the non-ergodic behavior in terms of an Onsager model [1].

However power law sojourn times are not limited to blinking Quantum dots. They are found in a very broad range of of dynamics stochastically modeled by the continuous time random walk theory. Such random walks exhibit, anomalous sub-diffusion and aging which in turn is related to the profound concept of weak ergodicity breaking introduced by Bouchaud. The same type of ergodicity breaking describes other dynamical systems and models [2, 3, 4].

Hence the basic question is what theory replaces standard ergodic statistical mechanics for such systems? A general theory of weak ergodicity breaking [5], based on Lévy's generalized central limit theorem, gives the distribution of the time averages of physical observables for these systems. Let $\mathcal{O}$ be a physical observable, in a system with $x = 1, \cdots, L$ states. When the system is in state x the physical observable attains the value $\mathcal{O}_x$. Let α describe the power law waiting times, specifically in the well known continuous time random walk model $\langle x^2 \rangle \underset{\sim}{} t^\alpha$ so α is the anomalous sub-diffusion exponent. The probability density function of the time average $\overline{\mathcal{O}}$ is

$$f_\alpha\left(\overline{\mathcal{O}}\right) = -\frac{1}{\pi}\lim_{\epsilon\to 0}\mathrm{Im}\frac{\sum_{x=1}^{L} P_x^{\mathrm{eq}}\left(\overline{\mathcal{O}} - \mathcal{O}_x + i\epsilon\right)^{\alpha-1}}{\sum_{x=1}^{L} P_x^{\mathrm{eq}}\left(\overline{\mathcal{O}} - \mathcal{O}_x + i\epsilon\right)^{\alpha}}. \quad (1)$$

where P_x^{eq} is the probability in ensemble sense to occupy state x. Validity of this equation is discussed in the talk. For models with thermal detailed balance P_x^{eq} is Boltzmann's canonical law. Eq. (1) applies in the long time limit, and when $\alpha \to 1$ we have ergodic behavior $f_\alpha\left(\overline{\mathcal{O}}\right) = \delta(\mathcal{O} - \langle\mathcal{O}\rangle)$.

There are many open questions with regard to this approach to non-ergodicity. For example can this approach describe physical systems in the thermodynamic limit, or is it applicable only for out of equilibrium systems (e.g. quantum dots driven by a laser field). When an ensemble of blinking dots is measured one cannot identify easily the non-ergodic behavior since the signal is averaged over many particles. If a single particle exhibits a non-ergodic behavior, how do we describe the transition to the many particle behavior? Is this transition smooth? Further recent experiments on single mRNA diffusing in a cell exhibit irreproducible results of the time average anomalous diffusion constant, which might be related to weak ergodicity breaking. There is therefore an open challenge to describe this biological system in terms of non-ergodic noise.

References

[1] G. Margolin, E. Barkai, *Non-ergodicity of Blinking Nano Crystals and Other Levy Walk Processes* **Phys. Rev. Letters** 94 080601 (2005).

[2] G. Bel, E. Barkai, *Weak Ergodicity Breaking with Deterministic Dynamics* **Europhysics Letters** 74 15 (2006).

[3] G. Bel, E. Barkai *Weak Ergodicity Breaking in the Continuous-Time Random Walk* **Phys. Rev. Lett.** 94 240602 (2005).

[4] S. Burov, E. Barkai, *Occupation Time Statistics in the Quenched Trap Model* **Phys. Rev. Lett.** 98 250601 (2007).

[5] A. Rebenshtok, E. Barkai, *Distribution of Time Averaged Observables for Weak Ergodicity Breaking* **Phys. Rev. Lett.** 99, 210601 (2007).

Heat fluctuations in systems in contact with heat baths at different temperatures

Giuseppe Gonnella and Antonio Piscitelli
Dipartimento di Fisica, Universitá di Bari,
I.N.F.N. Sezione di Bari,
via Amendola 173, Bari I-70123 Italia

A general symmetry has been recently discovered in the fluctuations of nonequilibrium systems [1, 2]. Further Fluctuation Relations (FRs), for both stochastic and deterministic systems, have subsequently been obtained; for recent reviews, see e.g. Refs.[3, 4, 5]. FRs are expected to be relevant for nano– and biological sciences [3, 6], where typical thermal fluctuations are of the same magnitude of applied forces. However, most of these relations still need to be tested in experiments or numerical simulations and their applicability has to be clarified for interacting systems which can undergo phase transitions.

We first consider here the case of systems in contact with two heat baths at temperatures T_j $(j = 1, 2)$, exchanging with them the heats $\mathcal{Q}_{j,\tau}$ in the time interval τ. Under stationary conditions, the fluctuation relation reads as

$$\ln \frac{\mathcal{P}(\mathcal{Q}_{j,\tau})}{\mathcal{P}(-\mathcal{Q}_{j,\tau})} \sim -\mathcal{Q}_{j,\tau} \left(\frac{1}{T_i} - \frac{1}{T_j} \right) \qquad at \quad large \quad \tau \tag{1}$$

where $\mathcal{P}(\mathcal{Q}_{j,\tau})$ is the pdf for the heat $\mathcal{Q}_{j,\tau}$. The relation essentially connects the probability of positive to that of negative values of the entropy production.

We will study the above relation in the context of the Ising model and of an intrinsically nonequilibrium model where the temperature at each lattice site depends on the local spin configuration [7]. These models have been chosen as paradigmatic examples of statistical systems with many interacting degrees of freedom and phase transition. An example of behavior of probability distribution function for the exchanged heat is given in fig.1 for the case of the Ising model at temperatures $T = 3$ and $T = 4$.

In both models the pdfs have a maximum at positive (negative) values of the heat exchanged at higher (lower) temperature. We find that the FR (1) is verified above the critical point and the pdfs are gaussian. When one or both the temperatures of the heat baths are below the critical region, the corresponding pdf's are very narrow, not gaussian, with a maximum close to the origin of zero heat exchanged. Also in this case the fluctuation relation is verified, at very late times, longer than above the critical point. Moving from low temperatures towards the critical point, larger fluctuations occur and the pdfs become wider with the typical behaviour of high temperature. We discuss this phenomenology in relation with the behaviour of the characteristic times required to restore ergodicity in the systems.

We want also to show and discuss results for more open problems concerning the nonequilibrium behaviour of heat fluctuations. For systems in contact with more than two heat baths we find that the fluctuations of the currents flowing in the systems are still related by a FR to the entropy production. Finally, we consider steady states of Ising systems subject to external driving [8]. In transient processes between different steady states corresponding to different driving, we show numerically that the mechanical work and not the heat verifies a Fluctuation Relation. We will discuss this behaviour.

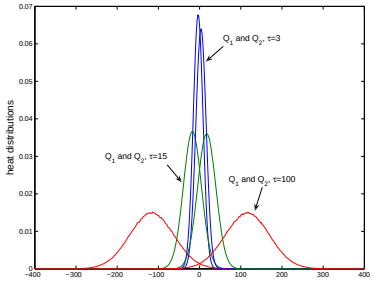

Figure 1: Heat pdfs for the Ising model on a lattice 2×100 where the two lines of spins are in contact with heat baths at $T = 3$ and $T = 4$. Heat values are collected over times of $\tau = 3, 15, 100$ Monte Carlo Sweeps (MCS) in a history of 10^8 MCS.

References

[1] D. J. Evans, E. G. D. Cohen and G. P. Morriss, Phys. Rev. Lett. **71**, 2401 (1993)

[2] G. Gallavotti and E.G.D. Cohen, J. Stat. Phys. **80**, 931 (1995)

[3] F. Ritort, Advances in Chemical Physics (to appear)

[4] L. Rondoni and C. Mejia-Monasterio, Nonlinearity **20**, R1 (2007)

[5] R.J. Harris and G.M. Schütz, J. Stat. Mech. P07020 (2007)

[6] C. Bustamante, J. Liphardt and F. Ritort, Phys. Today **58**, 43 (2005)

[7] A. Piscitelli, F. Corberi and G. Gonnella, in preparation.

[8] G. Gonnella and M. Pellicoro, J. of Phys. A: Mathematical and General **33**, 7043 (2000)

Posters

Applications of noise in measurements, technologies and informatics

A.1 – Ondrej Pokora
Classification of input signals based on input-output curves *70*

A.2 – Markus Niemann
Asymptotic continuous-time random walk models for deterministic diffusion *71*

A.3 – Jan Dolensky
Comparisons of noise spectroscopy analyze and microplasma noise sources *72*

A.4 – Mikhael Myara
Frequency Noise Contributions in External Cavity VCSELS using Homodyne Spectrum Analysis *73*

A.5 – Bernardo Spagnolo
The problem of analytical calculation of barrier crossing characteristics for Levy flights *74*

A.6 – Pierre Borgnat
Stationarization via surrogates *75*

Classification of input signals based on input-output curves

Ondrej Pokora
Department of Mathematics and Statistics, Masaryk University
Janackovo namesti 2a, 60200 Brno, Czech Republic

Petr Lansky
Institute of Physiology, Academy of Sciences of Czech Republic
Videnska 1083, 14220 Prague 4, Czech Republic

Neuronal responses evoked in sensory neurons by static stimuli are usually quantified by firing frequency which is plotted versus stimulus level, the frequency transfer (stimulus-response, input-output) function. The aim of the present contribution is to summarize and illustrate what is the range of important signals under two different points of view and we show that the role of noise is crucial in both approaches.

To obtain the range of stimuli which are identified at best, we propose to use measures based on Fisher information [1, 2, 3]. as known from the theory of statistical inference. To classify the most important stimuli from information transfer point of view, we suggest methods based on information theory [4, 5, 6]. These are two very different criteria as for example very informative signal may happen to be difficult to identify. We show that the most suitable signal, from the point of view of its identification, is not unique and the same holds for the most informative signal. A generic model of the response function is studied under the influence of several different types of noise. Finally, the methods are illustrated on a model of olfactory sensory neuron and data registered from such a neuron [7]. The open problem is classification of the input signals if the assumption of the rate coding is violated.

References

[1] Greenwood, P. E., Lansky, P., *Fluct. Noise Letters* **7**, L79–L89 (2007)

[2] Stemmler, M., *Network* **7**, 687–716 (1996)

[3] Lansky, P., Sacerdote, L., Zucca, C., *Math. Biosci.* **207**, 261–274 (2007)

[4] Bezzi, M., *BioSystems* **89**, 4–9 (2007)

[5] Brunel, N., Nadal, J.-P., *Neural Comput.* **10**, 1731–1857 (1998)

[6] DeWeese, M. R., Meister, M., *Network* **10**, 325–340 (1999)

[7] Pokora, O., Lansky, P., *Math. Biosci.*, in press (2008)

Asymptotic continuous-time random walk models for deterministic diffusion

Markus Niemann and Holger Kantz
Max-Planck-Institut fü Physik komplexer Systeme
Nöthnitzer Str. 38, 01187 Dresden, Germany

Abstract

Since the introduction of the continuous-time random walk (CTRW) by Montroll and Weiss [7], its concept has been successfully applied to model sub- and superdiffusive processes. Some recent examples are: blinking quantum dots [5], wind modeling [6], human travel [3] and economics [8].

We extend the description by Fogedby [4] with two independent stochastic differential equations by setting up a general description of a (possibly) space-time coupled version of a CTRW with continuous "virtual time". We identify the self-affine ones which emerge as long time limits. The method allows to give an interpretation of a result obtained by Becker-Kern, Meerschaert and Scheffler [2].

In a setting similar to Beck and Roepstorff [1], we identify the components of such CTRWs from the probabilistic behavior of these maps. In particular, we include classes with non-normalizable ergodic measure. Hence, we obtain a stochastic model for the long time behavior. This setup is exemplified analytically and numerically in a Manneville-Pomeau like setting. Depending on the ranges of the parameter we obtain sub- and superdiffusion.

References

[1] C. Beck and G. Roepstorff. *Physica A*, 145(1-2):1–14, 1987.

[2] P. Becker-Kern, M. M. Meerschaert, and H.-P. Scheffler. *Ann. Prob.*, 32(1B):730–756, 2004.

[3] D. Brockmann, L. Hufnagel, and T. Geisel. *Nature*, 439(7075):462–465, Jan. 2006.

[4] H. C. Fogedby. *Phys. Rev. E*, 50(2):1657 – 1660, 1994.

[5] Y. Jung, E. Barkai, and R. J. Silbey. *Chem. Phys.*, 284(1-2):181–194, Nov. 2002.

[6] D. Kleinhans, R. Friedrich, H. Gontier, and A. P. Schaffarczyk. In *Proceedings of DEWEK 2006*, 2006.

[7] E. W. Montroll and G. H. Weiss. *J. Math. Phys.*, 6(2):167 – 181, 1965.

[8] E. Scalas. *Physica A*, 362(2):225–239, Apr. 2006.

Comparisons of noise spectroscopy analyze and microplasma noise sources

Dolensky J., Vanek J., Jandova K., Chobola Z.*, Jurankova V.*
Department of Electrotechnology, Faculty of Electrical Engineering and Communication,
Brno University of Technology, Udolni 53, 602 00 Brno, Czech Republic
* Department of Physics, Faculty of Civil Engineering
University of Technology Brno,Žižkova 17, 602 00 Brno, Czech Republic

This paper deals with comparisons of noise spectroscopy and detection of microplasma noise sources in the three new type of solar cells G1, G3 and G5.

The passivation and antireflection structure of G1/1 and G1/4 specimens comprises a double layer formed by thermal silicon oxide (about 10 to 15 nm) and silicon nitride LP CVD (about 70 nm). The ARC layer of G1/5 and G1/7 specimens consists of a Si3N4 layer of a thickness of 75 nm.

The solar cells of type G3: after the double sided n-type diffusion process is completed and, prior to the subsequent deposition of the ARC (anti-reflection layer), this junction (of a thickness of about 1 um) is etched away from the rear side. For two cells, the passivation and antireflection layer of G3 specimens consists of an LP CVD Si3N4 layer (80 nm) and, for two other cells, of a double layer of thermal silicon oxide (about 10 to 15 nm) and silicon nitride LP CVD (about 70 nm).

The solar cells of type G5:For two cells, the passivation and antireflection layer of G5 specimens consists of an LP CVD Si3N4 layer (80 nm) and, for two other cells, of a double layer of thermal silicon oxide (about 10 to 15 nm) and silicon nitride LP CVD (about 70 nm).

The generation of microplasma is influenced by several factors. The first of them is defected silicon crystal-grid causing non-homogeneity of parameters that, in turn, creates visible defect. The second is dislocation of PN junction. At places where junction is thinner or mechanically damaged, the microplasma discharge and emission of light is present.

Another sign of observed microplasma is noise, which has random spectrum in frequency range. Microplasma noise is measurable even before the creation of light emissions. That provides a way to obtain information about microplasma creation with exiguous reverse voltage. Voltage needed for observation of microplasma highly depends on solar cell area and reverse voltage.

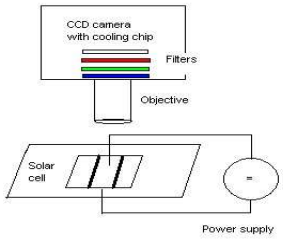

Fig. 1 – microplasma method workplace

Fig. 2 – Sample – microplasma method: scanning time 30s, current 0,11A, voltage 4,0V, clear filter

The basic principle of measuring method is connecting the solar cell to the source of reverse voltage. Creation of microplasma takes place at spots with non-homogeneity in structure of PN junction. Light emission is exhibited in full spectrum range. The whole process is observed with a special CCD camera in a dark special cryogenic box. CCD camera G2-3200 with low noise Kodak chip KAF-3200ME is used for measuring.

Compared second method we used for quality evaluation was the noise voltage spectral density measurement in forward biased voltage. The noise voltage being picked up across a load resistance R_L=100 Ω, at a band mean frequency of 1 kHz and a bandwidth of 20 Hz.

According to the transport and noise characteristic analysis of the mentioned double-sided alkali texture silicon solar cells, it is obvious that better quality has been achieved by the structure of the G3A/5 and G3A/7 specimens, this junction (of a thickness of about 1 um) is etched away from the rear side.

The G1/1 and G1/4 specimens in which an oxide - nitride passivation double layer has been used, show much worse noise properties. The noise parameters are likely to have deteriorated in the course of the high-temperature oxidation as a consequence of additional activation of phosphorus donors in the n+- layer and the subsequent diffusion spreading of the doped layer (which can be recognized from the layer resistance value change). The high thermal stress the Si chips are exposed to can also reduce the minority carrier life time.

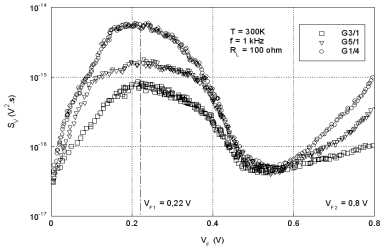

Fig.3. The noise spectral density as a function of forward voltage for nos. G1/4, G3/1 and G5/1 solar cells in forward direction.

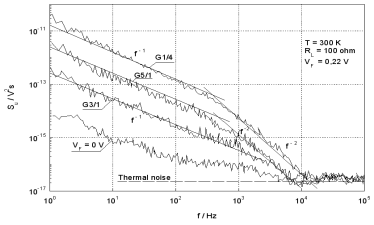

Fig.4. The noise spectral density versus frequency for mos. for nos. G1/4, G3/1 and G5/1 solar cells in forward direction

References

[1] VAN DER ZIEL, A., , H., Low frequency noise predicts when a transistor will fail, Electronics, 39(24), 95-97 (1966).

[2] VANDAMME, L.K.J., ALABEDRA, R. and ZOMMITI, M., 1/f noise as a reliability estimation for solar cells, Solid-State Electron., 26, 671-674 (1983).

[3] KLEINPENNING, T.G., 1/f noise in electronic devices, Proc.of Noise in Physical Systems (A. Ambrozy ed.), 443-454, Budapest (1989).

[4] CHOBOLA, Z., "Noise as a tool for non-destructive testing of single-crystal silicon solar-cells", in Microelectronics Reliability, vol. 41, no. 12, Dec. 2001, pp. 1947 – 1952.

[5] VANDAMME, L.K.J. "Opportunities and limitations to use low-frequency noise as a diagnostic tool for device quality", in Proceedings of the 17th International conference ICNF 2003, Prague 2003, pp. 735 – 748.

[6] CHOBOLA, Z.: Impulse noise in silicon solar cells. Microelectronics Journal, Vol.32/9 (2001), ISSN 0026-2692, pp.707-711.

[7] CHOBOLA, Z.: Noise as a tool for non-destructive testing of single-crystal silicon solar cells. Microelectronics Reliability, Vol.41/12 (2001), pp.1947-1952.

Frequency Noise Contributions in External Cavity VCSELS using Homodyne Spectrum Analysis

M. Myara ,A. Garnache , A. Bouchier, J.-P. Perez , P. Signoret
Institut d'Electronique du Sud, CNRS UMR5214, 34095 Montpellier, France
I. Sagnes
(2) Laboratoire de Photonique et Nanostructures, CNRS UPR20, 91460 Marcoussis, France
D. Romanini
(3) Laboratoire de Spectromtrie Physique, CNRS UMR5588, 38402 Saint Martin d'Heres, France

Laser technology is maturing rapidly and is finding applications in areas such as high resolution spectroscopy, medicine, optical telecoms, metrology, where highly coherent tunable low noise sources are required. Single frequency tunable high-power solid-state lasers rely on intracavity filtering. A more compact design can be achieved using a simple External-cavity VCSELs (VeCSELs), to develop high power highly coherent laser. VeCSELs exhibit single-frequency operation in the $0.8 - 2.5\mu m$ range and wide mode-hope-free tuning range. They offer continuous wave operation at 300 K with high output power and a TEM_{00} beam [1, 2]. In terms of frequency noise, the linewidth of these lasers is well known to be limited by the mirror mechanical fluctuations. In this paper, we study the influence of these fluctuations on the linewidth measurements using the heterodyne technique.

1 VeCSEL Design and Single Frequency Operation

Here, we present a GaAs-based VeCSEL emitting at $1\mu m$ formed by a half-VCSEL (fig. 1-a and b), a $10 - 25mm$ air gap to stabilize single longitudinal mode operation, and a commercial concave mirror (99% of reflectivity). The half-VCSEL structure is composed of a HR AlAs/GaAs Bragg Miror, 6 InGaAs/GaAs(P) strain compensated quantum-wells (QWs) and a SiN antireflection coating.

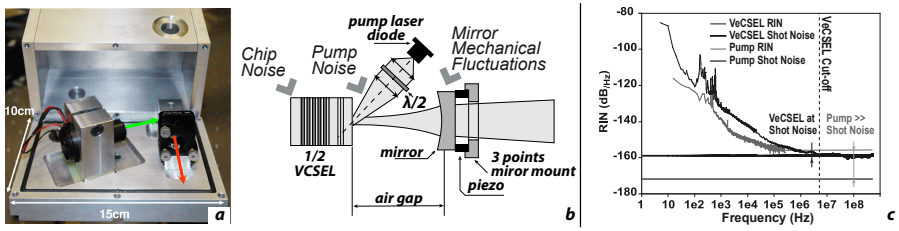

Figure 1: VeCSEL device, Schematic View and RIN Spectrum.

The external mirror is held by an ultra-stable mirror mount. A low noise $200mW$ single transverse mode 800 nm commercial pump laser diode (battery biased) is focused on a $30\mu m$ spot size at 65 degrees incidence angle. The components are glued on the breadboard and inserted in a metallic box. Single frequency operation ($SMSR > 40dB$) is obtained up to $50mW$ output power (pump power limited, 35% slope efficiency) at 295K, without any intracavity spectral filter thanks to the QW homogeneous gain [1]. The VeCSEL was linearly polarized along the [110] crystal axis due to QW gain dichrosm.

2 Frequency Noise Study using the Homodyne Spectrum

Besides the fundamental white noise sources, VeCSELS exhibit some excess noise sources (fig. 1-b). In this paper, we will consider the following ones : the mirror position fluctuations *(that will be identified by some specific vibrations at low frequencies)*, the noise from the pumping system *(that operates like a modulation signal)*, and the noise from the VeCSEL chip itself *(usually $1/f$ noise due to cristal defects or surface state effects [4])*.

A good picture of these noise contributions can be obtained thanks to amplitude noise measurements. The RIN (Relative Intensity Noise) spectrum displayed in fig. 1-c clearly shows the white noise (quantum noise) contribution, the $1/f$ slope and some mechanical spikes in the $100Hz - 1kHz$ range. This figure also demonstrates that the VeCSEL under test is not disturbed by the noisy pump, because the VeCSEL reaches the fundamental laser quantum noise level in spite of a super-poissonian pump source.

To obtain the VeCSEL Frequency Noise, we study the spectrum obtained thanks to the delayed homodyne technique, using a $5\mu s$ delay between the two paths. The photo-detected signal at the output of the interferometer is amplified and then Fourier-transformed thanks to a high resolution FFT Analyser. The distinct FM Noise contributions are extracted by fitting the measured spectra with an FFT-transformed $\Gamma(\tau, \tau_0)$ autocorrelation function, with τ the time and τ_0 the time delay. Whereas the $\Gamma(\tau, \tau_0)$ functions associated to $1/f$ and white noise are well known [3], we established the $\Gamma(\tau, \tau_0)$ for mechanical fluctuations, assumed to be a simple direac peak in the FM noise spectrum :

$$\Gamma_{mechanics}(\tau, \tau_0) = \exp\left(-8A_0 \frac{\sin^2(\pi\tau f_0)\sin^2(\pi\tau_0 f_0)}{f_0^2}\right)$$

with f_0 the peak frequency and $A0$ its frequency fluctuation power in Hz^2.

For lasers dominated by white and $1/f$ frequency noise, the homodyne spectrum obtained with too small delays or too narrow linewitdth lasers is known to be composed by an exact dirac peak at $0\ Hz$ (the so-called "coherence peak"), followed by oscillating wings at higher frequencies (fig. 2-a and -b) which shape strongly depends on the $1/f$ and white noise levels [3]. If we introduce a mechanical contribution in the frequency noise spectrum (a dirac peak at a given frequency in the $100Hz - 1kHz$ range, inset fig. 2-b), the resulting homodyne spectrum becomes nearly Gaussian around $0\ Hz$ and the wings become stronger in magnitude with exacly the same shape (fig. 2-a). Thus, neglecting the mechanics contribution (which is the strongest one in VeCSELs) leads to erroneous results for both the $1/f$ and the white noise PSD (Power Spectrum Density) values.

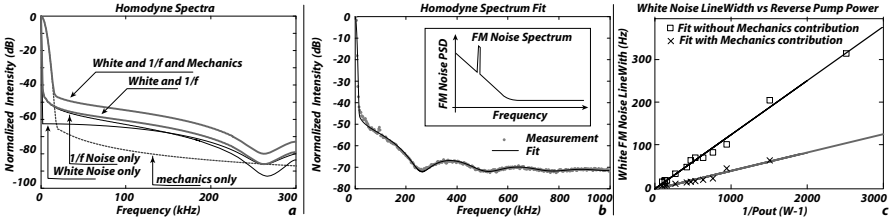

Figure 2: VeCSEL Homodyne spectrum for $5\mu s$ delay and Frequency Noise.

To illustrate this, we fitted twice the measured homodyne spectra, once considering only the $1/f$ and white FM noise in the expression of the autocorrelation function, and once more introducing the mechanical contribution in this function ($f_0 = 500Hz$, fluctuation power $A0 = 7.10^{10}\ Hz^2$). The white FM noise results shown in fig. 2-c clearly exhibit an error stronger than 300%, whereas both sets of values follow the classical $1/P_{out}$ slope.

A similar error were observed for the $1/f$ noise, estimated at $5.10^5 Hz^2/Hz$ at $1Hz$ for the mechanical contribution free fit, and at $2.10^5 Hz^2/Hz$ in the other one.

References

[1] A. Garnache, A. Ouvrard, and D. Romanini, *Optics Express* **15** p. 9403 (2007)

[2] A. Ouvrard, A. Garnache et al. *IEEE Photonics Technology Letters* **17** p. 2020 (2005)

[3] J.P. Tourrenc, P. Signoret, M. Myara et al., *IEEE J. Quantum Electronics* **41** p. 549 (2005)

[4] L.K.J. Vandamme, *IEEE Transactions on Quantum Electronics* **36** p. 549 (1989)

The problem of analytical calculation of barrier crossing characteristics for Lévy flights

Alexander Dubkov
Radiophysics Faculty, Nizhniy Novgorod State University,
23 Gagarin Ave., 603950 Nizhniy Novgorod, Russia

Bernardo Spagnolo
Dipartimento di Fisica e Tecnologie Relative,
Università di Palermo and INFM-CNR,
pad. 18, Viale delle Scienze, 90128 Palermo, Italy

The problem of escape from a metastable states investigated by Kramers [1] is ubiquitous in almost all scientific areas (see the review [2]). The main tool to investigate the barrier crossing problem remains the first passage times technique. But for anomalous diffusion in the form of Lévy flights this procedure meets with some difficulties. First of all, the fractional Fokker-Planck equation describing the Lévy flights is integro-differential, and the conditions at absorbing and reflecting boundaries differ from those using for ordinary diffusion. Lévy flights are characterized by the presence of jumps, and, as a result, a particle can reach instantaneously a boundary from arbitrary position. One can mention some erroneous results obtained in [3], because author used the traditional conditions at two absorbing boundaries. There are a lot of numerical results regarding the different time characteristics of Lévy flights, but obtaining analytical results remains an open problem (see Ref. [4]).

In our opinion, the nonlinear relaxation time technique is suitable for analytical investigations of Lévy flights temporal characteristics, because does not request a constraint of some boundary conditions. According to definition, the mean residence time in the interval (L_1, L_2) reads

$$T(x_0) = \int_0^\infty dt \int_{L_1}^{L_2} P(x,t|\,x_0,0)\,dx, \tag{1}$$

where x_0 is the initial position of all particles ($x_0 \in (L_1, L_2)$) and $P(x,t|\,x_0,0)$ is the probability density of transitions. Changing the order of integration in Eq. (1) we obtain

$$T(x_0) = \int_{L_1}^{L_2} Y(x,x_0,0)\,dx, \tag{2}$$

where $Y(x,x_0,s)$ is the Laplace transform of the transient probability density $P(x,t|\,x_0,0)$

$$Y(x,x_0,s) = \int_0^\infty P(x,t|\,x_0,0)\,e^{-st}dt. \tag{3}$$

Making the Laplace transform in the fractional Fokker-Planck equation for Lévy flights in the potential profile $U(x)$

$$\frac{\partial P}{\partial t} = \frac{\partial}{\partial x}\left[U'(x)\,P\right] + D\frac{\partial^\alpha P}{\partial |x|^\alpha} \tag{4}$$

and taking into account the initial condition $P(x,0|\,x_0,0) = \delta(x-x_0)$, we get

$$\frac{d}{dx}\left[U'(x)\,Y\right] + D\frac{d^\alpha Y}{d|x|^\alpha} - sY = -\delta(x-x_0). \tag{5}$$

If we put $s=0$ in Eq. (5) and make the Fourier transform we obtain

$$U'\left(-i\frac{d}{dk}\right)\widetilde{Y} - iD|k|^{\alpha-1}\operatorname{sgn}(k)\,\widetilde{Y} = \frac{e^{ikx_0}}{ik}, \tag{6}$$

where

$$\widetilde{Y}(k,x_0) = \int_{-\infty}^{+\infty} Y(x,x_0,0)\,e^{ikx}dx \tag{7}$$

and $\operatorname{sgn} x$ is the sign function. After solving Eq. (6) we can calculate the mean residence time as

$$T(x_0) = \frac{1}{2\pi i}\int_{-\infty}^{+\infty}\frac{e^{-ikL_1} - e^{-ikL_2}}{k}\,\widetilde{Y}(k,x_0)\,dk. \tag{8}$$

Although Eqs. (6) and (8) are useful tool to analyze the temporal characteristics of Lévy flights in different potential profiles $U(x)$, obtaining the exact analytical results even for the case of Cauchy stable noise excitation ($\alpha = 1$) remains the one of unsolved problem in this area.

This work has been supported by Russian Foundation for Basic Research (project 08-02-01259).

References

[1] Kramers, H. A., *Physica* **7** 284–304 (1940).

[2] Hänggi, P., Talkner, P., and Borkovec, M., *Rev. Mod. Phys.* **62** 251–341 (1990).

[3] Gitterman, M., *Phys. Rev. E* **62** 6065–6070 (2000).

[4] Chechkin, A. V., Gonchar, V. Yu., Klafter, J. and Metzler, R., *Adv. Chem. Phys.* **133** 439–496 (2006).

Stationarization via surrogates*

Pierre Borgnat & Patrick Flandrin
Université de Lyon, École Normale Supérieure de Lyon
Laboratoire de Physique (UMR 5672 CNRS),
46, Allée d'Italie, 69364 Lyon Cedex 07, France
Prenom.Nom@ens-lyon.fr

When facing with experimental data, making a distinction between stationary and nonstationary behaviours is often an important pre-processing step that may condition any subsequent analysis or modeling. Whereas the concept of stationarity (in short, independence of statistical properties with respect to some absolute time) seems to be unambiguous, its practical use turns out to be more subtle, with additional implicit assumptions regarding, e.g., observation scales and a need for statistical decisions aimed at assessing the significance of observed fluctuations over time (or space) in a single observation.

Those questions have recently been revisited from a time-frequency perspective, the basic ingredient being a comparison between local and global frequency features [1, 2]. In order to cope with unavoidable fluctuations when dealing with one single observation, the second ingredient of the approach is the introduction of some "controlled noise" in the problem so as to characterize in a data-driven way the null hypothesis of stationarity. More precisely, a family of *stationarized* time series is constructed from the observation, each of them having a global frequency spectrum that exactly identifies with that of the data, while being also reproduced locally. It therefore becomes possible to get from this set of time series a statistical knowledge from which some significance for the rejection of the null hypothesis of stationarity can be granted. A simple way of achieving the outlined program is to stationarize the initial data by randomizing the phase of its Fourier transform. This is in fact a new use of the well-known technique of *surrogate data* [3, 4] but, in contrast with more classical uses of surrogate data analysis where nonlinearity is to be assessed (with furthermore a possible sake of conservation of nonstationary properties), the key point here is to get rid of local frequency fluctuations in a transformed (time-frequency) domain.

This simple technique already proved efficient in some typical situations, but it also naturally calls for extensions and leaves a number of questions open. More precisely, the presentation is proposed to be organized as follows:

1. It will first outline the general framework of stationarization via surrogates as it has been introduced so far in [1] and [2].
2. Two new variations will then be proposed:
   - The first one is concerned with the general problem of *transient detection*, where the existence of a time-frequency "patch" in a fluctuating background has to be given a level of significance. In this case, the approach consists of constructing directly *surrogate time-frequency distributions* (as opposed to distributions of surrogate time series) via phase randomization in the domain of their 2D Fourier transforms.
   - The second one deals with the detection of *nonstationary correlations* in multivariate data. The problem is to find whether correlations between random signals stay the same along the time, or if there is some kind of non-stationarity pertaining to the correlations between signals. This question is solved in an equivalent manner, using here the multivariate formulation of surrogates [5] that aims at keeping the cross-spectrum by multiplying, for a given frequency, all the phases of the Fourier transforms for each variable by the same random rotation.
3. Finally, since all considered stationarization techniques involve some randomization, the question of possible relationships with other resampling plans (such as bootstrap, jacknife, cross-validation,... [6]) naturally surfaces and will be addressed as an open issue.

*This is part of an undergoing work supported by ANR StaRAC and conducted with the collaboration of Pierre-Olivier Amblard (GIPSA-lab, Grenoble), Cédric Richard (UTT, Troyes) and Jun Xiao (ENS Lyon & ECNU, Shanghaï).

References

[1] J. Xiao, P. Borgnat and P. Flandrin, "Testing stationarity with time-frequency surrogates," *Proc. EUSIPCO-07*, Poznan (PL), 2007.

[2] J. Xiao, P. Borgnat, P. Flandrin and C. Richard, "Testing stationarity with surrogates – A one-class SVM approach," *Proc. IEEE Stat. Sig. Proc. Workshop SSP-07*, Madison (WI), 2007.

[3] J. Theiler *et al.*, "Testing for nonlinearity in time series: the method of surrogate data," *Physica D*, Vol. 58, No. 1–4, pp. 77–94, 1992.

[4] T. Schreiber and A. Schmitz, "Improved surrogate data for nonlinearity tests," *Phys. Rev. Lett.*, Vol. 77, No. 4, pp. 635–638, 1996.

[5] D. Prichard and J. Theiler, "Generating surrogate data for time series with several simultaneously measured variables," *Phys. Rev. Lett.*, Vol. 73, No. 7, pp. 951–954, 1994.

[6] B. Efron, *The Jacknife, the Bootstrap and Other Resampling Plans*. Philadelphia: SIAM, 1982.

Biological noise

B.1 – Cecilia Pennetta
Extreme Value Analysis of Heart Beat Intervals RR 77

B.3 – Akio Nozawa
Evaluation of sleepiness by facial skin thermogram 78

B.4 – Zbigniew R. Struzik
The Origins of Behavioural Organisation in Humans 79

B.5 – Maria Teresa Giraudo
Some examples on the role of noise in neuronal modelling problems 80

B.6 – Pietro Lio
Noise and nonlinearities in biological and socio-psychological data 81

B.7 – Cheng-Hung Chang
Stochastic resonance of ion pumps on cell membranes 82

B.8 – Elisabetta Marras
Mining Protein-Protein Interaction Networks: Denoising Effects 83

B.9 – Igor A. Khovanov
Charge fluctuations in ion channels 84

B.10 – Denis S. Goldobin
Proteasomal Degradation of Proteins: Reconstruction of Translocation Rates 85

B.11 – Nicola Pizzolato
Noise induced effect in polymer translocation 86

B.12 – Ryota Kobayashi
Influence of firing mechanisms on gain modulation 87

Extreme Value Analysis of Heart Beat Intervals RR

Cecilia Pennetta[1] and Danuta Makowiec[2]
[1] Dipartimento di Ingegneria dell'Innovazione, Università del Salento and CNISM, Italy,
[2] Institute of Theoretical Physics and Astrophysics, Gdańsk, Poland

In recent years it has become clear that many physiological signals display fairly complex dynamics, like for example long-term correlations, multifractality, non-Gaussianity etc., which reflect the complex interplay of different biological mechanisms acting and competing in highly-organized organisms [1, 2, 3]. In particular, it has been realized that many biomedical signals contain much more information than that catched directly "by eyes". Moreover, such hidden information cannot be extracted by using conventional statistical tools. For this reason, advanced statistical methods, conceived in the context of complex physical systems, like detrended fluctuation analysis (DFA) [1, 2, 3, 4, 5], multifractal detrended fluctuation analysis (MDFA) [1, 2, 3, 4, 5] or wavelet transform modulus maxima (WTMM)[5] have been applied to the analysis of biomedical time series, like for example series made by heart beats or neural records [6]. On the other hand, very recently, some authors [7, 8, 9, 10] have highlighted the effectiveness of extreme value analysis (EVA) in the study of complex systems, in particular for what concerns the development of forecasting techniques. Thus, our aim here is to explore the ability of EVA to extract significant information from physiological time series. Precisely, we consider heart beat intervals RR series, i.e. time series whose records are the time intervals between two subsequent picks of the so called R waves, as measured in 24-h ECG Holter signals [5, 6]. These signals are known to fluctuate in a way that reflects autonomic neural control on the sinus node [11, 12] - the heart first pacemaker. A great number of tools have been developed to provide quantitative assessments of these fluctuations and then to obtain indices of neural regulation of the heart rate [13]. Nevertheless, new methods of processing are still looked forward.

Two sets of signals are analysed, corresponding to healthy and non-healthy patients with reduced left ventricular systolic function (rlvs) [5, 6]. The analysis is performed by considering the return time (RT) distribution, i.e. the distribution of the time intervals associated with two consecutive overcomings by the signal of a given threshold value [8, 9, 10]. Our preliminary results seem to indicate that the parameter values of the RT distribution are able to discriminate between the two sets of data. By MDFA and WTMM methods it is found that the control of the autonomic system is significantly weaken when one compares between the group averages healthy patients and patients with rlvs[5]. However, neither MDFA nor WTMM method provides a tool to classify an individual signal.

References

[1] P. Ch. Ivanov, L. A. N. Amaral, A. Goldberger, S. Havlin, M. G. Rosenblum, Z. R. Struzik, H.E. Stanley, *Nature*, **399**, 461-465 (1999).

[2] A. Bunde, S. Havlin, J. W. Kantelhardt, T. Penzel, J. H. Peter, K. Voigt, *Phys., Rev. Lett.*, **85**, 3736-3739 (2000).

[3] Z.R. Struzik, J. Hayano, R. Soma, S. Kwak, Y. Yamamoto, *IEEE Trans. of Biomed. Engin.*, **53**, 89-94 (2006).

[4] S. Tong, D. Jiang, Z. Wang, Y. Zhu, R. G. Geocadin, N. V. Thakor, *Physica A*, **380**, 250-258 (2007).

[5] D. Makowiec, R. Galaska, A. Dudkowska, A. Rynkiewicz, M. Zwierz, *Physica A*, **369**, pp. 632-644 (2006).

[6] PhysioNet Data Bank: *http://circ.ahajournals.org/cgi/content/full/101/23/e215.*

[7] D. Sornette, *Critical Phenomena in Natural Sciences, Chaos, Fractals, Selforganization and Disorder: Concepts and Tools*, Springer, Berlin (2004).

[8] E. G. Altmann. H. Kantz, *Phys. Rev.* E, **71**, pp. 056106-1-9 (2005).

[9] A. Bunde, J. F. Eichner, J. W. Kantelhardt, S. Havlin, *Phys. Rev. Lett.*, **94**, 048701-1-4 (2005).

[10] C. Pennetta, *Eur. Phys. J. B* **50**, pp. 95-98 (2006).

[11] M. P. Freneaux, *Heart* **90** 1248 (2004).

[12] M. J. De Jong and D. C. Randall. *J. Cardiovasc. Nurs.* **20** 186 (2005).

[13] Task Force of the European Society of Cardiology and North American Society of Pacing and Electrophysiology, *Eur.Heart J.* **17** 354 (1996).

Evaluation of sleepiness by facial skin thermogram

Correlation analysis on α–attenuation and nasal skin temperature

Akio Nozawa, Munecazu Tacano
School of Science and Engineering, Department of Electrical Engineering, Meisei Universit
2-1-1 Hodokubo, Hino, Tokyo 191-8506, Japan

Introduction

In recent years, the serious accident caused by decline of arousal level, such as a traffic accident and a mechanical control mistake, serves as a social concern. The physiologic index obtained by human body measurement is expected as a leading tool of evaluation arousal level as an objective indicator.

In this study, evaluation arousal level by nasal skin temperature was conducted. As the arousal level declining, the parasympathetic nerve activity is inihibited, and blood flow at peripheral vessels is decreased. Since a peripheral vessel exists directly under the skin in the nose, psychophisiological state appears on the displacement of skin temperature caused by changing blood flow volume[1]. Objective of the experiment is to obtain assessment criteria for decline arousal level by nasal skin temperature by using present technique, α–wave attenuation coefficient of EEG, as a reference benchmark[2]. Furthermore, psychophysiccal index of the sleepiness feeling was also measured by Visual Analogue Scale(VAS). And correlation with a nasal skin temperature index and a ECG index was analyzed.

Experiment

A measurement system and an experiment protocol are expressed below. Infrared thermography (AVIONICS, TVS–200EX) is installed 1m ahead subject. Facial skin thermogram is measured with 1s of sampling periods. Image resolution of the thermogram shall be 320x240 pixels, and room temperature sets 23±1.0 degrees cercius and the infrared emissivity of skin is ϵ= 0.98. A subject shall keep seating position and a resting state. Electrode helmet (Brain Function Laboratory) and headphone is put on the subject. Electroencepharogram (EEG) is recorded by 200Hz of sampling frequencies using biological amplifier/sampler (NF Electronic Instruments, 5102 EEG HEAD BOX) and digital signal processor unit (NF Electronic Instuments, 5101 PROCESSOR BOX). Differnt electrodes are C3, O1 and O2 based on the international 10-20 method, and a reference electrode is A2.

Subjects are four 22-years-old adult males. The α–wave attenuation test (AAT) is conducted, which consists of six times one-minute measurement segment. three of them are eye-closed session, other three are eye-opened session. The eye-closed sessions and eye-opened sessions are alternately arranged in sequence. Six minutes AAT is between four minutes resting segment. Psychophisical subjective arousal level, "sleepiness", is measured just after 1st resting started and just after AAT segment finished. Physiological indeces, which are EEG and thermogram, are measured from first resting segment to last resting segment by using VAS. Four kind of music, which are ballade, classic, rap and rock, are presented as auditory stimulus to subject in AAT segment in order to give a variation on arousal level. Experiment limited to be conducted once a day.

A frequency range of α–wave of EEG is defined from 8Hz to 13Hz. A α–wave power spectrum, P_α, of each one-minute measurement section is calculated. Then, power spectrum of α–wave is averaged on eye-closed sessions and eye-opened sessions, which are $\bar{P}_\alpha$(closed) and $\bar{P}_\alpha$(opened). α–wave attenuation coefficient(AAC) is derived from the following equation. AAC will approaches to 1 as the arousal level declining.

$$\mathrm{AAC} = \frac{\bar{P}_\alpha(\mathrm{opened})}{\bar{P}_\alpha(\mathrm{closed})} \tag{1}$$

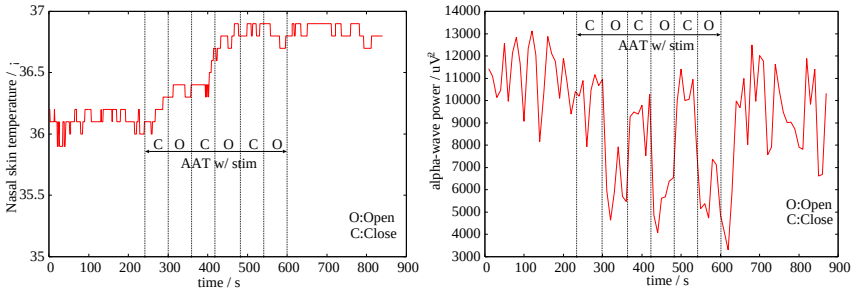

(a) Nasal skin temperature time series (b) alpha-wave power time series

Figure 1: Average nasal skin temperature and α-wave power spectrum time series.

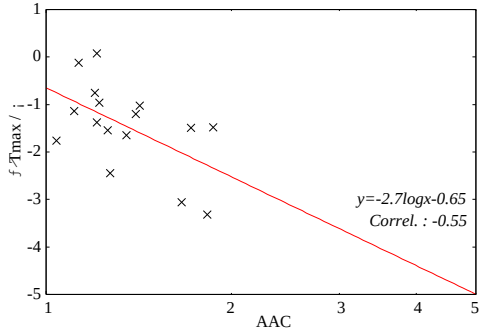

Figure 2: AAC and $\Delta T_{\max}$

Results

Fig.1(a) shows areal-averaged nasal skin thermogram time series, $\bar{T}(t)$. $\bar{T}(t)$ is obviously rose up in AAT segment. The arousal level declining is infered. Where, T_{ave} is defined as time-averaged $\bar{T}(t)$ of 1st resting segment, and $\Delta T_{\max}$ is absolute maximum as $|\bar{T}(t) - T_{\mathrm{ave}}|$ for t in AAT segment. $\Delta T_{\max}$ is defined "maimum temperature displacement", which corresponds to characteristics on nasal skin termperature variation relating to decline arousal level.

Fig.1(b) shows α–wave power spectrum time series, P_α. In general, α–wave evokes while resting, eye-closed and arousal status and attenuates with the declining arousal level. On the other hand, α–wave attenuates with eye-opened and increases with the declining arousal level. The figure expresses that α–wave power of eye-closed session attenuates.

Fig.2 gives a relationship between AAC and maximum temperature displacement $\Delta T_{\max}$ for all the subjects and stimuli. Where a variation on nasal skin temperature results from a variation on blood flow of peripheral vessel in nasal region. And blood flow of peripheral vessel is sympathetically-innervated. Thus, $\Delta T_{\max}$ is presumed an index of activity of sympathetic nervous system. Fig.2 expresses that AAC and $\Delta T_{\max}$ has a clear negative-correlation, and correlation coefficient between AAC and $\Delta T_{\max}$ is -0.55.

References

[1] H. Tanaka, H. Ide and Y. Nagashima, Attempt of Feeling Estimation by Analysis of Nasal Skin Temperature and Arousal Level, *Human interface. The Transaction of Human Interface Society*, **1**(4) pp. 51–56 (1999)

[2] A. Michimori, Relationship between the alpha attenuation test, subjective sleepiness and performance test, *10th Symposium on Human Interface*, **1413** pp. 233–236 (1994)

The Origins of Behavioural Organisation in Humans

Toru Nakamura[1], Zbigniew R. Struzik[2], and Yoshiharu Yamamoto[2]
1 The Center for Advanced Medical Engineering and Informatics,
Osaka University, Osaka, Japan
2 Educational Physiology Laboratory, Graduate School of Education,
The University of Tokyo, Tokyo, Japan

The quest for a principle underlying human behaviour is considered to be a difficult task, since actions are subject to the individual's constant conscious deliberation and psyche, resulting in a continuously changing type and level of activity, arising from interaction with dynamically changing environmental demands. Yet recent studies by Barabàsi et al. [1, 2] have pointed towards the existence of a universal statistical law governing waiting times of inter-human communication, such as e-mail exchange, Web browsing and trade transactions. Very recently, Nakamura et al. [3] also studied the nature of human behavioural organisation, specifically how resting and active periods are interwoven throughout daily life, and found that the duration statistics exhibit universal behaviour, which can be generalised across individuals. Specifically, thresholded activity (similar to that considered in records of earthquakes [4] or solar flare activity [5]), was there shown to follow universal laws (data collapse), of stretched exponential type for active intervals, and power law type for resting periods.

The significance of this study [3] is in providing evidence at the 'mesoscopic' level of complexity of the system under consideration, inaccessible for modelling both phenomenologically and from first-principles. Indeed, in recent years, the concept of universality has provided a powerful paradigm, allowing for a conceptual grasp of this otherwise inaccessible (either phenomenologically or from first-principles) 'mesoscopic' level of a system's complexity. This applies both to the application of the universality concept across different unrelated systems, and also across different levels of abstraction of hierarchical systems.

Current understanding of human social interactions, as presented by Barabasi et al. [1, 2], is indeed phenomenological, and the model used is built around a concept of priority - this is a consciousness-rooted, psychological concept, and as such does not lend itself well to explaining *all* human (motoric) activity. More specifically, power laws in waiting time statistics, as observed in resting times of human activity[3], have been associated with strongly priority-driven task scheduling [1]. One could hypothesise that humans and animals are, at all times, guided by such a high priority scheduling mechanism in their activity, yet it is not possible to prove or disprove this at the current level of insight.

On the other hand, activity durations and size, as discussed in [3], could indicate that the problem may be mapped onto a generic class of problems displaying critical phenomena statistics - indeed, universal laws of PDF collapse have been observed in thresholded activity considered in records of model sand pile avalanches [6], earthquakes [4] or solar flare activity [5]. In addition, quiet times (between thresholded avalanches) in generic models of self-organisation [6] also display power law behaviour, (in particular in the presence of correlated driving). In Ref [3], we have established these power laws, and thus correlation, in resting times of human activity [3], corresponding with waiting inter-burst times (or more accurately, quiet times), providing the basis for further investigation of the underlying cause(s).

Indeed, a body of research exists which points to criticality and phase transitions in brain function, optimising memory function or space allocation [7, 8, 9, 10, 11, 12, 13]. The question as to whether neural criticality can be scaled up to human behaviour cannot yet be answered. Yet, it is known from animal experiments that a direct correspondence between brain activity and behaviour exists [14]. Such experiments cannot be conducted on humans. Monitoring human brain activity by imaging in order to gain insight into its characteristics in daily behavioural organisation is also not feasible for practical reasons. It is only done in small-scale experiments [15], and indeed it points to critical processes as those responsible for large-scale synchronisation and multi-stability and multi-functionality across neurons.

At present we are, therefore, of the opinion that it is beyond the capacity of today's science to disprove either of the generic reasons (high task priorities or inherent, possibly neurogenic, correlated driving) as the underlying source of this correlation - exhibited in the universal scaling laws observed in human behavioural organisation, as shown in Ref [3].

Indeed, we expect that the findings described in Ref [3] and highlighted in this submission will contribute to elucidating the role of the universality insight at the 'mesoscopic' level of the complexity of behavioural organisation.

References

[1] Barabasi A.-L., *Nature* **435** pp. 207-211, (2005)

[2] Vazquez A. et al, *Phys. Rev. E* **73**, p. 036127, (2006)

[3] Nakamura T. et al, *Phys. Rev. Lett.* **99**, p. 138103, (2007)

[4] Bak, P. et al, *Phys. Rev. Lett.* **88**, p. 178501, (2002)

[5] Baiesi M. et al, *Phys. Rev. Lett.* **96**, p. 051103, (2006)

[6] Sanches R. et al, *Phys. Rev. Lett.* **88**, p. 068302, (2002)

[7] de Arcangelis L. et al, *Phys. Rev. Lett.*, p. 028107, (2006)

[8] Kinouchi O. et al, *Nature Physics*, **2**, pp. 348-252, (2006)

[9] Haldeman C. et al, *Phys. Rev. Lett.*, **94**, pp. 058101-1-4, (2005)

[10] Grinstein G. et al, *PNAS*, **102**, pp. 9948-9953, (2005)

[11] Fujisawa S. et al, *Cerebral Cortex* **16**, pp. 639-654, (2005)

[12] Eguiluz V.M. et al, *Phys. Rev. Lett.* **94**, p. 018102, (2005)

[13] Zhou C. et al, *Phys. Rev. Lett.* **97**, p. 238103, (2006)

[14] Vaadla E. et al, *Nature* **373**, pp. 515-518, (1995)

[15] Briggman K.L. et al., *Science* **307**, pp. 896-901, (2005)

Some examples on the role of noise in neuronal modelling problems

Maria Teresa Giraudo and Laura Sacerdote
Dept. of Mathematics, University of Torino,
Via C. Alberto 10, 10123 Torino, Italy

Noise influences all physical observations either as an intrinsic property of the studied system or in the form of fluctuations added by the measurement instrument (for a brief survey see [3] and references quoted therein). Filters can destroy its contribution in observed data improving the comprehension on the phenomena, but they can also determine the distruction of important pieces of information when the noise influences the system dynamics. Indeed the noise plays a positive role in a variety of instances, eventually changing in an important way the global behavior of the system. Many experimental and theoretical studies show that a suitable amplitude of noise can enhance signal transmission in biological context (cf. [9], [12] for surveys on the subject), linearizing the response to suprahreshold signals (cf. [14]), increasing input-output correlation and coherence or allowing the detection of subthreshold periodic signals (cf. for example [1]). Examples also exist showing the role of noise in determining optimum values of signal detection when the detector is unable to recognize signals of intensity lower then a fixed level (cf. [7], [8])

Here we review some of the important instances in neurobiological context where the contribution of noise has been recognized to be particularly relevant focusing on different unexpected features and open problems that arise in this context. To perform this goal we use as a reference model the so called Leaky Integrate and Fire model for the neuronal membrane potential that is described by means of the Ornstein-Uhlenbeck process $\{X_t,\ t>0\}$ (cf. [10]), solution of the stochastic differential equation

$$dX_t = \left(-\frac{X_t}{\theta}+\mu\right)dt+\sigma dW_t; X_0 = x_0, \tag{1}$$

or of its variants. In eq. (1) the parameter μ identifies the input (deterministic) signal while the membrane potential decays spontaneously with time constant θ and is affected by random fluctuations accounted for by the diffusion parameter $\sigma>0$. The neuron acts as a threshold device since an action potential or spike is generated when X_t reaches a constant value $S>x_0$. The mathematical counterpart of the time between successive spikes (interspike interval or ISI) is the first passage time T of the process X_t through the threshold S:

$$T = inf\left\{t>0:\ X_t \geq S;\ X_0 = x_0\right\}. \tag{2}$$

The analysis of this simple model allows us to illustrate a set of features related to the presence of noise such as the linearization of the response, the amplification of the coding range due the presence of noise or the existence of optimal noise level for signal detection.

We also focus on the effect of the composition of different types of noise by introducing a variant of model (1) where the membrane potential is described by the process $\{Y_t,\ t>0\}$ (cf. [10]), solution of the following stochastic differential equation

$$dY_t = \left(-\frac{Y_t}{\theta}+\mu\right)dt+\sigma dW_t + a dN_t^- - a dN_t^-; Y_0 = y_0,. \tag{3}$$

The membrane potential dynamics is then modelled as a diffusion process to which jumps of constant amplitude a occurring at random times are superimposed (cf. [11]). In this case the composition of two types of randomness such as the diffusion and the jump processes and the presence of a nonlinearity determined by the absorbing boundary determine the arising of unexpected dynamics. Indeed the ISI distributions can become multimodal with shapes very similar to those characterizing model (1) when μ is substituted by a periodic function $\mu(t)$, i.e. in the case of periodically modulated inputs. This feature hints to the existence of characteristic times in the system and suggest a possible role of noise to get synchronization phenomena. A challenging open problem in this framework consists in the determination by means of suitable theoretical tools of analytical relationships among the parameters characterizing model (3) that can generate this kind of phenomena and optimize the specific role of noise.

When the source of noise is inherent in the system, as in the neuronal modelling case, and the observed signal is periodic even a feeble signal can be amplified and optimized with the assistance of noise. The best known example of this type of behavior is the so called stochastic resonance phenomenon (cf. [4], [13] and references quoted therein) whereby a right tuning of the noise intensity can optimize the signal detection in threshold devices. We focus our attention here also on the phenomenon of ghost stochastic resonance (cf. [2]) by which an excitable neuron driven by (at least) two sinusoidal inputs, harmonic of the same fundamental frequency, responds to the missing fundamental thanks to an active role of noise in specific ranges that optimizes the response. If the signals are rendered anharmonic by adding the same shift to all the input frequencies the neuron responds with a shift in the output frequency. We consider both a single neuron model ([5]) and a model where a couple of periodic input signals is carried by two different neurons acting on a third processing one ([6]) as further examples on the importance of noise in neuronal coding. The study of further improvements of these models could be of great interest in the understanding of the contribution of noise in the neuronal response to different kinds of periodic inputs.

References

[1] Bulsara, A.R., Elston, T.C., Doering, C.R., Lowen, S.B. and Lindberg, K., *Phys. Rev. E* **53** pp. 3958-3969 (1996)

[2] Chialvo, D.R., Calvo, O., Gonzales, D.L., Piro, O. and Savino, G.V. *Phys. Rev. E* **65(5)** Art. No. 050902(R) (2002)

[3] Cohen, L. *IEEE Signal Processing Magazine* **20** pp. 20-45 (2005)

[4] Gammaitoni, L. Hanggi, P., Jung, P. and Marchesoni, F. *Modern Phys.* **70** pp. 223-287 (1998)

[5] Giraudo, M.T. and Sacerdote, L. *Sc. Math. Japon.* **64(2)** pp. 299-312 (2006)

[6] Giraudo, M.T., Sacerdote, L. and Sicco, A. *Lect. Notes Comp. Sc.* **4729** pp. 398-407 (2007)

[7] Lánský, P., Sacerdote, L. and Zucca, C. *Math. Biosc.* **207** pp. 261-274 (2007)

[8] Lánský, P., Sacerdote, L. and Zucca, C. *Lect. Notes Comp. Sc.* **4729** pp. 368-377 (2007)

[9] F. Moss, A. Bulsara and M. F. Schlesinger (Eds.) *Proceedings of the NATO ARW on Stochastics in Physics and Biology* J. Stat. Phys. **70** (1993)

[10] Ricciardi, L.M. and Sacerdote, L. *Biol. Cyb.* **35** pp. 1-9 (1979)

[11] Sacerdote, L. and Sirovich, R. *Sc. Math. Japon.* **58(2)** pp. 307-321 (2004)

[12] Segundo, J.P., Vibert, J.F., Pakdaman, K., Stiber, M. and Diez-Martinez, O. In *K. Pribram (Ed.) Origins: Brain and Self-Organization* pp. 300-331 (1994)

[13] Shimokawa, T., Pakdaman, K. and Sato, S. *Phys. Rev. E* **59** pp. 3427-3443 (1999)

[14] Yu, X. and Lewis, E.R. *IEEE Trans. Biomed. Eng.* **36** pp. 36-43 (1989)

Noise and nonlinearities in biological and socio-psychological data.

Franco Bagnoli
Department of Energy, University of Florence; also CSDC and INFN, sez. Firenze
Pietro Lió
Computer Laboratory, University of Cambridge, Cambridge CB3 0FD, UK

1 Introduction

Life and social sciences are becoming more and more quantitative, with experiments that generates large amounts of data. The results of such experiments can often be summarized in a large matrix, in which rows represent repetition of the experiment in different context, and the columns are the output of a single measurement. In particular, we consider the following cases: microarray sampling, protein-substrate affinity, socio-psychological surveys. Let us illustrate the similarities of these examples.

Microarray data. DNA microarray technology can simultaneously monitor the expression levels of thousands of genes across experimental conditions or treatments. A DNA microarray (gene chip) can be seen as an ordered collection of spots, on each of which there is a different probe formed by known sequences of cDNA. A sample of mRNA, supposed to represent the gene expressed in a given tissue under investigation, is let hybridize with the probes. Fluorescent techniques allows to detect the hybridized sports. The idea is that of using probes specific for a unique region of a gene, therefore detecting the gene expressed in a a tissue. The current approach to achieve sensitivity and specificity is to use multiple probe pairs to target a single gene; one of each pair is supposed to exactly match a fragment of the gene (PM probe), while the other contains a single mismatch in the center (MM probe). The MM probes offer a measure of specificity of the probe. Since about 30% of the probe pairs yield negative signals, the use of MM probe is rather unreliable [1]. The traditional experimental approach to improving precision of inherently noisy microarray data is by performing experimental replicates. Replicated observations also allow us to quantify precisely the experimental noise in measurements for each gene at each experimental condition. The experiment is moreover repeated for many tissue, from different part of the body, or from different patients, or from a different phase of the cellular cycle. The data can therefore be arranged using the probe numbering as column index, and tissue numbering as row index. The goal is that of identifying the difference in gene expressions in the different cases. There are many problems in extracting information from these data. Some data may be missing, MM spots are sometimes more hybridized that PM ones, low-intensity data cannot be easily distinguished from noise.

Protein-substrate affinity. A similar problem is that of investigating the shape of a protein or of a peptide. The interaction of proteins with the outer world (in particular concerning the immune response) depends on the shape and on the biochemical interaction network. Genetic and protein networks may contain ensemble of positive and negative feedbacks which may challenge the analysis even in presence of large data [2, 3]. At present, it is not possible to reconstruct the tri-dimensional shape of a protein from its primary sequence (easily obtained by mRNA sequence). Moreover, proteins are very often glycosylated, and these sugar chains attached to the outer surface may be the most important factor for inflammation. On the other hand, direct visualization of protein surface, using NMR, electronic microscopy, etc. is a very slow and costly process. A method for obtaining information about this shape is that of using proteins or antibody arrays, similar to DNA microarrays. Again, in this case, the pattern of matches can be represented as a matrix, with columns corresponding to substrates (probing proteins or antibodies) and rows to different proteins under investigation. One interesting application of the missing data problem is that of forecasting the interactions of a new drug in the cellular environment, given the affinity of this drug with a collection of substrates, and the affinity of a large sample of known "objects" with the same collection.

Questionnaires and other psycho-sociological data. The high-level investigation of the human mind take often the form of the study of responses to stimuli. The stimulus may be planned and targeted, like in the case of questionnaires, or occasional like for instance those that lead to choosing some good, emerging from pattern analysis of renting of DVDs, opinions on books, supermarket tickets. These data can be represented in matrix form, with rows corresponding to customers, and columns corresponding to items or goods. In this case, in addition to the usual problems of consistency an noise, there is a special meaning in missing data: an accurate method for "anticipating" them from the knowledge stored in the matrix would constitute a valuable tool for personal advertising [4]. However, in the case of humans, one should consider also that the tastes change and evolve in time.

2 Knowledge networks

The extraction of information about the properties of the gene, proteins and humans is performed using statistical tools, mainly based on variations of singular value decomposition [5]. The goal is that of extracting the most robust characteristics of patterns, clustering the data in similarity classes, reconstruct missing data, detect outliers, reduce noise. It is rather unusual to take into consideration an explicit model for the generation of data, *i.e.*, for the matching mechanism. The problem may be reformulated in geometrical terms. We shall denote with the word "probe" the substrates or the questionnaires, and with the word "subject" the mRNAs, the proteins and the individuals of the three examples. A subject can be visualized as an array of "tastes", and the probes as a complementary array of "characteristics". In the case of mRNA, this space is just the sequence space of basis, in case of proteins it is a way of coding the surface, in case of psychological data, these are mental modules, often called "dimensions" or factorial analysis. The match between tastes and characteristics is denoted "opinion". The match between tastes and characteristics may be linear, like a scalar product, or highly nonlinear, as in the case of protein-antibody interaction. In case of one-or-none interaction, there is no noise and no inference can be performed on missing data. In the linear case, the results are much more blurred, there is a non-zero overlap between different samples, and it has been shown [6] that, if one knows a sufficient number of overlaps between subjects, there is a rigid percolation threshold that in principle allows the reconstruction of any "taste" once that one is known. However, tastes are in general hidden or difficult to be obtained. If one has at his disposition a sufficient amount of data, it can be shown [7] that the correlation between expressed opinions approximates the real overlap among tastes. This would in principle allow the perfect reconstruction of missing opinion and detection of outliers. In this work we investigate the role of nonlinearities and noise in the matching phase. In particular, we show that nonlinearities appear as noise when linear investigation tools are used. We study the influence of nonlinearities in the rigid percolation transition. We apply a recursive technique [6, 7] to synthetic data, obtained from nonlinear matching models, and investigate the limits of the "black box" reconstruction model.

References

[1] Y. Zhou, R. Abagyan Curr. Opin. Drug Discov. Devel. **6**, 339 (2003).

[2] S. Hooshangi, R. Weiss Chaos **16**, 026108 (2006=.

[3] C. Tan, F. Reza, L. You Biophys. J. **93**, 3753 (2007)

[4] The Netflix DVD rental store issued a 1 million prize for improving the accuracy of their predictions: http://www.netflixprize.com/

[5] O. Troyanskaya, M. Cantor, G. Sherlock, P. Brown, T. Hastie, R. Tibshirani, D. Botstein, R. Altman Bioinformatics **17**, 520 (2001).

[6] S. Maslov, Y-C. Zhang Phys. Rev. Lett. **87** (24), 248701 (2001).

[7] F. Bagnoli, A. Berrones, F. Franci Physica A **332**, 509 (2004).

Stochastic resonance of ion pumps on cell membranes

Cheng-Hung Chang[1,2] and Tian Yow Tsong[3]

[1] Institute of Physics, National Chiao Tung university,
Hsinchu 300, Taiwan
[2] Physics Division, National Center for Theoretical Sciences,
Hsinchu 300, Taiwan
[3] Institute of Physics, Academy of Sciences,
Taipei 115, Taiwan

Ion pumps are biological motors capable of transporting ions through cell membranes, even against the transmembrane ion concentration gradient. While *in vivo* this nanoscale machine consumes ATP, *in vitro* it may be driven by external fluctuating electric fields, no matter they are periodic or random (see [1, 2, 3] and references therein). Theoretically, the motor conformations can be described by a conformation vector $V(t)$ governed by a multi-dimensional kinetic equation $dV(t)/dt = M(t)V(t)$. Given an oscillating electric field with a slight fluctuation, the Boltzmann distribution in different conformations will change with time and the matrix $M_{ij}(t) = a_{ij}\exp(f(t) + \xi(t))$ will contain a signal term $f(t)$ and a noise term $\xi(t)$. The instantaneous transported ion flux is then a functional of the quasi-cyclic trajectory $V(t)$ of this non-autonomous dynamical system. Various interesting dynamical properties of ion pumps, including stochastic resonance [4], have been discovered experimentally [2] and confirmed theoretically [1]. However, the theoretical approach is based on time-consuming simulations on above Langevin-kind equation, with a noise embedded in the exponential term. A more elegant Fokker-Planck formalism describing the probability evolution of this equation is still missing. This formalism would enable a more systematic study on how general biological small systems, e.g., proteins, receptors, or enzymes, (as long as they contain a non-negligible charge or magnetic dipole) response to external fields.

Key problem: the density evolution of a dynamical system with a noise in the exponential term.

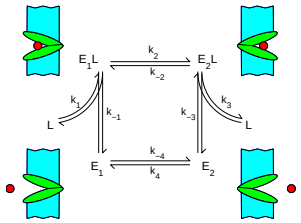

Figure 1: A four-state kinetic model of Na, K-ATPase. This motor (pacman) can open to the left or the right hand side of the membrane with or without captured Na^+ or K^+ ion, denoted by ligand L (red ball). Thus it has 4 conformations and 8 kinetic rate constants k_i's. Suppose under some $k_{\pm1}$ ($k_{\pm3}$) the motor opening to the left (right) hand side prefers to adapt L (release L). Then the motor concentrations tend to flow from E_1 to E_1L (E_2L to E_2) and converge to an equilibrium state, with more probability on E_1L and E_2. However, when an external force is applied to change $k_{\pm2}$ ($k_{\pm4}$), a flow from E_1L to E_2L (E_2 to E_1) is activated to approach a new equilibrium state, which shifts L across the membrane (empty motor opening returns to E_1). When the force is lifted, the motor releases L (adapts a new L) on the right (left) hand side and returns to the original equilibrium state. Therefore, a force oscillation may generate a clockwise flow and transport the ion from left to right.

To take a concrete example, let us consider the ion pump Na, K-ATPase. The kinetic equation for the concentrations of the four conformations in Fig. 1 is a 4-dim non-autonomous dynamical system

$$\frac{d}{dt}V(t) = M(t)V(t), \qquad M(t) = \begin{pmatrix} -k_3 - k_{-2} & k_2 & k_{-3}[L_3] & 0 \\ k_{-2} & -k_{-1} - k_2 & 0 & k_1[L_1] \\ k_3 & 0 & -k_4 - k_{-3}[L_3] & k_{-4} \\ 0 & k_{-1} & k_4 & -k_{-4} - k_1[L_1] \end{pmatrix}, \quad (1)$$

with the concentration vector $V(t) = ([E_2L], [E_1L], [E_2], [E_1])^T$ and $[L_1]$ and $[L_3]$ the concentrations of L on the left respectively right hand side of the membrane. The rate constants $k_i = h_i \exp(q_i\phi(t)a_i/RT)$ consist of the gas constant R, the temperature T, the effective charge q_i of different motor conformations, the transmembrane potential $\phi(t)$, the rate constant h_i in zero potential $\phi(t) = 0$, and the apportionment constant a_i. Under a varying external field, k_i's are time-dependent and have the form $k_i = h_i \exp(d_i\Psi(t))$, where h_i, d_i denotes some parameters and $\Psi(t) = A\sin(\omega(t) + \xi(t))$ consists of a signal $A\sin(\omega t)$ and a noise $\xi(t)$. The instantaneous transported ion flux is $j(t) = k_3[E_2L] - k_{-3}[E_2][L_3]$, which determines the transported amount $S(t) = \int_0^t j(t')dt'$ and the averaged flux $J = \lim_{t\to\infty} S(t)/t$.

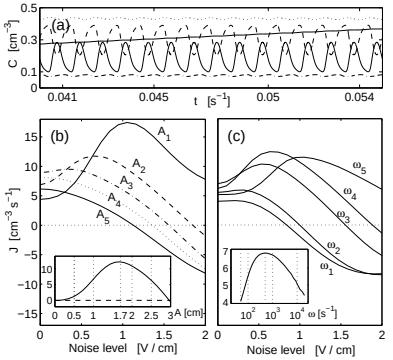

Figure 2: (a) The oscillations of different concentrations $[E_1]$ (dotted), $[E_2]$ (dash-dotted), $[E_1L]$ (thin solid), $[E_2L]$ (dashed), induced by $\Psi(t) = A\sin(\omega t)$, and the positive transported amount $S(t)$ across the membrane (thick solid). (b) The averaged flux J versus the noise level η under five different amplitudes of sinusoidal signal with signal frequency $\omega = 10^3$ and $\omega_n/\omega = 10^3$, where $A_1 = 0.5$, $A_2 = 1$, $A_3 = 1.4$, $A_4 = 1.7$, and $A_5 = 2$. The inset shows the signal amplitude dependence of the averaged flux J without noise. (c) The averaged flux J versus the noise level η under five different signal frequencies ω's with signal amplitude $A = 1$ and $\omega_n/\omega = 10^3$, where $\omega_1 = 50$, $\omega_2 = 10^2$, $\omega_3 = 500$, $\omega_4 = 10^3$, and $\omega_5 = 10^4$. The inset shows the frequency dependence of the averaged flux J without noise.

Inserting biologically relevant parameters into Eq.(1), the transport efficiencies with and without noises can be found in Fig. 2. These numerical results, consistent with previous experimental observation, reveal that the noise is destructive, when a signal magnitude A is at the optimal transport efficiency, but is constructive and stochastic resonance shows up when the signal is apart from this optimal magnitude. However, because of lack of a probability evolution formalism, these results are obtained from rather time-consuming simulation on the noise in Eq.(1).

References

[1] Chang, C.-H. and Tsong, T.Y., *Phys. Rev. E* **69**, 021914 (2004)

[2] Tsong, T.Y. and Xie, T.D., *Appl. Phys. A* **75**, 345 (2002)

[3] Tsong, T.Y. and Astumian, R.D., *Bioelectrochem. Bioenerg.* **15**, 457 (1986); Tsong, T.Y. and Astumian, R.D., *Prog. Biophys. Mol. Biol.* **50** pp. 1-45 (1987)

[4] Fulinski, A., *Phys. Rev. Lett.* **79**, 4926 (1997); Chaos 8, 549 (1998)

Mining Protein-Protein Interaction Networks: Denoising Effects

Elisabetta Marras and Enrico Capobianco
CRS4 Bioinformatics Laboratory,
Science & Technology Park of Sardinia,
09010 Pula (Cagliari), Sardinia - ITALY

A typical instrument to pursue analysis in complex network studies is determining statistical distributions for standard quantities or measures computed to characterize network topology, structure and dynamics.

Protein-Protein Interaction Networks (PPIN) have also been characterized by several measures, each one coming with a corresponding distribution. In general, a power law is considered to be a reasonable feature; a certain measure y is said to obey a power law when its probability distribution is given by $p(y) \approx y^{-\gamma}$, where usually $2 < \gamma < 3$. Equivalently, a log-transform leads to a doubly logarithmic plot from where it is simple to check whether a straight line results.

However, a mix of noise cover, long tails effects from outlying information, and other inherent fluctuations of the computed measures make the empirical detection of the power law not an easy task, which adds uncertainty when looking at the observed sample on whether the feature under exam may be reliably considered to follow a power law distribution.

Our Contribution

We address noise problems in applications to yeast and human interactomes, where both decomposition and denoising techniques are implemented to reduce the impact of factors potentially affecting power law detection.

1 Preliminary Results

We have some initial results on the dataset provided by [1]. Among many suggested methods, with a majority concentrating on perturbation techniques, we compare decomposition results from Principal Component and Independent Component Analysis (PCA [2], and ICA [3], respectively) applied to the computed interactome features.

These decomposition methods have built-in some denoising power, mainly embedded in the natural selection among eigenvalues from the obtained spectrum.

Furthermore, we apply wavelet decomposition to the same selected set of measures, representing topological features or network characteristics from which a summary of the informative content of all protein interactions is obtained.

The advantage of PCA or ICA is that we can reduce the global dimensionality of the problem from the original network to a core of it, where we believe the most significant information is present. By wavelets, we also dissect the observed features scale-wise, thus trying to look into a dynamic more than a static interaction map.

References

[1] Bader et al., Gaining Confidence in High-throughput protein interaction networks. *N*ature Biotech. **22**, pp. 78-85 (2003).

[2] Jolliffe, I.Y., *P*rincipal Component Analysis (New York: Springer, 1986).

[3] Cardoso, J.F., Source separation using higher order moments. *P*roc. ICASSP, pp. 2109-2112 (1989).

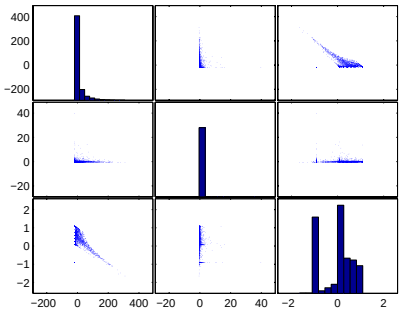

Figure 1: PCA of degree distribution, betweenness and clustering coefficients.

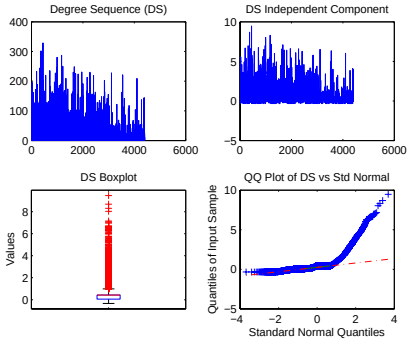

Figure 2: Degree demixing via ICA.

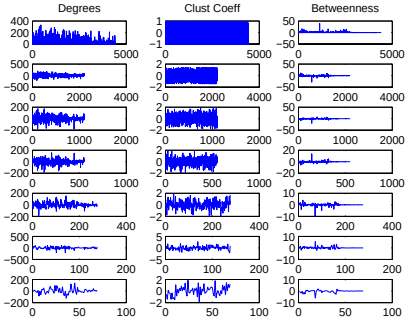

Figure 3: Wavelet decomposition of network features.

Charge fluctuations in ion channels

D. G. Luchinsky[1,2,5], R. Tindjong[1], I. Kaufman[3],
P.V.E. McClintock[1], R.S. Eisenberg[4]
[1]Department of Physics, Lancaster University, Lancaster LA1 4YB, UK.
[2]NASA Ames Research Center, MS 269-3, Moffett Field, CA, 94035, USA.
[3] VNII for Metrological Service, Gosstandart, Moscow, 119361, Russia.
[4]Department of Molecular Biophysics and Physiology, Rush Medical college,
1750 West Harrison, Chicago, IL 60612, USA.
[5]MCT Inc., 2041 Rosecrans Ave., Suite 225 El Segundo,CA 90245

Noise in ion channels. Ion channels are natural nanotubes in cellular membranes that control a vast range of biological functions in health and disease. The main properties of ion channels – their structure, conformational changes, selectivity, conductivity, and gating – are the subject of intensive, ever-growing, fundamental and applied research in biology, physics, and nanotechnology. Understanding the structure-function relationship for ion channels is one of the most fundamental unsolved problems of biophysics. The main challenges in modeling an ion's permeation through a channel are related to the fact that this is a many-body problem with long range interactions and with widely-varying timescales, ranging from sub-ps (atomic motion) to sub-ms (gating dynamics). It is therefore of particular importance to build low-dimensional models that incorporate most important many body effects at various time-scales and yet allow for analytical insight. Below we introduce a model of ion permeation that takes into account the noise corresponding to charge fluctuations and we demonstrate that the latter has a leading order effect on the transition probabilities.

Model. We consider electrostatic interactions between ions in an ionic channel and the charge fluctuations in the channel mouth. The motion of the ions is modeled within a self-consistent framework of Brownian dynamics (BD) (1) coupled to the Poisson equation (2).

$$m_i\ddot{\vec{x}}_i = -m_i\gamma_i\dot{\vec{x}}_i + \sum_{j=1}^{N}\left[\frac{q_iq_j}{4\pi\varepsilon\varepsilon_0 r_{ij}^2} + \frac{9U_0R_e^9}{r_{ij}^{10}} + AU_0\exp\left(\frac{R_{ij}-r_{ij}}{a_e}\right)\sin\left(2\pi\frac{R_{ij}-r_{ij}}{a_w}-\alpha\right)\right]\frac{\vec{r}_{ij}}{r_{ij}} + \vec{F}_{ch} + \sqrt{2m_i\gamma_ik_BT}\vec{\xi}_i(t) \quad (1)$$

$$-\nabla\cdot(\epsilon(\vec{r})\nabla\phi(\vec{r})) = \rho(\vec{r}), \qquad \vec{D} = \epsilon\vec{E}, \qquad \vec{E} = -\vec{\nabla}\phi, \quad (2)$$

Here $\vec{r}_{ij} = \vec{x}_i - \vec{x}_j$, $r_{ij} = |\vec{r}_{ij}|$, $A = \sqrt{1+(\frac{a_w}{2\pi a_e})^2}$, $\alpha = \arctan(\frac{a_w}{2\pi a_e})$, m_i, $\vec{x}_i$ and q_i, $m_i\gamma_i$ and $\sqrt{2m_i\gamma_ik_BT}\,\vec{\xi}_i(t)$ are the mass, position ,charge, friction coefficient and the stochastic force of the ith ion. The distance between ions i and j is r_{ij}. The parameters in the short range and hydration terms are given by [1]. The dielectric force acting on the ion as it moves on the channel axis F_{ch} is calculated numerically. It is shown that the charge fluctuations can be enhanced in channels of low dielectric constant, resulting in strong modulation of the potential barrier at the selectivity site as can be seen in Fig. 1(b). It become therefore possible to build a simple model capable of coupling the motion of ions in the channel to the bathing solution. To this end, we propose the one dimensional dynamics of a single ion moving from the middle of the channel to the right mouth, with two sources of noise. In the high friction limit, diffusion across the barrier is governed by the Langevin equation

$$m\gamma\dot{x} = -\frac{dV(x,t)}{dx} + \eta(t) + \sqrt{2m\gamma k_BT}\,\xi(t) \quad (3)$$

where $\xi(t)$ is a white Gaussian noise arising from thermal fluctuations. Taking into account that the charge fluctuations at the channel mouth occur on a sub-nanosecond time scale with an exponential distribution of arrival times [2], we approximate this term by a Poisson random force with an experimentally determined distribution of modulation amplitudes. $\eta(t)$ is the corresponding dichotomic noise

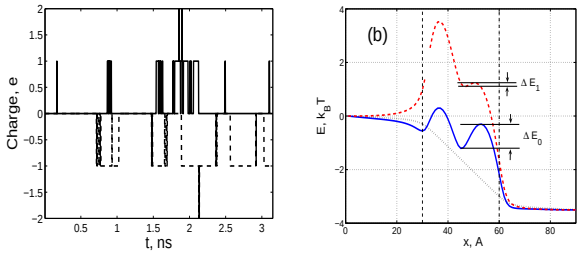

Figure 1: (a) Charge fluctuations at the channel mouth. (b) The potential energy profiles as a function of the position of the ion when: the first ion is fixed at the channel mouth (dashed line) and the second is moving along the channel axis. The (dotted line) correspond to the potential energy on a single ion moving on the channel axis; The potential energy of the passive channel (dotted line). The vertical dashed lines show the channel entrance and exit. The height of the potential energy barrier seen by a single ion at the selectivity site as it moves from left hand to right hand of the channel is denoted ΔE_0. In the presence of a second ion at the channel's left mouth this barrier is reduced to ΔE_1.

arising from the charge fluctuations. $V(x,t)$ is a fluctuating barrier with potential well at its middle (corresponding to the centre of the channel) and a barrier at one end (corresponding to the channel exit) as plotted in Fig. 1(b). The fluctuation in the potential arises from the interaction between an ion arriving at the channel mouth and an ion which was initially trapped in the middle of the channel at it selectivity filter. The dichotomic noise therefore controls the barrier fluctuations between two states with respective barriers ΔE_0 and ΔE_1, with $\Delta E_0 > \Delta E_1$. These two energy limits are a direct result of the charge fluctuations at the channel mouth which has shown that ions arrive at the channel mouth ones at a time and very rarely two at a time as is shown in Fig. 1(a). A direct analogy can be made between the model described by Eq. (3) and the model described by Stein [3] whose barrier fluctuation is controlled by a Gaussian process. The similarity of the two problems suggest that there is a possibility of some semi-analytical estimations of the effect of the charge fluctuations. The work is in progress and contains a plethora of unsolved problems.

Unsolved problems include the following –

(i) The role of the membrane fluctuations
(ii) The role of the electrostatic potential of interaction between the selectivity site and the ion, which can be strongly oscillating in the radial direction.
(iii) The role of additional binding sites outside the selectivity filter.
(iv) The energetics of the ion transition including energy relaxation due to the coupling to the protein phonon modes (wall oscillations)
(v) The coupling of the ion-wall interaction to the gating mechanism

In all of these, noise seems to play a crucial role that is only starting to be elucidated. Our preliminary research shows that the model can be extended to take these effects into account.

References

[1] Moy, G., Corry, B., Kuyucak, S., and Chung, S.-H. "Tests of continuum theories as models of ion channels. I. Poisson-Boltzmann theory versus Brownian dynamics" *Biophys. J.* **78**(5), 2349-2363, (2000).

[2] Luchinsky, D. G., Tindjong, R., Kaufman I., McClintock, P. V. E. and Eisenberg, R. S. "Ionic channels as electrostatic amplifiers of charge fluctuation" *IOP JPCS, Electrostatics 2007*, in press.

[3] Stein, D. L., Doering C. R., Palmer, R. G. Van Hemmen, J. L., and McLaughin, R. M. "Escape over fluctuating barrier: the white noise limit" *J. Phys. A: Math. Gen* **23**(5), L203-L208 (1990).

Proteasomal Degradation of Proteins: Reconstruction of Translocation Rates

D.S. Goldobin,[1,2] J. Kurths,[2] and A. Zaikin[3]

[1]Department of Physics, University of Potsdam, Postfach 601553, D–14415 Potsdam, Germany

[2]Department of Theoretical Physics, Perm State University, 15 Bukireva street, 614990, Perm, Russia

[3]Department of Mathematical Sciences, University of Essex, CO4 3SQ, Colchester, United Kingdom

The process of degradation of proteins by proteasomes (barrel-shaped macromolecules) cleaving the retracted proteins into peptides, short amino acid chains, is essential for the normal functioning of the immune system. Some of degradation fragments are transported onto the cell surface where T-lymphocytes scan them in order to recognize the cells to be killed because of an abnormal functioning. Therefore the cleavage pattern for a degraded protein and its statistical properties are of importance. While the scissility of a specific peptide bond is determined by the sequence of the nearest amino acids, the probability of the cleavage of this bond during the degradation process is also essentially affected by the translocation process.

In quantum chemistry the conventional approach to such kind problems is a direct numerical simulation with account to all the interactions between the ions. But here it is not applicable because the usual characteristic times for the processes simulated in such a way are microseconds, while the process of degradation of one protein takes about 3 min, what signifies a **stochastic diffusional** nature of the mechanism of the protein translocation within the proteasome and the need in developing of an adequate approximate **stochastic model** of the process. Here we use the model assuming on translocation
(1) the retraction of the protein into proteasome with a rate depending on the length of the protein part inside this proteasome, and
(2) a quick escaping of cleaved fragments from the proteasome. For the model utilized the Master-equations have been derived and is investigated.

We study the influence of the translocation rate on cleavage patterns and have developed the algorithms for the reverse engineering of the translocation rate from the experimental data on the cleavage pattern for (1) **relatively short synthetic polypeptides** (25-50 amino acids), (2) **long proteins with a periodic amino acid sequence**, and (3) **natural proteins**. From the viewpoint of the algorithm tolerance to experimental data inaccuracies, the utilizing of periodic proteins is most desirable, but for the moment the data only for short artificial and long natural proteins are available. We have obtained some preliminary results of the reverse engineering of the translocation rate for the short polypeptides degraded by the proteasome 20S, but for reliable conclusions more precise data or the experiments we suggest (for periodic proteins) are in demand.

An additional **open question** here is a specific stochastic mechanism of the translocation process. The stochastic model we use covers the broad class of possible mechanisms (ratchets, diffusion in a titled periodic potential, *etc.*). With having the translocation rates reliably reconstructed from experiments, one may (i) evaluate the physical soundness of the stochastic model used, and (ii) get an additional guiding information for revealing the specific underlaying physical mechanism.

The authors acknowledge the VW-Stiftung (proj. I/80 448), the BRHE program (Award PE–009–0 of CRDF), and the Foundation “Perm Hydrodynamics” for financial support.

Noise induced effects in polymer translocation

N. Pizzolato[a], A. Fiasconaro[ab], B. Spagnolo[a]
[a]Dipartimento di Fisica e Tecnologie Relative,
Università di Palermo and CNISM-INFM, Group of Interdisciplinary Physics,
Viale delle Scienze, edificio 18, I-90128 Palermo, Italy
[b]Mark Kac Complex Systems Research Center, Institute of Physics,
Jagellonian University, Reymonta 4, 30-059 Kraków, Poland

The transport of molecules across membranes represents one of the most important process in biology. DNA and RNA translocate across nuclear membrane channels, proteins can travel from the cytosol into the endoplasmatic reticulum. Recently, polymer translocation has been found to play a fundamental role in the acquisition of multidrug resistance to cancer chemotherapeutics [1].

Fundamental experiments in polymer translocation show a linear dependence of the crossing time on the chain length [2] and a temperature dependence as T^{-2} [3], which cannot be explained by a simple Arrhenius description of the polymer dynamics. In other experiments, shorter DNA molecules have shown longer crossing times, suggesting the existence of a quasi-equilibrium state of the polymer during the translocation [4].

The motion of a polymer in a cellular environment is strongly affected by thermal fluctuations. The dependence of the mean translocation time from the length of the chain molecule critically changes with the noise intensity [5]. In this work we study the noise induced effects on the dynamics of a polymer crossing a potential barrier, in the presence of a metastable state. An improved version of the Rouse model for a flexible polymer has been adopted to mimic the molecular dynamics by taking into account both the interactions between adjacent monomers and introducing a Lennard-Jones potential between non-adjacent beads. A bending recoil torque has also been included in our model. The polymer dynamics is simulated in a two-dimensional domain by numerically solving the Langevin equations of motion with a Gaussian uncorrelated noise. We find a nonmonotonic behavior of the mean first passage time (MFPT) and its standard deviation (SD), of the polymer centre of inertia, as a function of the noise intensity. These quantities (MFPT, SD) have been computed using different initial position of the molecule in the unstable region of the potential. We find that the starting position strongly influences the polymer dynamics during the translocation and the related noise induced effect. In this context, the role played by the length of the molecule in the translocation time is also investigated.

References

[1] C. F. Higgins, Nature **446**, 749 (2007)

[2] J. J. Kasianowicz, E. Brandin, D. Branton, and D. W. Deamer, Proc. Natl. Acad. Sci. USA **93**, 13770 (1996).

[3] A. Meller & D. Branton, Electrophoresis **23**, 2583 (2002).

[4] J. Han, S. W. Turner, and H. G. Craighead, Phys. Rev. Lett. **83**, 1688 (1999).

[5] N. Pizzolato, A. Fiasconaro, B. Spagnolo, Int. J. Bifurc. Chaos, accepted for publication, (2008).

Influence of firing mechanisms on gain modulation

Ryota Kobayashi
Kyoto University Department of Physics
Kyoto 606-8502, Japan

A neuron receives a thousands of synaptic inputs. The synaptic inputs are considered to be very noisy. Recently, the role of synaptic noise in neural computation has discussed [1, 2]. Chance et. al. [2] investigated experimentally the influence of synaptic noise on the firing rate of a neuron. They found the synaptic noise modulates the firing rate of a neuron. This effect is called gain modulation and experimental studies have shown gain modulation plays an important role in neural computation [3].

However the understanding of the underlying mechanism of gain modulation is currently lacking. The questions are, how does the firing mechanism of a neuron affect gain modulation, and how dose the statistical property of synaptic noise affect gain modulation?

To answer these questions, we studied the firing rate of model neurons receiving constant currents I_0 along with stochastic synaptic currents $I_{\rm syn}(t)$ [2]

$$C\frac{dV}{dt} = F(V) + I_0 + I_{\rm syn}(t), \tag{1}$$

where V is the membrane potential of a neuron, and C is the membrane capacitance of a neuron, and $F(V)$ describes the dynamics of the membrane potential. The functional form of $F(V)$ depends on a neuron model. We assumed the synaptic currents $I_{\rm syn}(t)$ are given by the following equations

$$\begin{aligned} I_{\rm syn}(t) &= g_{\rm E}(t)(V_{\rm E} - V(t)) + g_{\rm I}(t)(V_I - V(t)), \\ g_{\rm E,\,I}(t) &= \sum_j a_{\rm E,\,I} \exp\left(-\frac{t - t_j^{\rm E,\,I}}{\tau_{\rm E,\,I}}\right), \end{aligned} \tag{2}$$

where $t_j^{\rm E,\,I}$ is the jth spike time of the excitatory(E) and the inhibitory(I) presynaptic neuron, and $\tau_{\rm E,I}$ is the time constant of the synaptic conductance. The spike times of the excitatory(E) and the inhibitory(I) presynaptic neuron are generated by a homogeneous Poisson process with rate $\lambda_{\rm E,I}$ respectively.

To investigate the effect of the firing mechanism on gain modulation, we analyzed three neuron models, Leaky-integrate-and-fire (LIF) model [4] and Leaky-integrate-and-fire with dynamic threshold (LIFDT) model [5] and the Hodgkin-Huxley (HH) model [4]. We examined the influence of the synaptic currents $I_{\rm syn}(t)$ on the relationship between the firing rate and the constant input currents I_0. We found only the LIFDT model can accurately reproduce this relationship observed in the experiment [2]. This result indicates that cortical neurons may have an adaptation mechanism and it is not included in the HH model.

References

[1] Mainen, Z.F., and Sejnowski, T.J., *Science* **268** pp. 1503-1506 (1995)

[2] Chance, F. S., Abbott, L. F., and Reyes A. D., *Neuron* **35** pp. 773-782 (2002)

[3] Salinas, E., and Sejnowski T. J., *Neuroscientist* **7** pp. 430-440 (2001)

[4] Gerstner, W., and Kistler, W., *Spiking neuron models: single neurons, populations, plasticity* (Cambridge Univ. Press, Cambridge UK, 2002)

[5] Lindner, B., and Longtin, A., *J. Theor. Biol.* **232** pp.505-521 (2005).

Crackling noise

C.1 – Fabio Leoni
Fluctuations and collective behavior in a dislocation pile-up *89*

C.2 – Alvarro Corral
Critical propagation of tropical cyclones *90*

C.3 – Alvarro Corral
Waiting-Time Scaling Law without Power-Law Distributed Sizes in Italian Forest Fires *91*

Fluctuations and collective behavior in a dislocation pile-up

F. Leoni[1] and S. Zapperi[2,3]
[1] Dipartimento di Fisica, Sapienza Università di Roma,
P.le A. Moro 2, 00185 Roma, Italy.
[2] CNR-INFM, S3, Dipartimento di Fisica, Università di Modena e Reggio Emilia,
via Campi 213/A, I-41100, Modena, Italy
[3] ISI Foundation Viale San Severo 65, 10133 Torino, Italy

Recently the traditional paradigm of 'stable' plastic deformation as a smooth and steady flow process has been challenged both from an experimental and from a theoretical point of view [1]. Instead of the incoherent motion of individual defects, one finds coherent bursts of activity with long-range correlations both in space and in time. Here we describe, from a microscopic point of view, scale-free fluctuation phenomena and collective behavior for a particular configuration of dislocations, the pile-up, that can be observed in deforming crystals.

Crystal dislocations typically arrange into complex assemblies, affecting the mechanical properties of the materials. Non-local elastic properties arising naturally from long-range dislocation interactions, and the presence of disorder influence dramatically the plastic deformation process. Random disorder, in the form of solute atoms or other spatial heterogeneities, is responsible for a wealth of phenomena including surface roughening, non-linear dynamic response, stick-slip behavior and temporal intermittency, which are also observed in other physical systems ranging from domain walls in magnets and sheared granular matter to vortices in type II superconductors. Under the effect of an external force, these systems exhibit a complex behavior arising from the competition between elasticity and disorder. Disorder tends to perturb the system, which reacts by opposing elastic restoring forces. This complex small scale dynamics determines the macroscopic behavior of irreversibly deforming materials.

Several approaches have been employed in the literature to study dislocation assemblies. Molecular dynamics simulations provide a very accurate description of the dynamics, but suffer from numerical limitations, since it is difficult to reach the asymptotic regime. An alternative method is provided by the Langevin approach in which the dislocations are assumed to evolve stochastically [1]. In fact, the dynamics of the underlying crystalline medium enters in the problem only through the noise term (due to phonons and electrons) and eventually the periodic potential (Peierls-Nabarro). Hence, the equation of motion of the atoms or molecules are not directly relevant. Indeed there is experimental evidence in supporting of separation of time scales in plastic flow [2] and it is thus possible to integrate out the fast degrees of freedom (phonons and electrons) and consider only the slow ones (dislocations position).

A pile-up is schematized by an effective one-dimensional model in which an array of N points dislocations (with Burgers vector parallel to the array direction) move along a line, interacting with each other and with a disordered stress landscape provided by solute atoms, or other defects [3]. The presence of solute atoms changes the local properties of the host material, resulting in a pinning force on nearby dislocations. The purpose of this study is to analyze the dynamics of the pileup for different configurations and conditions. First we consider, the pile-up in a landscape of immobile defects with open boundary conditions. Dislocations are nucleated on the left side of the line and absorbed on the right. We find a scaling collapse for the dislocation density as a function of stress and system size that is indicative of a second order non-equilibrium phase transition. As a second step, we consider the pileup in a landscape of mobile solute atoms, performing a biased diffusion process. Mobile solute atoms are relevant to understand plastic instabilities in the Portevin-Le Chatelier effect (PLC). We find that the interplay between solute atom mobility and dislocation interaction leads to interesting fluctuation phenomena.

References

[1] M. Zaiser, *Adv. Phys.* **55** pp. 185-245 (2006)

[2] G. Ananthakrishna, *Phys. Rep.* **440** pp. 113-259 (2007)

[3] P. Moretti, M. C. Miguel, M. Zaiser and S. Zapperi, *Phys. Rev. B* **69** pp. 214103(11) (2004)

Critical propagation of tropical cyclones

Albert Ossó Castillón, Josep Enric Llebot
Grup de Fisica Estadistica, Departament de Fisica,
Facultat de Ciencies, Universitat Autonoma de Barcelona,
E-08193 Cerdanyola (Barcelona), Spain.
Alvaro Corral
Centre de Recerca Matematica, Edifici Cc, Campus UAB Bellaterra,
E-08193 Cerdanyola (Barcelona), Spain

Tropical cyclones, or, roughly speaking, hurricanes, are complex structures that have been studied for a long time; nevertheless, many aspects of the physics of hurricanes remain unknown [1]. For instance, although there have been substantial improvements on the prediction of their trajectories, the sudden intensifications they experience preclude the possibility of obtaining reliable forecasts. We analyze different measures of hurricane size, trying to establish connections with out-of equilibrium critical phenomena, in particular with self-organized criticality [2, 3]. Moreover, this new perspective can help to understand the complexity of the fluctuations in climate-change processes [4].

References

[1] K. Emanuel. *Divine wind: the history and science of hurricanes.* Oxford University Press, New York, 2005.

[2] P. Bak. *How Nature Works: The Science of Self-Organized Criticality.* Copernicus, New York, 1996.

[3] O. Peters and J. D. Neelin. Critical phenomena in atmospheric precipitation. *Nature Phys.*, 2:393–396, 2006.

[4] A. O. Castillón, A. Corral and J. E. Llebot, preprint (2008).

Waiting-Time Scaling Law without Power-Law Distributed Sizes in Italian Forest Fires

Alvaro Corral
Centre de Recerca Matematica, Edifici Cc, Campus UAB Bellaterra,
E-08193 Cerdanyola (Barcelona), Spain
Luciano Telesca and Rosa Lasaponara
Istituto di Metodologie per l'Analisi Ambientale
CNR, C. da S. Loja, 85050 Tito (PZ), Italy

Forest-fire waiting times, defined as the time between successive fires above a certain size in a given region, are calculated for Italy. The probability densities of the waiting times are found to verify a scaling law, despite that fact that the distribution of fire sizes is not a power law. The meaning of such behavior in terms of the possible self-similarity of the process in a nonstationary system is discussed. We find that the scaling law arises as a consequence of the stationarity of fire sizes and the existence of a nontrivial instantaneous scaling law, sustained by the correlations of the process; as a consequence, the nonstationary Poisson process model does not account for all the complexity of the structure of fire occurrence [1].

References

[1] A. Corral, L. Telesca, and R. Lasaponara. Scaling and correlations in the dynamics of forest-fire occurrence *Phys. Rev. E* **77**, 016101 (2008).

Noise in complex and non-linear systems

C&NL.1 – Toru Ohira
Stochasticity and Non-locality on the Time Axis *93*

C&NL.2 – Denis S. Goldobin
Generation of Localized Convective Flows under Parametric Disorder *94*

C&NL.3 – Francisco J. Cao
Optimal operation of feedback flashing ratchets *95*

C&NL.4 – Alessandro Magni
Avalanches visualization in magnetic thin films: temporal processing *96*

C&NL.5 – Alessandro Fiasconaro
Active Brownian motion with stochastic energy reservoir *97*

C&NL.6 – Denis L'Hôte
A device to measure locally the magnetic noise of physical systems *98*

C&NL.7 – Saverio Morfu
Noise induced breather generation in a sin-Gordon chain *99*

C&NL.8 – Sylvain Joubaud
Fluctuations at a critical point *100*

Stochasticity and Non-locality on the Time Axis

Toru Ohira
Sony Computer Science Laboratories, Inc.
Tokyo, 141-0022, Japan

The main theme of this paper is to consider concepts of stochasticity and non-locality on the time axes within the framework of classical dynamics through a presentation of rather simple models. These concepts are normally associated in the space variable, not in the time variable. We try to illustrate here the question of what happens if we transfer these concepts on the time axis.

More concretely, time is normally viewed as not having stochastic characteristics. This is so in normal dynamical systems, whether they are classical, quantum, or relativistic. In stochastic dynamical theories, we consider noise and fluctuations with only space variables, such as the position of a particle, and not with the time variable. In quantum mechanics, the concept of fluctuation is embodied in the time-energy uncertainty principle. However, time is not a dynamical quantum observable, and clear understanding of the time-energy uncertainty has yet to be found.

The similar situations in our cognition of non-locality in space and time. Non-local effects in space are incorporated in physical theories through wave propagation, fields, and so on. In quantum mechanics, the issue of spatial non-locality is more subtle, as appearing in the Einstein-Podolsky-Rosen paradox. With respect to time, there have been investigations of memory or delay effects in dynamical equations. In general, however, less attention has been paid to non-locality in time, and behaviors associated with non-locality in time, such as delay differential equations, are not yet fully understood.

Against this background, we present simple classical dynamical models to illustrate the idea of introducing stochasticity and non-locality into the time variable. For non-locality in time, we discuss delayed and anticipating dynamics which involve two points separated on the time axis. The general differential equation of the class of delayed dynamics is

$$\frac{dx(t)}{dt} = F(x(t), \bar{x}(\bar{t})). \tag{1}$$

Here, x is the dynamical variable, F is the "dynamical function" governing the dynamics, and $\bar{x}(\bar{t})$ is the state of x at some time point $t \neq \bar{t}$. Thus, the dynamics of x depends not only on its state at the current time t, but also on that at $\bar{t}$, which is separated from t the time axis. The level of temporal non-locality is the time interval between these two points.

If we take

$$\bar{t} = t - \tau, \quad \bar{x}(\bar{t}) = x(t - \tau) \tag{2}$$

we have a delayed dynamical system with "delay" $\tau > 0$.

On the other hand, we can take

$$\bar{t} = t + \eta \tag{3}$$

with "advance" $\eta > 0$. Given a suitable definition of $\bar{x}(t + \eta)$, this leads to "anticipative" or "predictive" dynamics, in which the dynamics of x depends on the state of x in the future. We present how the change in the level of non-locality as represented by delay τ and advance η affects the dynamics, leading to complex behaviors.

Similarly with respect to stochasticity on the time axis, we discuss a model which includes noise in the time variable but not in the space variable. Let us call such time variable as "stochastic time". The general differential equation of the class of delayed dynamics with stochastic time is given as

$$\frac{dx(\bar{t})}{d\bar{t}} = f(x(\bar{t}), x(\bar{t} - \tau)). \tag{4}$$

Here, as before, x is the dynamical variable of time t, and f is the "dynamical function" governing the dynamics. τ is the delay. The difference from the normal delayed dynamical equation appears in $\bar{t}$, which now contains stochastic characteristics. We show, through a study of a concrete model, that we can observe a resonance effect by a suitable combination of stochasticity in time and delay. This effect is similar to stochastic resonance, which arises through a combination of oscillating behavior and spatial noise and has been studied in variety of fields. We mention some of the difficulties in analyzing these types of models with a stochastic time.

We would like to discuss how these models may be developed to fit a broader context of generalized dynamical systems where fluctuations and non-locality are present in both space and time. Also, directions of further investigations toward possible applications, such as stick balancing on the human fingertips and the classical theory of electrons, will be discussed.

References

[1] Ohira, T., Stochasticity and Non-locality of Time *Physica A* **379** p. 483 (2007)

[2] Ohira, T. and Y. Sato, Resonance with Noise and Delay *Phys. Rev. Lett.* **82** p. 2811 (1999)

[3] Ohira, T. and Yamane, Y., Delayed Stochastic Systems *Phys. Rev. E* **61** p. 1247 (2000)

[4] Cabrera, J. L. and Milton, J. G., On–Off Intermittency in a Human Balancing Task *Phys. Rev. Lett.* **89** 158702 (2002).

[5] Rohrlich, F.,*Classical Charged Particles*, (Addison-Wesley, Reading, Mass., 1965).

[6] Sidarth, B. G., The Lorents-Dirac and Dirac equations, arXive:physics/0701237 (2007).

Generation of Localized Convective Flows under Parametric Disorder

Denis S. Goldobin[1,2] and Elizaveta V. Shklyaeva[1]

[1]Department of Theoretical Physics, Perm State University,
15 Bukireva street, 614990, Perm, Russia

[2]Department of Physics, University of Potsdam,
Postfach 601553, D–14415 Potsdam, Germany

Random spatial inhomogeneity of parameters of extended systems may lead to significant nontrivial effects. Here the most noteworthy examples are the Anderson localization effect, the problem of transparency of randomly inhomogeneous medium for light, *etc.* Nevertheless, in fluid dynamics (specifically, in thermal convection), the effects essentially caused by parametric disorder, *e.g.* Anderson localization, remain not widely studied in spite of they are of interest. First, there is *an interest from the viewpoint of mathematical physics* due to *the dissipativeness of convective problems* and, consequently, an equation type *different* than the Schrödinger equation or equations of *nondissipative* acoustic processes. Moreover, there is *a considerable difference in observability of the effects related to formal properties of equations describing the processes essentially different in their nature.* Second, these problems are of interest from the viewpoint of applications: for instance, random spatial inhomogeneity of the permeability of porous medium can effect flows through this medium, considerably affecting heat and mass (including pollutions) transfer in underground waters (what is of interest for ecologists), reactor cooling systems, and filters.

In this work, a thin horizontal layer of porous medium saturated with a fluid is heated from below, and there is a stationary in time random inhomogeneity of parameters (the heating intensity or the porous medium permeability). Remarkably, the same kind equations remain valid for a broad variety of physical problems (large-scale thermal convection in homogeneous and turbulent fluids, and some other excitable extended systems). In accordance with the described motives for the interest to this problem, we put emphasis on

a) interpretation of the localization effect of formal solutions to the linearized equations of the problem;
b) determining the localization properties and the effect of a imposed longitudinal advection of fluid on them;
c) observation of these properties in the nonlinear (not linearized) system;
d) determining the influence of the effects under consideration on the convectional transport of pollutant through the porous medium.

The points (a) and (c) are, to some extent, *venturing* in the sense that procedures for them are not predefined *unambiguously* by certain reasons. An additional *open question* here is a possible qualitative difference between 1-D (parameters are inhomogeneous in one of the horizontal directions) and 2-D cases like for Anderson localization, where, in the 1-D case, all the solutions are localized, while, in the 2-D case, unlocalized solutions appear. The first apparent topological effect here is the possibility of a percolation transition in 2-D (not possible in 1-D), where the domain of an intensive convective flow may be either globally connected or not connected. But even here not all points are clear for the moment.

The authors acknowledge the BRHE program (Award PE–009–0 of CRDF), RFBR (Grant No. 08-01-00537-a) and the Foundation “Perm Hydrodynamics” for financial support.

Optimal operation of feedback flashing ratchets

M. Feito, F. J. Cao
Departamento de Física Atómica, Molecular y Nuclear,
Universidad Complutense de Madrid,
Avenida Complutense s/n, 28040 Madrid, Spain.

Brownian motors or ratchets are rectifiers of thermal fluctuations. Usually two conditions are sufficient to rectify thermal fluctuations and induce direct transport without an a priori bias, namely, the breaking of thermal equilibrium and the breaking of spatial inversion symmetry [1]. Ratchets are relevant from the theoretical point of view of studying non-equilibrium processes, and from a practical point of view due to their applications in nanotechnology and biology [1, 2, 3].

In flashing ratchets the rectification of thermal fluctuations is achieved by switching on and off a periodic potential. Recently, it has been shown that a significant increase for the net flux in a flashing ratchet can be obtained if feedback on the state of the system is used by the protocol that switches on and off the ratchet potential [4]. Experimental implementations of these feedback flashing ratchets have been proposed [4, 5, 6], and their realization is currently under way [6]. In addition, feedback ratchets have been suggested as a mechanism to explain the stepping motion of the two-headed kinesin [7].

In this context determining the optimal protocol for the operation of a feedback flashing ratchet is a relevant question. However, this question has only received partial answers.

In the *maximization of the instant-velocity protocol* [4] the control policy depends on the sign of the net force per particle at each instant of time. More specifically, the potential is switched on if the net force per particle is positive and it is switched off otherwise. This protocol was found to be the optimal protocol for a feedback flashing ratchet consisting on a single particle. However, for a large number of particles the system dynamics gets trapped with the potential 'on' or 'off' and for a thousand of particles it already gives less flux than a simple periodic switching protocol that do not receives any feedback from the system.

The undesired trapping of the dynamics is settled in the *threshold protocol* [8], in which the potential switching is imposed provided the absolute value of the net force per particle is below certain threshold values. For an adequate value of the thresholds, this new strategy gives the same flux as the optimal periodic switching protocol for an infinite number of particles. Note that for an infinite number of particles no appreciable advantage over the optimal periodic switching can be obtained by using a feedback scheme, as only one degree of freedom control is performed (switching on and off). Therefore, the threshold protocol succeeds to get the optimal protocol both for the one particle case and for the infinite particle case, yielding in between fluxes greater or equal than open-loop protocols for all numbers of particles.

It is interesting to note that an exact optimization study in the framework of a discrete ratchet-like system revealed that the optimal protocol was a kind of threshold operation [9]. On the other hand, it was reported very recently [6] an attempt to beat the threshold protocol, the so-called *maximal net displacement* strategy. This new protocol was numerically found to slightly beat the threshold strategy for collective ratchets of two and three particles and enormous potential heights (greater than $50k_BT$).

The previous results seem to indicate that the threshold protocol gives fluxes close to the optimal protocol. However, which is the optimal protocol for a feedback flashing ratchet is still an open question.

References

[1] P. Reimann, *Phys. Rep.* **361**, 57 (2002).

[2] H. Linke, *Appl. Phys. A* **75**, 167 (2002).

[3] E. R. Kay, D. Leigh, and F. Zerbetto, Angew. Chem. Int. Ed. **46**, 72 (2007).

[4] F. J. Cao, L. Dinis, and J. M. R. Parrondo, *Phys. Rev. Lett.* **93**, 040603 (2004).

[5] M. Feito and F. J. Cao, *Phys. Rev. E.* **76**, 061113 (2007); E. M. Craig, B. R. Long, J. M. R. Parrondo, and H. Linke, *Europhys. Lett.* **81**, 10002 (2008).

[6] E. M. Craig, N. J. Kuwada, B. J. Lopez, H. Linke, *Ann. Phys.* **17**, 115 (2008).

[7] M. Bier, Biosystems **88**, 301 (2007).

[8] L. Dinis, J. M. R. Parrondo, and F. J. Cao, *Europhys. Lett.* **71**, 536 (2005); M. Feito and F. J. Cao, *Phys. Rev. E* **74**, 041109 (2006).

[9] B. Cleuren and C. Van der Broeck, *Phys. Rev. E* **70**, 067104 (2004).

Avalanches visualization in magnetic thin films: temporal processing

Magni, A.[1]; Durin, G.[1]; Zapperi, S.[2,3]; Sethna, J.P.[3,4]

April 14, 2008

[1]Istituto Nazionale di Ricerca Metrologica, Torino, Italia.
[2]Dep. of Physics, University of Modena and Reggio Emilia, CNR-INFM National Center on nanoStructures and bioSystems at Surfaces (S3), Modena, Italy.
[3]ISI Foundation, Torino, Italy.
[4]Physics Department, LASSP, Cornell University, Ithaca, NY, USA.

The motion of domain walls in soft magnetic materials, a basic example of complexity in materials science, has been the subject of a long and continuing series of studies. In bulk systems, most of the statisticals properties are understood in terms of the depinning transition [1]. In thin films similar processes are believed to happen. In many recent works (e.g. [2, 3]), avalanches are measured optically, in a small sub-window of the entire sample, and comparing windows of varying sizes. Yet their statistical description, in terms of the avalanche size distribution $P(S) = S^{\tau} f(S/S_0)$, is still not clear.

We acquired images of domains on Py films using a high-resolution Kerr microscope, under a slowly varying in-plane field. The determination of avalanche size from images is complex, due to the rich space-time information provided. To address this question, we determined a reliable procedure to identify the domains in the images. An effective method is to ignore at first the spatial information and consider only the time evolution for each pixel: a significant jump in the measured intensity represents the switching time for the magnetization at that point. Spatial information must then be used to correct for the small number of pixels which appear to switch at the wrong time.

We then considered the effect of the window size of the images. Generally, the window size effect is both to suppress the largest avalanches and to add extra truncated avalanches at small sizes. We thus simulated an elastic line moving in a random environment, from which we calculated size distributions including/excluding the avalanches touching the window borderes. We observe that large avalanches near to the depinning transition are increasingly anisotropic: an avalanche with width W will have typical height $H \sim W^{\zeta}$. If $\zeta < 1$, as in our case ($\zeta = 0.63$), large avalanches become short and fat. This means that the main effect of large windows is to cut off the widest avalanches, while at small window sizes a substantial number of tall avalanches may also be removed. Thus, unlike isotropic finite-size scaling, the effects of larger windows are not similar to the effects of small windows: they are similar to smaller windows *having different shape*. We can analyze the data using the finite-size scaling form $P(S, L) = S^{\tau} P_W(S/L^{1/\sigma\nu})$. Doing so, we find that the fitted exponents $\tau = 1.14$, $1/\sigma\nu = 1 + \zeta = 1.68$ are close to the theoretical expected values (1.13 and 1.63). In contrast, we found that the distribution including the avalanches touching the window borders has an exponent τ which continuously changes with window size, approaching the theoretical value only at the largest window sizes. This analysis enables us to conclude that the measurements at different window sizes must be taken with care, but, at the same time, when staistical distributions are properly rescales, other critical exponents which can better characterize the dynamics can be found.

References

[1] G.Durin, S.Zapperi, in "The Science of Hysteresis", Academic, II, 181 (2005)

[2] E.Puppin, Phys.Rev.Lett. 84,5415 (2000)

[3] K.-S. Ryu et al., Nat.Phys. 3,547 (2007)

Active Brownian motion with stochastic energy reservoir

A. Fiasconaro[ab], E. Gudowska-Nowak[a] and W.Ebeling [c]
[a]Mark Kac Complex Systems Research Center and M.Smoluchowski Institute of Physics, Jagellonian University, Reymonta 4, 30-059 Kraków, Poland
[b]Dipartimento di Fisica e Tecnologie Relative and CNISM-INFM, Università di Palermo Viale delle Scienze, edificio 18, I-90128 Palermo, Italy
[c]Institute of Physics, Humboldt University Berlin, Newtonstr. 15, 12489 Berlin, Germany

The aim of this presentation is to give a brief overview over recent studies on models of nonequilibrium Active Brownian Motion (ABM) coupled to energy reservoirs. Having in mind biological applications where typically some transfer from chemical to mechanic or electric energy appears, we further focus on evolution equations governing time variations of the depot energy. The latter can be described as a stochastic machine able to acquire energy from the environment and converting it into kinetic energy of motion. We present characteristic features of the ABM system in the case of differentiable ratchet potentials and discuss their asymptotic properties as obtained in analytical calculus and in numerical simulations. In particular, the effect of stochastically driven directionality (i.e. noise-induced asymptotic flux reversal) is analyzed in systems acquiring additional energy from the shot noise. Possible application of such a scenario to the ATP molecular machine will be also discussed.

References

[1] F. Schweitzer, W. Ebeling, B. Tilch. Phys. Rev. Letters **80** 5044 (1998).

[2] F. Schweitzer, B. Tilch, W. Ebeling, Eur. Phys. J. B 14, 157 (2000)

[3] A. Fiasconaro, W. Ebeling, E. Gudowska-Nowak, Eur. Phys. J. B, (2008) submitted

[4] W. Ebeling, E. Gudowska-Nowak, A. Fiasconaro, Acta Phys. Pol. (2008) submitted

A device to measure locally the magnetic noise of physical systems

D. L'Hôte, S. Nakamae and F. Ladieu
Service de Physique de l'Etat Condensé (CNRS/MIPPU/URA 2464),
DSM/IRAMIS/SPEC, CEA Saclay, F-91191 Gif/Yvette Cedex, France
V. Mosser and A. Kerlain
ITRON SAS, 76 avenue Pierre Brossolette, F-92240 Malakoff, France
M. Konczykowski
Laboratoire des Solides Irradiés, Ecole Polytechnique, F-91128 Palaiseau, France

Many open problems in the physics of complex systems require local and microscopic measurements of the physical observables. This is particularly true in what concerns time fluctuations since correlations among the fluctuations of the elementary components of the system arise due to their interactions. Such correlations can be characterized by their size in space and time. A local microscopic probe of size W and bandwidth $[0, f]$ will allow to measure correlations having space-time size larger than $W \times 1/f$, that are experimentally unreachable in bulk measurements involving macroscopic sizes. Among many examples of the local noise measurements interest, let us mention the direct observation of molecular cooperativity near the glass transition in a polymer [1].

To mesure the local magnetization of physical systems, we developped an experimental setup based on micronic and sub-micronic magnetic sensors working at temperatures 4 K < T < 300 K. To allow for high resolution measurements, several techniques minimizing parasitic noise contributions have been used: Antivibration devices, complete anti-RF shieldings from the sample till the first amplification stage, use of very low noise preamplifiers (NF-LI75A ®) eventual use of the coincidence between two amplifiers to suppress their voltage noise contribution, etc. We used micro-Hall sensors made from a two-dimensional electron gas (2DEG) in AlGaAs/InGaAs/GaAs heterostructures [2-5]. The low density of the electron gas allows for a large Hall coefficient of 820 $\Omega.T^{-1}$ for 4K < T < 350K. The large T range and an unlimited B-field dynamics are very attractive features of such Hall sensors. We plan to use simple Hall crosses, as well as linear arrays of Hall crosses that will allow spatial correlations measurements. Note that in addition to the Hall sensors themselves, it is possible to pattern additional circuits such as thermometers, coils, front-end electronics, etc. At present, our Hall probes sizes range from 1x1 to 5x5 μm^2, and are patterned by photolithography at Thales Research Technology. Reaching submicronic sizes either by electron beam lithography, or by focussed ion beam passivation is also envisaged in our project.

With a simple Hall voltage measurement, the resolution we obtained ranges from 5 to 15×10^{-7} T (FWHM) for temperatures below 80 K and measurement rates of 0.1 – 10 Hz. The main limitation to the resolution comes from excess noise, with $1/f^{\alpha}$ ($0.3 < \alpha < 2$) or Lorentzian spectra and a power proportional to the squared bias current. However, we started to use the "spinning current" method (which cancels the Hall voltage offset) in order to improve the resolution [4]. The figure (left) shows a spectrum obtained with this method at ambient temperature. The striking result is that the excess noise has been suppressed and the noise is almost independent of the bias current, close to the Johnson-Nyquist level. The resolution improvement expected at low temperature is thus larger than one order of magnitude.

One of our goals is to measure the local magnetic fluctuations of spin or superspin glasses [6] (in particular, to investigate the violation of the fluctuation-dissipation theorem [7]), and more generally 2 and 3D assemblies of magnetic (or superconducting) interacting nano-objects with various disorder levels, aging ferromagnetic systems, etc. The fluctuations are related to the correlations among the elementary magnetic moments, thus their measurement will provide an information on the correlation length and lifetime. With our devices, the measurable space-time sizes should be larger than ~300 nm × ~1 ms. The physical system of interest can be microscopic, even smaller than the probe itself. We succeded in depositing a microdrop of 20 pl of a ferrofluid on the Hall probe surface. On the other hand, if the physical system of interest is macroscopic, the geometry of an experiment will consist in applying the local probe on the surface of the sample. Thus an important question to be adressed is that of the volume in the sample that will contribute to the measured signal. A simple calculation gives a first answer to this question. Assuming that the magnetic probe is at the distance d from the surface of the sample, which is supposed to have its three dimensions much larger than d and the probe size, it is possible to calculate the variance $\langle \delta B_z^2 \rangle$ of the magnetic field fluctuations along a direction z perpendicular to the sample surface. We assume that the field is due to independent magnetic moments fluctuating isotropically and uniformly distributed in the sample. On the figure (right), the spatial distribution of the magnetic moments contributing to the measured variance of the field is given as a function of their distance r to the probe. This distribution is peaked for $r \approx 1.2\ d$, and appoaches zero as r^{-4} when r increases. As a consequence, only the moments located at a distance to the surface of the order of d contribute to the fluctuations of the measured magnetic field. Thus, when the probe is used to measure fluctuations, it is truly 'local' provided that d is sufficiently small. This is due to the fact that the variance $\langle \delta B_z^2 \rangle$ is the sum of squares (the contributions of the elementary momenta which are proportional to r^{-6}) weighted by a geometrical jacobian $\propto r^2$. On the contrary, the measured magnetic field $\langle B_z \rangle$ (when the sample magnetization is non zero) is not 'local' in the sense that the distribution of the magnetic momenta contribution for large r varies as r^{-1}.

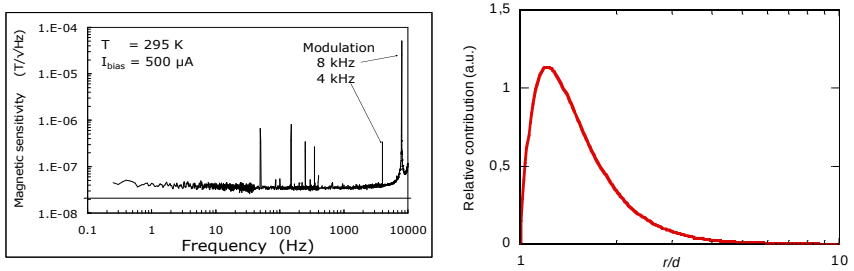

Figure: Left: Power noise spectra of the Hall voltage at ambient temperature obtained on a Hall cross by using the spinning current method. The horizontal line is the Johnson-Nyquist noise of the cross. Right : Calculated spatial distribution of the contributions to the variance of the measured magnetic field fluctuations, for a local magnetic probe placed on a macroscopic sample as a function of r/d (r : distance from the probe center to a microscopic volume element in the sample, d : distance between the probe and the surface of the sample).

References

1] Vidal Russell, E., and Israeloff ,N.E., *Nature* **408** pp. 695-697 (2000).

2] Mosser, V., Kobbi, F., Contreras, S., Mercy, J.M., Callen, O., Robert, J.L., Aboulhouda, S., Chevrier, J., and Adam, D., Proc. 9th Int. Conf. on Solid-State Sensors and Actuators, Chicago, USA, June 1997.

3] Mosser, V., Jung, G., Przybytek, J., Ocio, M., and Haddab, Y, SPIE Fluctuations and Noise Symposium, Santa Fe (NM), 1-4 June 2003, Proc. SPIE Vol. 5115, pp. 183-195 (2003).

4] Kerlain, A. and Mosser, V., *Sensor Letters* **5** pp. 192 (2007).

5] Mosser, V., et al., *Sensors and Actuators* **A43** pp. 135-140 (1994).

6] Parker, D., Dupuis, V., Ladieu, F., Bouchaud, J.-P., Dubois, E., Perzynski, R., and Vincent, E., *Phys. Rev.* B**77**, 104428 (2008)

7] Hérisson, D. and Ocio, M., *Phys. Rev. Lett.* **88**, 257202 (2002)

Noise induced breather generation in a sine-Gordon Chain

B. Bodo, S. Morfu, P. Marquié, B. Essimbi
Aile des sciences de l'ingénieur
BP 47870 21078 Dijon Cedex, France
smorfu@u-bourgogne.fr

For more than ten years now, the discovery of Stochastic Resonance (SR) by Benzi in the context of climate dynamics has changed forever the way to consider noise in nonlinear media [1]. Indeed, under certain conditions, it has been shown that the response of a nonlinear system to a deterministic excitation can be enhanced by an appropriate amount of noise via S.R. [2]. This counter intuitive phenomenon has naturally encouraged researchers to include the contribution of noise in their investigations, leading to interesting applications in different fields such as modeling of biological systems [3], signal processing [4, 5], image processing [6, 7] or nonlinear information transmission [8, 9, 10], to cite but a few. In this last area, it has been demonstrated that if we drove a nonlinear pass-band electrical transmission line beyond its high cut-off frequency with a periodic excitation, the addition of an appropriate amount of noise would trigger soliton generation in the medium with a given probability [11]. In the same way but in the absence of noise, Geniet and Leon [12], have theoretically studied a completely different nonlinear system. Indeed, considering a medium described by a sine-Gordon equation subjected to irradiation at a frequency in the stop gap, they have showed that, when the driving amplitude at the input boundary exceeds a threshold value, a large amount of energy flows through the medium by means of nonlinear modes generation. This phenomenon, known under the name of Nonlinear Supratransmission, has been reported in various nonlinear waveguides, but most often in the deterministic case. Contrary to the works presented in reference [11], we choose here a driving frequency in the stop gap and we consider media described by the sine-Gordon equation. In particular, we investigate if the addition of noise can induce the nonlinear supratransmission effect in a range of parameters where it does not occur. Therefore, the medium is ruled by the following differential equation:

$$\frac{d^2U_n}{dt^2} - c^2(U_{n+1} + U_{n-1} - 2U_n) + \omega_0^2 sinU_n + \gamma_n \dot{U}_n = 0. \quad (1)$$

Moreover, to assume an absorbing end, the damping coefficient γ_n in eq. (1) is null for all cells of the chain except for the last few cells. The profile of the damping coefficient is the following:

$$\gamma_n = 1 + tanh\left(\frac{2n - 2N + m}{2b}\right). \quad (2)$$

Lastly, the boundary conditions are almost exactly the same than those used by Geniet and Leon in [12], that is:

$$u_0(t) = A\sin(\Omega t) + \eta(t), \qquad u_n(0) = 0, \qquad \dot{u}_n(0) = A\Omega e^{-\lambda n}. \quad (3)$$

In eq. (3), $\eta(t)$ is a white gaussian noise of *R.M.S.* amplitude σ whereas the coefficient λ is defined by

$$\lambda = arcosh\left(1 + \frac{1 - \Omega^2}{2c^2}\right). \quad (4)$$

We have set the parameters of the chain to $\omega_0 = 1$, $c = 10$, while the angular frequency of the sinusoidal driving is adjusted to $\Omega = 0.95$. In addition, the time of the simulation is set to $T = 2000$ and the size of the chain is $N = 4000$. In absence of noise, the critical amplitude beyond which supratransmission occurs is then numerically obtained for $A^* = 1.24$. We consider a range of amplitudes of excitation A below the critical value A^* and we investigate the probability to induce supratransmission versus the noise intensity σ. We obtain the bifurcation diagram of fig 1 which allows to extend the supratransmission effect to the case of a more realistic signal, namely a noisy sinusoidal excitation. Usually, the media that display the supratransmission effect also exhibit a bistable behavior resulting from nonlinearity and generating hysteresis properties [13]. Since it has been proven that the bistable behaviour of nonlinear system can be used to realize stochastic detection [14], we trust that the sine-Gordon media which also shares a bistable feature could be used for signal processing purpose to enhance the detection of weak noisy signals.

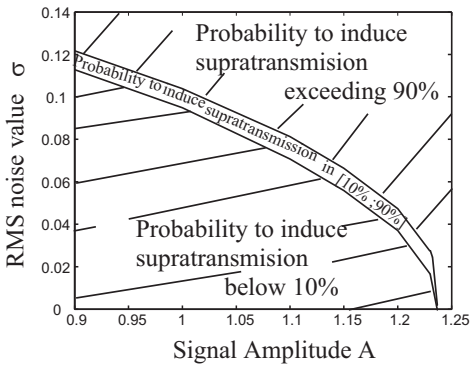

Figure 1: Bifurcation diagram of the sine-Gordon chain submitted to a noisy sinusoidal excitation. There exist three regions of parameters that allow to induce supratransmission with a given probability. Parameters: $N = 4000$, $m = 500$, $b = 140$, $\omega_0 = 1$, $c = 10$, $\Omega = 0.95$.

References

[1] R. Benzi, G. Parisi, A. Sutera and A. Vulpiani Tellus 34, 10–16 (1982).

[2] L. Gammaitoni, P. Hänggi, P. Jung and F. Marchesoni, Rev. Mod. Phys. 70, 223–282 (1998).

[3] F. Moss, L.M. Ward and W.G. Sannita, Clinical Neurophysiology 115, 267–281 (2004).

[4] S. Zozor and P.O. Amblard, IEEE Trans. on Signal Processing 53, 3202–3210 (2005).

[5] J.C. Comte and S. Morfu, Phys. Lett. A 309, 39-43 (2003).

[6] E. Simonotto, M. Riani, C. Seife, M. Roberts, J. Twitty and F. Moss, Phys. Rev. Lett. 78, 1186–1189 (1997).

[7] M. Hongler, Y. De Meneses, A. Beyeler and J. Jacquot, IEEE Trans. on Pattern Analysis and Machine Intelligence 25, 1051–1062 (2003), .

[8] J. F. Lindner, B. J. Breen, M.E. Wills, A.R. Bulsara and W. Ditto, Phys. Rev. E 63, 051107 (2001).

[9] A. A. Zaikin, J. Garcia-Ojalvo, L. Schimansky-Geier and J. Kurths, Phys. Rev. Lett. 88, 010601 (2002).

[10] S. Morfu, Phys. Lett. A 317, 73 (2003)

[11] S. B. Yamgoué, S. Morfu and P. Marquié, Phys. Rev. E 75, 036211-1/036211-7 (2007)

[12] F. Geniet and J. Leon, Phys. Rev. Lett. 89, 134102 (2002) ; and J. Phys. Cond. Matt. 15, 2933 (2003)

[13] R. Khomeriki, J. Léon and D. Chevriaux, Eur. Phys. J. B 49, 213-218 (2006).

[14] F. Duan and D. Abbott, Phys. Lett. A 344, 401–410 (2005).

Fluctuations at a critical point

S. Joubaud, A. Petrosyan and S. Ciliberto
Ecole Normale Supérieure de Lyon, Laboratoire de Physique,
C.N.R.S. UMR5672,
46, Allée d'Italie, 69364 Lyon Cedex 07, France

May 15, 2008

The mean orientations of the fluctuations of the director of a nematic liquid crystal are measured using a sensitive polarization interferometer. When an electric field is applied perpendicularly to the initial alignment of the molecules, there is a critical point for which molecules try to align to the field. This is called the Frédericksz transition which is expected to be second order phase transition. We show that near the critical value of the field the spatially averaged order parameter has a generalized Gumbel distribution instead of a Gaussian one. The latter is recovered away from the critical point. We investigate also experimentally the non equilibrium behavior of the liquid crystal during its critical relaxation. Correlation function and response function are measured during the quench and an aging like behavior is clearly displayed.

Noise in materials and devices

M&D.1 – Igor V. Bezsudnov
Internal Percolation Problem *102*

M&D.3 – Jevgenij Starikov
Anomalous behavior of electronic noise related to the onset of current instabilities in n^+nn^+ diodes *103*

M&D.5 – Oleg Gerashchenko
Power-law distribution of the flux avalanches in a Josephson medium. *104*

M&D.6 – Dominique Persano Adorno
Noise influence on electron dynamics in semiconductors driven by a periodic electric field *105*

M&D.7 – Jean-Marc Routoure
LSMO thermometers for uncooled bolometric applications *106*

M&D.8 – Chenghua Liang
1/f Noise in polyaniline / polyurethane (PANI/PU) blends *107*

M&D.9 – Nobuhisa Tanuma
Low-frequency noise monitoring of current collapse in AlGaN/GaN high-electron-mobility transistors on sapphire substrate *108*

M&D.10 – Svetlana A. Vitusevich
Noise spectroscopy of AlGaN/GaN HEMT structures with long channel *109*

M&D.11 – Valentina Andreoli
Transition process of superconducting nanogranular MgB2 films by current noise analysis in non-stationary conditions *110*

M&D.12 – Yossi Paltiel
1/f Resistance Noise in Low-doped $La_{1-x}Ca_xMnO_3$ Manganite Single Crystals *111*

M&D.13 – Julien Gabelli
Full Counting Statistics of Avalanche Transport: an Experiment *112*

Internal Percolation Problem

A. A. Snarskii[1], I. V. Bezsudnov[2]
[1] National Technical University of Ukraine "KPI",
Dep. of General and Theoretical Physics, Kiev, Ukraine
[2] Nauka Service JSC, Moscow, Russia

Investigated critical behaviour of $1/f$ noise in new kind of percolation problem - so called internal percolation problem (IP). For usual percolation current flows from top to bottom of the system and here it can be called as external percolation problem (EP) despite of the IP case when voltage is applied to the system through bars which are inside of the hole in system (see Fig.1).

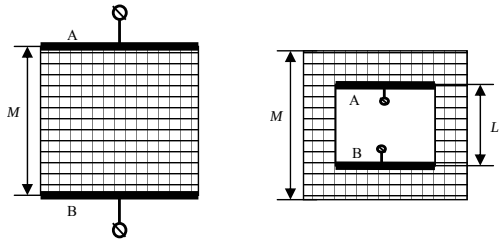

FIGURE 1. Schematic plot of the external (a) and internal (b) problems.

EP problem has two major parameters: M – size of system and a_0 – size of inclusion, lattice size etc. IP holds one more parameter – the size of hole - L.

In EP for sizes $M \gg \xi$, where ξ - correlation length, the conductance of whole system is not depend on realization of random media. In IP problem if $M \gg \xi$ two different cases exist: $L \gg \xi$ and $M - L \gg \xi$, when size of system where current flows is bigger then correlation length and realization of random media do not affect conductance of the whole system and the case when such condition is not true either $L \le \xi$ or $M - L \le \xi$ - the system looks like rectangle with one side less than correlation length and therefore conductance will depend upon random realization.

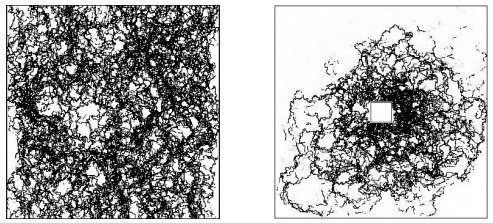

FIGURE 2. Averaged (over 50 random realizations) spatial distribution of 4-th moment in EP system (a) and IP system (b), with a hole in the centre.

Computer simulations of IP problem was performed see for example Fig.2. Results of computer simulation shows, that indexes of relative spectral noise density of $1/f$ noise and higher moments are really differs from those in EP problem.

The source of such behaviour is discussed and also possible further modifications of IP problem are introduced.

References

[1] B.A.Aronzon, N.K.Chumakov, A.A.Snarskii, J.-M.Brotto, H.Rokoto, J.Leotin // *Superlocalization in compensated InSb, The physics of semiconductors, 24th International Conferece*, Jerusalem, Israel, August 2-7, 1998, pp.43-50

[2] Albinet G., Tremblay R.R., Tremblay A.-M.S. // *J.Phys.I, France.* **3** pp.323-330

[3] Arcangelis L. de, Redner S., Coniglio A. // *Phys.Rev.B.* **34** pp.4656.

[4] Arcangelis L.de, Redner S., Coniglio A. // *Phys.Rev.B.* **31** pp. 4725-4727.

[5] Bergman D.J., Stroud D. // *Solid St.Phys.* **46** pp.147-269.

[6] Broadbent S.R., Hammersley J.M. // *Proc.Camb.Phyl.Soc.* **53** pp.629-633.

[7] Butterweck H. // *Philips Res.Rep.* **30** pp.316.

[8] Clerc J.P., Giraud G., Laugier J.M., Luck J.M. // *Advances in Physics.* **39** pp.191-309.

[9] Efros A.L., Shklovskii B.I. // *Phys.Stat.Sol.B.* **76** pp.475-485.

[10] Isichenko M.B. // *Rev.Mod.Phys.* **64** pp.961-1043.

[11] Rammal R., Tannous C., Brenton P., Tremblay A.-M.S. // *Phys.Rev.Lett.* **54** pp.1718-1727.

[12] Snarskii A.A., Morozovsky A.E., Kolek A., Kusy A. // Phys.Rev.E. 1996. **53** pp.5596-5605.

[13] Snarskii A.A., Bezsudnov I.V., Sevryukov V.A. // *Transport in macroscopically inhomogeneous media*, URSS, Moscow, 2007

[14] Stauffer D., Aharony A. // *Introduction to Percolation Theory*. 2nd ed., Taylor&Francis, 1992.

[15] Tremblay R.R., Albinet G., Tremblay A.-M.S. // *Phys.Rev.B.* 1991. **43** pp.11546-11549.

[16] Wolf M., Muller K.-H. // *Phys.St.Sol.A.* 1985. **92** pp.151.

Anomalous behavior of electronic noise related to the onset of current instabilities in n^+nn^+ diodes

E. Starikov[a], P. Shiktorov[a], V. Gružinskis[a],
L. Varani[b], C. Palermo[b], G. Sabatini[b], H. Marinchio[b], T. Laurent[b]
and L. Reggiani[c]
[a]Semiconductor Physics Institute
Goštauto 11, 01108 Vilnius, Lithuania
[b]Institut d'Électronique du Sud (CNRS UMR 5214)
Université Montpellier 2, Place Eugène Bataillon, 34095 Montpellier Cedex 5, France
[c]Dipartimento di Ingegneria dell'Innovazione, Università del Salento and CNISM
Via Arnesano s/n, I-73100 Lecce, Italy

It is well known that under nearly-thermal conditions the spectrum of current noise in homogeneous resistors exhibits a Lorentzian shape with a cutoff frequency determined by the momentum relaxation rate. In the case of n^+nn^+ diodes there appear an additional high-frequency spike (usually in the region 5-20 THz) caused by a hybrid plasma resonance at the n^+n-homojunctions. By increasing the static voltage applied between the diode terminals, the Lorentzian part of the noise spectrum can be transformed following two main scenarios which reflect: (i) the hot-electron velocity noise behavior in bulk materials, (ii) the dynamic behavior of electrons in the structure determined by carrier propagation and redistribution coupled with the self-consistent electric field. The most interesting case from both the fundamental and applied point of view corresponds to the second scenario when various current instabilities related to Gunn-effect, plasma effects, etc. can appear above some threshold value of the applied voltage. The onset of such instabilities can lead to a drastic change of the noise spectrum at frequencies below the hybrid plasma resonance frequency. Numerous Monte Carlo simulations for different situations evidence that such a transformation of the noise spectrum includes: (i) the appearance of noise spikes at resonant frequencies of the structure determined by physical effects responsible for the instability (Gunn-domain and the associated formation of an accumulation-layer and its propagation, plasma waves, etc.), (ii) the enhancement of the noise level (sometimes up to several orders of magnitude) and the appearance of extra resonances in the frequency region below (and even considerably below) the resonant frequency range. While the former phenomenon has an evident physical interpretation related to the appearance of spontaneous oscillations of the current at the resonant frequencies of the instability, the latter one has no evident connection with the resonances and can be considered as an anomalous behavior of noise. Usually, a considerable enhancement (up to 1-2 order of magnitude) of the low-frequency noise appears just below the instability threshold. With further increase of the applied voltage this anomalous extra noise practically disappears. One can suppose that such a noise is related to dynamic/stochastic processes formed at the initial stage of the instability because of transitions between "dynamic" states characterized by the presense and absence of current oscillations. Nevertheless, *the origin of such an enhancement of electronic noise can still be considered as an open question.* From an applied point of view such a low-frequency noise enhancement is very interesting since it can be used as an indicator of the onset of high-frequency intabilities, even without a precise identification of the physical processes responsible for the instability. Therefore, the investigation of its origin is of great practical interest especially having in mind that direct measurements of noise and microwave generation in the THz frequency region meet with a lot of difficulties. Accordingly, the aim of this work is to investigate in detail the formation and the possible origin of this anomalous low-frequency noise enhancement by using Monte Carlo Particle simulations of various current instabilities related with Gunn-effect, low-temperature optical phonon emission, plasma waves excitation, etc. in InP and nitride-based n^+nn^+ structures.

Power-low disribution of the flux avalanches in a Josephson medium

O. V. Gerashchenko
Petersburg Nuclear Physics Insninute,
188300 Gatchina, Russia

Avalanche flux penetration dynamics has been experimentally observed in a Josephson medium, a granular high-T_c superconductor, with slowly increasing an external magnetic field. The observed voltage spikes are associated with the stepwise penetration of the field into the superconductor and obey the power-law size distribution. The results directly confirm the hypothesis of self-organized criticality in such a system. But details of fluctuation dynamics in the self-organized critical state of such system is not clear completely.

Granular high-T_c superconductors are known to be strong-pinning multiply-connected Josephson media that can be described by the critical state concept (see, e.g., [1, 2]), proposed for ordinary type-II superconductors by Bean [3].

According to Ginzburg [4], the main parameter of a Josephson medium is the ratio of the characteristic granule area to the Josephson vortex area:

$$V = \frac{a^2}{\lambda_{eff}^2}, \quad \lambda_{eff}^2 = \frac{\Phi_0}{2\pi\mu_0\mu_{eff}j_c a}, \tag{1}$$

where μ_{eff} is the effective permeability of the Josephson medium, j_c is the critical current density. The continious approach of the Bean critical state is valid for the case $V \ll 1$. Taking $j_c = 10^6\ A/m^2$, $\mu_{eff} = 0.5$, and $a = 10\ \mu m$, we obtain $V \approx 2$. Thus, criterion (1) is violated. Physically, this implies that each elementary loop formed by adjacent granules serves as a discrete pinning center for the flux quanta. Therefore, strong pinning is an intrinsic property of the system. In this case, continuum equations are inapplicable and the Josephson medium is described by the equations with marked discreteness that are equivalent to those describing the system with self-organized criticality (SOC) [5]. Structurally, the critical state combines a large number of metastable critical states through which the system walks. An external perturbation drives the systems out of one such metastable critical state and generates a dynamic process (avalanches). The avalanches may be either small or large, involving the whole system, but both are induced by equally small perturbations. This behavior was called self-organized criticality, which manifests itself in a power-law size distribution of aches.

Ginzburg [4] showed that the self-organized critical state in the low-field electrodynamics of the Josephson medium appears ab initio from Maxwell's and Joseph-son equations, and, consequently, the avalanche dynamics is an intrinsic property of the system.

Thus, the appearance of a self-sustaining critical state (according to the Bean model [3]) and the characteristic scaling avalanche dynamics (according to the Bak model [5]) are the main attributes of the self-organized critical state in hard superconductors. Thus, the experimental study of the flux dynamics particularly in a Josephson medium with strong internal pinning on discrete Josephson loops, which is exemplified by a granular high-Tc superconductor, is of supreme importance for the confirmation of the self-organized critical state in such a system [6].

The pickup coil study was carrier out on the $YBa_2Cu_3O_{7-x}$ ceramic prepared by the standard procedure. An external magnetic field was generated by the coil fed with a self-made high-accuracy integrating current source, which provided an accurate long-term linear field sweep. The measurements were performed in at liquid nitrogen temperature.

The accumulation time was as long as several hours, depending on the time constant of the current source, and the rate of the flux variation in the sample was down to one quantum Φ_0 per second. Before each measurement, the sample was warmed up with a subsequent zero-field cooling.

The jumps of the flux penetrating into the sample were detected as short unipolar spikes of the voltage induced in the pickup coil. The apparatus allows us to observe avalanches of at least 100 flux quanta,

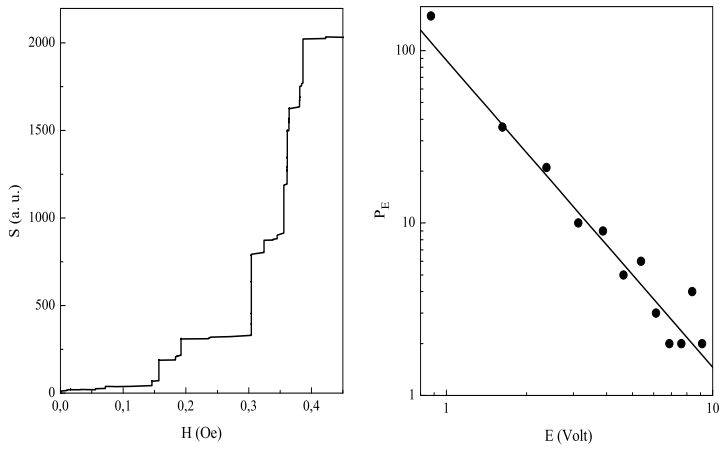

Figure 1: Accumulated amplitude of voltage spikes at the field ramping rate 13 Φ_0/s. The record time is 3600 s(left). Amplitude distribution of voltage spikes. The slope of the linear fit is $k = -1.8$ (right).

which is coobtained by Field [7].

The fragment of the accumulated amplitude of spikes $S \sim \Sigma E_i$, where E_i is the induced voltage exceeding the threshold value equal to five standard deviations, is shown in Figs. 1 (left). The quantity S is proportional to the flux that has entered the sample. Obviously, the flux jumps of the random amplitude are observed.

Figure 1 (right) presents the amplitude distribution of the voltage spikes. The flux penetration is seen to occur in the form of jumps that obey a power-law amplitude distribution $P_E \sim E^k$, where $k = -1.8 \pm 0.2$.

Such a scaling behavior is direct evidence of the existence of the self-organized critical state in the Josephson medium.

This work was supported by the Russian Foundation for Basic Research, and by the Division of Physical Sciences RAS (programs 'Macrophysics' and 'Strongly Correlated Electrons in Semiconductors, Metals, Superconductors, and Magnetic Materials').

References

[1] Sonin, E. B., *JETP Lett.* **47** p. 496 (1988).

[2] Clem, J. R., *Physica C* **50** p. 153 (1988).

[3] Bean, C. P., *Rev. Mod. Phys.* **36** p. 31 (1964).

[4] Ginzburg, S. L., *JETP* **79** p. 334 (1994).

[5] Bak, P., Tang, C., Wiesenfeld, K., *Phys. Rev. A* **38** p. 364 (1988).

[6] Gerashchenko, O. V., *JETP Lett.* **86** p. 470 (2007).

[7] Field, S., Witt, J., Nori, F., et al., *Phys. Rev. Lett.* **74** p. 1206 (1995).

Noise influence on electron dynamics in semiconductors driven by a periodic electric field

D. Persano Adorno[a], N. Pizzolato[ab], B. Spagnolo[ab]
[a]Dipartimento di Fisica e Tecnologie Relative,
Università di Palermo and CNISM-INFM, [b]Group of Interdisciplinary Physics,
Viale delle Scienze, edificio 18, I-90128 Palermo, Italy

Semiconductor based devices are always imbedded into a noisy environment that could strongly affect their performance. A study about the constructive aspects of noise and fluctuations in different non-linear systems has shown that the addition of external noise to systems with an intrinsic noise may result in a less noisy response [1]. The possibility to reduce the diffusion noise in semiconductor bulk materials by adding a random fluctuating contribution to the driving static electric field has been tested in ref. [2] and previous numerical results of noise-induced effects in semiconductors has shown that this opportunity exists also under cyclostationary conditions [3]. Moreover, recent studies on the modification of the spectral density of the electron velocity fluctuations in a GaAs bulk, caused by the mixing of two high-frequency periodic electric fields, have shown that the total power of the intrinsic noise is very sensitive to the amplitude and the frequency of the excitation signals [4, 5].

In the present work we investigate the noise-induced effects on the intrinsic carrier noise spectral density in low-doped GaAs semiconductor driven by a high-frequency periodic electric field. The electron dynamics is simulated by a Monte Carlo procedure which takes into account all the possible scattering phenomena of the hot electrons in the medium. The starting point for our analysis is the computation of the changes in the integrated spectral density (ISD) of the electron velocity fluctuations caused by the addition of an external correlated noise source.

The results reported in this work confirm that, under specific conditions, the presence of a randomly-fluctuating electric field added to an high-frequency periodic field can reduce the total noise power. Furthermore, we find a nonlinear behavior of the ISD with the noise intensity D. In particular, the ISD vs. D diagram shows the presence of a minimum which critically depends on the noise correlation time. This minimum could be ascribed to a combination effect of the external noise amplitude and the ratio between the noise correlation time and the characteristic time scale of the system. We have extensively investigated the details of the electron transport dynamics in the semiconductor. Our study reveals that the system receives a benefit by the constructive interplay between the random fluctuating electric field and the intrinsic noise.

References

[1] J. M. G. Vilar and J. M. Rubì, Phys. Rev. Lett. **86**, 950-953 (2001)

[2] L. Varani, C. Palermo, C. De Vasconcelos, J. F. Millithaler, J. C. Vaissiere, J. P. Nouger, E. Starikov, P. Shiktorov and V. Gruzinskis, Unsolved Problems of Noise and Fluctuations: UpoN 2005, pp.474-479 (American Institute of Physics, 2005)

[3] D. Persano Adorno, N. Pizzolato and B. Spagnolo, Acta Physica Polonica A **113**, in press (2008).

[4] D. Persano Adorno, M.C. Capizzo and M. Zarcone, J. Comput. Electron **5**, 475-477 (2006).

[5] D. Persano Adorno, M. C. Capizzo and M. Zarcone, Fluctuation and Noise Letters **8**, in press (2008).

LSMO thermometers for uncooled bolometric applications

B. Guillet, J.M. Routoure, S. Flament, L. Méchin

GREYC
C.N.R.S. UMR6072, ENSICAEN, Université Caen Basse-Normandie
6, Bd Maréchal Juin, 14050 Caen, France

We report measurements of the temperature coefficient of the resistance (TCR) and the low-frequency noise of epitaxial $La_{0.7}Sr_{0.3}MnO_3$ (LSMO) thin films deposited on Silicon (Si), $SrTiO_3$ (STO) substrates.

An x-ray-diffraction study showed that the films were (001) oriented. A normalized Hooge parameter of 9×10^{-31} m^3 was measured at 300 K in the case of a 10 µm-wide, 575 µm-long line patterned in the 200-nm-thick film grown on STO substrate. This value is among the lowest reported values for manganites and close to values measured in standard metals and semiconductors. The corresponding noise equivalent temperature (NET) was constant in the 300–340 K range and equal to 6×10^{-7} K $Hz^{-1/2}$ at 10 Hz and 0.15 mA for a 10 µm-wide, 575 µm long line patterned in a 200-nm-thick LSMO film [1]. This very low NET value is comparable to the best published results for manganites and was even found to be lower than the NET of other uncooled thermometers such as semiconductors (a-Si, a-Si:H, a-Ge, poly SiGe) and other oxide materials (semiconducting YBCO, VOx, other manganite compounds). The results show that despite a TCR of only 0.017 K^{-1} at 300 K, and thanks to a very low-noise level, LSMO thin films are real potential material for uncooled thermometry and bolometry. Optical responses of a LSMO sample at a wavelength of 533 nm in the 300–400 K range has been investigated [2]. We measured an optical sensitivity at I=5 mA of 10.4 V W^{-1} and corresponding Noise Equivalent Power (NEP) values of 8.1×10^{-10} W $Hz^{-1/2}$ and 3.3×10^{-10} W $Hz^{-1/2}$ at 30 Hz and above 1 kHz, respectively.

Simple considerations on bias current conditions and thermal conductance G are finally given for further sensitivity improvements using LSMO films. Finally, the possible use of these thermometers with such low NET characteristics for the fabrication of both membrane-type bolometers for mid-infrared detection and antenna coupled bolometers for THz applications is discussed. Investigations on the feasibility of multipixels camera will be also showed.

References

[1] F. Yang, L. Méchin, J.M. Routoure, B. Guillet, R. Chakalov, *J. Appl. Phys.* 99, 024903 (2006)

[2] L. Méchin, J.M. Routoure, B. Guillet, F. Yang, S. Flament, D. Robbes, R. Chakalov, *Appl. Phys. Lett.* 87, 204103 (2005)

1/*f* Noise in polyaniline / polyurethane (PANI/PU) blends

C. Liang*, G. Leroy, J. Gest
Université du Littoral Côte d'Opale, Laboratoire LEMCEL – UPRES –E.A. 2601
50 rue F. Buisson, B.P. 717, 62228 Calais, France
L. K. J. Vandamme
Eindhoven University of Technology, Department of Electrical Engineering
P.T. 9. 13 P.O. Box 513, 5600MB Eindhoven, The Nederlands
J-L. Wojkiewicz
Ecole des Mines de Douai, Laboratoire des Polymères Conducteurs et CEM
941 rue Charles Bourseul, 59500 Douai, France
*Contact : Liang@univ-littoral.fr

We investigated the electrical conductivity and the low-frequency noise at room temperature of polyanline / polyurethane (PANI/PU) blends with different compositions and deposited by spin coating. The concentration of PANI varies from 5% to 50%, and 3 specimens of 100% concentration have been respectively deposited on different substrates (on ceramic, PVC, and Teflon). The layer thickness was between 12 µm and 220 µm. The conductivity ranged from 10^2 S/m to 10^4 S/m and the sheet resistance was between 4 Ω and 50 Ω.

A morphological study by optical microscope and TEM revealed the formation of conductive meandering routes by self-assembly of the PANI component [Ref 1]. From their results it turned out that the PANI component seemed to be connected like a flexible net with a wire diameter of about 20 nm. The PANI/PU conductivity did not significantly change with the increase of the elongation in a tensile tester [Ref 1]. This indicates that the resistance is concentrated in the contact region between a pair of PANI wires and much less in the flexible wires. This implies that the flexible wire-net in a tensile test are slightly unwinded due to the elongation but the contacts between conducting paths are kept constant and not disconnected during the elongation.

According to Hooge's empirical relation under constant voltage conditions, 1/*f* noise results obtained on homogeneous fields can be described as [Ref 2],

$$\frac{S_r(f)}{r^2} = \frac{S_v(f)}{V^2} = \frac{\alpha}{fN} = \frac{\alpha}{fnWLt}$$

α, the 1/*f* noise parameter is volume independent with values between 10^{-6} and 10^{-3} for metals and semiconductors, *N* the number of free charge carriers. For layers of unknown thickness, it is convenient to characterize the layer with its sheet resistance $R_{sh} = RW/L = \rho/t$ and relative noise by C_{us} where *t* is the thickness, *L* the length between two line contacts and *W* is the width of the layer.

$$C_{us} = \frac{\alpha}{nt} = \frac{f.S_v}{V^2}WL \qquad C_{us} = \frac{\alpha}{nt} = \alpha q \mu R_{sh} = KR_{sh}$$

The characteristics of the different specimens are given in Table I, and the results are summarized in the C_{us} versus R_{sh} plot of figure 1. A proportion between C_{us} and R_{sh} is observed, and the proportionality factor *K* can be different for high ohmic samples compared to low ohmic samples (see table I and figure 1). Also, these *K* values are very high compared to values found in homogeneous materials (# 5×10^{-19}mm^2/Ω in Au for example [Ref 3]). To explain these extremes high values, we propose a model based on the typical morphology of the PANI component and type of contact between touching molecules (fig. 2). This model shows that the high values for *K* are due to a strong current crowding at the contact spot between two touching PANI wires and the spaghetti-like structure of the conducting network (fig. 3).

This study shows that the noise results can be used as a tool to understand better the transport mechanism and to propose technology improvements.

Table I. Characteristics of the different samples

No.	Sample	Thickness t (µm)	Sheet resistance R_{sh} (Ω)	Conductivity σ (S/m)	Normalized 1/*f* noise C_{us} (mm^2)	$K=C_{us}/R_{sh}$ (mm^2/Ω)	$[\alpha\mu]_{eff} = K/q$ (cm^2/V s)
1	PANI/PU 5% (free)	150	47.3	140	1×10^{-8}	2.1×10^{-10}	1.31×10^{7}
2	PANI/PU 5%-b (free)	170	26	230	5×10^{-9}	1.9×10^{-10}	1.19×10^{7}
3	PANI/PU 10% (free)	220	8	570	3×10^{-9}	3.8×10^{-10}	2.37×10^{7}
4	PANI/PU 20% (free)	70	9	1.6×10^{3}	2×10^{-9}	2.2×10^{-10}	1.37×10^{7}
5	PANI/PU 50% (free)	55	4.4	4.1×10^{3}	1×10^{-9}	2.3×10^{-10}	1.44×10^{7}
6	PANI (Ceramic)	12.5	10	8×10^{3}	5.6×10^{-10}	5.6×10^{-11}	3.50×10^{6}
7	PANI (Teflon)	12	7.7	1.1×10^{4}	1.3×10^{-10}	1.7×10^{-11}	1.06×10^{6}
8	PANI (PVC)	12.5	7	1.1×10^{4}	1.4×10^{-10}	1.9×10^{-11}	1.21×10^{6}

Figure 1. Comparison of the proportionality factor K between high ohmic samples and low ohmic samples

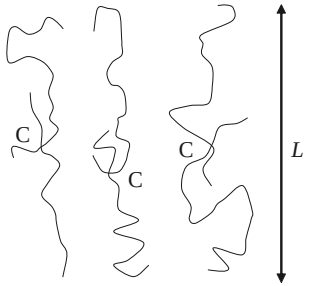

Figure 2. Spaghetti-like morphology of the PANI wires touching each other

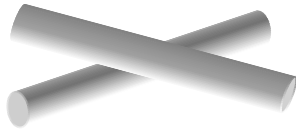

Figure 3. Contact between 2 crossed PANI wires

References

[1] H. Yoshikawa, T. Hino, and N. Kuramoto, *"Effect of temperature and moisture on electrical conductivity in polyaniline/polyurethane (PANI/Pu) blends"*, Synthetic Metals **156** (2006) pp 1187-1193

[2] F.N.Hooge, T.G.M.Kleinpenning, and L.K.J.Vadamme, *"xperimental studies on 1/f noise"*,Rep. On Prog. in Phys. 44 (1981) 479-532

[3] L. K. J. Vandamme, H. J. Casier, *"The 1/f noise versus sheet resistance in poly-Si is similar to poly-SiGe resistors and Au-layers"* Eds. R.P. Mertens and C.L. Claeys. no. IEEE Catalog number: 04EX851, pp. 365-368, (2004). Proc. of 34th ESSDERC . IEEE, Piscataway, NJ, USA

Low-frequency noise monitoring of current collapse in AlGaN/GaN high-electron-mobility transistors on sapphire substrate

N. Tanuma[1], M. Tacano[1], S. Yagi[2] and J. Sikula[3]
[1]Meisei University, Hino, Tokyo 191-8506, Japan
[2]Power Electronics Research Center, National Institute of Industrial Science and Technolo
Tsukuba, Ibaraki 305-8568, Japan
[3]Czech Noise Research Laboratory, Brno University of Technology,
Technicka 8, 616 00 Brno, Czech Republic

1 Introduction

GaN is a kind of wide-bandgap semiconductor suitable for high-power-density, high-frequency and high-temperature applications. Research is currently focused on the development of AlGaN/GaN high-electron-mobility transistors (HEMTs) and on the blue and ultraviolet light emitting diodes or laser diodes. The performance of these devices, however, can be limited by the defects within the AlGaN/GaN heterostructures typically appearing as the current collapse induced by drain bias stress [1]. The activation energy of the deep trap center causing the current collapse has not been clarified yet. The low-frequency-noise (LFN) measurement of semiconductor devices is known to identify the deep traps in the semiconductor [2], being rather effective method to assign those of low barrier height materials like those in the InGaAs heterostructures [3, 4]. We report the study of current collapse in AlGaN/GaN heterostructure devices by LFN measurement at low temperatures. Additionally, the effect of SiN surface passivation is reported.

2 Experiment and Results

The AlGaN/GaN heterojunction structure was grown on a 2-inch c-face of a sapphire substrate by metal organic chemical vapor deposition (MOCVD) for a high-breakdown-voltage metal-insulator-semiconductor HEMT (MIS-HEMT) [5, 6, 7]. The layer structure consists of a 4-μm-thick undoped GaN layer followed by the 15-nm-thick undoped $Al_{0.25}Ga_{0.75}N$ barrier layer. To form ohmic contacts at the drain and source electrodes were made by depositing Ti (25 nm thick), Al (100 nm), Ni (40 nm) and Au (50 nm) by electron-beam deposition and annealing by rapid thermal annealing at 700°C for 120 s in N_2. The specific contact resistivity was determined as 2.6×10^{-6} $\Omega \cdot$ cm^2 by the transmission line model (TLM) structure. Layers of Ni (25 nm) and Au (500 nm) were deposited by electron-beam deposition to form the gate contact. The gate length and source-drain distance was 2 μm and 6 μm, respectively. A 120-nm-thick SiN layer for surface passivation was deposited on the completed device by ECR sputtering.

LFN measurements were performed using the TLM structure patterned on the wafer used for dc characteristic measurements. The conducting channel of the device has a width 200 μm and a distance of 10 μm between the ohmic contacts. The device was mounted on a TO5 package and placed into a cryostat designed for high-sensitivity LFN measurement. The low-frequency spectra were measured in the frequency range from 1 Hz to 10 kHz and in the temperature range from 20 K to 290 K. The sample current was approximately 5 mA.

Figure 1 shows temperature dependence of noise density S_I at different frequencies (f = 1, 10, 100, 1000 and 10000 Hz) for the unpassivated (a) and passivated (b) devices. As shown in Fig. 1(a), there is peak (E_1) corresponding to generation-recombination (G-R) noise induced by electron traps in the epitaxial layer of the unpassivated device at temperatures from 50 K to 110 K. On the other hand, in the noise spectra of the passivated device, G-R noise at peaks E_2 and E_3 as well as E_1 were observed; however, the current noise density of E_1 for the passivated device is 12 dBA/$\sqrt{\text{Hz}}$ lower than that of the unpassivated device. It is supposed that G-R noise at peaks E_2 and E_3 also occurred in the unpassivated

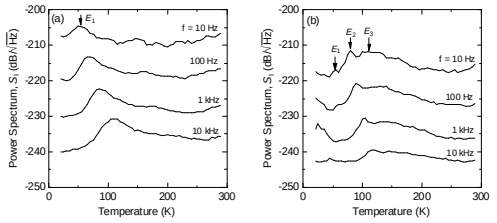

Figure 1: Temperature dependences of current noise characteristics for AlGaN/GaN heterostructures without SiN passivation (a) and with SiN passivation (b), for different frequencies (10, 100, 1000 and 10000 Hz).

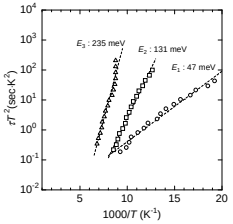

Figure 2: Arrhenius plots of the fluctuation time constant, τ, for AlGaN/GaN heterostructures.

device; however, they were not observed, because the G-R noise at E_1 is much larger than those at E_2 and E_3. The activation energies of these G-R noises correspond to deep traps.

The Arrhenius plots of G-R noise at E_1, E_2 and E_3 illustrated in Fig. 1 are shown in Fig. 2. The activation energies of the G-R noise at E_1, E_2 and E_3 extracted from the Arrhenius plots were 47 meV, 131 meV and 235 meV, respectively. It is supposed from the results shown in Fig. 1 that the activation energy of 47 meV for the G-R noise at peak E_1 corresponds to the deep trap center causing current collapse.

3 Conclusion

The effect of surface passivation on LFN for AlGaN/GaN heterostructure devices was studied. The measurement results of the temperature dependence of LFN for the AlGaN/GaN heterostructure device showed that the current noise density of the G-R noise at E_1 for the unpassivated device is much larger than that of the passivated device. The activation energy of the G-R noise at E_1 was 47 meV, which corresponds to the deep trap center causing current collapse. All these results show the importance of decreasing the deep trap of activation energy 47 meV for improving the performance of AlGaN/GaN HEMTs.

References

[1] P. B. Klein and S. C. Binari and K. Ikossi and A. E. Wickenden and D. D. Koleske and R. L. Henry, *Appl. Phys. Lett.* **79** pp. 3527 (2001)

[2] P. Dutta and P. M. Horn, *Rev. Modern Phys.* **53** pp. 497 (1981)

[3] M. Tacano and K. Tomisawa and H. Tanoue and Y. Sugiyama, *Proceedings of the international conference on noise in physical systems and 1/f fluctuations, ICNF'91* pp. 167 (1991)

[4] M. Tacano, *AIP conference proceedings: Quantum 1/f noise & other low frequency fluctuations in electronic devices* pp. 21 (1992)

[5] S. Yagi and M. Shimizu and M. Inada and Y. Yamamoto and G. Piao and H. Okumura and Y. Yano and N. Akutsu and H. Ohashi, *Solid-State Electron.* **50** pp. 1057 (2006)

[6] S. Yagi and M. Shimizu and M. Inada and H. Okumura and H. Ohashi and Y. Yano and N. Akutsu, *Phys. Stat. Sol. (c)* **40** pp. 2682 (2007)

[7] S. Yagi and M. Shimizu and H. Okumura and H. Ohashi and Y. Yano and N. Akutsu, *Jpn. J. Appl. Phys.* **46** pp. 2309 (2007)

Noise spectroscopy of AlGaN/GaN HEMT structures with long channels

S.A.Vitusevich[1], M.V.Petrychuk[2], A.M.Kurakin[1], S.V.Danylyuk[1], Z. Bougrioua[3], A.V.Naumov[4], A.E.Belyaev[4], and N.Klein[1]

[1]Institut für Bio- und Nanosysteme and CNI- Center of Nanoelectronic Systems for Information Technology, Forschungszentrum Jülich,D-52425 Jülich, Germany

[2]Taras Shevchenko National University, 01033 Kiev, Ukraine

[3]Centre de Recherche sur l'Hétéroépitaxie et ses Applications, CNRS, rue Bernard Gregory, F-06560 Valbonne, France

[4]Institute of Semiconductor Physics, NASU, Pr. Nauki 41, 03028 Kiev, Ukraine

In this paper we discuss the effect of dissipated power on characteristic time of noise spectra transformation of wide-band gap AlGaN/GaN transistor structures with long channels. It is found that this time as a function of temperature demonstrates exponential dependence with definite activation energy. Obtained results are explained based on developed model of nonequilibrium fluctuations of the sample resistance.

INTRODUCTION

Over the last decade, there has been growing interest in study of GaN-based structures owing to their unique fundamental properties. Despite the progress made in the production of these structures, including AlGaN/GaN high electron mobility transistors (HEMTs), the quality and reliability of the obtained structures are still below that predicted and required for commercial application. Several models were developed to explain deterioration in time of transistors characteristics, but specific features and their evolution is still under debate[1,2]. This paper provides an alternative way to study transport properties by investigating dynamic of noise spectral characteristics. Analysis of the noise behaviour allows us to study nonequilibrium effects induced by lateral electric field redistribution.

EXPERIMENTAL DETAILS

The investigated devices were fabricated from $Al_{0.25}Ga_{0.75}N$/GaN undoped heterostructures grown by MOCVD on sapphire substrates. The conducting channel with two dimensional electron gas (2DEG) was formed at the AlGaN/GaN interface due to spontaneous and piezoelectric polarization effects. Lateral devices with 200 μm width and different distances between contacts from 5 to 200 μm were studied. The noise behaviour is studied in long channel samples to remove influence of contact regions. Standard ohmic contacts were processed. Spectral noise characteristics were measured in the frequency range from 1Hz to 100KHz using a low noise preamplifier and spectrum analyzer HP 35670A. I-V characteristics of the HEMTs were simultaneously recorded within a temperature range T=70-300K

RESULTS AND DISCUSSION

The measured current-voltage characteristics demonstrate a linear behaviour until approximately V=1V. With higher voltages the curves become sublinear and for highest voltages the differential resistance becomes negative.

The noise spectra for long samples are changing significantly with applied voltage. The set of nonequilibrium noise spectra normalized on equilibrium noise (V = 100-200 mV) for samples of different length is shown at Fig.1a. One can notice a drastic (6-7 orders of magnitude) increase of maximal noise level for the 200μm long sample. Similar behaviour is observed at lower temperatures with very weak temperature dependence of maximal value of normalized nonequilibrium noise. On the other hand, a characteristic time, determined in this work by frequency of transition to high-frequency fall-off of the spectrum, is strongly changing with temperature (Fig.1b). Taking into account that dissipated power P is proportional to the temperature of a self-heating, one can estimate a temperature dependence of characteristic time as exponential, i.e. determined by an activation process.

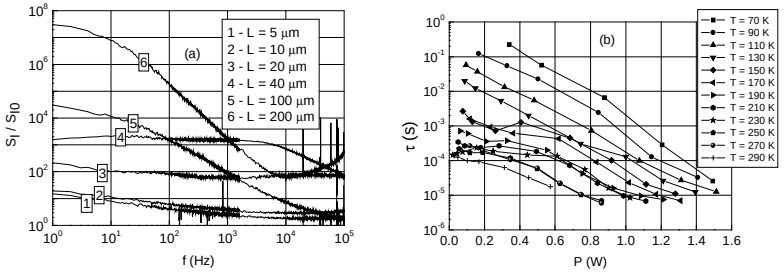

Fig.1 (a) nonequilibrium noise spectra of TLM-structures with different channel length normalized on equilibrium noise. Applied voltage V = 8 V, sample temperature at V = 0 equals to T_0 = 290K
(b) dependence of characteristic time on dissipated power at different starting temperatures for sample with channel length equal L = 40 μm

To explain the observed behaviour we are suggesting a model of nonequilibrium low-frequency noise in TLM HEMTs. Low-frequency part of the noise spectrum is increasing due to a feedback between dynamic potential redistribution in the barrier and fluctuation of electron concentration in the channel. The latter is determined by the space, occupied by the electrons, i.e. by channel length. Therefore increase of the length leads to increase of the amplitude of fluctuations as observed in the experiment. In the same time the high-frequency part of the spectrum, separated from low frequency part by steep transition region with characteristic time τ, does not undergo any significant changes.

CONCLUSION

In summary, we demonstrated an alternative way to study characteristics of AlGaN/GaN HEMT structure in high dissipated power regime using noise spectroscopy. Transport and low frequency noise spectra measurements allowed us to analyze the mechanisms of current formation in the HEMT structures. Two regions of noise spectra with different behaviour were registered. The characteristic time constant extracted from the spectra demonstrate exponent dependence on dissipated power and temperature with definite activation energy. Our results show that III-Nitride based heterostructures in conjunction with improved technology will provide one of the most promising solutions for high-frequency high-power applications. We propose the model of nonequilibrium fluctuations excited by thermal activation of carriers, captured by traps in the barrier layer, to the conducting channel. This model is satisfactorily applied to explain our experimental results.

References

[1] J.Kotani, M.Tajima, S.Kasai, and T.Hashizume., *Appl.Phys.Lett.* **91** pp.093501-1-3 (2007)

[2] J.M.Tirado, J.L.Sanchez-Rojas, and J.I.Izpura., *IEEE Trans. on Electron. Dev.* **54**, pp.410-417 (2007)

Transition process of superconducting nanogranular MgB_2 films by current noise analysis in non-stationary conditions

M. Rajteri, C. Portesi, M. Accardo, E. Taralli, E. Monticone
Istituto Nazionale di Ricerca Metrologica INRIM
Strada delle Cacce 91, 10135 Torino, Italy

G. Gandini, A. Masoero
Dipartimento di Scienze e Tecnologie Avanzate, Università del Piemonte Orientale
Corso Borsalino 54, 15100 Alessandria, Italy

V. Andreoli, P. Mazzetti
Dipartimento di Fisica, Politecnico di Torino, Corso Duca degli Abruzzi 24
10129 Torino, Italy

A rather simple model [1] for the interpretation of the noise produced during the resistive transition of disordered granular superconductive films, induced by a slow temperature change, has been recently developed and tested on MgB_2 films. The model is based on the onset of correlated transitions of large sets of grains, forming resistive layers through the film cross-section area during the transition process. The strong non-linear behaviour and correlation of the grains produces abrupt resistance variations, giving rise to the large noise, of the $1/f^3$ type, observed in experiments. Alternative models, found in the literature, describe the transition of mono-crystalline or grain-oriented superconductive films in terms of quantum fluxoids depinning and motion. In this case a much lower noise, of the $1/f^n$ type, with n between 1 and 2, is expected. Very few experimental data are found in the literature concerning this case, and, since the power spectra are always given in arbitrary units, a clear proof of the validity of these models, when the transition takes place at low bias currents and near to the critical temperature, is not established. There is the possibility that, in the presence of a magnetic field, a mixed state of superconductive and normal state domains might be evidenced by measurement and analysis of the transition noise. While these experiments, at the moment, cannot be performed, owing to the difficulty of obtaining MgB_2 single crystals of sufficiently large dimensions, in the present paper preliminary results will be given on the transition noise of MgB_2 granular films produced by the application of an external magnetic field. A comparison with the spectra obtained when the transition is induced by a temperature change might give some evidence of the possible role played by fluxoids depinning, at least during the first stage of the transition.

References

[1] Mazzetti P., Gandini C., Masoero A., Rajteri M., and Portesi C., to be published on Phys. Rev. B 77 (2008)

1/f Resistance Noise in Low-doped $La_{1-x}Ca_xMnO_3$ Manganite Single Crystals

G. Jung[1], X. D. Wu[1,2], V. Markovich[1], M. Belogolovskii[3], B. Dolgin[1], Y. Yuzhelevski[1], Ya. M. Mukovskii[4]
1) Department of Physics, Ben Gurion University of the Negev, 84105 Beer-Sheva, Israel
2) Department of Materials Engineering, Monash University, Clayton, Australia 3800
3) Donetsk Physical and Technical Institute, National Academy of Sciences of Ukraine, 83114 Donetsk, and Scientific and Industrial Concern 'Nauka', 04116 Kyiv, Ukraine
4) Moscow State Steel and Alloys Institute, 119049, Moscow, Russia

April 3, 2008

Fundamental interest in mixed-valence manganese perovskites arises from their strongly spin-dependent conductivity and pronounced manifestations of phase separation (PS). In a complex and rich phase diagram of $La_{1-x}Ca_xMnO_3$ (LCMO) manganites the critical doping level $x_C = 0.225$ separates ferromagnetic (FM) insulating ground state at $x < x_C$ from FM metallic ground state above x_C. In the doping range 0.17 <x< 0.25 a mixed FM state composed of insulating and metallic FM phases with different levels of orbital ordering appears below Curie temperature T_C. Therefore, transport properties of low-doped LCMO, $x \leq x_C$, became markedly different when the temperature is changing.

Hopping conductivity controls transport in the paramagnetic (PM) insulating regime at high temperatures $T > T_C$. Intrinsic PS associated with metal-insulator (M-I) transition at T T_C leads to percolation conductivity in the FM state at $T < T_C$. Low temperature resistivity is likely dominated by tunneling across intrinsic barriers associated with extended structural defects, such as twins and grain boundaries, and/or with inclusions of insulating FM phase interrupting metallic percolating paths.[1]

In such complex system as low-doped LCMO one expects that noise data will allow to get a deeper insight into the dynamics of dissipation processes associated with different transport mechanisms. In this presentation we discuss electric noise properties of dc current biased low-doped $La_{0.82}Ca_{0.18}MnO_3$ single crystals at zero applied magnetic field.

The noise was found to have 1/f spectral form in a wide temperature range, independently of the changing dissipation mechanism. Moreover, changes in the noise intensity with changing temperature follow resistivity changes suggesting that resistivity fluctuations constitute a fixed fraction of the total resistivity, independently of the dissipation mechanism and magnetic state of the system. At all temperatures the noise scales as a square of the current as expected for noise resulting from bias independent resistivity fluctuations probed by the current flow. However, at low temperatures where transport is dominated by tunneling mechanism the noise intensity decreases with increasing bias at bias exceeding some threshold value.

We find correlations between behavior of the noise at low temperatures and that of d^2I/dV^2, known to be related to the density of states involved in the tunneling process. At low bias the noise increases, as the square of the current, until the first peak of d^2I/dV^2 appears. Above the peak the noise decreases with increasing voltage in a certain bias range. In general, a peak in d^2I/dV^2 is a signature of a step-like conductivity increase. One can therefore attribute d^2I/dV^2 peaks to openings of additional tunneling channels with higher conductivity, as predicted by theoretical models of indirect nonelastic tunneling through a chain of localized states.[2] The theory predicts that the probability of indirect inelastic tunneling through increased number of localized states N increases with increasing bias. The conductivity of an inelastic channel increases exponentially with increasing N. Let us underline that in the investigated system the force exercised by electric field of the bias can directly influence the topology of PS by stretching insulating FM phase and thus increasing the effective width of intrinsic tunnel barriers.[3]

Analysis performed in the framework of Dutta-Horn-Dimon 1/f noise model [4] suggests that increasing bias does not modify distributions of activation energies in elementary two0level fluctuator ensembles responsible for generation of 1/f noise, except for the low temperature case. The nature of the low temperature fluctuators, their relation to those active at higher temperatures as well as physical mechanisms involved in changing their energy distributions exclusively at low temperatures are the UPON that will be discussed.

References

[1] Y. Yuzhelevski, et al. Phys. Rev. B **64**, 224428 (2001).

[2] L. I. Glazman and K. A. Matveev, Sov. Phys. JETP **67**, 1276 (1988).

[3] M. Viret, et al. Phys. Rev. B **72**, 140403 (2005).

[4] P. Dutta and P. M. Horn, Rev. Mod. Phys. **53**, 497 (1981).

Full Counting Statistics of Avalanche Transport: an Experiment

J. Gabelli and B. Reulet
Laboratoire de Physique des Solides,
UMR8502 bâtiment 510, Université Paris-Sud 91405 ORSAY Cedex, France

Current noise, *i.e.* the variance of the current fluctuations, is the simplest measure of the statistical aspect of electronic transport in a conductor, beyond the dc current. Its study as a function of other parameters (voltage, temperature, etc.) has been a powerful way to check our understanding of the conduction process in many systems, and a tool to obtain information that is hidden in the mean current.

In order to probe the statistics of the conduction more in depth, a better knowledge of the distribution function $P(I)$ of the fluctuating current I is necessary, beyond the average $\langle I\rangle$ and the variance $S_2 = \langle i^2\rangle$ with $i = I - \langle I\rangle$. Most of the time the full measurement of $P(I)$ is not possible, but a finite number of the moments $S_n = \langle i^n\rangle$ of the distribution can be measured, which give some insight into the statistics of I. For example, the third moment S_3 reveals the asymmetry of the distribution around the average: $S_3 = 0$ if $P(i) = P(-i)$. For a Gaussian process, $S_3 = 0$; for a Poissonian process, $S_3 \propto \langle I\rangle$.

While the calculation of the full counting statistics of current fluctuations in a quantum conductor has been achieved 15 years ago, the measurement of moments of current fluctuations beyond the second has started only five years ago. In these recent measurements, the statistics of transport is driven by the finite rate at which electrons can pass a barrier, this rate being influenced by the voltage across the sample.

We present the first measurement of high order cumulants of current fluctuations in avalanche diodes (up to the sixth cumulant is detected with reliable calibration). In such samples, the process that is responsible for current fluctuations is not the transport at the one electron level, but arises from the complex statistics of charge multiplication due to spontaneous creation of electron-hole pairs that occurs in semi-conductors in the presence of a high electric field. This mechanism has been analyzed in the regime where no current is injected but individual e-h pairs are photo-created, giving rise to well separated current pulses, the statistics of which being driven by the avalanche mechanism. Here we work in a very different regime, where the sample sustains a stationary dc current. Our measurement of the current fluctuations in the bandwidth 25MHz - 100MHz reveals a mechanism that strongly differs from the case of single e-h pair injection.

Our experiment raises general questions, both technical and conceptual, about what can be learned from the measurement of the statistics of current fluctuations:

1. The finite bandwidth (from f_1 to f_2) of the detector is of no importance for the measurement of the second moment of noise, which is simply proportional to the $f_2 - f_1$. This is no longer correct for the third and higher cumulants (for example the third one is strictly zero if $f_2 < 2f_1$). So how can one extract true statistical information about current statistics from a measurement ? How precise has to be the knowledge of the experimental setup in order to be sure of the measurement of the Nth cumulant ? What are the effects of finite sampling, quantization noise, etc ?

2. How the results can help us infer the mechanism that is responsible for charge transfer in the conductor ? Can one learn something simply from the measured statistics, without varying a single parameter ?

Quantum noise and coherence

Q.1 – Anatoly Golub
Shot noise in the interacting spinless resonant level model *114*

Q.2 – Alessandro Braggio
Counting Statistics of Non-Markovian Quantum Stochastic Processes *115*

Q.3 – Adam Bednorz
Positive operator valued measure in electron counting statistics of quantum point contacts *116*

Shot noise in the interacting spinless resonant level model

Anatoly Golub
Department of Physics, Ben-Gurion University of the Negev, Beer-Sheva 84105, Israel

INTRODUCTION

The shot noise power and the Fano factor of a spinless resonant level model is calculated. The Coulomb interaction which in this model acts between the lead electron and the impurity is considered in the first order approximation. The logarithmic divergencies which appeared in the expressions for shot noise and the transport current are removed by renormalization group analysis. By passing to the bosonized form of the resonant model we show that in the strong interaction limit the tunnelling becomes irrelevant and decreases.

The transport properties of quantum impurity have attracted great interest as a basic problems in nanophysics. Recently, spinless interacting resonant level model (IRLM) has become a subject of a special attention. This interest, in particular, was related to the extending the Bethe ansatz out of equilibrium to calculate the transport current in the steady state of a quantum dot [1]. The IRLM served as a simplest test and toy model.

The principal purpose of this work is the calculation of the current-current correlation function, in particular, the zero frequency shot noise power. This value is very important experimentally measured characteristic and technically it is much more difficult to obtain. Shot noise has not been considered yet. The calculations of shot noise causes a special difficulties for Bethe ansatz approach in nonequilibrium. Here we obtain [2] the shot noise power for a general position of bear impurity level ϵ_d relative to the Fermi energy which is taken at zero.

1 Hamiltonian

The standard form of the hamiltonian of IRLM has a form

$$\begin{aligned} H &= H_0 + t(\sum_i \psi_i(0)d^\dagger + h.c) + \epsilon_d d^\dagger d \\ &\quad + U\sum_i \psi_i(0)^\dagger \psi_i(0) d^\dagger d \end{aligned} \tag{1}$$

The first term corresponds to non-interacting electrons in the two leads

$$H_0 = \sum_{ik} \varepsilon_i(k)\psi^\dagger_{ik}\psi_{ik}$$

where ψ_{ik}, $\varepsilon_i(k)$ are the electron field operator and the electron energy of a lead i, respectively. Index $i = L, R$ indicates left (right) lead. The second term describes the tunnelling processes. The last one presents an important interacting term with Coulomb capacitive coupling U. For non-equilibrium transport properties we use Keldysh technique and go to the action generalized for Keldysh space. We develop a perturbation theory in U.

2 Shot noise

The current noise power is given by current-current correlation function

$$S_{tt_1} = 1/2(< I(t)I(t_1) > + < I(t_1)I(t) >) - < I >^2$$

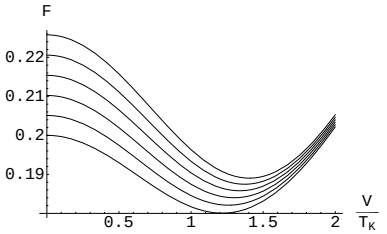

Figure 1: Fano factor as function of applied voltage for different values of u. The numerical values of chosen parameters: $\mu/T_K = 3, \epsilon_d/T_k = -0.5$. The Coulomb coupling u/π is changed from 0 (lowest curve) up to u/π=0.1

where the current operator is obtained by a commutation of the density operator of the left or right lead with the hamiltonian. In a symmetric presentation the current operator acquires a form

$$I = \frac{ite}{2} < \hat{\psi}(0)^\dagger d - d^\dagger \hat{\psi}(0) >; \hat{\psi} = \psi_L - \psi_R \tag{2}$$

In the limit $U \to 0$ transport current $I_0 = \frac{e\Gamma}{2\pi} j_-$ and shot noise S_0 depend on parameters of noninteracting resonant level

$$S_0 = \frac{e^2\Gamma}{4\pi}(j_- - j_1) \tag{3}$$

$$j_1 = \Gamma[\epsilon_+(\epsilon_+^2 + \Gamma^2)^{-1} - \epsilon_-(\epsilon_-^2 + \Gamma^2)^{-1}] \tag{4}$$

where here and below $j_\pm = \arctan\frac{\epsilon_+}{\Gamma} \pm \arctan\frac{\epsilon_-}{\Gamma}$, , $\epsilon_\pm = \epsilon_d \pm eV/2$ and Γ is a tunnelling width. In the linear regime (small voltages: $V/(\epsilon^2 + \Gamma^2) << 1$) we immediately recognize standard expressions $I_0 = (e^2/h)\bar{T}$, $S_0 = (e^3/h)\bar{T}(1-\bar{T})$, where $\bar{T} = \Gamma^2/(\Gamma^2 + \epsilon_d^2)$ is the transmission coefficient. In the last formulas we have returned to the usual units (here $2\pi \to h$).

To consider the Coulomb interacting contribution we expand the average in the noise and current formulaes to the first order in U. Direct calculations lead to the shot noise power $S = S_0 + S_U$ where

$$\begin{aligned} S_U &= \frac{u\Gamma}{4\pi^2}\{[j_- - 3j_1 - \Gamma^2\frac{\partial(j_1/\Gamma)}{\partial\Gamma}]L + j_2 j_+(1-j_3)\} \\ j_2 &= \Gamma^2[(\epsilon_+^2 + \Gamma^2)^{-1} - (\epsilon_-^2 + \Gamma^2)^{-1}] \\ j_3 &= \Gamma^2[(\epsilon_+^2 + \Gamma^2)^{-1} + (\epsilon_-^2 + \Gamma^2)^{-1}] \\ L &= \ln[\frac{D}{[(\epsilon_+^2 + \Gamma^2)(\epsilon_-^2 + \Gamma^2)]^{1/4}}] \end{aligned} \tag{5}$$

Similarly, the capacitor coupling leads to a contribution to the transport current

$$I_U = \frac{u\Gamma}{2\pi^2}\{(j_- - j_1)L + \frac{\pi}{8}\ln\frac{\epsilon_-^2 + \Gamma^2}{\epsilon_+^2 + \Gamma^2} + \frac{1}{2}j_2 j_+\} \tag{6}$$

In equations (5) and (6) D is the large cut-off of the order of band width, and we also introduced the notation $u = 2\pi UN(0)$. In Figure we plot Fano factor $F = S/eI$ as a function of voltage for different values of Coulomb coupling U.

References

[1] P. Mehta and N. Andrei, Phys. Rev. Lett **96**, 216802 (2006)

[2] A. Golub, Phys. Rev. B 76, 193307 (2007).

Open questions in Counting Statistics of Non-Markovian Processes

A. Braggio[1], C. Flindt[2], T. Novotný[3], M. Sassetti[1], A.-P. Jauho[2,4]
[1]LAMIA-INFM-CNR & Dipartimento di Fisica, Università di Genova, Genoa, Italy
[2] Laboratory of Physics, Helsinki University of Technology, Helsinki Finland
[3] Department of Condensed Matter Physics, Charles University, Prague, Czech Republic
[4] Department of Micro and Nanotechnology, Technical University of Denmark, Kongens Lyngby, Denmark

The concept of Full Counting Statistics (FCS) has recently attracted intensive theoretical [1] and experimental [2, 3, 4] attention in the field of electron transport. In the contest of mesoscopic transport, the FCS was introduced to determine the noise properties of nanodevices [5] but after it was demonstrated to be a sensitive diagnostic tool in the detection of quantum-mechanical coherence, entanglement, disorder, and dissipation [1].

Mathematically, FCS encodes the complete knowledge of the probability distribution $P(n,t)$ of the transmitted particles number n during the measurement time t or, equivalently, of all corresponding cumulants. The study of counting statistics for stochastic processes in general is of broad relevance for a wide class of problems. For example, non-zero higher order cumulants describe non-Gaussian behavior and contain information about rare events, whose study has become an important topic within non-equilibrium statistics in physics, chemistry, and biology. Efficient methods for evaluating the counting statistics of general stochastic processes are therefore of urgent need.

In recent years a number of important results was obtained in the Markovian Master Equation framework. Bagrets and Nazarov have shown that the Cumulant Generating Function (CGF) is given by the dominant eigenvalue of the Markovian master equation kernel having included the counting field factors[6]. Flindt *et al.* have shown that it is possible to calculate an arbitrary order of cumulants using an appropriate pertubative approach in the counting field[7].

For cases described by non-Markovian master equation but with a short range memory, no power-law tails, was shown that a CGF scales linearly with time, as in Markovian processes, and can be calculated via a peculiar non-Markovian expansion[8].

Here we present a method which unifies extending those earlier approaches[9]. We will consider systems governed by a generic non-Markovian GME of the form [10]

$$\frac{d}{dt}\rho(n,t) = \sum_{n'} \int_0^t dt' \mathcal{W}(n-n', t-t')\rho(n',t') + \gamma(n,t). \qquad (1)$$

where, the reduced density matrix has been resolved into components $\rho(n,t)$ corresponding to the number of particles n passing through the system within time-span $[0,t]$. The memory kernel $\mathcal{W}$ describes the influence of the environment on the dynamics of the system, while the inhomogeneity γ accounts for initial correlations between system and environment. We will consider systems with $\mathcal{W}$ and γ decaying with time faster than any power law, short range in memory. The inhomogeneity γ does, however, play a crucial role at finite times because take in account of the initial correlations between the reduced system and the bath. The probability distribution for the number of transferred charges is given by $P(n,t) = \mathrm{Tr}\{\rho(n,t)\}$. For the systems described by Eq.1 we demonstrated that the long-time limit of the CGF is determined by a single dominating pole of the resolvent of the memory kernel. An open issue is to consider the case of systems with long range memory. In what measure previous results con be generalized?

We defined also a *recursive* scheme extremely efficient in calculating high order cumulants both analytically than numerically. We tested the numerical stability of the methods for very high orders of cumulants (> 20) on simple models. The main advantage of our method is the possibility to evaluate the zero-frequency high order current cumulants in non-Markovian systems with many states.

The method allows to develop a general approach to the finite-frequency current noise of non-Markovian transport processes. We found the finite-frequency noise is governed not only by the full set of poles of the resolvent of Eq.1 but also by initial system-environment correlations γ are crucial. Such correlations can be, and have been [8, 11], neglected for non-Markovian processes at low frequencies, but must be included at frequencies comparable with the internal frequencies of the system. It not yet clear if it is possible to develop a similar scheme for finite frequency cumulants of higher order. We will investigate which are the possibilities of this extension.

We applied our methods in transport through a double quantum dot qubit coupled with a phonon bath. In particular we studied the effects of dissipation and temperature on the current cumulants of very high orders and the finite-frequency current noise. We will compare our results with known theories to identify the discrepancies and the role of common bath correlations approximations. We will show that our method may easily be applied also to other electronic (or photonic) counting systems, as well as other counted quantities, such as heat or work, in non-equilibrium systems.

References

[1] *Quantum Noise in Mesoscopic Physics* ed. Yu. V. Nazarov (Kluwer, Dordrecht,2003)

[2] Reulet B., Senzier J. and Prober D.E, *Phys. Rev. Lett.* **91**, 196601 (2003).

[3] Bomze Y. *Phys. Rev. Lett.* **95**, 176601 (2005).

[4] Fujisawa T., Hayashi T., Tomita R. and Y. Hirayama, *Science* **312**, 1634 (2006).

[5] Levitov L.S., Lee H. and Lesovik G. B., *J. Math. Phys.* **37**, 4845 (1996).

[6] Bagrets and A., Nazarov Y., *Phys. Rev. B* **67**, 085316 (2003).

[7] Flindt C., Novotný T. and Jauho, A.-P., *Europhys. Lett.* **69**, 475 (2005).

[8] A. Braggio, J. König, and R. Fazio, *Phys. Rev. Lett.* **96**, 026805 (2006).

[9] Flindt C., Novotný T., Braggio A., Sassetti M. and Jauho A.-P., submitted to Phys. Rev Lett., condmat/0801.3723.

[10] R. Zwanzig, *Nonequilibrium Statistical Mechanics* (Oxford University Press, 2001).

[11] R. Aguado and T. Brandes,*Phys. Rev. Lett.* **92**, 206601 (2004).

Positive operator valued measure in electron counting statistics of quantum point contacts

Adam Bednorz[a,b] and Wolfgang Belzig[a]
[a]Department of Physics, University of Konstanz, D-78457 Konstanz, Germany
[b]Department of Physics, University of Warsaw, PL-00-681 Warsaw, Poland

The description of the statistics of charge transfer in quantum point contacts requires to take care of the ordering of the electric current operators at different times. We construct a positive operator valued measure based on the inaccuracy of the current measurement, which leads to a well defined probability functional. The corresponding generating function of charge transfer reduces to that obtained by direct application of Keldysh order in the limit of negligible influence of the detector. An experimentally observable prediction of our approach is a large offset noise, which can be detected by comparing the measured high-frequency current noise with the measured low-frequency noise. We discuss differences between the generating functions obtained by the two methods in various limits – low and high frequency, short and long characteristic measurement times.

Theoretical trends in fluctuations

T.1 – Takaaki Monnai
Diffusion process induced by an external force and a spatio-temporal correlated noise *118*

Diffusion process induced by an external force and a spatio-temporal correlated noise

Takaaki Monnai
Department of Applied Physics, Waseda University
3-4-1 Okubo Shinjuku-ku 169-8555 Tokyo, Japan

It has been a long standing problem to systematically treat the spatio-temporal colored noise. In the context of path coalescence, Deutsch[1] examined the free-diffusion of damped particles subjected to a force fluctuating both space and time. Wilkinson, Mehlig and coworkers[2, 3] pursued similar subject where the turbulant flow amounts to the spatio-temporal correlated noise acting on the suspended particles, and analyzed the spectrum of the Fokker-Planck operator of the corresponding generalized Ornstein Uhlenbeck process in momentum space.

It is thus a next important step to consider the case where an additional potential-induced systematic force is present. In this contribution, we shall address this issue and explore how the potential is radically affected by the spatio-temporal correlation[4]. We shall explore the overdamped case described by the Langevin equation with a colored noise $f(x,t)$

$$\begin{aligned}&\eta\dot{x}(t) = -U'(x(t)) + f(x(t),t)\\ &\langle f(x,t)\rangle = 0,\ \langle f(x,t)f(x',t')\rangle = C(x-x',t-t'),\end{aligned} \tag{1}$$

where η stands for the friction coefficient and $U(x)$ is a potential. The autocorrelation function is assumed to be decorrelated $C(x,t) \to C_0\delta(x)\delta(t)$ in the short correlation limit of both the spatial correlation length ξ and temporal relaxation constant τ. As a typical case, we can take $C(x,t) = 2\eta k_B T/\tau\sqrt{\pi}e^{-x^2/\xi^2 - t^2/\tau^2}$ with k_BT the strength of the noise.Other form of the autocorrelation function will be discussed also. Then a Fokker-Planck equation is well-defined in a certain Markovian limit specified by the scaling relation between ξ and τ

$$\frac{\partial}{\partial t}P(x,t) = \frac{1}{\eta}\frac{\partial}{\partial x}\left(U'(x)(1-\kappa) + k_BT\frac{\partial}{\partial x}\right)P(x,t), \tag{2}$$

with a dimensionless parameter $\kappa = 2\tau k_BT/\xi^2\eta\sqrt{\pi}$ which is kept finite as $\tau, \xi \to 0$. *It is notable that the drift velocity is renormalized by the memory of the noise.* The diffusion process with a spatially and temporally correlated noise is thus, in the above-mentioned Markovian limit, equivalently replaced by that with purely temporal white noise.

Our theoretical predictions are numerically confirmed by calculating the escape rate for the double-well potential and also the steady state distribution with use of the stochastic simulations of corresponding Langevin equation. We should note that our symmetric doubly-stochastic noise can enhance the diffusion which is in contrast to the localization observed in Sinai's random walk in random environment[5].

References

[1] J. M. Deutsch, *J. Phys. A* **18** pp. 1457 (1985).

[2] B. Mehlig, M. Wilkinson, K. Duncan, T. Weber and M. Ljunggren, Phys. Rev. E **72** 051104 (2005).

[3] V. Bezuglyy, B. Mehlig, M. Wilkinson, K. Nakamura and E. Arvedson, J. Math. Phys. **47** 073301 (2006).

[4] T. Monnai, A. Sugita, and K. Nakamura, *e-print cond-mat* 0712.0551

[5] Ya. G. Sinai, *Proceedings of the Berlin Conference on Mathematical Problems in Theoretical Physics*, pp. 12 (1982)

Scientific Committee

Derek Abbott *(Adelaide University, Australia)*
Dean Astumian *(University of Maine, USA)*
Robert Austin *(Cornell University, USA)*
Kamal Bardhan *(Saha Institute of Nuclear Physics, India)*
Sergey Bezrukov *(National Institutes of Health, USA)*
Gijs Bosman *(University of Florida, USA)*
Adi Bulsara *(SPAWAR Systems Center, USA)*
Markus Büttiker *(University of Geneva, Switzerland)*
Anna Carbone *(Torino Polytechnic, Italy)*
David Deamer *(University of California, USA)*
Jamal Deen *(McMaster University, Canada)*
Charlie Doering *(University of Michigan, USA)*
Gianfranco Durin *(Istituto Elettrotecnico Nazionale, Italy)*
Christian Glattli *(CEA Saclay, France)*
Peter Hanggi *(University of Augsburg, Germany)*
Laszlo Kish *(Texas A&M University, USA)*
Mikhail Levinshtein *(Ioffe Physico-Technical Institute, Russia)*
Andre Longtin *(University of Ottawa, Canada)*
Massimo Macucci *(University of Pisa, Italy)*
Peter McClintock *(University of Lancaster, England)*
Frank Moss *(University of Missouri, USA)*
Nossal Ralph *(National Institutes of Health, USA)*
Xavier Oriols *(Autonomous University of Barcelona, Spain)*
Cecilia Pennetta *(University of Lecce, Italy)*
Lino Reggiani *(University of Lecce, Italy)*
Stefano Ruffo *(University of Florence, Italy)*
Marco Sampietro *(Polytechnic of Milano, Italy)*
Lutz Schimansky-Geier *(Humboldt University, Germany)*
Michael Shlesinger *(Office of Naval Research, USA)*
Eugene Stanley *(Boston University, USA)*
Jevgenij Starikov *(Semiconductor Physics Institute, Lithuania)*
Charles Stevens *(Salk Institute for Biological Studies, USA)*
Munecazu Tacano *(Meisei University, Japan)*
Lode Vandamme *(University of Eindhoven, The Netherlands)*
Nico Van Kampen *(Institute of Theor. Physics, The Netherlands)*
Luca Varani *(Montpellier CNRS, France)*
Michael Weissman *(University of Illinois, USA)*
Kurt Wiesenfeld *(Georgia Institute of Technology, USA)*
Stefano Zapperi *(University of Rome, Italy)*

List of participants

Mr. Guillem Albareda
Universitat Autonoma de Barcelona
Departament d'Enginyeria Electrònica
ESTE
08193-Bellaterra-Barcelona
Spain
guillem.albareda@uab.es

Dr. Pierre-Olivier Amblard
GIPSAlab, CNRS
BP 46
38402 saint martin d'hères cedex
France
bidou.amblard@gipsa-lab.inpg.fr

Dr. Valentina Andreoli
Politecnico di Torino
Corso Duca degli Abruzzi, 24, 10129 Torino
Italy
valentina.andreoli@polito.it

Pr. Daniele Andreucci
Dipartimento di Metodi e Modelli Matematici
via A.Scarpa 16 00161 ROMA
Italy
andreucci@dmmm.uniroma1.it

Ms. Debjani Bagchi
Laboratoire de Physique, Ecole Normale Supérieure de Lyon
46, Allée d'Italie, Lyon
Cedex 07
France
debjani.bagchi@ens-lyon.fr

Dr. Kamal Kumar Bardhan
Saha Institute of Nuclear Physics
1/AF Bidhannagar
Kolkata 700 064
India
kamalk.bardhan@saha.ac.in

Pr. Eli Barkai
Bar Ilan University
Physics Department
Bar Ilan University
52900 Ramat Gan
Israel
barkaie@mail.biu.ac.il

Dr. Adam Bednorz
University of Konstanz
Fachbereich Physik, M703
D-78457 Konstanz
Germany
Adam.Bednorz@uni-konstanz.de

Pr. Roberto Benzi
Univ. Roma "Tor Vergata"
Dip. of Physics
Via della Ricerca Scientifica 1
00133, Roma
Italia
roberto.benzi@gmail.com

Mr. Igor V. Bezsudnov
NPP Nauka-Sevice
127473 Moscow
1-st Volkonskii per. 11
Russian Federation
biv@akuan.ru

Dr. Pierre Borgnat
Université de Lyon, ENS Lyon CNRS, Laboratoire de Physique
46 allé d'Italie
69364 Lyon cedex 07
France
pierre.borgnat@ens-lyon.fr

Mr. Freddy Bouchet
INLN
1361, route des lucioles
06560 Valbonne Sophia Antipolis
France
Freddy.Bouchet@inln.cnrs.fr

Dr. Hélène Bouchiat
Université Paris-Sud
LPS
Bat 510 91405 Orsay
France
bouchiat@lps.u-psud.fr

Dr. Alessandro Braggio
LAMIA-INFM-CNR & Dipartimento di Fisica, Università di Genova
Dipartimento di Fisica
Via Dodecaneso 33
16146
Genova (GE)
Italy
braggio@fisica.unige.it

Dr. Francisco J. Cao
Universidad Complutense de Madrid
Dpto. Física Atómica
Facultad de Ciencias Físicas
Av. Complutense s/n
28040 Madrid
Spain
francao@fis.ucm.es

Pr. Bernard Castaing
Université de Lyon
École Normale Supérieure de Lyon, Laboratoire de Physique
C.N.R.S. UMR5672
46, Allée d'Italie
69364 Lyon Cedex 07
France
Bernard.Castaing@ens-lyon.fr

Dr. Edvige Celasco
Dept, Physics Politecnico di Torino
Corso Duca Degli Abruzzi 24, 10129 Torino
Italy
edvige.celasco@polito.it

Pr. Ho Bun Chan
University of Florida
PO Box 118440
New Physics Building
U.S.A.
hochan@phys.ufl.edu

Pr. Cheng-Hung Chang
Institute of Physics, National Chiao-Tung University
1001 Ta Hsueh Rd
Hsinchu 300
Taiwan
chchang@phys.cts.nthu.edu.tw

Pr. Francois Chapeau-Blondeau
LISA, University of Angers
62 avenue Notre Dame du Lac
49000 ANGERS
France
chapeau@univ-angers.fr

Pr. Shih Chun-Hsing
Department of Electrical Engineering, Yuan Ze University
135 Yuan-Tung Road, Chung-Li
Taoyuan 320
Taiwan
Taiwan
chshih@saturn.yzu.edu.tw

Dr. Francesco Ciccarello
Dipartimento di Fisica e Tecnologie Relative
Viale delle Scienze, Edificio 18 Palermo
Italy
ciccarello@difter.unipa.it

Dr. Alvaro Corral
Centre de Recerca Matematica
Edifici Cc, Campus UAB Bellaterra,
E-08193 Cerdanyola (Barcelona)
Spain
alvaro.corral@uab.es

Mr. Fabien Crauste
IXXI - Complex Systems Unstitute
5 rue du vercors
69007 Lyon
France
crauste@math.univ-lyon1.fr

Dr. Ferenc F. Csikor
Eotvos University Budapest, Department of Materials Physics
H-1117 Budapest
Pazmany Peter setany 1/a
Hungary
csikor@metal.elte.hu

Dr. Karin Dahmen
University of Illinois
Department of Physics
1110 West Green St.
Urbana, IL 61801-3080
U.S.A.
dahmen@uiuc.edu

Dr. Fergal Dalton
Istituto dei Sistemi Complessi
Via del Fosso del Cavaliere 100
00133 Roma
Italy
fergal.dalton@isc.cnr.it

Dr. Serhiy Danylyuk
Forschungszentrum Juelich
Leo Brandt str.1
52425 Juelich
Germany
s.vitusevich@fz-juelich.de

Ms. Stéphanie Deschanel
INSA Lyon, MATEIS
Bâtiment Blaise Pascal, 20 Av Albert Einstein
69621 Villeurbanne Cedex
France
stephanie.deschanel@insa-lyon.fr

Ms. Francesca Di Patti
CSDC - Centro Interdipartimentale per lo Studio delle Dinamiche Complesse, Università degli Studi
via di Santa Marta 3, 50139 Firenze
Italy
f.dipatti@gmail.com

Mr. Kai Dierkes
Max Planck Institute for the Physics of Complex Systems
Kai Dierkes (Room 1A07)
Noethnitzer Strasse 38
01187 Dresden
Germany
kai@mpipks-dresden.mpg.de

Mr. Jan Dolensky
Brno University of Technology - FEEC
Udolni 53
60200
Brno
Czech republic
xdolen00@stud.feec.vutbr.cz

Dr. Alexander Alexandrovich Dubkov
Nizhniy Novgorod State University
Gagarin Ave. 23
Nizhniy Novgorod
603950
Russian Federation
dubkov@rf.unn.ru

Mr. Andrea Duggento
Lancaster University
Bailrigg
Lancaster
LA1 4YW
UK
a.duggento@lancs.ac.uk

Dr. Roberto Eggenhoffner
Physycs Department University of Genova
via Dodecaneso 33
16146 GENOVA
Italy
eggen@fisica.unige.it

Dr. Alessandro Fiasconaro
Marian Smoluchowski Institute of Physics
Jagellonian University
Reymonta 4 30-059
Poland
fiascona@th.if.uj.edu.pl

Mr. Julien Gabelli
Laboratoire de Physique des Solides
Bât. 510 Université Paris Sud
91405 Orsay
France
gabelli@lps.u-psud.fr

Pr. Iouri Galperine
University of Oslo
Department of Physics
PO Box 1048 Blindern
0316 Oslo
Norway
iouri.galperine@fys.uio.no

Dr. Oleg Gerashchenko
B.P.Konstantinov Nuclear Physics Insnitute
PNPI, Gatnina, Leningrad distr., 188300
Russia
gerashch@pnpi.spb.ru

Dr. Maria Teresa Giraudo
Dept. of Mathematics University of Torino
Via C. Alberto 10, 10123 Torino
Italy
mariateresa.giraudo@unito.it

Dr. Denis S. Goldobin
Nonlinear Dynamics Group
Institute of Physics,
University of Potsdam,
Postfach 601553,
D-14415 Potsdam
Germany
Denis.Goldobin@gmail.com

Mr. Anatoly Golub
Ben-Gurion University
Department of Physics, Ben-Gurion University, Beer-Sheva 84105, Israel
Israel
agolub@bgu.ac.il

Pr. Giuseppe Gonnella
Dipartimento di Fisica
via Amendola 173
70123 Bari
Italy
gonnella@ba.infn.it

Mr. Josep Maria Huguet
Universitat de Barcelona
Diagonal, 647
Departament de Física Fonamental
Small Biosystems Lab
08028 Barcelona
Spain
huguet@ffn.ub.es

Mr. Sylvain Joubaud
Laboratoire de Physique. ENS Lyon
46 allee d'italie
69007 Lyon
France
sylvain.joubaud@ens-lyon.fr

Dr. Holger Kantz
Max Planck Institute for the Physics of Complex Systems
Noethnitzer Str. 38
01187 Dresden
Germany
kantz@pks.mpg.de

Dr. Igor A. Khovanov
Lancaster University
Lancaster
LA14YB
United Kingdom
i.khovanov@lancaster.ac.uk

Pr. Laszlo B. Kish
Texas A&M University, ECE Department
TAMU, Mailstop 3128, College Station, TX-77843-3128, USA
U.S.A.
Laszlokish@tamu.edu

Mr. Ryota Kobayashi
Kyoto university
Department of Physics,
Graduate School of Sciences, Kyoto University
Kyoto 606-8502, Japan
Japan
kobayashi@dora3.scphys.kyoto-u.ac.jp

Dr. Takayuki Kobayashi
Shiga University of Medical Science
Seta, Otsu
Shiga
Japan
jokyo-ji@ever.ocn.ne.jp

Dr. Peter M. Kotelenez
Case Western Reserve University
Department of Mathematics
Yost Hall
Cleveland, OH 44106
U.S.A.
pxk4@cwru.edu

Dr. Ferenc Kun
Department of Theoretical Physics, University of Debrecen
H-4010 Debrecen, Bem ter 18/b
Hungary
feri@dtp.atomki.hu

Dr. Denis L'Hôte
CEA
Service de Physique de la Matière Condensée
CE Saclay
91191 Gif/Yvette Cedex
France
denis.lhote@cea.fr

Mr. Gaetan Lassere
Universite de Bourgogne, ESIREM LE2I
Laboratoire LE2I UMr. 5158
Aile des sciences de l'ingénieur BP 47870
21078 Dijon Cedex
France
gaetan.lassere@u-bourgogne.fr

Mr. Thibault Laurent
University Montpellier 2
place Eugène Bataillon
CC 084
34095 Montpellier
France
thibault.laurent@ies.univ-montp2.fr

Mr. Lasse Laurson
Laboratory of Physics, Helsinki University of Technology
P.O.Box 1100
FIN-02015 HUT
Finland
lla@fyslab.hut.fi

Dr. Fabio Leoni
Sapienza, Università di Roma
P.le A. Moro 2
00185, Roma
Italy
leoni@pil.phys.uniroma1.it

Mr. Chenghua Liang
Université du littoral côte d'opale
50 rue F. Buisson, B.P. 717, 62228 Calais, France
France
Liang@univ-littoral.fr

Dr. Benjamin Lindner
Max Planck Institute for the Physics of Complex Systems
Noethnitzer Str. 38
01187 Dresden
Germany
benji@pks.mpg.de

Mr. Pietro Lio
Computer Laboratory
15 J Thomson avenue
cb30fd
Cambridge
United Kingdom
pl219@cam.ac.uk

Mr. Lukasz Machura
University of Silesia
Institute of Physics
ul. Uniwersytecka 4
40 - 007 Katowice
Poland
lukasz.machura@us.edu.pl

Dr. Alessandro Magni
INRIM
S.delle Cacce 91
10135 Torino
Italia
magni@inrim.it

Mr. Hugues Marinchio
University Montpellier 2
place E. Bataillon
34095 Montpellier cedex 5
France
marinchio@ies.univ-montp2.fr

Dr. Elisabetta Marras
CRS4 Bioinformatics
loc Pixinamanna bldg 3
09010 Pula (Ca)
Italy
lisa@crs4.it

Pr. Peter Vaughan Elsmere McClintock
Lancaster University
Department of Physics
Lancaster University
Lancaster
LA1 4YB
UK
p.v.e.mcclintock@lancaster.ac.uk

Dr. Mark Damian McDonnell
University of South Australia
Institute for Telecommunications Research
SPRI Building
Mawson Lakes Boulevard
Mawson Lakes SA 5095
Australia
mark.mcdonnell@unisa.edu.au

Mr. Jean-Francois Millithaler
Universita' degli Studi del Salento
Dipartimento di Ingegneria dell' Innovazione
Via Arnesano s/n
73100 Lecce, ITALY
Italy
jf.millithaler@unile.it

Ms. Fatemeh Momeni
Physics Department of Purdue University
Fatemeh Momeni, Department of Physics
525 Northwestern Avenue, West Lafayette, IN
47907-2036
U.S.A.
fmomeni@purdue.edu

Dr. Takaaki Monnai
Waseda University
Department of Applied Physics
3-4-1 Okubo, Shinjuku-ku, 169-8555, Tokyo
Japan
monnai@suou.waseda.jp

Mr. Saverio Morfu
Université de Bourgogne, ESIREM, LE2I
Laboratoire LE2I UMr. 5158
Aile des sciences de l'ingénieur BP 47870
21078 Dijon Cedex
France
smorfu@u-bourgogne.fr

Mr. Mikhael Myara
Institut d'Electronique du Sud - UMR5214
Université Montpellier II
Place Eugène Bataillon - cc. 084 - Bat 21
34095 Montpellier
France
myara@opto.univ-montp2.fr

Dr. Gianni Niccolini
Istituto Nazionale di Ricerca Metrologica
Strada delle Cacce,91
TORINO
Italy
g.niccolini@inrim.it

Mr. Markus Niemann
Max-Planck-Institut für Physik komplexer Systeme
Nöthnitzer Straße 38
01187 Dresden
Germany
niemann@pks.mpg.de

Dr. Tomas Novotný
Charles University in Prague
Department of Condensed Matter Physics
Faculty of Mathematics and Physics
Ke Karlovu 5
CZ-121 16 Prague
Czech Republic
tno@karlov.mff.cuni.cz

Dr. Akio Nozawa
Meisei University
2-1-1 Hodokubo, Hino, Tokyo 191-8506
Japan
akio@ee.meisei-u.ac.jp

Dr. Toru Ohira
Sony Computer Science Laboratories, Inc.
3-14-13 Higashigotanda
Shinagawa, Tokyo 141-0022
Japan
ohira@csl.sony.co.jp

Mr. Elvis Obi
African information Technology Holdings
29 Bolong Street, Off Pipeline
Pipeline-The Gambia
The Gambia
aith@fastermail.com

Dr. Xavier Oriols
Universitat Autonoma de Barcelona
Departament d'Enginyeria Electrònica
ETSE
Universitat Autonoma de Barcelona
08193 - Bellaterra - Barcelona
Spain
xavier.oriols@uab.es

Mr. Bernard Orsal
Université Montpellier 2
Place Eugène Bataillon
34095 MONTPELLIER CEDEX
France
orsal@opto.univ-montp2.fr

Dr. Yossi Paltiel
Soreq NRC
Yavne 8100
Israel
paltiel@soreq.gov.il

Dr. Paolo Paradisi
Istituto di Science dell'Atmosfera e del Clima (ISAC - CNR), Unità di Lecce
Strada Provinciale Lecce-Monteroni Km 1,2 , I-73100 Lecce
Italy
p.paradisi@isac.cnr.it

Pr. Cecilia Pennetta
Universita' del Salento
Via Arnesano, Ed. "Stecca",
73100 Lecce, Italy
Italy
cecilia.pennetta@unile.it

Dr. Dominique Persano Adorno
Dipartimento di Fisica e Tecnologie Relative - Università di Palermo
Viale delle Scienze, Ed. 18
90128 PALERMO
Italy
dpersano@unipa.it

Dr. Estelle Pitard
CNRS-Laboratoire des Colloides, Verres et Nanomateriaux
Universite Montpellier 2
Place Eugene Bataillon
34095 Montpellier cedex 5
France
estelle@lcvn.univ-montp2.fr

Dr. Nicola Pizzolato
University of Palermo
Viale delle Scienze, Ed. 18
90128 Palermo
Italy
npizzolato@gip.dft.unipa.it

Mr. Ondrej Pokora
Department of Mathematics and Statistics, Masaryk University
Janackovo nameti 2a
60200 Brno
Czech Republic
pokora@math.muni.cz

Mr. Jean-Marc Routoure
GREYC/ENSICAEN & Univ Caen
Bd du marechal Juin
14050 Caen Cedex
France
routoure@greyc.ensicaen.fr

Mr. Giulio Sabatini
University Montpellier 2
Place E. Bataillon
34095 Montpellier cedex 5
France
sabatini@ies.univ-montp2.fr

Mr. Mahamadou Sahanoho
African information Technology Holdings
29 Bolong Street, Off Pipeline
Pipeline-The Gambia
The Gambia
aithinfo@fastermail.com

Dr. Pavel Shiktorov
Semiconductor Physics Institute
Goshtauto 11, LT-01108 Vilnius
Lithuania
pavel@pav.pfi.lt

Pr. Shigeru Shinomoto
Department of Physics, Kyoto University
Sakyo-ku, Kyoto
Japan
shinomoto@scphys.kyoto-u.ac.jp

Pr. Andrew Snarskii
Kiev Plitechnics Institute, Ukrain
127473 Moscow
1-st Volkonskii per 11,
(address for communications)
Russian Federation
asnarskii@gmail.com

Dr. Dorottya Sohler
Institute of Nuclear Research (ATOMKI)
Bem ter 18/c
Debrecen
H-4026
Hungary
sohler@atomki.hu

Pr. Bernardo Spagnolo
University of Palermo
Dipartimento di Fisica e Tecnologie Relative,
Viale delle Scienze, pad.18
Palermo
Italy
spagnolo@unipa.it

Dr. Jevgenij Starikov
Semiconductor Physics Institute
Goshtauto 11, LT-01108 Vilnius
Lithuania
jane@pav.pfi.lt

Pr. Zbigniew R. Struzik
Graduate School of Education, The University of Tokyo
7-3-1 Hongo, Bunkyo-ku, 113-0033, Tokyo
Japan
zbigniew.struzik@p.u-tokyo.ac.jp

Mr. Eugene Sukhorukov
University of Geneva
Department of Theoretical Physics, University of Geneva
24, quai Ernest Ansermet
CH-1211 Geneva
Switzerland
Eugene.Sukhorukov@physics.unige.ch

Dr. Noboru Tanizuka
Graduate School of Science, Osaka Prefecture University
1-1 Gakuen-cho, Naka-ku, Sakai, Osaka, 599-8531
Japan
tanizuka@mi.s.osakafu-u.ac.jp

Dr. Nobuhisa Tanuma
Meisei University
Hino, Tokyo 191-8506
Japan
tanuma@amrc.meisei-u.ac.jp

Dr. Ekkehard Ullner
Universitat Politecnica de Catalunya, Departament de Fisica i Enginyeria Nuclear
Colom 11
E-08222 Terrassa
Spain
ekkehard.ullner@upc.edu

Dr. Eric Vanden-Eijnden
New York University
Courant Institute
251, Mercer street
New York, NY, 10012
U.S.A.
eve2@cims.nyu.edu

Pr. Luca Varani
University Montpellier 2
Place E. Bataillon
34095 Montpellier cedex 5
France
luca.varani@univ-montp2.fr

Pr. Jesús Enrique Velázquez-Pérez
Universidad de Salamanca
Pza. de la Merced s/n
Edificio Trilingüe
E-37008 Salamanca
Spain
js@usal.es

Dr. Alexey Zaikin
University of Essex
Department of Mathematics
Wivenhoe park
CO4 3SQ Colchester
UK
zaikin@essex.ac.uk

Dr. Steeve Zozor
GIPSA-Lab
961 rue de la Houille Blanche
B.-P. 46
38402 Saint Martin d'Hères Cedex
France
steeve.zozor@gipsa-lab.inpg.fr

Index of Authors

Accardo, M. 110
Akin, O. C. 21
Alarcón , A. 60
Alava, M. J. 28
Albareda, G. **50**
Amblard, P.-O. 19, 20
Andreoli, V. **110**
Andreucci, D. **25**

Bagchi, D. **37**
Bagliani, D. 58
Bagnoli, F. 81
Baldassarri, A. 34
Bardhan, K. K. **56**
Barkai, E. **67**
Barone, C. 49
Bednorz, A. **116**
Bellon, L. 37
Belogolovskii, M. 111
Belyaev, A. E. 109
Belzig, W. 116
Ben Simon, A. 47
Benzi, R. **64**
Berger, V. 47
Bezsudnov, I. **102**
Billangeon, P. 46
Bodo, B. 99
Borgnat, P. **75**
Bouchet, F. **43**
Bouchiat, H. **46**
Bouchier, A. 73
Bougrioua, Z. 109
Braggio, A. **115**
Buceta Fernández, J. 22
Bustamante, C. 23

Cambras Riu, T. 22
Cao, F. J. **39**, **95**
Capobianco, E. 83
Castaing, B. **36**
Castillón, A. O. 90
Celasco, E. **58**
Celasco, M. 58
Chan, H. B. **38**
Chang, C.-H. **82**
Chapeau-Blondeau, F. **12**
Chobola, Z. 72
Chun-Hsing, S. **57**
Ciccarello, F. **55**
Ciliberto, S. 29, 37, 100
Corral, A. **31**, **90**, **91**
Csikor, F. **32**

Dahmen, K. **27**
Dalton, F. **34**
Danylyuk, S. V. **109**
Deblock, R. 46
Deschanel, S. **29**
Di Patti, F. **16**
Dierkes, K. **15**
Díez Noguera, A. 22
Dolensky, J. **72**
Dolgin, B. 111
Dubkov, A. **42**, 74
Duchêne, C. 20
Duggento, A. **41**
Dureisseix, D. 11
Durin, G. 33, 96

Ebeling, W. 97
Eggenhöffner, R. 58
Eisenberg, R. S. 84
Essimbi, B. 99

Fadil, D. 49
Fanelli, D. 16
Feito, M. 39, 95
Ferrari, L. 58
Fiasconaro, A. 86, **97**
Flament, S. 49, 106
Flandrin, P. 75
Flindt, C. 115
Fobelets, K. 53
Forns, N. 23

Gabelli, J. **61**, **112**
Galperine, I. **48**
Gandini, G. 110
García-Ojalvo, J. 22
Garnache, A. 73
Gatti, F. 58
Gerashchenko, O. **104**
Gest, J. 107
Giraudo, M. T. **80**
Godin, N. 29
Goldobin, D. S. **85**, **94**
Golub, A. **114**
Gong, J. 57
Gonnella, G. **68**
González, T. 54
Goychuk, I. 42
Grigolini, P. 21
Gružinskis, V. 51, 103
Gudowska-Nowak, E. 97
Guillet, B. 106

Halász, Z. 30
Hänggi, P. 42
Herrmann, H. J. 30
Hochin, T. 24
Huguet, J.M. **23**

Jandova, K. 72
Jauho, A.-P. 115
Jiménez, D. 50

Joubaud, S. **100**
Jülicher, D. 15
Jung, G. 47, 111
Jurankova, V. 72

Kantz, H. **10**, 71
Kaufman, I. 84
Kerlain, A. 98
Khan, M. R. 24
Khovanov, I. A. **18**
Kish, L. **44**
Kiyono, K. 17
Klein, N. 109
Knap, W. 54
Kobayashi, R. **87**
Konczykowski, M. 98
Kotelenez, P. M. **66**
Kun, F. **30**
Kurakin, A. M. 109
Kurths, J. 85

Ladieu, F. 98
Lansky, P. 70
Lasaponara, R. 91
Laurent, T. 103
Laurson, L. **28**
Leitman, M. J. 66
Leoni, F. **89**
Leroy, G. 107
L'Hôte, D. **98**
Liang, C. **107**
Lien , C. 57
Lindner, B. **14**, 15
Lío, P. **81**
Liu, Y. 27
Llebot, J. E. 90
Luchinsky, D. G. 41, 84

Machura, L. **40**
Magni, A. **96**
Makowiec, D. 77
Marinchio, H. 51, 103
Markovich, V. 111
Marquié, P. 99
Marras, E. **83**
Masoero, A. 110
Mateos, J. 54
Mazzetti, P. 110
McClintock, P. V. E. 41, 84
McDonnell, M. D. **19**
Méchin, L. 49, 106
Millithaler, J.-F. **54**
Monnai, T. **118**
Monticone, E. 110
Morfu, S. **99**
Morita, H. 43
Mosser, V. 98
Motz, C. 32
Mukherjee, C. D. 56
Mukovskii, Ya. M. 111
Myara, M. **73**

Naert, A. 37
Nakamae, S. 98
Nakamura, T. 79
Naumov, A. V. 109
Niccolini, G. **33**
Niemann, M. **71**
Ninios, K. 38
Novotný, T. **62**, 115
Nozawa, A. **78**

Ohira, T. **93**
Oriols, X. 50, **60**
Orsal, B. **11**

Palermo, C. 54, 103
Paltiel, Y. **47**
Paradisi, P. **21**
Pardo, D. 54
Pennetta, C. **77**
Perez, J.-P. 73
Perez, S. 54
Perna, P. 49
Persano Adorno, D. **105**
Petri, A. 34
Petrosyan, A. 100
Petrychuk, M. V. 109
Piscitelli, A. 68
Pizzolato, N. **86**, 105
Pokora, O. **70**
Pontuale, G. 34
Portesi, C. 110
Pousset, J. 54

Rajteri, M. 110
Reggiani, L. 51, 54, 103
Reulet, B. 61, 112
Ritort, F. 23
Romanini, D. 73
Rousseau, D. 12
Routoure, J.-M. **49**, **106**

Sabatini, G. 51, 103
Sacerdote, L. 80
Sagnes, I. 73
Sassetti, M. 115
Schneider, H. 47
Sethna, J. P. 96
Shiktorov, P. 51, 103
Shklyaeva, E. V. 94
Signoret, P. 73
Sikula, J. 108
Simonnet, E. 43
Smelyanskiy, V. N. 41
Smith, S.B. 23
Snarskii, A. A. 102
Spagnolo, B. **74**, 86, 105
Stambaugh, C. 38
Starikov, J. 51, **103**
Stocks, N. G. 19
Struzik, Z. R. **17**, **79**
Sukhorukov, E. **52**

Tacano, M. 78, 108
Tanizuka, N. **24**
Tanuma, N. **108**
Taralli, E. 110
Telesca, L. 91
Tindjong, R. 84
Tsong, T. Y. 82

Ullner, E. **22**

Vacher, R. 11
Valle, R. 58
Vandamme, L. K. J. 107
Vanden-Eijnden, E. **65**
Vanek, J. 72
Vanel, L. 29
Varani, L. **51**, 54, 103
Velázquez-Pérez, J. E. **53**
Vigier, G. 29
Vitusevich, S. A. 109

Weygand, D. 32
Wojkiewicz, J.-L. 107
Wu, X. D. 111

Yagi, S. 108
Yamamoto, Y. 17, 79
Yeh, S.-P. 57
Yuzhelevski, Y. 111

Zaikin, A. 85
Zaiser, M. 32
Zammito, S. 55
Zapperi, S. 32, 34, 89, 96
Zarcone, M. 55
Zozor, S. **20**

Document compiled by L. Bellon with LaTeX – Last update: June 4, 2008